

Атомная
Энергия

Volume 3, Number 10, 1957

The Soviet Journal of
ATOMIC
ENERGY

IN ENGLISH TRANSLATION



CONSULTANTS BUREAU, INC.

227 WEST 17TH STREET, NEW YORK 11, N. Y.

ATOMNAYA ENERGIYA

Academy of Sciences of the USSR

Volume 3, Number 10, 1957

EDITORIAL BOARD

A. I. Alikhanov, A. A. Bochvar, V. I. Veksler, A. P. Vinogradov,
N. A. Vlasov (Acting Editor in Chief), V. S. Emelyanov, V. F. Kalinin,
G. V. Kurdyumov, A. V. Lebedinsky, I. I. Novikov (Editor in Chief),
B. V. Semenov (Executive Secretary), V. S. Fursov

The Soviet Journal

of

ATOMIC ENERGY

IN ENGLISH TRANSLATION

Copyright, 1958

CONSULTANTS BUREAU, INC.

227 West 17th Street

New York 11, N. Y.

Printed in the United States

Annual Subscription \$75.00
Single Issue 20.00

Note: The sale of photostatic copies of any portion of this copyright translation is expressly prohibited by the copyright owners. A complete copy of any article in the issue may be purchased from the publisher for \$12.50.

SIGNIFICANCE OF ABBREVIATIONS MOST FREQUENTLY ENCOUNTERED IN SOVIET PHYSICS PERIODICALS

AN SSSR	<i>Academy of Sciences, USSR</i>
FIAN	<i>Physics Institute, Academy of Sciences USSR</i>
GITI	<i>State Scientific and Technical Press</i>
GITTL	<i>State Press for Technical and Theoretical Literature</i>
GOI	<i>State Optical Institute</i>
GONTI	<i>State United Scientific and Technical Press</i>
Gosenergoizdat	<i>State Power Press</i>
Gosfizkhimizdat	<i>State Physical Chemistry Press</i>
Gozkhimizdat	<i>State Chemistry Press</i>
GOST	<i>All-Union State Standard</i>
Goztekhizdat	<i>State Technical Press</i>
GTTI	<i>State Technical and Theoretical Press</i>
GUPIAE	<i>State Office for Utilization of Atomic Energy</i>
IF KhI	<i>Institute of Physical Chemistry Research</i>
IFP	<i>Institute of Physical Problems</i>
IL	<i>Foreign Literature Press</i>
IPF	<i>Institute of Applied Physics</i>
IPM	<i>Institute of Applied Mathematics</i>
IREA	<i>Institute of Chemical Reagents</i>
ISN (Izd. Sov. Nauk)	<i>Soviet Science Press</i>
I YaP	<i>Institute of Nuclear Studies</i>
Izd	<i>Press (publishing house)</i>
KISO	<i>Solar Research Commission</i>
LETI	<i>Leningrad Electrotechnical Institute</i>
LFTI	<i>Leningrad Institute of Physics and Technology</i>
LIM	<i>Leningrad Institute of Metals</i>
LITMiO	<i>Leningrad Institute of Precision Instruments and Optics</i>
Mashgiz	<i>State Scientific-Technical Press for Machine Construction Literature</i>
MATI	<i>Moscow Aviation Technology Institute</i>
MGU	<i>Moscow State University</i>
Metallurgizdat	<i>Metallurgy Press</i>
MOPI	<i>Moscow Regional Institute of Physics</i>
NIAFIZ	<i>Scientific Research Association for Physics</i>
NIFI	<i>Scientific Research Institute of Physics</i>
NIIMM	<i>Scientific Research Institute of Mathematics and Mechanics</i>
NII ZVUKSZAPIOI	<i>Scientific Research Institute of Sound Recording</i>
NIKFI	<i>Scientific Institute of Motion Picture Photography</i>
OIYaI	<i>Joint Institute of Nuclear Studies</i>
ONTI	<i>United Scientific and Technical Press</i>
OTI	<i>Division of Technical Information</i>
OTN	<i>Division of Technical Science</i>
RIAN	<i>Radium Institute, Academy of Sciences of the USSR</i>
SPB	<i>All-Union Special Planning Office</i>
Stroiiizdat	<i>Construction Press</i>
URALFTI	<i>Ural Institute of Physics and Technology</i>

NOTE: Abbreviations not on this list and not explained in the translation have been transliterated, no further information about their significance being available to us.—*Publisher.*

FORMATION OF Na^{24} AND P^{32} IN THE INTERACTION OF HIGH-ENERGY PROTONS WITH COMPOUND NUCLEI

A. K. Lavrukhina, L. P. Moskaleva, L. D. Krasavina and I. M. Grechishcheva

The variation of the yields of Na^{24} and P^{32} nuclei from copper, lanthanum, gold, and thorium with the proton energy has been studied by a radiochemical method. The curves show that the yields of these nuclei increase considerably with increase of the proton energy from 120 to 660 mev. It was found that the yields of Na^{24} and P^{32} nuclei depend to a considerable extent on the atomic number of the target element. A comparison of the calculated formation thresholds of Na^{24} and P^{32} nuclei in spallation and fission reactions with experimental estimates of these thresholds led to the conclusion that they are formed by strongly asymmetric fission of copper, lanthanum, and gold nuclei. An exception is P^{32} , which is formed from copper as the result of a spallation reaction. This last process plays a significant role in the formation of Na^{24} from copper.

INTRODUCTION

It follows from a number of investigations [1-6] that when high-energy protons interact with compound nuclei the cross section of light element nucleus formation decreases with increase in atomic numbers of the light elements and of the atomic number of the irradiated nuclei. It has also been shown that the cross section of light nucleus formation increases considerably with increasing energy of the bombarding particles.

However, the mechanism of the formation of nuclei of light elements is still not clear, and investigation of it presents considerable interest. Studies of the formation of such nuclei by the interaction of protons artificially accelerated to energies close to cosmic radiation energies may assist solution of the problem concerning the presence of light nuclei in the primary component of cosmic radiation.

The present authors have studied the mechanism of formation of Na^{24} and P^{32} nuclei during bombardment of copper, lanthanum, gold, and thorium by protons of energies between 120 and 660 Mev. The cross sections of nuclear formation were determined by a radiochemical method.

METHOD

The materials used were spectroscopically pure copper, gold, thorium, and lanthanum oxide. Spectral analysis of the copper showed the presence of $Ca \sim 2 \cdot 10^{-4} \%$, $Mn \sim 5 \cdot 10^{-3} \%$, $Ag \sim 2 \cdot 10^{-4} \%$ and $Fe, Ni, Cd \sim 10^{-3} \%$. The metallic thorium contained $Na \sim 1 \cdot 10^{-2} \%$, $Mg \sim 5 \cdot 10^{-3} \%$, $Ca < 10^{-4} \%$, $Mn \sim 10^{-3} \%$ and $Pb \sim 10^{-3} \%$. The lanthanum oxide contained $Pr_2O_3 \leq 0.02 \%$ and $Ce_2O_3 \leq 0.02 \%$. Targets of these materials $15 \times 5 \times 0.5$ mm in size were bombarded for 1.5-2 hours by an internal beam of protons with energies of 660, 480, 340, 220 and 120 Mev in the synchrocyclotron of the Laboratory of Nuclear Problems, OIAl. *

After the bombardment the targets were dissolved in appropriate acids, containing isotopic carriers of the isotopes to be isolated, and this was followed by chemical isolation and purification. Various methods were used for this.

*Joint Institute for Nuclear Studies.]

Isolation of sodium. Sodium was isolated from the bombarded copper in the form of the chloride after previous precipitation of copper and bismuth sulfides in a weakly acid medium, of manganese sulfide in an ammoniacal medium, and of ferric hydroxide and potassium perchlorate, and sorption of the cations from 0.3 N HCl solution in a chromatographic column filled with KU-2 resin in the H⁺ form. Ammonium salts were removed by strong heating. The sodium chloride precipitate was reprecipitated and dried at 130°. In the analysis of irradiated lanthanum and gold, lanthanum hydroxide was first precipitated with ammonia, and gold was precipitated by means of SO₂ from 40% HCl solution.

Isolation of phosphorus. In the analysis of copper, phosphorus was precipitated as ammonium phosphomolybdate in presence of 20 mg Be⁺² after preliminary precipitation of copper sulfide. The precipitate, after twofold reprecipitation, was dissolved in concentrated ammonia and phosphorus was isolated from the solution by means of magnesia mixture (this operation was performed twice). The precipitate was dissolved in 0.3 N HCl solution and passed through a chromatographic column filled with KU-2 resin in the H⁺ form; bismuth phosphate was separated from the solution and dissolved in HCl. Bismuth was removed by means of H₂S. Iron was then precipitated twice by cupferron. Phosphorus was finally precipitated in the form of zirconium phosphate. This was reprecipitated and ignited at 900° to ZrP₂O₇.

The isolation of phosphorus from irradiated lanthanum and gold was carried out by the procedure described above, with the additional operations of lanthanum precipitation as the oxalate in presence of 50 mg Ce⁺³, and of gold by means of SO₂ from 40% HCl solution.

RESULTS

The results of identification of the Na²⁴ and P³² radioisotopes from different targets are given in Table 1, which also contains, for comparison, the corresponding literature data [7].

TABLE 1

Radioisotope	Half-life		Energy of β -radiation, mev	
	found	literature data	found	literature data
Na ²⁴	15.0 hrs	15.0 hrs	1.4	1.39
P ³²	14.5 days	14.3 days	1.7	1.701

Data on the cross sections of Na²⁴ and P³² formation from different nuclei are given in Table 2. Each value is the mean of two or three determinations.

TABLE 2

Proton energy, Mev	Cross sections, 10^{-29} cm ²							
	Cu		La		Au		Th	
	Na ²⁴	P ³²	Na ²⁴	P ³²	Na ²⁴	P ³²	Na ²⁴	P ³²
120	0.09	0.07	0.099	—	—	—	—	—
220	0.22	0.22	0.3	Traces	0.59	Traces	—	—
340	1.3	1.8	0.5	0.73	0.13	0.3	—	—
480	5.6	24	2	1.4	3.7	1.1	18	3
660	25	31	21	—	8.1	2.2	—	—

The variations of the cross sections of the formation of Na^{24} and P^{32} isotopes from different nuclei with the proton energy are shown in Figures 1-5. The following principal conclusions can be drawn from the results obtained:

1. The cross sections of Na^{24} and P^{32} formation increase sharply with increase of proton energy from 120 to 660 mev. The yield of Na^{24} from copper and lanthanum increases more than 200-fold in this energy range, and the yield of phosphorus from copper increases \approx 440-fold.

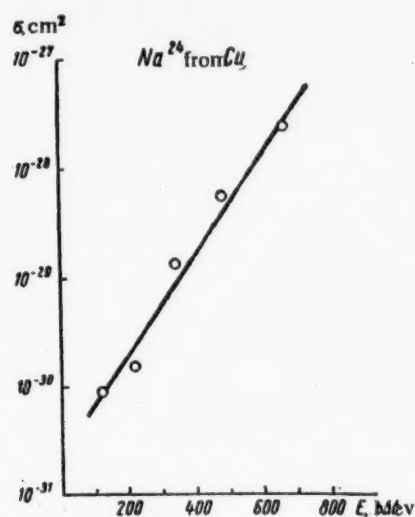


Fig. 1. Variation of the yield of Na^{24} from copper with the proton energy.

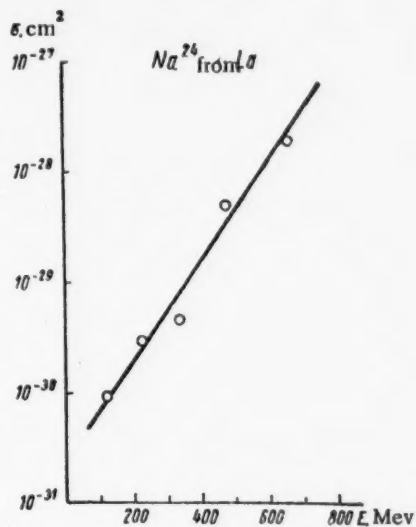


Fig. 2. Variation of the yield of Na^{24} from lanthanum with the proton energy.

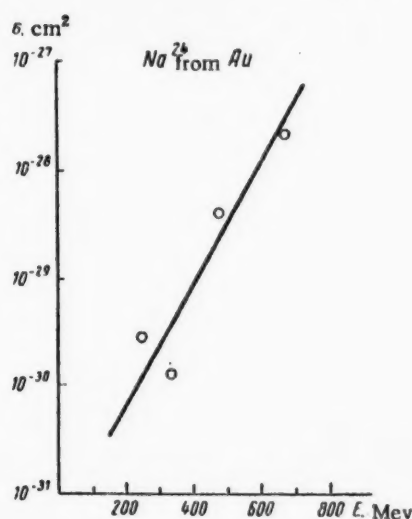


Fig. 3. Variation of the yield of Na^{24} from gold with the proton energy.

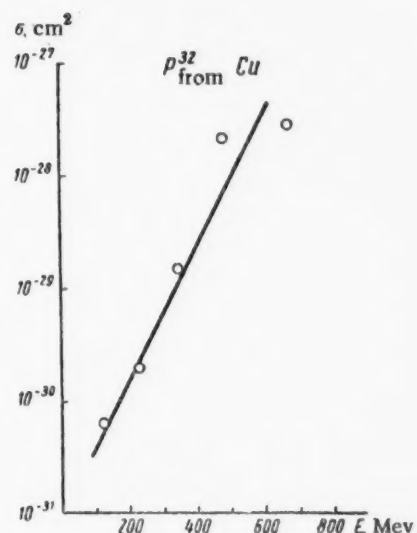


Fig. 4. Variation of the yield of P^{32} from copper with the proton energy.

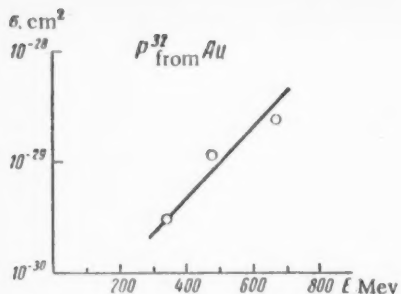


Fig. 5. Variation of the yield of P^{32} from gold with the proton energy.

the thresholds of P^{32} formation from lanthanum and gold, below 220 Mev, and of Na^{24} formation from gold, below 220 Mev.

To determine the relationship between the yields of the nuclei and the atomic numbers of the target elements, we consider the curves in Figure 6. This graph shows the yields of Na^{24} and P^{32} (with proton energies 420-480 Mev) plotted against the atomic numbers of the bombarded nuclei. Data on the cross section of F^{18} formation at proton energy 1 Bev are taken from [10].

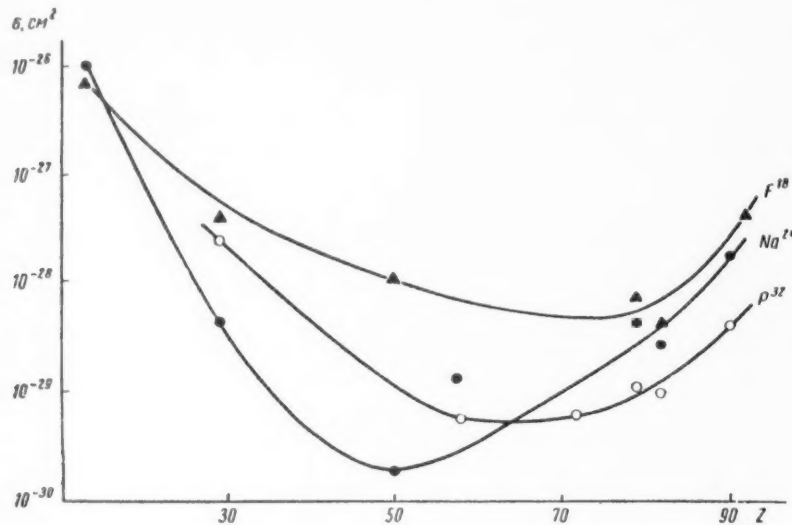


Fig. 6. Variations of the yields of Na^{24} and P^{32} with the atomic numbers of nuclei bombarded by protons of 480-Mev energy, and of F^{18} for 1-Bev protons. Data used:

- σ of Na^{24} formation from Al and Sn [1];
- σ of Na^{24} formation from La [5];
- σ of Na^{24} and P^{32} formation from Pb [9].

The yields of Na^{24} and P^{32} depend to a considerable extent on the atomic number of the target element. There is a 2000-fold decrease of yields from aluminum ($Z = 13$) to tin ($Z = 50$), and a gradual increase toward thorium ($Z = 90$).

2. The yields of Na^{24} and P^{32} are practically the same for copper and lanthanum nuclei in the proton energy range of 120-660 Mev. In the bombardment of gold, the yield of Na^{24} is two to three times the yield of P^{32} . Therefore for nuclei of medium atomic weight the yield of nuclei of light elements with $Z = 11-15$ does not depend on their atomic number. This is in agreement with earlier findings [8]. When protons of energies between 350 and 660 Mev interact with nuclei of a photographic emulsion, multinuclear particles with $Z \geq 4$ are formed; the yields of nuclei with $Z \geq 9$ are practically the same.

3. The curves for the yields of Na^{24} and P^{32} against the proton energy can be used for estimation of their formation threshold, i. e., the proton energy at which these nuclei cannot be identified. The thresholds of Na^{24} formation from copper and lanthanum and P^{32} formation from copper lie below 120, and of Na^{24} formation from gold, below 220 Mev.

The relative positions of the curves for Na^{24} , P^{32} and F^{18} show that with increasing proton energy the difference between the yields of light nuclei from different elements diminishes, and becomes very slight at high proton energies. With 3-Bev protons the yields of F^{18} from aluminum ($Z = 13$) and silver ($Z = 47$) differ only by a factor of 4.7 [10].

DISCUSSION OF RESULTS

It is known that when high-energy particles (100-700 Mev) interact with compound nuclei, two nuclear processes take place: spallation and fission.

It is not possible to determine from the curves, obtained in this investigation, for the yields of Na^{24} and P^{32} isotopes against the proton energy by which of these processes the isotopes are formed. To solve this problem, the thresholds for the formation of these nuclei by the spallation and fission reactions were calculated. Use was made of the mass differences between the initial and final products and the excitation energy necessary for overcoming the potential barrier by the charged particles or fission fragments. Either experimentally determined values of the masses [11], [12] were used, or they were calculated by the Fermi semiempirical equation:

$$M(A, Z) = 1.01464A + 0.014A^{2/3} - \\ - 0.041905\frac{(Z - Z_A)^2}{Z_A} +$$

$$+ \begin{cases} \pm 0.036/A^{1/4} \\ 0 \end{cases} \begin{array}{ll} Z - \text{odd}, & A - \text{even} \\ Z - \text{even}, & A - \text{even} \\ A - \text{odd}, & \end{array}$$

where

$$\frac{Z_A}{A} = \frac{1}{1.9807 + 0.01496A^{2/3}}.$$

The spallation thresholds were calculated for the case most favorable from the energy aspect, when the maximum possible number of α -particles is emitted from the original nucleus.

The height of the Coulomb potential barrier of a nucleus of charge $(Z - 2)e$ for an α -particle is given by the equation

$$B_\alpha = \frac{2(Z - 2)e^3}{R + R_\alpha},$$

where R is the radius of the final nucleus ($Z - 2, N - 2$); R_α is the radius of an α -particle.

The height of the barrier preventing fission of the fragments is

$$B_{\text{fiss}} = \frac{Z_1 Z_2 e^3}{R_1 + R_2},$$

where Z_1e , Z_2e and R_1 , R_2 are the charges and the radii of the resultant nuclei after fission of the target nucleus.

The thresholds of the spallation and fission reactions determined in this way are given in Table 3.

Comparison of the calculated and experimental values of the thresholds for Na^{24} and P^{32} formation by the spallation and fission reactions shows that the calculated thresholds of Na^{24} formation by fission of copper, lanthanum, and gold, and of P^{32} formation by fission of lanthanum and gold are in good agreement with the

TABLE 3

Spallation reaction	Threshold Mev	Fission reaction	Threshold, Mev
$\text{Cu}^{63} + p \rightarrow p + 3n + 9x + \text{Na}^{24}$	170	$\text{Cu}^{63} + p \rightarrow \text{Na}^{24} + \text{K}^{39} + n$	60
$\text{La}^{139} + p \rightarrow p + 23n + 23x + \text{Na}^{24}$	560	$\text{La}^{139} + p \rightarrow \text{Na}^{24} + \text{Ag}^{113} + 3n$	70
$\text{Au}^{197} + p \rightarrow p + 37n + 32x + \text{Na}^{24}$	840	$\text{Au}^{197} + p \rightarrow \text{Na}^{24} + \text{Tu}^{171} + 3n$	100
$\text{Cu}^{63} + p \rightarrow p + 3n + 7x + \text{P}^{32}$	450	$\text{Cu}^{63} + p \rightarrow 2\text{P}^{32}$	50
$\text{La}^{139} + p \rightarrow p + 23n + 21x + \text{P}^{32}$	530	$\text{La}^{139} + p \rightarrow \text{P}^{32} + \text{Tc}^{101} + 7n$	110
$\text{Au}^{197} + p \rightarrow p + 37n + 32x + \text{P}^{32}$	800	$\text{Au}^{197} + p \rightarrow \text{P}^{32} + \text{Tb}^{161} + 5n$	140

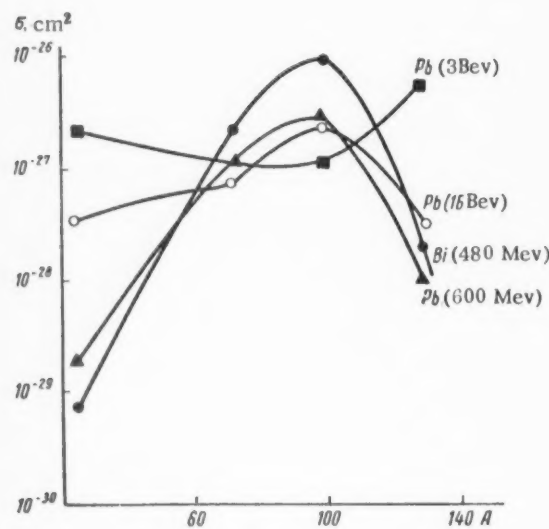


Fig. 7. Variations of the yields of Na^{24} , Ga^{72} , Mo^{99} and Ba^{129} with the proton energy in the bombardment of bismuth and lead by protons of 480 and 600 Mev, and 1 and 3 Bev energy.

The fact that the mechanism of Na^{24} and P^{32} formation depends on the atomic weight of the original element is also confirmed by the curves for the yields as functions of the atomic number of the target element (see Fig. 6). These curves show that the probability of Na^{24} and P^{32} formation by spallation decreases from aluminum to tin. The ascent of the curve beyond tin indicates increasing probability of a new process — strongly asymmetric fission. At very high energies of the bombarding particles the difference between the probabilities of these two processes diminishes, and therefore the dependence of the yield of the nuclei in question on the atomic number of the bombarded nucleus becomes less pronounced. This explanation of the course of the curves in Figure 6 is consistent with the modern views on the probabilities of fission and spallation processes in different nuclei.

The data obtained by us on Na^{24} and P^{32} nuclei can probably be considered in the light of the postulated "fragmentation" process which has recently been the subject of frequent discussion in the American literature.

experimental estimates. The experimental value of the threshold of P^{32} formation from copper differs considerably from the calculated value for the fission reaction and is close to that for the spallation reaction. It can therefore be concluded that Na^{24} nuclei are formed from all the nuclei studied, and P^{32} nuclei from lanthanum and gold, as the result of strongly asymmetric fission of these nuclei. Formation of P^{32} from copper occurs by spallation.

The relatively low calculated value (170 Mev) for the threshold of Na^{24} formation by spallation of copper indicates that this process may play an appreciable role at high proton energies. The very high thresholds for the spallation of lanthanum and gold nuclei with formation of Na^{24} and P^{32} indicate that the role of this process is small even at the highest proton energy. Figure 7 shows curves for the yields of Na^{24} , Ga^{72} , Mo^{99} and Ba^{129} nuclei formed by fission of bismuth [1] and lead [9], against proton energy. The yields of the strongly asymmetric fission products, Na^{24} and Ba^{129} , increase with increase of the proton energy from 480 Mev to 3 Bev. The yield of Mo^{99} formed by symmetrical fission, decreases at the same time. These facts confirm that Na^{24} and P^{32} are formed by strongly asymmetric fission of nuclei of heavy elements and of elements of moderate atomic weight.

According to this postulate, if the energy of the bombarding particles is very high the nucleus can receive a fairly high excitation energy which may be concentrated in small regions of the nucleus. Under such conditions it is possible for fragments of the nuclear substance to be emitted until the energy has become distributed uniformly over the whole nucleus. However, as the fragmentation process has not yet been studied in detail, it is difficult to assess its role in the formation of Na^{24} and P^{32} at relatively low proton energies (≤ 660 Mev). For this, further determinations of the angular and energy distributions of the nuclei in question are necessary.

LITERATURE CITED

- [1] L. Marquez, Phys. Rev. 86, 405 (1952).
- [2] A. P. Vinogradov, I. P. Alimarin, V. I. Baranov, A. K. Lavrukhina, T. V. Baranova, F. I. Pavlotskaya and Iu. V. Iakovlev, Session of AN SSSR on the Peaceful Use of Atomic Energy, July 1-5, 1955 (Meetings of the Division of Chemical Sciences) [In Russian] (Izd. AN SSSR, 1955) p. 97.
- [3] A. K. Lavrukhina, Doctorate Dissertation (Geochemical Institute AN SSSR, 1955).
- [4] S. Wright, Phys. Rev. 79, 838 (1950).
- [5] L. Marquez and I. Perlman, Phys. Rev. 81, 953 (1951).
- [6] R. Batzel and G. Seaborg, Phys. Rev. 82, 606 (1951).
- [7] G. Seaborg, I. Perlman and D. Hollender, Table of Isotopes (Russian Translation) (IL, 1956).
- [8] O. V. Lozhkin and N. A. Perfilov, J. Exptl.-Theoret. Phys. (USSR), 31, 913 (1956).*
- [9] R. Wolfgang, E. Baker, A. Caretto, J. Cumming, G. Cumming, G. Friedlander and J. Hudis, Phys. Rev. 103, 394 (1956).
- [10] J. Hudis and A. Caretto, Bull. Am. Phys. Soc. 1, 229 (1956).
- [11] B. S. Dzhelepov and L. N. Zyrianova, Uspekhi Fiz. Nauk, 48, 466 (1952).
- [12] V. A. Kravstov, Uspekhi Fiz. Nauk, 47, 341 (1952).

Received May 31, 1957

*See English translation.



THE MEASUREMENT OF THE ABSOLUTE INTENSITY OF NEUTRON SOURCES
BY A COMPARISON WITH THE REACTION $T(d, n)He^4$

N. N. Flerov and V. M. Taluzin

A method for the measurement of the absolute intensity of neutron sources by a comparison with the neutron intensity from the reaction $T(d, n)He^4$ is described. For the comparison of the intensities a detector was used which has an almost constant sensitivity for a wide range of neutron energies. The detector consisted of a graphite prism in which, at a definite distance from the source ("constant"-sensitivity distance), the density of thermal neutrons was measured. The sensitivity of such a detector is constant, to an accuracy of 1-2 %, in the interval of neutron energies 0.1-8 Mev and is 13% lower for neutrons of energy 14 Mev. In 1953 this method was used for the measurement* of the absolute intensity of a Ra- α -Be source with an accuracy of 4%.

For the determination of the absolute intensity of neutron sources various methods have been used [1], [2]. In a series of experiments, [3-5], the method of comparing the neutron flux from the source with the neutron flux obtained from the reactions $D(\gamma, n)H$; $D(d, n)He^3$; $T(d, n)He^4$ was used. In these reactions the neutrons are accompanied by charged particles whose flux can be determined sufficiently accurately.

In this way the determination of the absolute intensity of the neutron sources is reduced to the counting of the number of charged particles produced in the reaction used and the comparison of the neutron fluxes from the source investigated and from the reaction

$$J_s = \frac{N_s}{N_r} J_r \quad (1)$$

where N_s and N_r are the counting rates for neutrons from the source and the reaction, respectively; $J_r = \frac{4\pi}{\Omega} N_\alpha$ is the absolute intensity of the neutrons from the reaction; Ω is the solid angle of the charged-particle counter; N_α is the charged-particle counting rate.

The comparison of the neutron fluxes must be made using a detector having a constant sensitivity in the whole of the neutron-energy interval.

In the present work the detector used consisted of a graphite prism in which the density of thermal neutrons was measured at a definite distance from the neutron source.

The intensity of the source was compared with the neutron intensity from the reaction $T(d, n)He^4$. This reaction is suitable because the angular distribution of neutrons with an energy of 14 Mev is isotropic, while the α particles with an energy of 3 Mev are easily registered. A slight disadvantage of the detector is the high neutron energy.

*G. N. Flerov, L. B. Poretskii and S. M. Polikanov took part in the initial stages of the work.

Description of the Apparatus

Figure 1 shows the graphite prism in whose central cavity the various neutron sources were placed. To obtain neutrons with energies of 2.5 and 14 Mev zirconium targets, saturated with deuterium or tritium, were used and were irradiated by a beam of deuterons of energy 140 kev. For the relative measurements of the fluxes of neutrons with energies of 2.5 and 14 Mev, proton and α -particle proportional counters, placed at an angle of $\sim 170^\circ$ to the deuteron beam, were used as monitors. During the absolute measurements of the neutron flux at an energy of 14 Mev an α counter, with a definite solid angle, was used and placed perpendicularly to the beam. The fast-neutron fluxes were measured by the thermal-neutron density in the graphite prism by a proportional BF_3 counter.

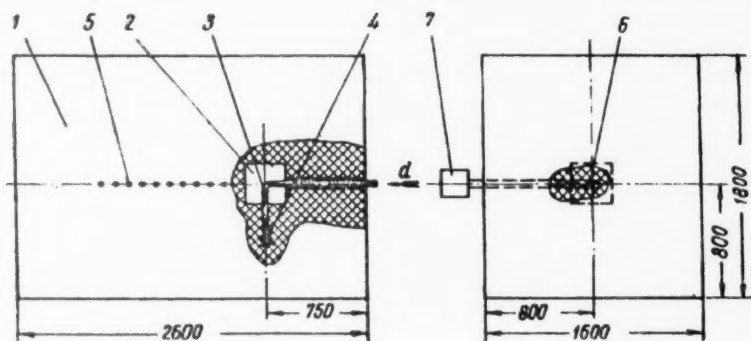


Fig. 1. Block diagram of the apparatus. 1) Graphite prism; 2) cavity; 3) target; 4) proportional α counter; 5) channels, closed by graphite plugs, into one of which the BF_3 counter was placed; 6) proportional BF_3 counter; 7) amplifier.

Neutron Detector

If sources of mono-energetic neutrons of various energies are placed at any point of an infinite medium then it is possible to find a distance from the sources at which the thermal-neutron density is almost independent of the fast-neutron energy and is mainly determined by the intensity of the source. This is correct for moderating media in which the slowing-down length is less than the diffusion length. Consequently, if a thermal-neutron detector is placed at this distance from the source, called in the following the "constant"-sensitivity distance then it is possible to compare the intensities of neutron sources having different energy spectra. If the sources are placed at the center of a cavity, and not directly into the medium, the "constant"-sensitivity distance is somewhat altered.

A graphite prism having a cubical cavity, at the center of which the neutron source was placed, was used in practice (Fig. 1). The choice of graphite for the moderator was governed by the small absorption of fast neutrons and the absence of neutron multiplication.

The effective diffusion length of thermal neutrons in the prism is less than the diffusion length in an infinite medium and depends on the dimensions of the prism. To determine the dependence of the "constant"-sensitivity distance on the effective diffusion length calculations were made of the thermal-neutron density as a function of the distance from the source, the slowing-down length (i. e., the fast neutron energy) and the radius of a spherical cavity, at the center of which the fast-neutron source was placed. The calculations were made using Equation (6.3 a) of Reference [6] for an infinite medium. It was shown that the "constant"-sensitivity distance depends very little on the diffusion length L in the interval from 40 to 52 cm and on the cavity radius a_1 from 15 cm to 20 cm. In further calculations it was assumed that the cubical cavity with a side of 30 cm is equivalent to a spherical cavity of radius $a_1 = 18.6$ cm (cavities of equal volume).

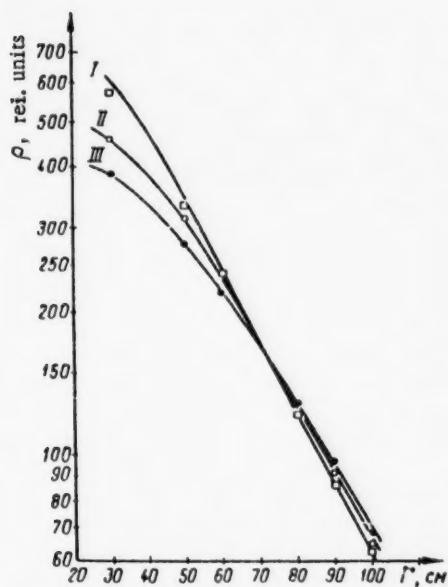


Fig. 2. The thermal-neutron density in the graphite prism as a function of the distance from the source. Theoretical curves for neutrons with energies: I) 0.13 Mev; II) 2.5 Mev; III) 14 Mev. Experimental points, normalized to the theoretical at $r = 70$ cm: \square) Ra- γ -Be source; \circ) 2.5 Mev neutrons; \bullet) 14 Mev neutrons.

The small dependence of the "constant"-sensitivity distance on the effective diffusion length was verified experimentally. At this distance the ratios of the thermal-neutron densities from three sources of fast neutrons (Ra- γ -Be, Ra- α -Be and the reaction $T(d, n)He^4$) were measured in prisms of three sizes: $1200 \times 1600 \times 2000$; $1200 \times 1600 \times 2600$ and $1600 \times 1800 \times 2600$. The ratio of the thermal-neutron densities for all these sources in the three prisms remained constant within 0.5%. All measurements following were made with the prism $1600 \times 1800 \times 2600$ (Fig. 1). The effective diffusion length for this prism was $L = (45 \pm 1)$ cm.

Figure 2 gives the theoretical curves of the thermal-neutron density as a function of distance with $L = 45$ cm and $a_1 = 18.6$ cm for three slowing-down lengths $\sqrt{\theta}$: 13.5; 18.5 and 21.7 cm.

Source	Ra- γ -Be	$D(d, n)He^3$	$T(d, n)He^4$	
Energy, Mev	0.13	0.5	2.5	5.0
Slowing-down length $\sqrt{\theta}$, cm	13.5	15.0	18.5	20.0

Figure 3 gives the theoretical curves of the ratios of the thermal-neutron densities for neutrons with a slowing-down length $\sqrt{\theta} = 21.7$ cm and neutrons with values of $\sqrt{\theta}$ equal to 13.5, 15.0, 18.5 and 20.0 cm.

The Table gives the slowing-down lengths of fast neutrons in graphite calculated from the age theory* [7].

In Figures 2 and 3 experimental results, normalized to the theoretical values at the point $r = 70$ cm, are also given. These results for neutrons from the Ra- γ -Be source and the reaction $D(d, n)He^3$ ($E_n = 2.5$ Mev) are in sufficiently good agreement with the theoretical curves. A small discrepancy for the Ra- γ -Be source can be explained by the presence of neutrons with an energy of ~ 0.5 Mev. The experimental data for neutrons with an energy of 14 Mev are in good agreement with the theoretical curve for $\sqrt{\theta} = 21.7$ cm. The decrease of the slowing-down length by comparison with the value given in the Table is explained by the inelastic scattering of neutrons on carbon (reactions (n, n') and $(n, 3\alpha n)$ [8-9]) which were not taken into account in the calculation of $\sqrt{\theta}$. From these data it follows that the "constant"-sensitivity distance of the detector can be taken to be equal to 70 cm (Fig. 4, solid curve).

However, in the region of high energies the sensitivity of such a detector is lower than that calculated, which is due to the absorption of fast neutrons by carbon as the result of the reaction (n, α) . To calculate the absorption of neutrons through the reaction $C^{12}(n, \alpha)Be^9$ ($Q = -5.75$ Mev, threshold ~ 8.2 Mev) it is necessary to know the energy dependence of the cross section from the reaction threshold to 14 Mev. Up to the present, this reaction has been little investigated [10, 11].

* The authors are grateful to E. P. Kunegin and Iu. N. Zankov for the calculations.

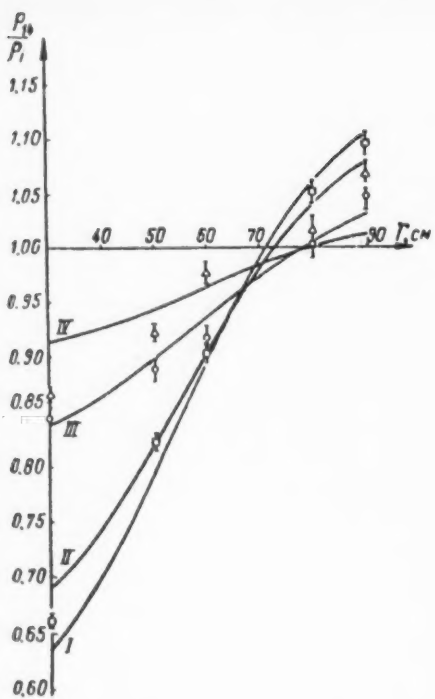


Fig. 3. The ratio of thermal-neutron density as a function of the distance from the source in the graphite prism. Theoretical curves of the ratios of thermal-neutron densities for fast neutrons with the following ratios of the slowing-down lengths: I) $\frac{21.7}{13.5}$; II) $\frac{21.7}{15.0}$; III) $\frac{21.7}{18.5}$; IV) $\frac{21.7}{20.0}$. Experimental values, normalized to the theoretical at the point $r = 70$;
 □) $\frac{14 \text{ Mev}}{\text{Ra}-\gamma\text{-Be}}$; ○) $\frac{14 \text{ Mev}}{2.5 \text{ Mev}}$; Δ) $\frac{14 \text{ Mev}}{\text{Ra}-\alpha\text{-Be}}$.

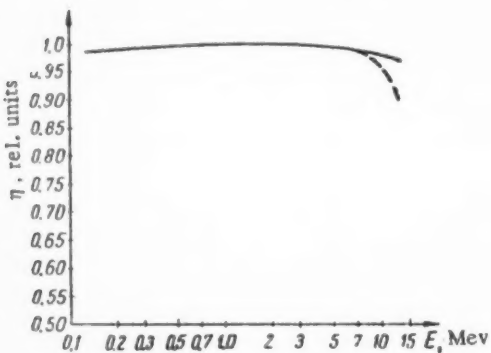


Fig. 4. Detector sensitivity as a function of the neutron energy. Solid curve) without taking into account the absorption of fast neutrons in carbon, dashed curve) taking absorption into account.

In the present work the measurement of total effect of absorption of 14-Mev neutrons by carbon during the slowing-down process was carried out.

Let x denote the fraction of 14-Mev neutrons absorbed by carbon during the slowing-down process. Then the counting rate of the detector will be equal to

$$N_0 = k J_0 (1 - x), \quad (2)$$

where J_0 is the intensity of the 14-Mev neutron source; k is the sensitivity of the detector to these neutrons. If a certain fraction of the 14-Mev neutrons are slowed down to an energy below the reaction threshold E_n before they interact with the graphite then the thermal-neutron density at the "constant"-sensitivity distance and the counting rate must correspondingly increase: $N_1 = N_0 (1 + \gamma_0)$. The most suitable moderator in this case is hydrogen.

If a fraction β of the 14-Mev neutrons is singly scattered by hydrogen nuclei, then the detector counting rate is

$$N_1 = k J_0 \left\{ (1 - \beta) (1 - x) + \beta \left[\frac{E_n}{E_0} \frac{1}{k_1} + \frac{E_0 - E_n}{E_0} (1 - \delta x) \right] \right\}, \quad (3)$$

where $k_1 = 0.98 \pm 0.01$ is the ratio of the sensitivity of the detector to neutrons of energy E_0 and to neutrons of energy less than E_n (Fig. 3); δ is the mean coefficient taking into account the decrease in the absorption by graphite of neutrons with the energy from E_n to E_0 by comparison with neutrons of energy E_0 . Then

$$\frac{N_1}{N_0} = 1 + \gamma_0 = \frac{(1 - \beta) (1 - x) + \beta \left[\frac{E_n}{E_0} \frac{1}{k_1} + \frac{E_0 - E_n}{E_0} (1 - \delta x) \right]}{1 - x}. \quad (4)$$

The introduction of hydrogen into the graphite-prism cavity, in addition to lowering the absorption of 14-Mev neutrons by graphite, leads to the absorption of slow neutrons and to a change of the conditions for the slowing down of

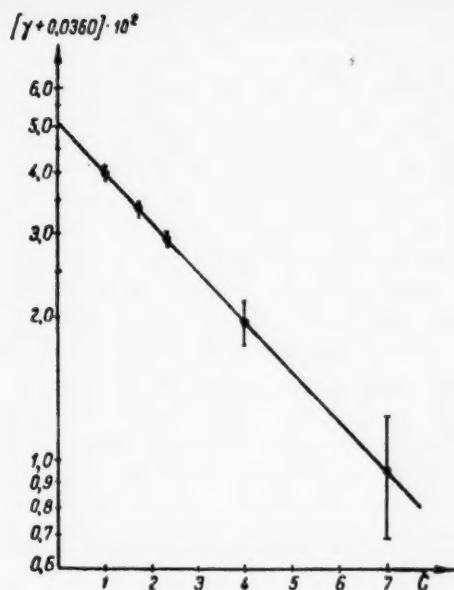


Fig. 5. Graph of the function $\ln(y + \text{const}) = f(C)$ for samples 9.5 cm in diameter.

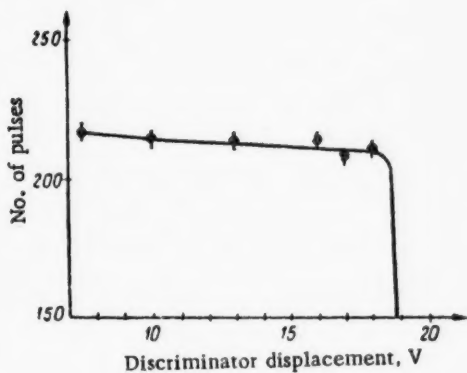


Fig. 6. The counting characteristic of the proportional α -counter.

ment of the absolute intensity of a neutron source having a wide energy spectrum or for the comparison of neutron sources having different spectral compositions. Further, the presence of a cavity in the prism enables measurements to be made with samples of various substances, i. e., to study the process of inelastic interaction.* The main advantage of such a detector is the very low background.

* This detector was used for the study of the inelastic interaction of fast neutrons with matter (unpublished results, 1954). The results of measurements on the cross section of the $(n, 2n)$ reaction are being prepared for publication.

neutrons in the prism, i. e., to a change of the effective size of the cavity. Therefore, when the quantity x is measured all three effects must be taken into account.

The moderator used was paraffin from which spherical samples were prepared 9.5 and 6.8 cm in diameter. To take into account the absorption of slow neutrons by hydrogen, samples were also made of paraffin with an admixture of amorphous boron. The values of the quantity γ , obtained from samples having different absorption, can be well approximated by the equation

$$\gamma = \gamma_0 - a(1 - e^{cb}), \quad (5)$$

where $c = \frac{n_H \sigma_H + n_B \sigma_B}{n_H \sigma_H}$; n_H and n_B are the number of nuclei in 1 cm^3 ; σ_H and σ_B are the thermal-neutron absorption cross sections for hydrogen and boron respectively.

In Figure 5 are shown the results of measurement on samples 9.5 cm in diameter. The values of γ_0 were obtained by an extrapolation of the experimental values of γ to the case of no absorption ($c = 0$). From Equation (4), taking into account secondary scattering, the following values of the quantity x were obtained:

$$x_1 = (7.0 \pm 1.0) \cdot 10^{-2} \text{ for samples 9.5 cm in diameter;}$$

$$x_2 = (8.8 \pm 2.5) \cdot 10^{-2} \text{ for samples 6.8 cm in diameter.}$$

To take into account the different conditions for the slowing down of neutrons in the prism these values were extrapolated to samples of zero dimensions. Finally, the fraction of 14-Mev neutrons absorbed during the slowing-down process is $x = (10.6 \pm 2.8) \cdot 10^{-2}$.

If the coefficient k_1 is taken into account then the relative sensitivity of the detector to 14-Mev neutrons by comparison to neutrons with energy from 0.1 to 0.8 Mev will be equal to $\eta = 0.874 \pm 0.030$.

In this way the graphite prism, in which the density of thermal neutrons is measured at a certain distance from a fast-neutron source, can be used for the measurement of the absolute intensity of a neutron source having a wide energy spectrum or for the comparison of neutron sources having different spectral compositions.

Comparison of Source Intensities

A proportional α -particle counter, filled with methane to a pressure of 200 mm Hg, 7 mm in diameter with a nichrome wire 0.05 mm in diameter and 20 mm long, was used for the measurement of the absolute flux of 14-Mev neutrons. A window, (0.693 ± 0.002) mm in diameter, was made in the side wall of the counter. The counter was placed at a distance of (412.7 ± 0.5) mm from the center of a zirconium-tritium target, at an angle of 90° to the deuteron beam. The target was arranged at an angle of 45° to the deuteron beam. The solid angle subtended by the α counter was $\Omega = (2.22 \pm 0.02) \times 10^{-6}$ ster. In the path of the α particles, from the target to the counter window, 5 diaphragms were placed to limit the scattering of the α particles from the walls of the vacuum system. It was found that the scattering of α particles from the diaphragms was negligibly small. Figure 6 gives the relation between the number of pulses, registered by the α counter, and the discrimination threshold after subtraction of the background due to the recoil protons in methane. The background was determined with the window closed and was equal to $(0.5 \pm 0.2)\%$ at a discriminator working voltage of 15 v.

The comparison of the neutron fluxes from the target and the source investigated, placed at the center of the cavity in the graphite prism, was made from the ratio of the thermal-neutron densities at the "constant-sensitivity distance, $r = 70$ cm. The thermal-neutron densities were measured with a proportional BF_3 counter, 20 mm in diameter and 60 mm long. The counter background was taken into account and was less than 0.3% of the total counting rate.

For the determination of the absolute intensity of the Ra- α -Be source H-28, four series of measurements were made, in each of which there were a large number of determinations of N_s , the counting rate of the detector of neutrons from the Ra- α -Be source, and of the ratios of the counting rates N_α , of the α -particle counter, and N_r , of the neutron detector.

The mean value of the product of these quantities $\frac{N_\alpha}{N_r} N_s$ is equal to $(9.50 \pm 0.06) \times 10^{-2}$. Substituting this value into Equation (1) and taking into account the coefficient η , we obtain for the source intensity

$$J_s = (4.71 \pm 0.17) \times 10^5 \text{ neutrons/sec.}$$

It is necessary to introduce experimental corrections into this result:

- 1) for the background of neutrons with an energy of 2.5 Mev from the deuterium reaction $D(d, n) \text{He}^3$ in the zirconium-tritium target - $(0.3 \pm 0.2)\%$;
- 2) for the multiplication of neutrons in the target supports as the result of the reaction $(n, 2n) - (0.7 \pm 0.3)\%$;
- 3) for the background due to the recoil protons in the α counter - $(0.5 \pm 0.2)\%$;
- 4) for the α -particle anisotropy - $(0.9 \pm 0.3)\%$.

After correction, the intensity of the Ra- α -Be source H-28 was found to be

$$J_{\text{H-28}} = (4.78 \pm 0.18) \cdot 10^5 \text{ neutrons/sec.}$$

Simultaneously with the determination of the absolute intensity of the Ra- α -Be source H-28, a comparison was made between the intensities of this source and that of the Ra- γ -Be source H-29, as the result of which the following ratio of intensities was obtained:

$$\frac{J_{\text{H-28}}}{J_{\text{H-29}}} = 1.28 \pm 0.01.$$

It follows that the intensity of the Ra- γ -Be source H-29 is

$$\frac{J_{H-23}}{J_{H-29}} = 1,018 \pm 0,010.$$

A comparison of the intensities of the sources H-28 and H-23 is of interest, since in reference [2] the results of the comparison of a number of sources with source H-23 are given.

This comparison was made by G. A. Dorofeev,* who obtained

$$J_{H-23} = (4,86 \pm 0,19) \cdot 10^5 \text{ neutrons/sec.}$$

By using this relation and the values of J_{H-28} derived above, we find that the intensity of the Ra- α -Be source H-23 is $J_{H-23} = (4,86 \pm 0,19) \cdot 10^5$ neutrons/sec. Our results are in good agreement with those of Reference [12]** and of a comparison of USSR and Swedish sources [13].

It must be pointed out that the results of the measurement of the intensity of neutron sources in the USSR, reported by Bezotosny and Zamiatnin [2], and also the results of the present work and those of references [12, 13] are grouped about two values which differ by approximately 10%, which is outside the limits of experimental error.

In conclusion, it must be pointed out that the proposed method for the measurement of the intensity of neutron sources is comparatively simple and enables a high accuracy to be attained. The main source of error with this method lies in the determination of the absorption of 14-Mev neutrons by carbon during the slowing-down process. The error can be considerably reduced by a further study of the reaction $C^{12}(n, \alpha)Be^9$. Because graphite is used as the moderator the correction for the absorption of fast neutrons from the Ra- α -Be source during the slowing-down process need not be introduced, while if water is used as the moderator it is necessary to take into account the absorption of fast neutrons by oxygen.

We consider it a pleasant duty to express our gratitude to G. N. Flerov for valuable advice and a constant interest in the work, to D. V. Timoshuk for discussion of the results and to S. N. Solov'ev for constant help during the experiments.

LITERATURE CITED

- [1] D. J. Hughes, Nucleonics 12, No. 12, 26 (1954).
- [2] V. M. Bezotosnyi and Iu. S. Zamiatnin, J. Atomic Energy (USSR) 2, 313 (1957).***
- [3] K. A. Petrzhak, M. A. Bak, and B. A. Fersman, J. Atomic Energy (USSR) 2, 319 (1957).***
- [4] G. N. Flerov and L. B. Poretskii, unpublished results quoted in reference [2].
- [5] K. Larson, Ark. f. Fys. 9, 318 (1955).
- [6] P. R. Wallace, Nucleonic 4, No. 3, 48 (1949).
- [7] R. E. Marshak, Rev. Mod. Phys. 19, 185 (1947).
- [8] L. L. Green, and W. M. Gibson, Proc. Phys. Soc. 62A, 296 (1949).
- [9] G. M. Frye, L. Rosen and L. Stewart, Phys. Rev. 99, 1375 (1955).
- [10] J. E. Draper, Rev. Sci. Instr. 25, 558 (1954).
- [11] E. R. Graves and R. W. Davis, Phys. Rev. 97, 1205 (1955).
- [12] B. G. Erozolimskii and P. E. Sptvak, J. Atomic Energy (USSR) 2, 327 (1957).***
- [13] G. A. Dorofeev, I. E. Kutikov and A. M. Kucher, J. Atomic Energy (USSR) 3, 328 (1957).***

*Private communication.

**A standardization of the Ra- γ -Be source H-29 was made in reference [12].

***Original Russian pagination. See C. B. Translation.

Received May 30, 1957

INVESTIGATIONS OF THE PERFORMANCE OF GAS-DISCHARGE COUNTERS WITH A CONTROLLED PULSED POWER SUPPLY

V. V. Vishnyakov and A. A. Tyapkin

With a pulsed power supply for gas-discharge counters, counting errors, determined by the dead time, are eliminated. Because of this, the possibility arises of using hodoscope systems of counters with a controlled pulsed power supply in experiments carried out with accelerators having a large background of extraneous radiation. In the present work the counting characteristics were investigated, and also measurements were carried out of the efficiency and the resolving power of self-quenching factory-produced counters with a controlled pulsed power supply. It is found that in the case of short-duration pulses (pulse length $\sim 10^{-6}$ sec) the counters can work under over-voltages of up to 2 kv. At the same time there is no necessity to amplify the pulses in the hodoscope channel or to use a discriminator to obtain their coincidences with the control pulse. Each channel, in this case, in addition to the counter contains a load resistance and a neon lamp. The considerable simplification of the system, by comparison with the usual type of hodoscope, and also the reliable performance of counters with pulsed power supplies, make such systems also useful for the study of cosmic radiation.

In using gas-discharge counters in hodoscope systems there is a possibility of eliminating counting errors, determined by the dead time, by employing a controlled pulsed high-tension power supply for the counters. In this case the high tension is applied to the counters only after they have been traversed by the ionizing particles which operated the control system of the hodoscope. It is possible to register these particles because the primary ionization electrons are delayed in reaching the counter wire.

To realize a hodoscope system with pulse-fed counters in practice, it is important to determine experimentally the possible values of the efficiency and the resolving time, and also to obtain the counting characteristics of the various factory-produced counters with pulsed power supplies.

In the present work the properties of argon-methylal counters MS-6, MS-7 and MS-9, as well as the halogen counters STS-8, were studied from this point of view.

Experimental Arrangement

Cosmic-ray particles, which traversed the counters whose performance with a pulsed power supply was being investigated, were registered by a telescope consisting of three groups of counters. The output pulse from the telescope coincidence circuit was used to control the pulsed power supply whose circuit is shown in Figure 1. The pulse from the coincidence circuit, after a preliminary amplification, triggered the blocking generator, the circuit of tube 6AG7. The pulse from the blocking generator was amplified by the GI-30 tube and applied to the cathode of the controlled counter to which, in addition, a constant voltage V_0 was applied. The rise time of the output pulse was about 0.1 μ sec. The performance of the pulse-fed counters was studied for two values of the supply-pulse duration: 0.8 and 0.3 μ sec. The delay of the supply pulse relative to the passage of the cosmic-ray particle through the counter was $\sim 0.7 \mu$ sec. The circuit also allowed the possibility of

introducing an additional delay of the control pulse from the triple-coincidence circuit. The pulse which appeared on the counter wire due to the discharge of the counter was registered by an electromechanical counter SB1M. Because of the capacity of the counter, the supply pulse produced a potential on the counter wire for whose compensation a pulse of reverse polarity was applied from the blocking generator.

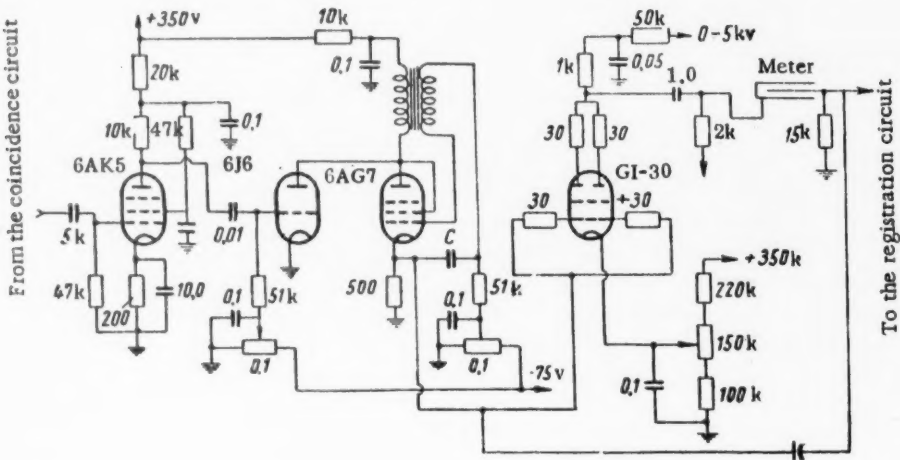


Fig. 1. Diagram of the high-voltage pulse generator.

The Performance of Pulse-Fed Counters with Small Values of the Constant Applied Potential

The main discharge characteristics in pulse-fed counters. The amplitude characteristics, i. e., the dependence of the size of the potential pulse on the counter wire on the amplitude of the supply pulse for different pulse lengths and for different values of the constant potential V_0 , are shown in Figure 2 for counters MS-6 and MS-9. The main feature of the characteristics given is the rapid rise of the pulse size beginning at a certain amplitude of the supply pulse. As can be seen from the curves, the amplitude of the supply pulse, at which the rapid increase of the discharge takes place, depends on the constant potential applied to the counter and on the duration of the high-voltage supply pulse. For counters of different diameters (MS-6, MS-7 and MS-9) * but with the same filling, the amplitude characteristics are similar.

The discharge occurring in the pulse-fed counter has the streamer character. During the discharge the internal resistance of the counter, which is several thousand ohms, falls rapidly. With the application to the counter of a supply pulse of shorter duration, the breakdown in the counter occurs for a big amplitude of the supply pulse. With decreasing pulse duration, from 0.8 to 0.3 μ sec, its amplitude has to be increased by 200-300 v. Consequently, the counter breakdown does not occur immediately after the counter potential reaches its maximum value but only after a few tenths of a microsecond. The oscillogram of the pulse, observed on the counter wire, confirms this deduction (Fig. 3).

*These counters have a copper cathode with diameters 2, 1.2 and 3 cm, respectively. The diameter of the wire is 0.1 cm. The pressure of the argon-methylal mixture is 80-100 mm Hg. The threshold of the Geiger region is about 800 v.

By increasing the amplitude of the supply pulse it is possible to obtain pulses of up to 1500 v from the counter without interfering with its normal performance. With a small load resistance ($R < 1 \text{ k}\Omega$) the counter breakdown is accompanied by visible radiation and the characteristic crackling sound.

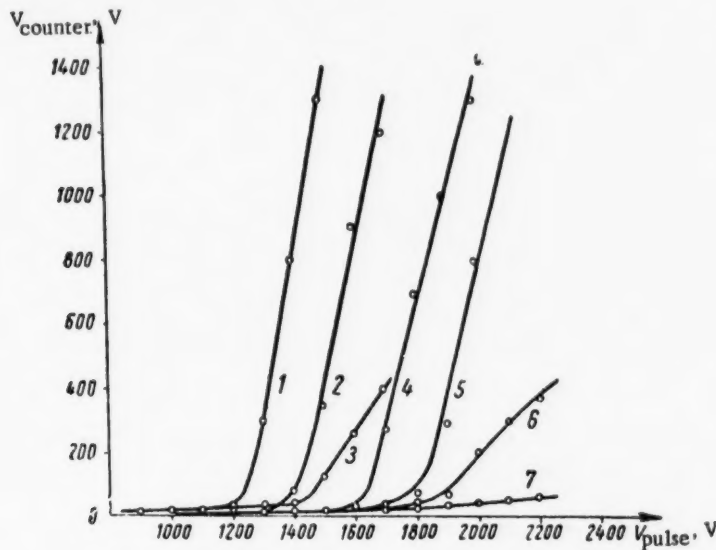


Fig. 2. Amplitude characteristics of the MS-9 and MS-6 counters.
 MS-9: 1) $V = -350 \text{ v}$, $T_p = 0.8 \mu\text{sec}$; 3) $V = -350 \text{ v}$, $T_p = 0.3 \mu\text{sec}$; 4) $V_0 = -75 \text{ v}$, $T_p = 0.8 \mu\text{sec}$; 5) $V_0 = 65 \text{ v}$, $T_p = 0.3 \mu\text{sec}$; 6) $V_0 = -75 \text{ v}$, $T_p = 0.3 \mu\text{sec}$; 7) $V_0 = 65 \text{ v}$, $T_p = 0.3 \mu\text{sec}$.
 MS-6: 2) $V_0 = -75 \text{ v}$, $T_p = 0.8 \mu\text{sec}$.

The efficiency and resolving time of pulse-fed counters. To determine the counter efficiency, the ratio of the number of particles registered by the counters investigated to the number of triple coincidences was measured. These measurements were made both with pulsed and with normal power supplies for the counters being investigated. The efficiency of pulse-fed counters was determined from the ratio of the result of these measurements, during which the efficiency of the counters with normal power supplies was taken equal to 100%.

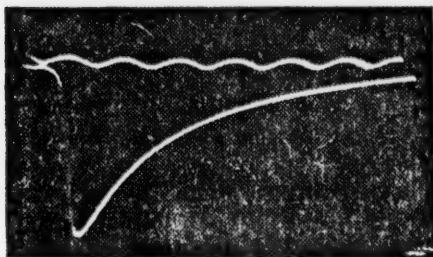


Fig. 3. Oscillogram of the pulse on the counter wire.

The counting characteristics of the counters MS-6 and MS-9, being the dependence of the counter efficiency on the amplitude of the supply pulse, are given in Fig. 4. The characteristics show that the counters have a constant counting rate (plateau) for a wide range of the supply pulse amplitude. When the constant potential $V_0 \sim 0$, the efficiency of a pulse-fed counter is near that of a counter with the usual supply, i. e., it is near 100%. When $V_0 = -20 \text{ v}$, there is a plateau in the counting characteristic of counter MS-6; however, the counter efficiency is less than 100%. Curves 3 and 4 of Figure 4 show the dependence of the counting characteristic on the duration of the supply pulse.

The region which is most suitable for operation begins at a sufficiently high amplitude of the supply pulse when breakdown occurs in the counter. At even

higher amplitudes of the supply pulse, spontaneous breakdown, not connected with the presence of ionization in the counter, occurs. The value of the supply-pulse amplitude at which spontaneous breakdown begins to occur depends on the magnitude of the constant potential, and for counter MS-6 (Fig. 4) it is higher than 2000 v. The width of the working region of supply-pulse amplitude is 500-600 v.

The possibility of registering particles with a counter controlled by a pulsed power supply is explained by the presence of a delay of the electrons produced in the counter gas by the passage of a charged particle. Increasing the efficiency for registering particles by choosing a sufficiently low constant potential leads to an impairment of resolving power of the hodoscope system. In this connection it is necessary to determine the conditions in which a high counting efficiency can be combined with a sufficiently small resolving time. With this aim, the dependence of the efficiency on the constant potential V_0 , which removes electrons, was investigated for various delays of the control pulse. The average maximum value of the electron-delay time T_0 for small values of the electric field potential is connected with V_0 , the magnitude of the constant potential on the counter, by the relation $T_0 = \frac{k}{V_0}$, where k is a coefficient which depends on the cathode diameter, the gas pressure and the electron mobility.

Figure 5 gives the efficiency of counter MS-9 as a function of the constant potential. The experimental data are in good agreement with the results of calculations carried out by A. A. Tyapkin.* The results of the calculation are given by the solid curves. In constructing these curves the value of k in the expression $T_0 = \frac{k}{V_0}$ was obtained from the experimental data given in the same figure. For counter MS-9, the coefficient k was found to be equal to $1.0 \cdot 10^{-4}$ v \cdot sec.

In calculating the efficiency of a counter working with a pulsed power supply, counting errors were taken into account which were determined by the premature removal of the electrons, both by the constant electric field, as well as by the growing field produced in the counter by the application of a high-voltage pulse. During the time the counter potential rises to the threshold value V_t at which the discharge develops in the counter, the electric field removes the primary-ionization electrons to the counter wire. If the counting errors, determined by the delay in the commencement of the supply pulse, can be decreased by a choice of a sufficiently small value of the constant potential V_0 , then the counting errors determined by the growing field can only be decreased at the expense of decreasing the pulse rise time.

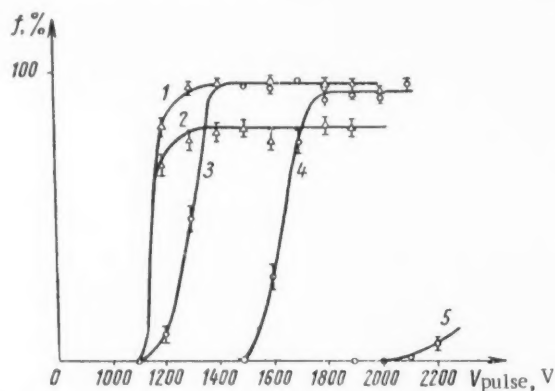


Fig. 4. Counting characteristics (dependence of the counting efficiency on the supply-pulse amplitude) and the relative number of spurious discharges (Curve 5). MS-6:
 1) $V_0 = 0$, $T_p = 0.8 \mu\text{sec}$; 2) $V_0 = -20$ v, $T_p = 0.8 \mu\text{sec}$;
 MS-9: 3) $V_0 = -10$ v, $T_p = 0.8 \mu\text{sec}$; 4) $V_0 = -10$ v,
 $T_p = 0.3 \mu\text{sec}$; MS-6: 5) $V_0 = -75$ v, $T_p = 0.8 \mu\text{sec}$.

* See *Pribory i tekhnika experimenta*, No. 3, 51 (1956).

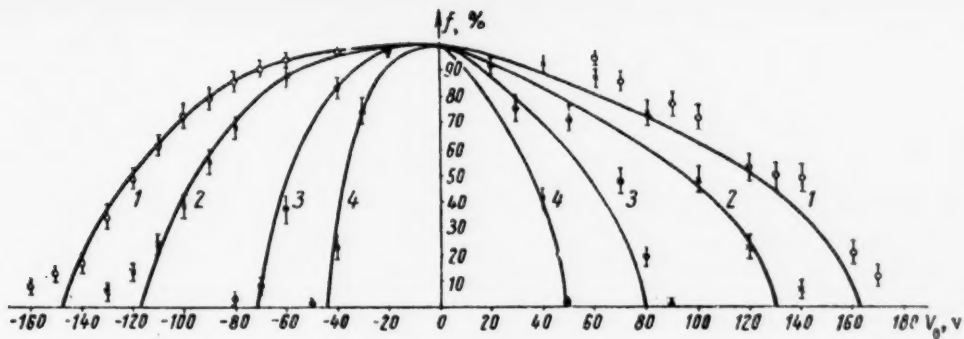


Fig. 5. The dependence of the efficiency on the constant potential for counter MS-9. 1) $T_d = 0.6 \mu\text{sec}$; 2) $T_d = 0.8 \mu\text{sec}$; 3) $T_d = 1.3 \mu\text{sec}$; 4) $T_d = 2.1 \mu\text{sec}$; $V_{\text{pulse}} = 1800 \text{ v}$, $T_p = 0.8 \mu\text{sec}$.

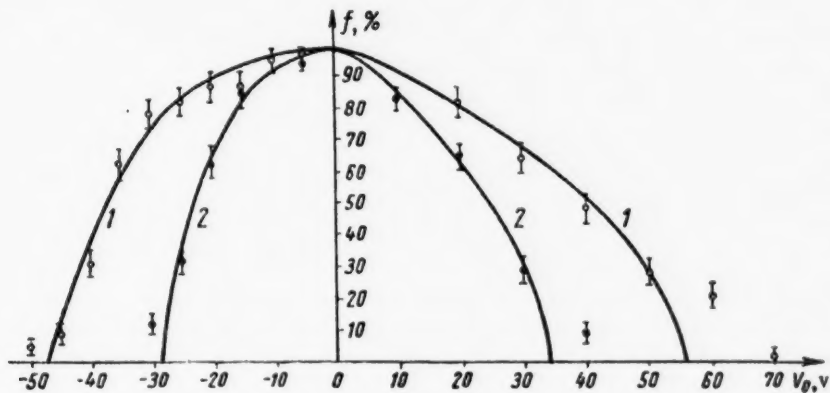


Fig. 6. The dependence of the efficiency on the constant potential for counter MS-6. 1) $T_d = 0.8 \mu\text{sec}$; 2) $T_d = 1.3 \mu\text{sec}$.

If, during the calculation of the radius of the noneffective zone, the drift velocity of the electrons is taken to be proportional to the square root of the electric field strength then the counter efficiency (cathode diameter 0.7 cm), with τ_r (the time of rise of the potential to V_t) equal to 10^{-7} sec, will be close to zero. In agreement with these calculations, for counter MS-7 (cathode diameter 1.2 cm) with $\tau_r \sim 10^{-7}$ sec the maximum efficiency observed at $V_0 = 0$ is considerably less than one (0.65).

The relation for the magnitude of the counting error, given by A. A. Tyapkin, can be applied for the determination of the counting errors because of the premature removal of electrons to the counter wire by the constant negative potential applied to the counter cathode. In the case when a positive constant potential is applied to the cathode the electrons, during the delay time of the control pulse, are removed to the cathode and, consequently, the noneffective zone is situated near the cathode. The efficiency of a pulse-fed counter with a positive potential applied to the cathode is given by the relation

$$f \approx \sqrt{1 - \frac{T_d}{T_0} \left(1 - e^{-\frac{\pi}{4} \frac{R_0}{x_0} \sqrt{1 - \frac{T_d}{T_0}}} \right)},$$

where R_0 is the radius of the counter cathode, $1/x_0$ is the mean number of electrons produced per unit path length in the counter. This expression is obtained without taking into account the supply-pulse rise time. With a positive constant potential on the counter the removal of electrons to the wire only begins when

$$\tau_r \geq \frac{2T_d}{\frac{V_t}{V_0} - \frac{V_0}{V_t}}.$$

In this case the removal of the electrons will be the same as that by a constant negative potential in a certain effective time

$$T_{\text{eff}} = \left(\frac{V_t}{V_0} - \frac{V_0}{V_t} \right) \frac{\tau_r}{2} - T_d$$

From Figure 5 it can be seen that for counter MS-9, for the region of positive constant potential the agreement between the experimentally-determined efficiencies and those calculated is somewhat less than the agreement for the region of negative potential. The dependence of the efficiency on the magnitude of the constant potential is of the same form for counter MS-6 (Fig. 6) as for counter MS-9. Because the counter diameter is less, efficiencies close to zero are observed for lower potentials applied to the counter. The coefficient k for MS-6 counters is equal to $0.46 \cdot 10^{-4} \text{ v} \cdot \text{sec}$. The measured values of the efficiency of counter MS-6 are in good agreement with the calculated ones, both for negative, as well as positive potentials applied to the counter.

From the curves shown in Figure 5 the time characteristics of the counters can be obtained, i. e., the dependence of the efficiency on the control-pulse delay time for a constant T_0 (Fig. 7). A comparison of the experimentally determined dependence of the counter efficiency on the magnitude of the additional delay of the control pulse with the results of the corresponding calculation shows that the minimum delay time in the control system is approximately $0.6 \mu\text{sec}$.

The curves shown in Figure 7 enable the resolving time of pulse-fed counters to be determined. The resolving time is the sum of the effective delay time, equal to $\sim 0.7 T_0$, and a certain fraction (α) of the supply-pulse length: $T_{\text{res}} \approx 0.7 T_0 + \alpha T_p$. Therefore, to decrease the resolving time T_0 must be decreased, i. e., a higher constant potential must be applied to the counter and this, for a given value of the control-pulse delay time, leads to a decrease of the efficiency. However, as can be seen from Figure 7, the efficiency is initially little dependent on the delay time and by increasing the delay time to $T_0/2$ the efficiency is reduced by only 10%. For a further increase of the delay time a rapid decrease of the counter efficiency is observed. This feature of the dependence of the efficiency on the supply-pulse delay time enables the registration of particles with the help of supply-controlled counters having an efficiency $\sim 90\%$ with a resolving time of about $2 \mu\text{sec}$.

When the discharge occurs in the counter a large number of ions are produced which are then removed by the weak constant field. Because of this, the next supply pulse can only be applied to the counter after the expiration of the de-ionization time during which the ions will be removed from the counter volume. The de-ionization time, of course, depends on the magnitude of the constant potential applied to the counter. This dependence was investigated experimentally in the case of counter MS-7 (Fig. 8). The measurements were made at one value of the total potential applied to the counter, equal to 1800 v. From Figure 8 it can be seen that as the constant potential V_0 is increased the de-ionization time decreases. At a potential near the threshold of the Geiger region the de-ionization time is of the order of the counter dead time. In the region of small constant potentials, required for the normal operation of pulse-fed counters, the de-ionization time is of the order of a few tenths of a second or longer. The same behaviour of the de-ionization time as a function of the constant potential is also observed for other counters of type MS.

The Registration of Discharges in Counters of a Hodoscope System

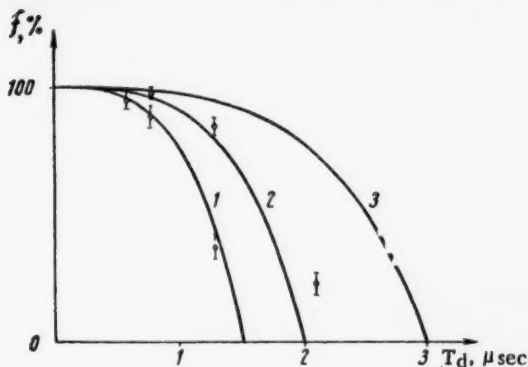


Fig. 7. The dependence of the efficiency on the delay time (time characteristics of counters MS-9). 1) $T_0 = 1.5 \mu\text{sec}$; 2) $T_0 = 2.0 \mu\text{sec}$; 3) $T_0 = 3.0 \mu\text{sec}$. The experimental data were obtained for $V_0 = -60$ and -40 v .

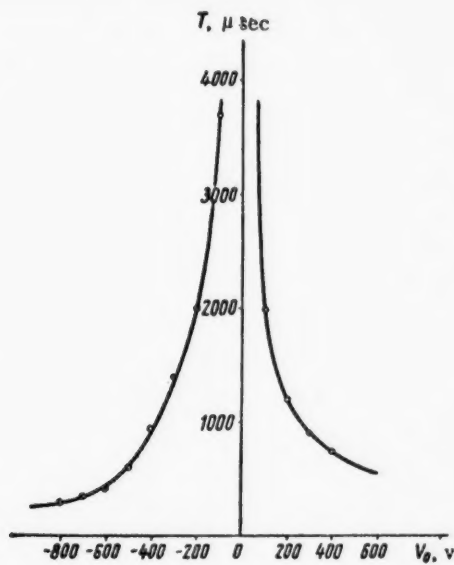


Fig. 8. The dependence of the de-ionization time on the constant potential applied to counter MS-7.

in this case the deionization time becomes $\leq 0.01 \text{ sec}$ and the fast action of the hodoscope system is determined by the time taken to photograph the neon lamp flashes.

Pulsed Power Supplies for Counters When the Constant Potential is Nearly Equal to the Geiger-Region Threshold

All of the above considerations referred to the case when a small constant potential, insufficient for the occurrence of a discharge, was applied to the counter. In this case the discharge could only occur during the short interval when a high-tension pulse was applied to the counter.

The possibility of obtaining large-amplitude pulses from pulse-fed counters enables the counter discharges to be easily registered. In addition, there is no necessity to introduce into the hodoscope channel an additional circuit for coincidence between the control pulse and the pulse from the counter, because the counter discharge can only occur from the passage of an ionizing particle through the counter during the resolving time, determined by the mean time for the removal of primary-ionization electrons and the duration of the supply pulse. For these two reasons, a neon lamp connected directly to the counter wire can be used as an indicator of a discharge in the counter.

The load for the counter was a resistance whose magnitude was $20-30 \text{ k}\Omega$. It was found that the amplitude of the output pulse depended little on the magnitude of the resistance.

The pulses from the counter load can be directly applied to the cathode of a neon lamp; a positive potential is applied to the anode of the lamp. Its magnitude must be greater than the extinction voltage and smaller than the striking voltage. The extinction of the lamp is produced by the removal of the anode potential.

In particular, good results for the registration of the counter discharges were obtained by using cold thyratrons MTKh-90, employing two electrodes. The tube trigger grid was left floating. One-hundred volts was applied to the anode. With the tube connected in this way, the pulse produced by the counter capacity did not ignite the tube and, therefore, there was no necessity to compensate for this pulse. The neon lamp was lit by pulses whose amplitude was greater than $500-700 \text{ v}$.

The neon lamp, in addition to registration, also has another duty. At the ignition of the neon lamp a potential difference of about 60 v occurs across the load resistance, and this leads to a significant decrease of the deionization time. In

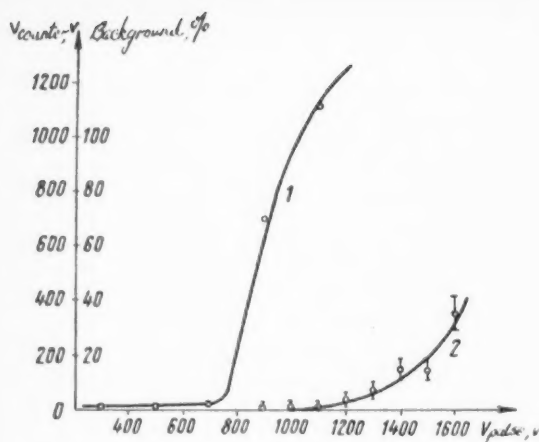


Fig. 9. The amplitude characteristic of counter MS-9 (1) and the relative number of spurious discharges (2).

of 800 v applied to it. The same figure shows the dependence of the number of spurious discharges, occurring in the absence of a source of radiation, on the supply-pulse amplitude. From the figure it can be seen that there exists a region of supply-pulse amplitude sufficiently useful for counter operation.

However, pulse-feeding can be applied in the usual hodoscope system, i. e., in the case when a large constant potential is applied leading to the occurrence of weak discharges when a particle passes through the counter. This will enable a considerable simplification to be made in the registering part of the hodoscope system. Of course, it must be remembered that in this case in self-quenching counters there remains a dead time, therefore such a hodoscope system can only operate under conditions of a small background, for example, in cosmic-ray investigations.* The additional potential pulses, applied to the counter after the passage of the particles, produce in it an intensification of the discharge and finally a breakdown such as that described earlier, i. e., in this case the supply pulse is necessary to increase the amplitude of the output pulses and also to fix the coincidence of the control pulse with the time of passage of the particle through the counter.

Figure 9 shows the amplitude characteristics of counter MS-9, which has a constant potential of 800 v applied to it. The same figure shows the dependence of the number of spurious discharges, occurring in the absence of a source of radiation, on the supply-pulse amplitude. From the figure it can be seen that there exists a region of supply-pulse amplitude sufficiently useful for counter operation.

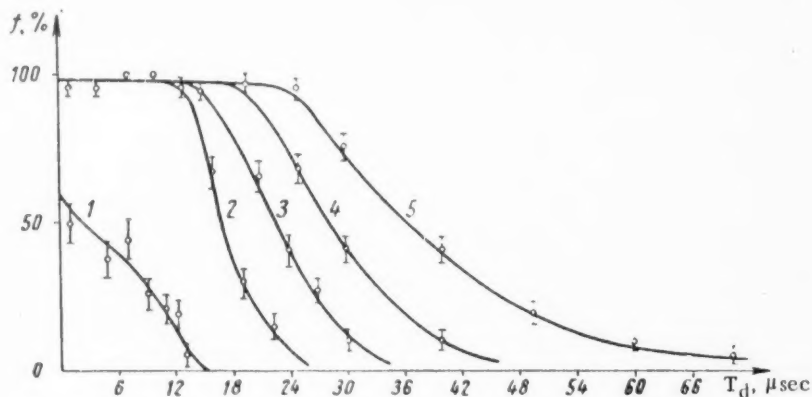


Fig. 10. The time characteristics of counters MS-9 with a high constant potential applied. 1) $V_0 = 660$ v, $V_p = 700$ v; 2) $V_0 = 720$ v, $V_p = 700$ v; 3) $V_0 = 800$ v, $V_p = 700$ v; 4) $V_0 = 800$ v, $V_p = 800$ v; 5) $V_0 = 800$ v, $V_p = 1100$ v.

The time characteristics of self-quenching counters with high constant potentials are different from the characteristics of these counters with small constant potentials. The dependence of the efficiency of counter MS-9 on the supply-pulse-delay time for various values of the constant potential and the supply-pulse amplitude is shown in Figure 10. In a small region of proportional amplification, occurring in these counters for $V_0 \sim 700$ v, a marked increase in efficiency is observed with increasing constant potential applied to the counter. As can be seen from Figure 10, the efficiency not only depends on the value of the constant potential, but also on the supply pulse amplitude.

* Such power supplies can be used for individual counter trays, which are simultaneously part of the control and hodoscope system.

The resolving time of MS-9 counters under these conditions is comparatively large — of the order of 20-30 μ sec, which is the same as the counter dead time, and this does not allow the use of counters operating under these conditions when the background is high.

The nature of the curves shown in Figure 10 enables the following ideas to be presented about the discharge of a pulse-fed counter with a high constant potential. When a particle passes through the counter a discharge occurs which leads to a rapid increase in the number of ions in the counter volume. The supply pulse is applied to the counter a certain time after the passage of the particle. The field near the wire rapidly grows and this can lead to excitation and ionization of the gas molecules by the positive ions, which did not succeed in moving far from the wire because of the small mobility. If even one electron is produced at this stage a discharge will again occur in the counter and this discharge, when the total applied potential is high, leads to a breakdown in the counter.

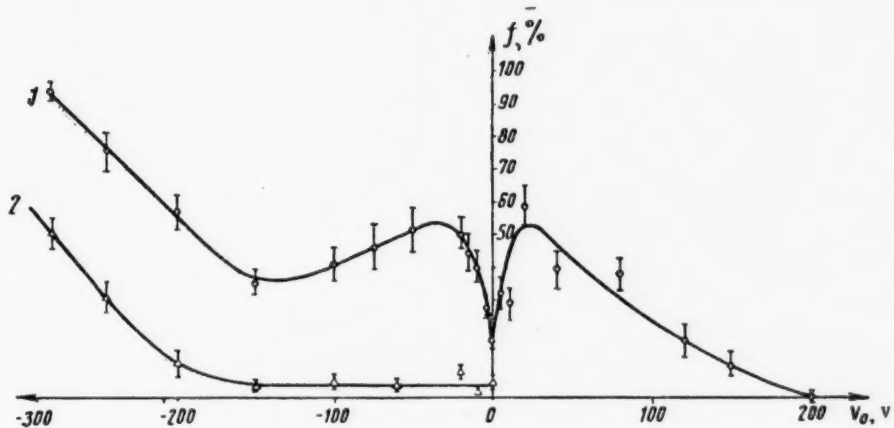


Fig. 11. The dependence of the efficiency on the constant potential for the halogen counters STS-8. 1) $T_p = 0.8 \mu\text{sec}$, $T_d = 0.6 \mu\text{sec}$; 2) $T_p = 0.8 \mu\text{sec}$, $T_d = 1.1 \mu\text{sec}$, $V_p = 1300 \text{ v}$.

From the point of view of this assumption, the dependence of the efficiency on T_d , V_0 and V_p (Fig. 10) becomes understandable. The constant potential V_0 determines the number of positive ions formed as the result of the primary discharge. The bigger the number of positive ions formed and the bigger the field at the wire, which is determined by the total potential $V_0 + V_p$, the higher is the probability for further ionization, and this is observed in practice.

With an increase of the supply-pulse delay time this probability decreases. The counter efficiency drops to zero when the supply-pulse delay is increased to a time in which the positive ions, formed near the wire, are able to leave the region where they can produce only a single electron.

Investigation of the Performance of Halogen Counters With a Pulsed Power Supply

The performance of pulse-fed counters containing an admixture of halogen gases is different from the performance of argon-methylal counters. In STS-8* halogen counters a different pattern is observed for the dependence of the efficiency on the constant potential applied to the counter (Fig. 11). The curves, shown in Figure 11, were obtained for $V_p = 130 \text{ v}$. The comparatively small supply-pulse amplitude is explained by

*The STS-8 counters have a cathode diameter of 1.8 cm, wire diameter of 0.06 cm. The pressure of the mixture $\sim 140 \text{ mm Hg}$ (99.2% neon, 0.4% argon and 0.4% bromine).

the fact that for these counters the amplitude curves, typical of operation with a pulsed power supply, are shifted into the region of smaller amplitudes because of the lower threshold of the Geiger region in the case of halogen counters.

In the case of halogen counters, when the constant potential is reduced to a value close to zero a rapid decrease of the efficiency is observed. In the absence of a constant potential applied to the counter an increase in the amplitude and the duration of the supply pulse does not lead to an increase of the efficiency. An increase of the supply-pulse-delay time from 0.6 to 1.1 μ sec leads to a sharp decrease of the sensitivity. It is possible that the effect observed is determined by the so-called preferential recombination of the ions (neutralization of ions formed from one and the same atom).

With a further increase of the constant potential, the efficiency again falls, this time because of the removal of electrons.

For negative constant potentials higher than 150 v a rise of the efficiency is observed. The difficulty of explaining such a rise of the efficiency is due to the fact that the rise of the efficiency begins at a potential V_0 which is considerably lower than the Geiger-region threshold, when discharges are not observed in the counter. There is no significant increase in the number of ions in the counter and, consequently, the observed rise of the efficiency cannot be explained by the appearance of electrons from the ionization of the gas by the positive ions. The maximum efficiency, close to 100 %, is observed with constant potentials nearly equal to the Geiger-region threshold, which in the given counters of type STS-8 is equal to 320-350 v. For these values of the constant potential, an increase in the delay of the supply pulse lowers the efficiency of the counter but not as markedly as for smaller potentials. From a comparison of the curves obtained at two values of the delay time it is possible to evaluate the resolving time of halogen counters with a pulsed power supply. It reaches $\sim 3 \mu$ sec for T_p and V_0 equal to $\sim 1 \mu$ sec and ~ 300 v, respectively.

The de-ionization time for halogen counters is small, and is equal to ~ 0.01 sec when $V_0 = 0$, i. e., considerably less than the de-ionization time for argon-methylal counters. This is explained by the high probability for the recombination of ions because of the presence of electronegative gases.

SUMMARY

The use of counters with a pulsed high-tension supply enables the construction of counter hodoscopes which have a number of advantages compared to the usual hodoscope systems.

In the operation of counters in a pulsed hodoscope, first of all, counting errors determined by the dead time are eliminated, which enables such hodoscope systems to be used in experiments carried out with accelerators, in conditions when the counters are heavily loaded. *

With pulse-fed counters there is no necessity for the amplification of the pulses and for the use of a circuit in each channel for obtaining coincidences between the counter output pulse and the control pulse. If a large number of counters are used, this leads to a considerable simplification of the whole hodoscope system.

Because of the large extent of the plateau with pulse-fed counters even a big difference in counter characteristics (for example, the spread in the value of the Geiger-region threshold) is found to be unimportant, which facilitates the use of a hodoscope system containing a large number of counters.

With a pulsed power supply, self-quenching counters can work for a considerable length of time. Thus, after 10^6 discharges there were no significant changes observed in counter MS-9. It is clear that a life time of this order is more than sufficient for a counter used in a hodoscope system with a pulsed power supply.

The resolving time of such a hodoscope system can be made to be comparatively small ($\sim 2 \mu$ sec).

Some disadvantages of a hodoscope system with pulse-fed counters can also be pointed out. To obtain a small resolving time ($\sim 2 \mu$ sec) it is necessary to have a lowered efficiency. As was already pointed out, the use of argon-methylal counters with a small diameter ($\lesssim 10$ mm) leads to a considerable decrease of the detection efficiency, which limits the possibility of increasing the accuracy of spatial resolution. This deficiency,

*At the present time in the Joint Institute for Nuclear Studies a pulsed-hodoscope system containing 450 Geiger counters is used for studying the angular distribution of π^- mesons scattered from hydrogen.

of course, can be eliminated by choosing a mixture of gases having a low electron mobility and by decreasing the time of growth of the potential on the counter.

In conclusion, the authors express their gratitude to A. N. Sinaev for help during the work.

Received February 28, 1957

DETERMINATION OF THE COMPOSITION AND INSTABILITY CONSTANTS OF COMPLEX Pu^{+3} OXALATE IONS

A. D. Gel'man, N. N. Matorina and A. I. Moskvin

The solubility of $\text{Pu}_2(\text{C}_2\text{O}_4)_3 \cdot 9\text{H}_2\text{O}$ in aqueous solutions of $\text{K}_2\text{C}_2\text{O}_4$ of various concentrations (0.01-2.4 moles/liter) has been determined at constant ionic strength of the solution at 20°. It was found that Pu^{+3} complexes are formed in these solutions. It was found from the results of $\text{Pu}_2(\text{C}_2\text{O}_4)_3 \cdot 9\text{H}_2\text{O}$ solubility determinations that in the region of $\text{K}_2\text{C}_2\text{O}_4$ concentrations studied the following complex ions are formed $[\text{Pu}(\text{C}_2\text{O}_4)_2]^-$, $[\text{Pu}(\text{C}_2\text{O}_4)_3]^{-3}$ and $[\text{Pu}(\text{C}_2\text{O}_4)_4]^{-5}$, the total instability constants of which are $4.9 \cdot 10^{-10}$; $4.10 \cdot 10^{-10}$ and $11.9 \cdot 10^{-11}$ respectively. The solubility of $\text{Pu}_2(\text{C}_2\text{O}_4)_3 \cdot 9\text{H}_2\text{O}$ in aqueous $(\text{NH}_4)_2\text{C}_2\text{O}_4$ solutions has also been determined in the range of ammonium oxalate concentrations from 0.07 to 0.7 mole/liter at 70°. It is shown that the composition of the complex ions under these conditions corresponds to $[\text{Pu}(\text{C}_2\text{O}_4)_2]^-$, $[\text{Pu}(\text{C}_2\text{O}_4)_3]^{-3}$ and $[\text{Pu}(\text{C}_2\text{O}_4)_4]^{-5}$. The calculated total instability constants of these complex ions are $11.6 \cdot 10^{-9}$; $5.6 \cdot 10^{-9}$ and $2.5 \cdot 10^{-9}$ respectively. The heats of formation of complex Pu^{+3} oxalate ions have been calculated for the reaction $\text{Pu}^{+3} + n\text{C}_2\text{O}_4^{-2} \rightleftharpoons [\text{Pu}(\text{C}_2\text{O}_4)_n]^{3-2n}$. $\Delta\bar{Q}$ for the $[\text{Pu}(\text{C}_2\text{O}_4)_2]^-$ ion is 1300 cal., for $[\text{Pu}(\text{C}_2\text{O}_4)_3]^{-3}$, 1200 cal., and for $[\text{Pu}(\text{C}_2\text{O}_4)_4]^{-5}$, 1300 cal.

Determinations of the composition and instability constants of complex plutonium compounds are of considerable interest as there are at present no data available in the literature, despite the exceptional importance of this question.

Various physicochemical methods are widely used for the study of complex ions in solutions [1-11]. We studied complex Pu^{+3} oxalate ions.

EXPERIMENTAL

The solubility of Pu^{+3} oxalate was determined at constant ionic strength in aqueous $\text{K}_2\text{C}_2\text{O}_4$ solutions of various concentrations at 20°. To maintain constant ionic strength, various amounts of KCl were added to the solutions in the region of potassium oxalate concentrations from 0.01 to 1.5 mole/liter. The precipitate was kept in a thermostat with stirring for 4-6 hours. This time was sufficient for equilibrium to be established between the solution and the Pu^{+3} oxalate precipitate. Nitrogen was passed through the solution to prevent oxidation of Pu^{+3} to Pu^{+4} . Ten to fifteen grams per liter of sodium formaldehyde sulfoxylate, $\text{NaHSO}_3 \cdot \text{CH}_2\text{O} \cdot 2\text{H}_2\text{O}$ was also added to the solution.

The increase in the solubility of plutonium oxalate caused by KCl and the sulfoxylate was determined in special experiments.

The Pu^{+3} content of the solution was determined radiometrically. The results of the solubility determinations are given in Table 1. The variation of the solubility of $\text{Pu}_2(\text{C}_2\text{O}_4)_3 \cdot 9\text{H}_2\text{O}$ with the $\text{K}_2\text{C}_2\text{O}_4$ concentration is shown in Figure 1. The same graph also gives the results of earlier experiments on the determination of the solubility of Pu^{+3} oxalate in aqueous $\text{K}_2\text{C}_2\text{O}_4$ solutions of various concentrations without any added electrolyte, i. e., at different ionic strengths.

The same curves plotted in logarithmic coordinates are shown in Figure 2. The logarithm of the ratio of the total complex ion concentration to the free plutonium ion concentration is taken along the ordinate axis, and the logarithm of the equilibrium concentration of oxalate is taken along the abscissa axis.

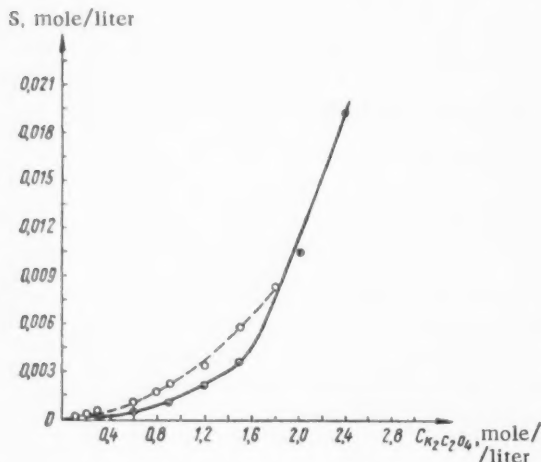


Fig. 1. Variation of the solubility of $\text{Pu}_2(\text{C}_2\text{O}_4)_3 \cdot 9\text{H}_2\text{O}$ with $\text{K}_2\text{C}_2\text{O}_4$ concentration. —) In absence of KCl ; ---) at constant ionic strength.

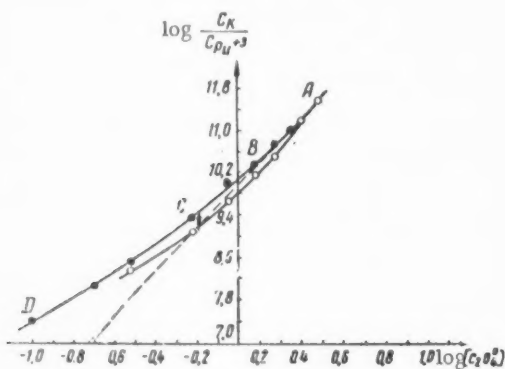


Fig. 2. Effect of $\text{K}_2\text{C}_2\text{O}_4$ concentration on the solubility of $\text{Pu}_2(\text{C}_2\text{O}_4)_3 \cdot 9\text{H}_2\text{O}$. ●) At different ionic strengths; ○) at constant ionic strength.

We found that the solubility of $\text{Pu}_2(\text{C}_2\text{O}_4)_3 \cdot 9\text{H}_2\text{O}$ in distilled water of 20° is $4.32 \cdot 10^{-6}$ mole per liter, which corresponds to a solubility product for the oxalate of Pu^{+3} $1.62 \cdot 10^{-25}$.

It follows from Figures 1 and 2 that in the region of $\text{K}_2\text{C}_2\text{O}_4$ concentrations studied changes in the ionic strength of the solution with increasing concentrations of the $\text{C}_2\text{O}_4^{2-}$ ion do not greatly influence the solubility of Pu^{+3} oxalate. Introduction of cations (K^+ in this instance) which are not involved in complex ion formation cannot affect the composition of the complex ions formed. However, variations of the concentration of K^+ ions and consequent changes in the ionic strength of the solution may affect the instability constant of the complex compound. In view of the fact that the solubility of Pu^{+3} oxalate did not show great differences at constant ionic strength of the solution, we also used data on the solubility of $\text{Pu}_2(\text{C}_2\text{O}_4)_3 \cdot 9\text{H}_2\text{O}$ in aqueous solutions of $(\text{NH}_4)_2\text{C}_2\text{O}_4$ at 70° * for determining the composition and instability constants of complex Pu^{+3} oxalates. The results of these experiments are given in Table 2. The variation of the solubility of $\text{Pu}_2(\text{C}_2\text{O}_4)_3 \cdot 9\text{H}_2\text{O}$ with the concentration of $(\text{NH}_4)_2\text{C}_2\text{O}_4$ at 70°C is plotted in logarithmic coordinates in Figure 3.

DISCUSSION OF RESULTS

It is seen from Figures 1-3 that the solubility of $\text{Pu}_2(\text{C}_2\text{O}_4)_3 \cdot 9\text{H}_2\text{O}$ increases with increasing concentration of $\text{C}_2\text{O}_4^{2-}$ ions; this is undoubtedly the result of Pu^{+3} complex formation. The expression for the solubility of $\text{Pu}_2(\text{C}_2\text{O}_4)_3 \cdot 9\text{H}_2\text{O}$ has the form:

$$S = \frac{L_p}{2 [\text{C}_2\text{O}_4^{2-}]^{3/2}} \left\{ \frac{[\text{C}_2\text{O}_4^{2-}]^{n_1}}{k_{n_1}} + \frac{[\text{C}_2\text{O}_4^{2-}]^{n_2}}{k_{n_2}} + \dots + \frac{[\text{C}_2\text{O}_4^{2-}]^{n_m}}{k_{n_m}} \right\} \quad (1)$$

or

$$\frac{2S}{[\text{Pu}^{+3}]} = k_1 [\text{C}_2\text{O}_4^{2-}]^{n_1} + \dots + k_2 [\text{C}_2\text{O}_4^{2-}]^{n_2} + \dots + k_m [\text{C}_2\text{O}_4^{2-}]^{n_m}, \quad (2)$$

* The solubility at 70° was determined in a stream of nitrogen without addition of reducing agent to the solution.

where L_p is the solubility product of trivalent plutonium oxalate; $[C_2O_4^{2-}]$ is the equilibrium concentration of free oxalate in the solution; $[Pu^{+3}]$ is the equilibrium concentration of free plutonium ions in the solution; n_1 is the number of oxalate groups per plutonium atom.

TABLE 1

Variation of the Solubility of $Pu_2(C_2O_4)_3 \cdot 9H_2O$ with $K_2C_2O_4$ Concentration at 20°C

Conc. of $K_2C_2O_4$ mole/liter	Solubility of $Pu_2(C_2O_4)_3 \cdot 9H_2O$ S, mole/liter	Conc. of free Pu^+ ions calcu. from L_p , mole/liter	Calculated concentration of complex ions, mole/liter			Calc. solubility of $Pu_2(C_2O_4)_3 \cdot 9H_2O$ mole/liter
			$[Pu(C_2O_4)_2]^-$	$[Pu(C_2O_4)_3]^{-3}$	$[Pu(C_2O_4)_4]^{-5}$	
0.010	$3.53 \cdot 10^{-5}$	$4.02 \cdot 10^{-10}$	$8.22 \cdot 10^{-5}$			$4.11 \cdot 10^{-5}$
0.025	$7.54 \cdot 10^{-5}$	$10.2 \cdot 10^{-11}$	$13.06 \cdot 10^{-5}$			$6.53 \cdot 10^{-5}$
0.050	$1.00 \cdot 10^{-4}$	$3.60 \cdot 10^{-11}$	$1.84 \cdot 10^{-4}$			$9.20 \cdot 10^{-5}$
0.075	$1.09 \cdot 10^{-4}$	$1.96 \cdot 10^{-11}$	$2.24 \cdot 10^{-4}$			$1.12 \cdot 10^{-4}$
0.10	$1.55 \cdot 10^{-4}$	$1.27 \cdot 10^{-11}$	$2.61 \cdot 10^{-4}$	$3.4 \cdot 10^{-5}$	$1.07 \cdot 10^{-5}$	$1.52 \cdot 10^{-4}$
0.2	$2.7 \cdot 10^{-4}$	$4.47 \cdot 10^{-12}$	$3.66 \cdot 10^{-4}$	$8.72 \cdot 10^{-5}$	$6.01 \cdot 10^{-5}$	$2.56 \cdot 10^{-4}$
0.3	$4.04 \cdot 10^{-4}$	$2.26 \cdot 10^{-12}$	$4.16 \cdot 10^{-4}$	$1.48 \cdot 10^{-4}$	$1.535 \cdot 10^{-4}$	$3.60 \cdot 10^{-4}$
0.6	$1.01 \cdot 10^{-3}$	$8.6 \cdot 10^{-13}$	$6.34 \cdot 10^{-4}$	$4.53 \cdot 10^{-4}$	$9.4 \cdot 10^{-4}$	$1.02 \cdot 10^{-3}$
0.8	$1.71 \cdot 10^{-3}$	$5.63 \cdot 10^{-13}$	$7.04 \cdot 10^{-4}$	$7.04 \cdot 10^{-4}$	$1.94 \cdot 10^{-3}$	$1.68 \cdot 10^{-3}$
0.9	$2.27 \cdot 10^{-3}$	$4.69 \cdot 10^{-13}$	$7.78 \cdot 10^{-4}$	$7.34 \cdot 10^{-4}$	$2.88 \cdot 10^{-3}$	$2.1 \cdot 10^{-3}$
1.2	$3.46 \cdot 10^{-3}$	$3.03 \cdot 10^{-13}$	$8.94 \cdot 10^{-4}$	$1.27 \cdot 10^{-3}$	$5.28 \cdot 10^{-3}$	$3.72 \cdot 10^{-3}$
1.5	$5.91 \cdot 10^{-3}$	$2.17 \cdot 10^{-13}$	$1.01 \cdot 10^{-3}$	$1.82 \cdot 10^{-3}$	$9.48 \cdot 10^{-3}$	$6.155 \cdot 10^{-3}$
1.81	$8.45 \cdot 10^{-3}$	$1.65 \cdot 10^{-13}$	$1.11 \cdot 10^{-3}$	$2.0 \cdot 10^{-3}$	$1.34 \cdot 10^{-2}$	$8.25 \cdot 10^{-3}$
2.00	$1.06 \cdot 10^{-2}$	$1.41 \cdot 10^{-13}$	$1.45 \cdot 10^{-3}$	$2.75 \cdot 10^{-3}$	$1.91 \cdot 10^{-2}$	$1.145 \cdot 10^{-2}$
2.41	$1.87 \cdot 10^{-2}$	$1.07 \cdot 10^{-13}$	$1.28 \cdot 10^{-3}$	$3.66 \cdot 10^{-3}$	$2.95 \cdot 10^{-2}$	$1.72 \cdot 10^{-2}$

TABLE 2

Variation of the Solubility of $(Pu_2C_2O_4)_3 \cdot 9H_2O$ with $(NH_4)_2C_2O_4$ Concentration at 70°C

Conc. of $(NH_4)_2C_2O_4$ mole/liter	Solubility of $Pu_2(C_2O_4)_3 \cdot 9H_2O$ S, mole/liter	Conc. of free Pu^+ ions calcu. from L_p , mole/liter	Calculated concentration of complex ions, mole/liter			Calc. solubility of $Pu_2(C_2O_4)_3 \cdot 9H_2O$ mole/liter
			$[Pu(C_2O_4)_2]^-$	$[Pu(C_2O_4)_3]^{-3}$	$[Pu(C_2O_4)_4]^{-5}$	
0.07	$2.02 \cdot 10^{-4}$	$8.57 \cdot 10^{-10}$	$3.65 \cdot 10^{-4}$	$5.24 \cdot 10^{-5}$		$2.08 \cdot 10^{-4}$
0.13	$2.90 \cdot 10^{-4}$	$3.38 \cdot 10^{-10}$	$4.96 \cdot 10^{-4}$	$1.33 \cdot 10^{-4}$		$3.14 \cdot 10^{-4}$
0.225	$4.70 \cdot 10^{-4}$	$1.49 \cdot 10^{-10}$	$6.55 \cdot 10^{-4}$	$3.03 \cdot 10^{-4}$		$4.79 \cdot 10^{-4}$
0.28	$5.66 \cdot 10^{-4}$	$1.07 \cdot 10^{-10}$	$7.31 \cdot 10^{-4}$	$4.21 \cdot 10^{-4}$		$5.76 \cdot 10^{-4}$
0.35	$6.90 \cdot 10^{-4}$	$7.65 \cdot 10^{-11}$	$8.11 \cdot 10^{-4}$	$5.86 \cdot 10^{-4}$		$6.98 \cdot 10^{-4}$
0.41	$8.19 \cdot 10^{-4}$	$6.05 \cdot 10^{-11}$	$8.83 \cdot 10^{-4}$	$7.44 \cdot 10^{-4}$		$8.14 \cdot 10^{-4}$
0.49	$9.75 \cdot 10^{-4}$	$4.63 \cdot 10^{-11}$	$9.55 \cdot 10^{-4}$	$9.75 \cdot 10^{-4}$		$9.76 \cdot 10^{-4}$
0.56	$1.14 \cdot 10^{-3}$	$3.79 \cdot 10^{-11}$	$1.03 \cdot 10^{-3}$	$1.19 \cdot 10^{-3}$		$1.11 \cdot 10^{-3}$
0.62	$1.49 \cdot 10^{-3}$	$3.26 \cdot 10^{-11}$	$1.09 \cdot 10^{-3}$	$1.38 \cdot 10^{-3}$	$0.43 \cdot 10^{-3}$	$1.45 \cdot 10^{-3}$
0.66	$2.05 \cdot 10^{-3}$	$2.985 \cdot 10^{-11}$	$3.79 \cdot 10^{-4}$	$1.53 \cdot 10^{-3}$	$2.08 \cdot 10^{-3}$	$2.08 \cdot 10^{-3}$
0.70	$2.25 \cdot 10^{-3}$	$2.71 \cdot 10^{-11}$	$2.12 \cdot 10^{-3}$	$1.66 \cdot 10^{-3}$	$2.63 \cdot 10^{-3}$	$2.25 \cdot 10^{-3}$

* L_p for $Pu_2(C_2O_4)_3 \cdot 9H_2O$, calculated from data on the solubility of Pu^{+3} oxalate in water at 70°C is $2.52 \cdot 10^{-22}$.

The total instability constants (k_1, k_2, \dots, k_{11}) can be found by the method of least squares [8], if the following are known: the compositions of these compounds, the variation of the solubility of $(Pu_2C_2O_4)_3 \cdot 9H_2O$ with concentration of the $C_2O_4^{2-}$ ion, and the solubility product of $Pu_2(C_2O_4)_3 \cdot 9H_2O$.

The nature of the relationship between the logarithm of the ratio of the total complex ion concentration to the free plutonium ion concentration, and the logarithm of the equilibrium oxalate concentration (see Fig. 2) shows that a mixture of several complex compounds is formed under these conditions. The points in the region AB lie almost on a straight line which slopes at an angle whose tangent is 4. In view of the stepwise character of processes of complex formation, and of the change in the region CD of the curve, it is natural to suppose that in these conditions complex ions with a smaller number of oxalate groups are formed, i. e., complex ions with coordination number 6 (three oxalate groups) and 4 (two oxalate groups). The concentration of these complex ions should rise with decrease of the addend concentration.

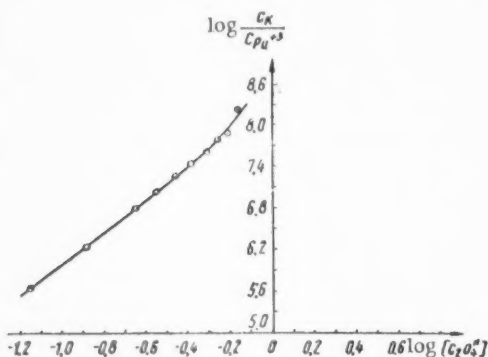


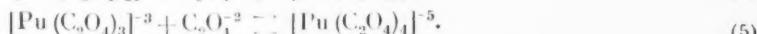
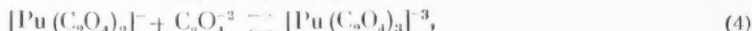
Fig. 3. Variation of the solubility of $\text{Pu}_2(\text{C}_2\text{O}_4)_3 \cdot 9\text{H}_2\text{O}$ with $(\text{NH}_4)_2\text{C}_2\text{O}_4$ concentration at 70°C .

These data can be used to estimate the metal/addend ratio in the complex ions. However, the number of oxalate groups contained in the inner sphere of the complex does not always determine the coordination number of the complex ion. Coordination number 8 has been ascribed to the hydrated Pu^{+3} ion [12]. It is very likely that the coordination number of complex ions containing two and three oxalate groups is also 8. In this case 4 and 2 water molecules respectively are within the complex. The number of water molecules present within the complex, and hence the true coordination number of the complex ion, cannot be determined by our method for studying complex compounds.

However, when the metal/addend ratio has been determined, it is possible to calculate the instability constants of the complex ions, as the presence of water molecules and variation of the

number of H_2O molecules within the complex has no influence on the magnitude of the instability constant. For this reason, in writing the equations for dissociation of the complex ions we attributed to the complex ions a composition corresponding only to a definite metal/addend ratio, without consideration of the number of water molecules within the complex. Therefore the composition of the complex ions established in the present investigation must be taken as referring only to a definite metal/addend ratio in the inner sphere of the complex ion. The instability constants of the complex ions were calculated from the values found for the metal/addend ratios. Calculation of the total instability constants by means of Equation (2) showed that the solutions contain complex ions with values of n_1 equal to 2, 3 and 4. Therefore the complex ions $[\text{Pu}(\text{C}_2\text{O}_4)_2]^-$, $[\text{Pu}(\text{C}_2\text{O}_4)_3]^{-3}$ and $[\text{Pu}(\text{C}_2\text{O}_4)_4]^{-5}$ are formed in the solutions.

Accordingly, the reactions of complex formation taking place in the solutions may be represented as:



The values of the total instability constants for the complex ions $[\text{Pu}(\text{C}_2\text{O}_4)_2]^-$, $[\text{Pu}(\text{C}_2\text{O}_4)_3]^{-3}$ and $[\text{Pu}(\text{C}_2\text{O}_4)_4]^{-5}$ formed when $\text{Pu}_2(\text{C}_2\text{O}_4)_3 \cdot 9\text{H}_2\text{O}$ is dissolved in aqueous $\text{K}_2\text{C}_2\text{O}_4$ solutions were found to be, respectively:

$$k_{n_1} = 4.9 \cdot 10^{-10}, \quad k_{n_2} = 4.4 \cdot 10^{-10}, \\ k_{n_3} = 1.2 \cdot 10^{-10}.$$

The total instability constant of the complex Pu^{+3} ion is

$$K_{n_i} = \frac{[\text{Pu}^{+3}] [\text{C}_2\text{O}_4^{2-}]^{n_i} \cdot \gamma_{\text{Pu}^{+3}} \cdot \gamma_{\text{C}_2\text{O}_4^{2-}}}{[\text{Pu}(\text{C}_2\text{O}_4)_{n_i}^{4-2n_i}] \cdot \gamma_{[\text{Pu}(\text{C}_2\text{O}_4)_{n_i}^{4-2n_i}]}}.$$

We calculated the total concentration instability constants of complex Pu^{+3} oxalate ions, corresponding to the equation

$$k_{n_i} = \frac{K_{n_i}}{B},$$

where B, the ratio of the activity coefficients of the corresponding ions, is constant for a given ionic strength of the solution.

These constants correspond to total decomposition of the complex ions according to the equation

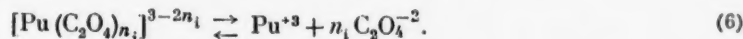


Table 1 gives the concentrations of each of these ions, calculated with the aid of the instability constants. The variation of the complex ion concentration with the concentration of $\text{C}_2\text{O}_4^{2-}$ ions in solution is shown in Figure 4.

TABLE 3

Heats of Formation of Complex Ions

Composition of complex ion	T_1 °C	T_2 °C	k_{n_i} at T_1	k_{n_i} at T_2	$\Delta \bar{Q}$, cal
$[\text{Pu}(\text{C}_2\text{O}_4)_3]^-$	20	70	$4 \cdot 9 \cdot 10^{-10}$	$11.6 \cdot 10^{-9}$	1300
$[\text{Pu}(\text{C}_2\text{O}_4)_2]^{-3}$	20	70	$4 \cdot 10 \cdot 10^{-10}$	$5.6 \cdot 10^{-9}$	1200
$[\text{Pu}(\text{C}_2\text{O}_4)_4]^{-5}$	20	70	$11.9 \cdot 10^{-11}$	$2.5 \cdot 10^{-8}$	1300

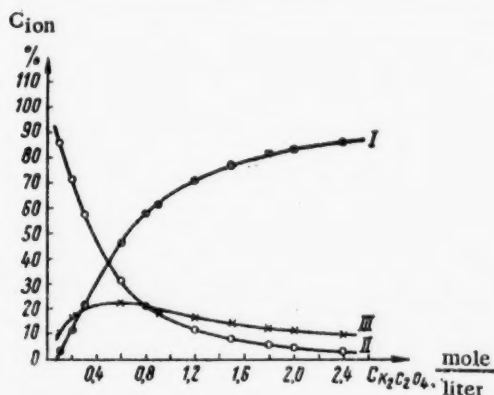


Fig. 4. Effect of concentration of $\text{C}_2\text{O}_4^{2-}$ ions on the concentration of complex Pu^{+3} ions.

I— $[\text{Pu}(\text{C}_2\text{O}_4)_4]^{-5}$; II— $[\text{Pu}(\text{C}_2\text{O}_4)_2]^{-3}$; III— $[\text{Pu}(\text{C}_2\text{O}_4)_3]^-$.

These results show that at low $\text{K}_2\text{C}_2\text{O}_4$ concentrations, from 0.01 to 0.4 mole/liter, the complex ion $[\text{Pu}(\text{C}_2\text{O}_4)_3]^-$ is predominantly formed, and its content in the solution decreases with increasing concentration of the $\text{C}_2\text{O}_4^{2-}$ ion. At the same time, the concentration of the other complex ion, $[\text{Pu}(\text{C}_2\text{O}_4)_2]^{-3}$ increases at first and, after reaching a maximum, decreases with increasing $\text{K}_2\text{C}_2\text{O}_4$ concentration. At $\text{K}_2\text{C}_2\text{O}_4$ concentrations of 1.5 moles per liter and over, the solubility is mainly determined by the formation of the complex ion $[\text{Pu}(\text{C}_2\text{O}_4)_4]^{-5}$, and increases in proportion to the fourth power of the oxalate concentration.

Examination of data on the solubility of Pu^{+3} oxalate in aqueous $(\text{NH}_4)_2\text{C}_2\text{O}_4$ solutions at 70°C

also leads to the conclusion that complex formation occurs between Pu^{+3} and $\text{C}_2\text{O}_4^{-2}$ ions. Determinations of the composition and instability constants by the method described showed that complex ions of the composition $[\text{Pu}(\text{C}_2\text{O}_4)_2]^{-}$, $[\text{Pu}(\text{C}_2\text{O}_4)_3]^{-3}$ and $[\text{Pu}(\text{C}_2\text{O}_4)_4]^{-5}$ are formed, with total instability constants of $k_{n_1} = 11.6 \cdot 10^{-9}$, $k_{n_2} = 5.6 \cdot 10^{-9}$, $k_{n_3} = 2.5 \cdot 10^{-9}$ respectively. Experimental data therefore show that as the $\text{C}_2\text{O}_4^{-2}$ ion concentration increases, formation of complex ions of high coordination numbers begins to prevail in solution, and at very high oxalate concentrations these processes become the predominant reactions of complex formation.

The values found for the total instability constants were used to calculate the heats of formation of the complex ions, given in Table 3.

These values of the total instability constants can be used for determining the progressive dissociation constants of the corresponding complex ions.

LITERATURE CITED

- [1] A. K. Babko, Zhur. Obshchel Khim. 15, 745 (1954).
- [2] M. Bobtelsky, J. Chem. Soc. 77, No. 7, 1990 (1955).
- [3] A. A. Grinberg, "Physicochemical investigations in the field of complex compounds" Izvest. Inst. Izucheniyu Platiny i Drug. Blagorod. Metal. 1932, No. 10.
- [4] I. M. Korenman, Zhur. Obshchel Khim. 16, 157 (1946).
- [5] W. H. Reas, The Transuranium Elements, pp. 4, 3, G. Seaborg, editor.
- [6] N. V. Tananaev and B. N. Detchman, Izv. An SSSR (OKhN) 2, 144 (1949).
- [7] V. V. Fomin, Zhur. Fiz. Khim. 29, 9, 1728 (1955).
- [8] K. B. Iatsimirskii, Zhur. Fiz. Khim. 25, 475 (1951).
- [9] C. E. Crouthamel, and D. S. Martin, J. Amer. Chem. Soc. 72, 3, 1383 (1950).
- [10] M. Bose and D. M. Chowdhury, J. Indian Chem. Soc. 32, 10, 673 (1955).
- [11] D. Dyrsen and L. C. Sillen, Acta Chem. Scandinavica 7, 4, 663 (1953).
- [12] G. Seaborg and J. Katz, editors, The Actinides, Chapter 9, 259 (IL, 1955).

Received January 19, 1957

INVESTIGATION OF THE FORMATION CONDITIONS AND STABILITY OF COMPLEX Pu^{+3} COMPOUNDS BY A SPECTROPHOTOMETRIC METHOD

A. D. Gel'man and A. I. Moskvin

The formation of Pu^{+3} complexes with $\text{C}_2\text{O}_4^{-2}$, CO_3^{-2} , $\text{C}_6\text{H}_5\text{O}_7^{-3}$ ions and with Trilon B has been demonstrated by a spectrophotometric method. It was found that their absorption spectra have the most characteristic maxima at the following wave lengths: 565, 605, 665, 780-790, 905-910, 1090 m μ .

Scarcely any information is available in the literature on complex Pu^{+3} compounds, and the existing scanty data are doubtful. For example, J. Hindman * states that Pu^{+3} oxalate can dissolve in saturated potassium oxalate solution but doubts the possibility of Pu^{+3} complex compound formation owing to the rapid oxidation of Pu^{+3} to Pu^{+4} ; he suggests that in this case a soluble Pu^{+4} complex is formed.

In view of the lack of adequate experimental data in the published literature on Pu^{+3} complex formation, this suggestion is fully justified. The question whether oxidation of Pu^{+3} to Pu^{+4} takes place at the instant of Pu^{+3} complex formation, or whether these complexes are relatively stable under these conditions, required further experimental investigation.

In the present investigation a spectrophotometric method was used to study the stability, to oxidation by atmospheric oxygen, of the complex Pu^{+3} ions formed when Pu^{+3} oxalate is dissolved in solutions containing $\text{C}_2\text{O}_4^{-2}$, CO_3^{-2} , $\text{C}_6\text{H}_5\text{O}_7^{-3}$ ions and Trilon B.

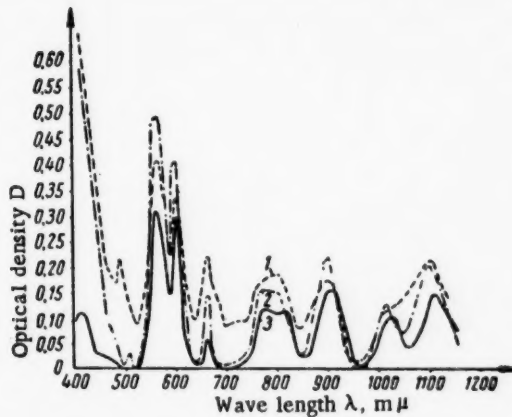


Fig. 1. Absorption spectra. 1) Pu^{+3} oxalate in 20% $\text{K}_2\text{C}_2\text{O}_4$ solution, determination immediately after preparation; Pu^{+3} concentration 1.07 g/liter; 2) the same solution, reduced again after oxidation by exposure in open air for 4 days; 3) Pu^{+3} solution in HNO_3 (2.7 N).

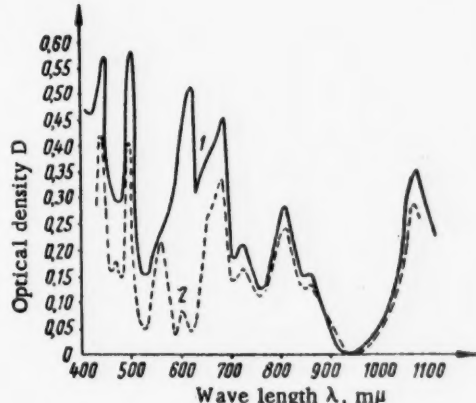


Fig. 2. Absorption spectra. 1) Pu^{+4} oxalate in 20% $\text{K}_2\text{C}_2\text{O}_4$ solution; 2) Pu^{+3} oxalate in 20% $\text{K}_2\text{C}_2\text{O}_4$ solution, determination 4 days after preparation of the solution.

* In the book: Actinides, edited by G. Seaborg and J. Katz (Russian translation) (IL, 1955) Chapter 9, p. 279.

The absorption spectra were measured at room temperature in the wave length region 400-1100 m μ by the SF-4 Instrument in open cuvettes with absorbing layers 10.01 mm long. The comparison standard in all the determinations was a solution containing all the components (except plutonium) present in the solution under test.

For preparation of the complex oxalate compounds, Pu^{+3} oxalate was first dissolved in 20% potassium oxalate solution in presence of excess reducing agent — hydrazine hydrate or sodium formaldehyde sulfoxylate. The resultant solution of the Pu^{+3} complex compound had a blue color and was fairly stable in a strongly reducing medium. A Pu^{+3} solution obtained by a similar method but with a deficiency of, or in absence of, reducing agent changed color rapidly, within 1-2 hours, from blue to green and then to reddish brown, characteristic of the Pu^{+4} complex. The absorption spectra of the solutions are given in Figures 1 and 2. Comparison of these curves shows that the absorption spectrum of Pu^{+3} oxalate in 20% $\text{K}_2\text{C}_2\text{O}_4$ solution, measured immediately after the solution is made, is similar to the absorption spectrum of a Pu^{+3} solution in nitric acid (Fig. 1). The absorption spectra measured 1-4 days after preparation of the complex compound solutions show sharp changes, indicating the atmospheric oxidation reaction $\text{Pu}^{+3} \rightarrow \text{Pu}^{+4}$ (the solutions were kept in open vessels). As the oxidation proceeds, the most characteristic maxima — at 563 and 605 m μ — decrease in intensity; the maxima at 780, 910, 1015 m μ disappear entirely, and new maxima arise, characteristic of the absorption spectrum of the corresponding Pu^{+4} complex.

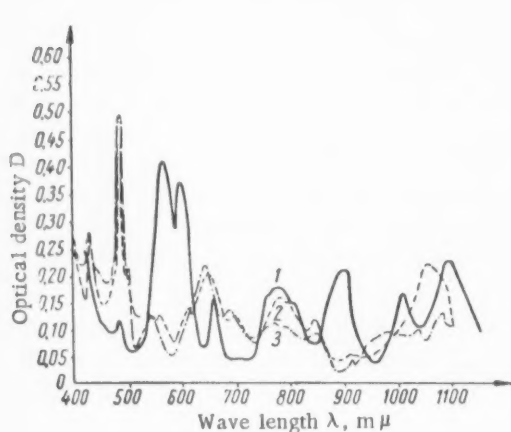


Fig. 3. Absorption spectra. 1) Pu^{+3} oxalate in 20% $(\text{NH}_4)_2\text{CO}_3$ solution, determination immediately after preparation; Pu^{+3} concentration 1 g/liter; 2) the same solution, determination 3 days after preparation; 3) Pu^{+4} oxalate solution in 20% $(\text{NH}_4)_2\text{CO}_3$ solution.

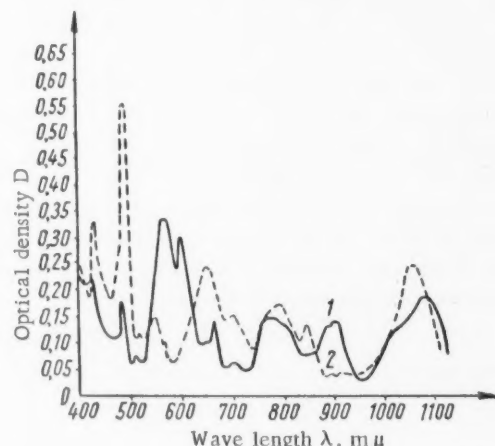


Fig. 4. Absorption spectra. 1) Pu^{+3} oxalate in 25% K_2CO_3 solution, determination immediately after preparation; 2) the same solution, determination 2 days after preparation of the solution.

The blue Pu^{+3} oxalate complex is also readily formed when Pu^{+3} oxalate is dissolved in saturated ammonium oxalate solution on heating to 80-90°. Cooling of the resultant solution to room temperature leads to partial decomposition of the complex and precipitation of Pu^{+3} oxalate. The solubility of $\text{Pu}_2(\text{C}_2\text{O}_4)_3 \cdot 9\text{H}_2\text{O}$ falls approximately from 5.40 to 0.24 g Pu^{+3} per liter owing to the decreased concentration of $\text{C}_2\text{O}_4^{2-}$ ions in the solution. The absorption spectrum of a solution of Pu^{+3} oxalate in $(\text{NH}_4)_2\text{C}_2\text{O}_4$ solution is quite analogous to the absorption spectra shown in Figure 1.

To prepare complex Pu^{+3} carbonate compounds, Pu^{+3} oxalate precipitates were dissolved in 20 and 25% solutions of $(\text{NH}_4)_2\text{CO}_3$ and K_2CO_3 respectively, in presence of hydrazine hydrate or sodium formaldehyde sulfoxylate. For comparison, a solution of the Pu^{+4} carbonate complex was prepared, and its absorption spectrum was compared with the absorption spectra of complex Pu^{+3} carbonate compounds, first prepared by Moore and Werner.* The absorption spectra of Pu^{+3} oxalate in $(\text{NH}_4)_2\text{CO}_3$ and K_2CO_3 solutions of various concentrations are shown in Figures 3 and 4 respectively.

* In the book: Actinides, edited by G. Seaborg and J. Katz (Russian translation) (IL, 1955) Chapter 9, p. 279.

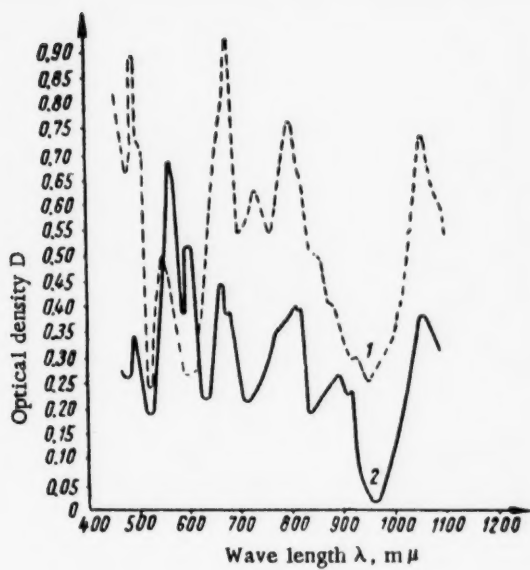


Fig. 5. Absorption spectra. 1) Pu^{+3} oxalate in 5% potassium citrate solution, determination immediately after preparation; 2) the same solution, determination 48 hours after preparation.

ciable changes in the absorption spectrum of Pu^{+3} , since the 5f electrons are strongly shielded and are therefore not readily susceptible to influence in the external field of the atomic nucleus.

When precipitates of Pu^{+3} oxalate were dissolved in 5% potassium citrate solution and 10% Tiron B solution, blue complex Pu^{+3} compounds were obtained, relatively resistant to oxidation in presence of excess reducing agent. The absorption spectra were determined both for the freshly prepared solutions and for solutions kept for 48 hours in open vessels. The absorption spectra of Pu^{+3} oxalate solution in 5% potassium citrate solution are given in Figure 5.

It is seen from Figures 3-5 that the absorption spectra of complex carbonate and citrate Pu^{+3} compounds are analogous to the absorption spectra of complex oxalate Pu^{+3} compounds. Examination of the absorption spectra of complex Pu^{+3} compounds shows that they are relatively stable in a strongly reducing medium; the stability is increased considerably if the experiments are carried out in a nitrogen atmosphere. The absorption spectra of Pu^{+3} complexes: oxalate, carbonate, citrate, and with Tiron B, have the most characteristic absorption maxima at wave lengths 565, 605, 665, 780-790, 905-910, 1090 mμ, and are similar to the absorption spectrum of a nitric acid solution of Pu^{+3} . This resemblance of the absorption spectra fully confirms J. Hindman's views, according to which complex formation may not produce appreciable changes in the absorption spectrum of Pu^{+3} , since the 5f electrons are strongly shielded and are therefore not readily susceptible to influence in the external field of the atomic nucleus.

Received January 19, 1957

LETTERS TO THE EDITOR

ON THE QUESTION OF NEUTRON THERMALIZATION

V. V. Smelov

The present article is devoted to the energy and spatial distributions of neutrons in a monoatomic gas moderator when the neutron velocities are comparable with the mean thermal velocities of the moderator nuclei.

As is well known, the neutron density $N(\vec{r}, \vec{v})$ satisfies the kinetic equation [1]

$$\vec{v} \nabla N(\vec{r}, \vec{v}) + [\gamma(v) + V(v)] N(\vec{r}, \vec{v}) = \int G_s(\vec{v}' \rightarrow \vec{v}) N(\vec{r}, \vec{v}') d\vec{v}' + s(\vec{r}, \vec{v}), \quad (1)$$

where $\gamma(v)$ and $V(v)$ are the probabilities for absorbing and scattering neutrons, $G_s(\vec{v}' \rightarrow \vec{v}) d\vec{v}'$ is the probability that a neutron with velocity \vec{v} , will be scattered into the velocity interval $d\vec{v}'$ about \vec{v}' and $s(\vec{r}, \vec{v})$ gives the distribution of neutron sources.

Assuming that $N(\vec{r}, \vec{v})$ is a slowly varying function of the direction of the velocity vector \vec{v} , we may attempt to find a solution of (1) in the form of a series of spherical harmonics and maintain only the first two terms [2]

$$N(\vec{r}, \vec{v}) = \frac{1}{4\pi} \left[N_0(\vec{r}, v) + 3 \frac{\vec{v}}{v} \vec{N}_1(\vec{r}, v) + \dots \right],^*$$

as a result of which we arrive at the following set of equations for the two unknown functions $N_0(\vec{r}, v)$ and $N_1(\vec{r}, v)$:**

$$\left. \begin{aligned} \vec{v} \nabla \vec{N}_1(\vec{r}, v) + [\gamma(v) + V(v)] N_0(\vec{r}, v) &= \\ &= \int G_0(v', v) N_0(\vec{r}, v') d\vec{v}', \\ \frac{v}{3} \nabla N_0(\vec{r}, v) + [\gamma(v) + V(v)] \vec{N}_1(\vec{r}, v) &= \\ &= \int G_1(v', v) \vec{N}_1(\vec{r}, v') d\vec{v}', \end{aligned} \right\} \quad (2)$$

*Henceforth we shall denote the vector \vec{v}/v by $\vec{\Omega}$.

** If the neutrons emitted by the source have high energy, the thermal neutron spectrum can be described by a homogeneous equation, and we may assume that $s(\vec{r}, \vec{v}) = 0$.

where

$$G_0(v', v) = \int G_s(\vec{v}' \rightarrow \vec{v}) d\vec{\Omega},$$

$$G_1(v', v) = \int G_s(\vec{v}' \rightarrow \vec{v}) \cos(\vec{v}, \vec{v}') d\vec{\Omega}.$$

All the functions $\gamma(v)$, $V(v)$, $G_0(v', v)$, $G_1(v', v)$ are well known for slowing-down of neutrons by infinitely heavy stationary nuclei* [3]. If, however, the mean thermal velocity of the moderator nuclei is comparable with the neutron velocity, this theory is inapplicable.

Accounting for the motion of the moderator nuclei complicates the determination of γ , V , G_0 and G_1 to a very large extent. Nevertheless, with certain definite properties of the moderator these functions can be obtained analytically.

In the case we are considering, as is well known, the moderator nuclei have a Maxwell velocity distribution given by

$$M(v_0) = \frac{4}{V\pi} \left(\frac{m}{2kT} \right)^{3/2} v_0^3 e^{-\frac{mv_0^2}{2kT}}.$$

Obviously, therefore,

$$\gamma(v) = \frac{1}{4\pi} \int_0^{2\pi} \int_{-1}^1 \int_0^\infty v_R \Sigma_a(v_R) M(v_0) dv_0 d\mu d\varphi, \quad (3)$$

$$V(v) = \frac{1}{4\pi} \int_0^{2\pi} \int_{-1}^1 \int_0^\infty v_R \Sigma_s(v_R) M(v_0) dv_0 d\mu d\varphi, \quad (4)$$

$$G_s(\vec{v} \rightarrow \vec{v}') =$$

$$= \frac{1}{4\pi} \int_0^{2\pi} \int_{-1}^1 \int_0^\infty v_R \Sigma_s(v_R) M(v_0) p(\vec{v} \rightarrow \vec{v}', \vec{v}_0) dv_0 d\mu d\varphi, \quad (5)$$

where

$$p(\vec{v} \rightarrow \vec{v}', \vec{v}_0) =$$

$$= \begin{cases} 0 & \text{for } v' < v_m \\ \frac{1}{2\pi} \frac{2v'}{v_M^2 - v_m^2} \delta\left(\frac{M+1}{2} \frac{v'}{v_M} - \frac{M-1}{2} \frac{v_M}{v'} - \mu'\right) & \text{for } v_m < v' < v_M \\ 0 & \text{for } v' > v_M, \end{cases}$$

$$v_M = \frac{m}{m+1} v_R + v_c, \quad v_m = \left| \frac{m}{m+1} v_R - v_c \right|,$$

$$\left\{ \begin{array}{l} \vec{v}_c = \frac{\vec{v} + m\vec{v}_0}{1+m}, \quad \vec{v}_R = \vec{v} - \vec{v}_0, \\ M = \frac{m}{1+m} \frac{v_R}{v_c}, \end{array} \right.$$

* In particular, $\gamma(v) = v \Sigma_a(v)$, $V(v) = v \Sigma_s(v)$.

where $\mu = \cos(\vec{v}, \vec{v}_0)$, $\mu' = \cos(\vec{v}', \vec{v}_c)$, m is the mass of the moderator nucleus, and $\delta(x)$ is the Dirac δ -function.

The functions V and G_0 were obtained analytically by E. Cohen [1] who considered the process of slowing-down of neutrons in an infinite medium and suggested that the scattering cross section is of the form $\Sigma_s =$

$= \sum_i \sigma_i e^{-\alpha_i v^2}$: he obtained

$$G_0(v, v') = \frac{(m+1)^2}{4m} \frac{\tau^3}{\lambda} \frac{x'}{x} \times$$

$$\times \{ e^{-\frac{\alpha \tau^2}{\beta^2} x^2} [\operatorname{erf}(x'0 - x\eta) + \epsilon \operatorname{erf}(x'0 + x\eta)] +$$

$$+ e^{x^2 - \lambda x'^2} [\operatorname{erf}(x0 - x'\eta) - \epsilon \operatorname{erf}(x0 + x'\eta)] \},$$

$$V(v) = \frac{\tau^3}{\beta} \left[\left(\tau^2 x + \frac{1}{2mz} \right) \operatorname{erf}(\sqrt{m} \tau x) e^{-\frac{\alpha \tau^2}{\beta^2} x^2} + \right.$$

$$\left. + \frac{\tau}{\sqrt{\pi m}} e^{-mx^2} \right],$$

where

$$x = \beta v, x' = \beta v', \beta = \frac{1}{\sqrt{2kT}}, \tau^2 = \frac{m \beta^2}{m \beta^2 + \alpha},$$

$$\theta = \frac{m+1}{2\tau \sqrt{m}}, \eta = \tau \sqrt{m} - \theta, \lambda = 1 + m(1 - \tau^2),$$

$$\epsilon = \begin{cases} 1 & \text{for } x > x', \\ -1 & \text{for } x < x'. \end{cases}$$

With this assumption one is also able to find $G_1(v, v')$ in analytic form, namely

$$G_1(v, v') = \frac{(m+1)^2}{4m} \frac{\tau^3}{\lambda} \frac{x'}{x} \left\{ e^{-\frac{\alpha \tau^2}{\beta^2} x^2} \times \right.$$

$$\times \left[v \left(\frac{x'}{x} 0 - \frac{x}{x'} \eta - \frac{v}{xx'} \right) (\operatorname{erf}(x'0 - x\eta) + \right.$$

$$+ \epsilon \operatorname{erf}(x'0 + x\eta)) + \frac{2}{\sqrt{\pi}} \left(\frac{v}{x'} + \theta(x - x') \right) \times$$

$$\times e^{-(x'0 - x\eta)^2} - \epsilon \frac{2}{\sqrt{\pi}} \left(\frac{v}{x'} - \theta(x + x') e^{-(x'0 + x\eta)^2} \right) +$$

$$+ e^{x^2 - \lambda x'^2} \left[v \left(\frac{x'}{x'} 0 - \frac{x'}{x} \eta - \frac{v}{xx'} \right) \times \right.$$

$$\times (\operatorname{erf}(x0 - x'\eta) - \epsilon \operatorname{erf}(x'\eta - x0)) +$$

$$+ \frac{2}{\sqrt{\pi}} \left(\frac{v}{x} + \theta(x' - x) \right) e^{-(x0 - x'\eta)^2} +$$

$$\left. + \epsilon \frac{2}{\sqrt{\pi}} \left(\frac{v}{x} - \theta(x + x') \right) e^{-(x0 + x'\eta)^2} \right] \} ,$$

where $v = (m+1)/(2\lambda\theta)$.

*We shall henceforth assume that $\Sigma_s(v) = e^{-\alpha v^2}$.

In conclusion, if the absorption in the moderator is given by a $1/v$ law, $\Sigma_\alpha(t) = \Sigma_\alpha(v_T) \frac{v_T}{v}$, then from Equation (3) it follows that

$$\gamma(v) \equiv \text{const} = v_F \Sigma_a(v_F).$$

The author expresses his gratitude to G. I. Marchuk for discussing the work and valuable remarks.

LITERATURE CITED

- [1] E. Kogen, "Experimental reactors and reactor physics," Reports of Foreign Scientists at the International Conference on the Peaceful Uses of Atomic Energy [in Russian] (Gostekhizdat, 1956), p. 257.
- [2] H. Hurwitz, M. S. Nelkin and G. J. Haberler, Nucl. Sci. Eng. 1, 280 (1956).
- [3] A. Akhiezer and I. Pomeranchuk, Some Problems in Nuclear Theory [in Russian] (Gostekhizdat, 1950).

Received May 24, 1957

• Transliteration of Russian—Publisher's note.

THE CHEMICAL BEHAVIOR OF Mo⁹⁹ FORMED ON IRRADIATION OF URANIUM COMPOUNDS BY NEUTRONS

L. V. Shiriaeva and G. M. Tolmachev

In recent years there have been many investigations of the chemical state of a number of radioactive isotopes formed in various nuclear reactions. For example, Smith and Aten [1] studied the (n, 2n) reaction for NaNO₃ and NH₄NO₃ and found that most of the N¹³ is present after it is formed in the form of nitrate and nitrite, and a small proportion is in the form of N₂O and molecular nitrogen.

Rao, Sharma and Shankar [2] found that most of the Mn⁵⁴ formed in solid Fe₂O₃ by the (n, p) reaction after irradiation is in the form of MnO₂, and a small proportion is present in the form of Mn⁺² compounds and as manganese in higher states of oxidation.

Walton and Croall [3] irradiated a mixture of uranium oxide and potassium iodate in a pile. The iodide ion I⁻¹³¹, elementary iodine I₂¹³¹, and a small amount of I¹³¹ compounds in higher states of oxidation found in the solid potassium iodate are justifiably regarded by the authors as being the reaction products of fragmentation iodine with solid potassium iodate. They did not investigate the chemical state of I¹³¹ in uranium oxide.

Up to the present time the literature does not contain any information on the chemical state of any fission fragments in irradiated uranium compounds.

The present paper gives the results of a preliminary investigation of the chemical behavior of Mo⁹⁹ formed in U₃O₈ and uranium dioxide in the fission reaction.

It was presumed that after Mo⁹⁹ has been formed it may occur in the uranium oxides in the form of elementary molybdenum, MoO₂ and MoO₃. It may also possibly form compounds with uranium. It was also presumed that the fission fragments, like other impurities, should be displaced to the surface of the U₃O₈ and UO₂ crystals on heating. The work of Chemla [4] and Libby [5] provides a thermodynamic basis for this process.

Experiments on the extraction of Mo⁹⁹ were carried out on irradiated samples of U₃O₈ and UO₂ which were heated for an hour and a half in oxygen and hydrogen after irradiation at temperatures between 400 and 1200°. Weighed samples of U₃O₈ (or UO₂) between 50 mg and 5 g (depending on the activity of the sample) were placed in a special vessel, to which 100 ml of a solution of inactive ammonium molybdate was then added. The mixture was stirred for two hours in a nitrogen atmosphere at 20°.

At the end of the experiment the solution was centrifuged and analyzed for Mo⁹⁹. It was found that: 1) the temperature of the solution, in the 20 to 60° range, does not influence the percentage extraction of Mo⁹⁹ from uranium oxide; 2) in the presence of a carrier — inactive ammonium molybdate — a change of solution pH from 2.0 to 10.0 does not affect the percentage extraction; 3) in an ammoniacal medium (pH from 8.0 to 10.0) the extraction of Mo⁹⁹, both in presence of the carrier and without it, reaches about 1%; 4) in weakly acidic solutions (pH from 2.0 to 5.5) in absence of carrier in the solution, losses of Mo⁹⁹ occur; 5) the optimum stirring time is 2 hours.

In all these experiments the percentage extraction of Mo⁹⁹ was determined as follows. A weighed sample of U₃O₈ (or UO₂) was dissolved in nitric acid in presence of a definite amount of ammonium molybdate (70 mg calculated as PbMoO₄). The Mo⁹⁹ was isolated from the solution together with the carrier and purified to remove

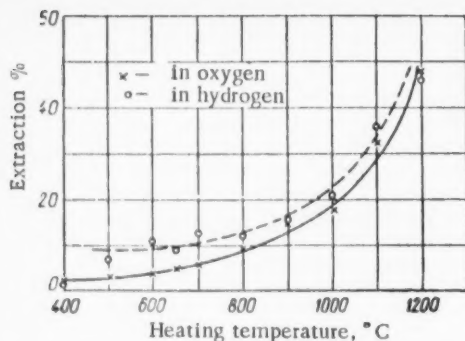


Fig. 1. Variation of percentage extraction of Mo⁹⁹ with the temperature of heating of U₃O₈ in oxygen and hydrogen. (The volatilization of Mo⁹⁹ was not taken into account in heating in an oxygen atmosphere at 1100 and 1200°).

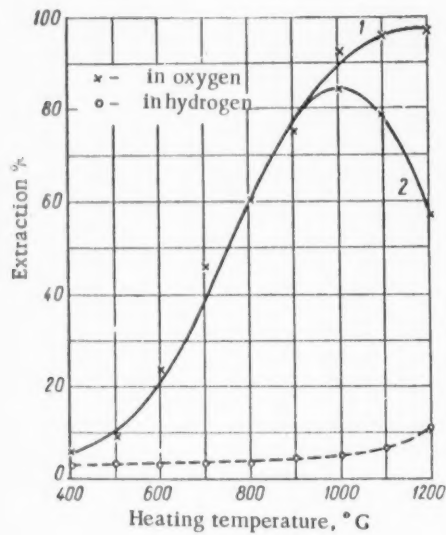


Fig. 2. Variation of percentage extraction of Mo⁹⁹ with the temperature of heating of UO₂ in oxygen and hydrogen. 1) Volatilization taken into account; 2) volatilization not taken into account.

fission fragments and uranium. The PbMoO₄ in the form of which Mo⁹⁹ was isolated was made into a target of definite shape and weight for determination of β -activity. This target was used as a standard. Similar targets were made for each experimental sample after isolation of molybdenum from the wash solution. The ratio of the Mo⁹⁹ activity in these targets to the activity of the standard target represents the degree of extraction of Mo⁹⁹. In some experiments the percentage of Mo⁹⁹ remaining in the U₃O₈ (or UO₂) was also determined.

Figures 1 and 2 give the results of experiments on the heating of U₃O₈ and UO₂ samples in oxygen and hydrogen.

In the extraction of Mo⁹⁹ from U₃O₈ (Fig. 1) the principal factor is the heating temperature and not the nature of the gas. Conversion of U₃O₈ into UO₂ when U₃O₈ is heated in hydrogen does not influence the degree of extraction. On heating in oxygen ($t = 1200^\circ$) about 15% of the molybdenum is volatilized from U₃O₈; in hydrogen, volatilization of Mo⁹⁹ was not detected over the temperature range studied.

The behavior of Mo⁹⁹ is different when UO₂ is heated. In hydrogen, the percentage extraction of Mo⁹⁹ slowly increases with the heating temperature, reaching 11% at 1200°. A sharp increase of the extraction of Mo⁹⁹ with temperature is found when UO₂ is heated in oxygen. The maximum extraction of Mo⁹⁹ (83.5%) corresponds to 1000°. The subsequent descent of the curves is the result of increased volatilization. At 1200° 40% Mo⁹⁹ is volatilized from UO₂, and after treatment of the sample with the solution a further 57% is extracted. Thus, by heating the sample in oxygen at 1100-1200° for 1 and 1/2 hours and subsequent elution it is possible to remove nearly all the Mo⁹⁹ from UO₂.

It is interesting to note that Mo⁹⁹ is extracted very rapidly from samples of U₃O₈ (or UO₂). As the table shows, over 50% of the Mo⁹⁹ extractable from the sample passes into solution in the first 5 minutes of stirring. However, complete extraction into solution takes 1-2 hours.

Variation of the Extraction of Mo⁹⁹ from U₃O₈ with the Time of Stirring

Time of stirring	5 min	1 hr	2 hr	10 hr
Percentage extraction	16	29	31	32

Qualitative experiments on the behavior of fragment Ba¹⁴⁸ showed that under analogous conditions the degree of extraction is low (1-2%).

The results indicate that a part of the Mo⁹⁹ formed in U₃O₈ during fission is in the form of MoO₃. We are now studying the effects of heating in vacuum and in an inert gas of Mo⁹⁹.

LITERATURE CITED

- [1] R. D. Smith and A. H. W. Aten, *J. Inorg. Nucl. Chem.* 1, 296 (1955).
- [2] C. L. Rao, H. D. Sharma and J. Shankar, *Proc. Indian Acad. Sci. A40*, 2, 102 (1954).
- [3] G. N. Walton and I. E. Croall, *J. Inorg. Nucl. Chem.* 1, 149 (1955).
- [4] M. M. Chemla, *Compt. Rend.* 232, 1553 (1951).
- [5] W. F. Libby, *J. Am. Chem. Soc.* 69, 2523 (1947).

Received April 18, 1957

ON THE MEASUREMENT OF NEUTRON ABSORPTION IN HETEROGENEOUS URANIUM-HEAVY WATER SYSTEMS

V. F. Belkin, P. A. Krupchitskii and Yu. V. Orlov

The probability of the resonance capture of U^{238} neutrons during their slowing down from fission to thermal energy is an important quantity entering the calculations dealing with nuclear reactors. In reference [1], an expression is given for φ — the resonance escape probability for a heterogeneous system consisting of an infinite lattice of cylindrical uranium rods with a diameter ρ :

$$-\ln \varphi = \psi = \frac{\alpha}{S_3} (\rho^{3/2} + A\rho^2),$$

where α and A are constants determined by the parameters of the U^{238} nuclear levels and the properties of the moderator; S_3 is the area of the moderator in a lattice cell. In this equation, the resonance capture of neutrons for a lattice with cylindrical lumps of uranium is represented as the sum of lump ($\sim \rho^{3/2}$) and non-lump ($\sim \rho^2$) capture. This form for the dependence of φ on the radius of the lump was used in references [2-5]. In references [6-11] a different form for the dependence of φ on the lump radius was used.

A large number of experimental determinations of φ have been made. In particular, the following methods were used: irradiation of natural uranium by neutrons, with the subsequent extraction of U^{239} or Np^{239} [2], [4], [5], [7] measurements with the help of a reactor oscillator [8], [11], exponential experiments [9], [10], the measurement of neutron capture by detectors of U^{238} [12], [13].

In reference [3], for the measurement of φ for the system uranium-heavy water the method of similar media was used, which is based on the assumption that the slowing-down density, measured at a definite location in a medium having a point source of neutrons, is decreased φ times when the absorber (U^{238}) is introduced into the medium. In addition, it is assumed that the neutron capture does not affect the spatial distribution of the density of neutrons being slowed down, i. e., the neutron density decreases in the same way (φ times) at all points in a cell of the system when the absorber is introduced. In reference [3], to measure the density of neutrons being slowed down a BF_3 -filled ionization chamber was placed at the center of a cell at the corners of which the rods were located. A mixture of radium and beryllium was used as the neutron source.

Similar measurements were made by the authors of the present work. The experiment was carried out in a tank, 76 cm in diameter and 78 cm high, containing heavy water and surrounded by a shield of boron and paraffin. At the center of the tank was situated a uranium converter, 3.5 cm in diameter and 10 cm in height, to which a beam of slow neutrons from the vertical experimental channel of the AN SSSR heavy-water reactor could be supplied through a special pipe. Three types of lattice, made from uranium rods 1.75, 1.1 and 0.586 cm in diameter with the spacing of the square cell being 10.0, 6.3 and 3.4 cm, respectively, could be introduced alternately into the tank. To obtain a similar medium without absorption the uranium rods were replaced by lead ones. To eliminate the fission of U^{235} the rods were placed in cadmium pipes whose walls were 0.09 cm thick. The density of the neutrons being slowed down was measured through the activation of indium (energy of the main resonance — 1.46 ev) placed at the centre of the cell. The indium detectors were in the form of foil with a thickness of 20 mg/cm². They were irradiated in cadmium sheaths 0.05 cm thick. Two low-background counting devices were used to measure alternately the intensity of activation of the indium. Each

device consisted of six β counters and cathode followers, as well as a scaling circuit with a resolving time of 10^{-5} sec.

TABLE 1

Results of Measurement of the Coefficients α and A in the Equation $-\ln\varphi = \psi = \frac{\alpha}{S_m} (\rho^{3/2} + A\rho^2)$

α (cm $^{1/2}$)	A (cm $^{-1/2}$)	Method of determination	References
5.6	0.55	The irradiation of natural uranium in the reactor followed by the extraction of U 239	[2]
7.4	0.21	The irradiation of natural uranium in the reactor followed by the extraction of Np 239	[5]
6.3	0.19	The combination of the method of similar media, (detector - boron chamber), critical experiments and theoretical calculations	[3]
4.4	0.40	The method of similar media (detector - indium)	present work

TABLE 2

Results of the Measurement of the Effective Resonance Integral for Absorption $\int_E^{E_0} \sigma_{u \text{ eff}} \frac{dE}{E}$

Expression for	Method of determination	References
$\int_E^{E_0} \sigma_{u \text{ eff}} \frac{dE}{E}$		
$7.3 \left(1 + 3.22 \frac{S}{M} \right)$	The irradiation of spherical uranium lumps by cyclotron neutrons	[7]
$5 \left(1 + 7 \frac{S}{M} \right)$	Exponential experiment	[9]
$9 \left(1 + \frac{3.34}{\frac{M}{S} + 0.11} \right)$	Reactor oscillator and the irradiation of U 238 by reactor neutrons	[11]

The results of measurement are given in Figure 1 and Table 1. In the same figure and in Tables 1 and 2 the results of resonance - absorption measurements carried out by the other authors—are given. In all cases the absorption which depends on the energy according to the $1/v$ law was excluded.

From these experimental data the dependence of the quantity $\psi S_m \rho^{-3/2}$ on $\rho^{1/2}$, in the case of an infinite periodic lattice of uranium rods, placed in heavy water, has been drawn in Figure 1. In the calculations the following value was used for the scattering length of neutrons in heavy water, $\lambda_s = 2.9$ cm, for the mean logarithmic energy loss of neutrons in heavy water, $\xi = 0.524$ and for the density of uranium $d = 18.7$ g/cm 3 .

From Figure 1 it can be seen that for the system uranium-heavy water the value of $\psi S_m \rho^{-3/2}$ obtained by the method of similar media lie lower than those obtained by the other methods. Thus, for example, for $\rho = 0.7$ cm and $S_m = 29.9$ cm 2 , from reference [2] $\psi = 0.161$ ($\varphi = 0.852$), from reference [3] $\psi = 0.129$ ($\varphi = 0.879$), while from the present work $\psi = 0.115$ ($\varphi = 0.891$).

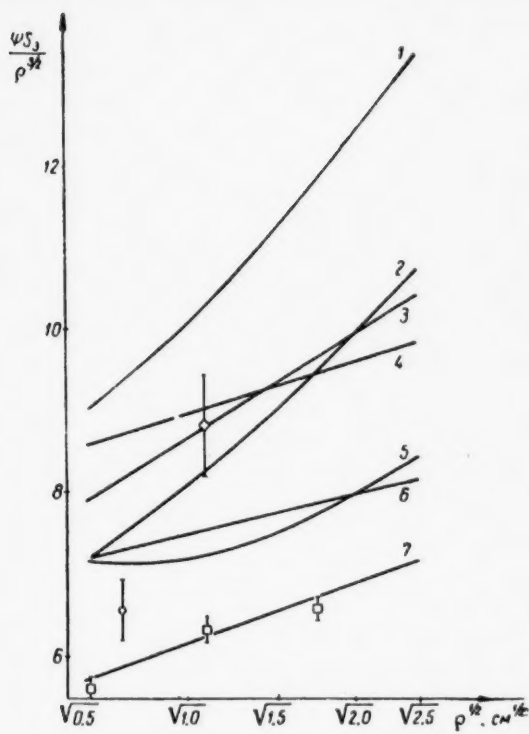


Fig. 1. The quantity $\psi S_m p^{-3/2}$ as a function of $p^{1/2}$.
 1) Data of Macklin and Pomerance [11]; 2) data of Creutz et al [7]; 3) data of Egiazarov et al [2]; 4) data of Hellstrand [5]; 5) data of Mummery [9]; 6) data of Burgov [3]; 7) data of the present work; \diamond —the value obtained in reference [3] from the critical experiments; \circ —the value obtained in reference [3] by the method of similar media; \square —values obtained in the present work.

2. A correction for the nonuniformity of the neutron density, carried out for a lattice with a spacing of 10 cm and $p = 1.75$ cm, enables the results of our measurements of φ to be brought into agreement with the results of reference [2].

In conclusion, the authors express their gratitude to S. Ya. Nikitin, A. D. Galanin, B. L. Ioffe and A. P. Rudik for unfailing interest in the work and for discussion of the results, and also to A. K. Dubasov and A. Ya. Diamant for help with the measurements.

In subsidiary experiments with a more widely spaced lattice (spacing 6.8 and 4.8 cm for $p = 0.568$ cm and 8.9 cm for $p = 1.1$ cm) the detector was not placed at the center of the cell. It was found that the values of $\psi S_m p^{-3/2}$ found with this arrangement of the detector were considerably higher than the values obtained when the detector was placed at the center of the cell.

For a more detailed study of this effect, the authors carried out an experiment to obtain the ratio of the density of neutrons being slowed down at the center of the cell to the density at the surface of a rod for the system uranium-heavy water(f_U) and lead-heavy water(f_{pb}). The same experimental arrangement was used for this as for the determination of φ . The measurements were made in a lattice with a spacing of 10 cm and $p = 1.75$ cm. In this experiment a Ra- α -Be neutron source was used and this replaced the uranium converter (Fig. 2). The indium detectors were placed in tubes which were bent in such a way that by rotating them the detector could be brought either into the center of a cell or near to the surface of one of the rods. The distance of the detector from the source was the same in both positions. The results of these measurements are given in Table 3.

The following conclusions can be drawn from the results of the measurement of f_U and f_{pb} :

1. When a scatterer (lead) is introduced into the heavy water the density of neutrons being slowed down becomes nonuniform; in the vicinity of the rods the density becomes smaller than the density at the center of the cell. This nonuniformity also depends on the distance between the detector and the source; when the lead is replaced by uranium the nonuniformity increases. From this it follows that the method of similar media is unsatisfactory for the measurement of the resonance absorption in heterogeneous systems of uranium-heavy water.

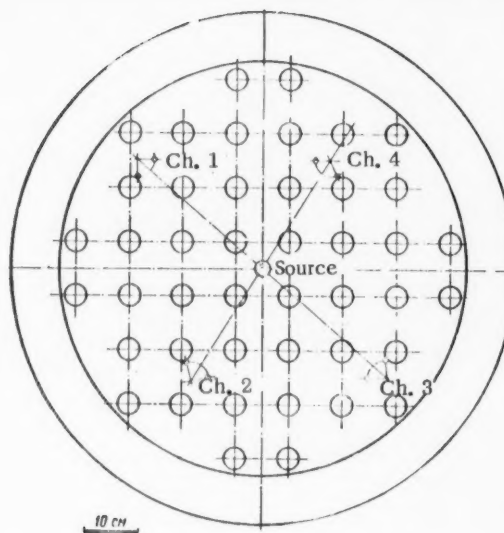


Fig. 2. The arrangement of the neutron detectors and the uranium rods for the measurement of the quantities f_U and f_{Pb} in a tank containing heavy water. (Ch. = channel No.)

TABLE 3

Results of Measurement of f_U and f_{Pb}

Measurement channel No.	Distance from the source, cm	f_U	f_{Pb}	$f_U - f_{Pb}$
2 4	22.4	1.089 ± 0.012	1.053 ± 0.012	0.036 ± 0.017
		1.104 ± 0.013	1.045 ± 0.010	0.059 ± 0.017
2 4	27.5	1.071 ± 0.032	1.018 ± 0.025	0.053 ± 0.039
		1.077 ± 0.035	1.020 ± 0.024	0.057 ± 0.042
1 3	28.4	1.070 ± 0.032	1.010 ± 0.020	0.060 ± 0.032
		1.061 ± 0.035	1.016 ± 0.022	0.045 ± 0.032
Mean value		0.050 ± 0.015		

LITERATURE CITED

[1] I. I. Gurevich, and I. Ya. Pomeranchuk, "Reactor building and reactor theory," Reports of the Soviet Delegation at the International Conference on the Peaceful Uses of Atomic Energy [in Russian] (Izd AN SSSR, Moscow, 1955) p. 220.

[2] M. B. Eglazarov, V. S. Dikarev and V. G. Madeev, AN SSSR Session on the Peaceful Uses of Atomic Energy July 1-5, 1955 (Meeting of the Physics-Mathematics Section) [in Russian] (Izd AN SSSR, Moscow, 1955) p. 53.

[3] N. A. Burgov, AN SSSR Session on the Peaceful Uses of Atomic Energy July 1-5, 1955 (Meeting of the Physics-Mathematics Section) [in Russian] (Izd AN SSSR, Moscow, 1955), p. 67.

[4] Z. I. Gromova, B. G. Dubovskii, A. V. Kamaev and V. V. Orlov, J. Atomic Energy (USSR) 2, 411 (1957).

[5] E. Hellstrand, Private communication.

[6] Nucleonics 10, No. 5, 64 (1952).

[7] E. Cruetz, H. Jupnik, T. Snyder and E. Wigner, J. Appl. Phys. 26, 257, 260, 271 (1955).

[8] V. O. Eriksen, P. W. Meier and P. Schmid, Proceedings of the International Conference on the Peaceful Uses of Atomic Energy 5, UN., N. Y., 1956, p. 105.

[9] P. W. Mummery, Proceedings of the International Conference on the Peaceful Uses of Atomic Energy 5, UN., N. Y., 1956, p. 282.

[10] R. Persson, E. Blomsjö, M. Bustraan and R. Meier, J. Nucl. Energy 3, 3, 188 (1956).

[11] R. L. Macklin and H. S. Pomerance, Progress in Nuclear Energy, Ser. I, 1 (Pergamon Press, London, 1956) p. 179.

[12] D. Hughes, "Neutron Measurements with Nuclear Reactors" [Russian translation] (IL, 1954) p. 180.

[13] V. S. Crocker, Proceedings of the International Conference on the Peaceful Uses of Atomic Energy 5, UN., N. Y., 1956, p. 102.

Received April 23, 1957

THE MEASUREMENT OF THE RESONANCE INTEGRALS OF ABSORPTION
FOR ZIRCONIUM SAMPLES

Yu. P. Dobrynin, G. A. Dorofeev and I. E. Kutikov

The method used by the authors has been developed by P. E. Spivak et al [1] and is based on the measurement of the probability for neutron capture through the perturbation of the neutron field produced by the sample being investigated.

The equipment consisted of a graphite prism $190 \times 190 \times 190 \text{ cm}^3$ with a central cavity $70 \times 70 \times 70 \text{ cm}^3$. The sample was placed at the center of the cavity in the path of a collimated neutron beam from the reactor VVR [2]. The required neutron spectrum was obtained by the use of a cadmium filter.

Sample	Weight of sample (in g)	No. of atoms in 1 cm^2	Admix-ture of hafnium, % by wt.	Admix-ture of hafnium, % of the No. of nuclei	$\int_{0.4 \text{ ev}}^{\infty} \frac{\sigma(E) dE}{E}$, barn	Hafnium contribution barn
Boron	0.256	$0.00374 \cdot 10^{24}$	—	—	375	—
Zirconium	26	$0.0423 \cdot 10^{24}$	0.03	0.015	2.65 ± 0.45	0.42 ± 0.12
Zirconium	27.2	$0.0435 \cdot 10^{24}$	0.04	0.02	3.0 ± 0.35	0.56 ± 0.15
Zirconium	27.2	$0.0435 \cdot 10^{24}$	0.14	0.07	3.4 ± 0.37	1.75 ± 0.6

The neutrons were registered by twelve proportional BF_3 counters uniformly distributed throughout the volume of the prism. A precision counting system enabled the number of pulses to be measured to an accuracy of 0.02%.

As shown in reference [1], the change in the total number of pulses registered in unit time on the introduction into the cavity of the sample being investigated is uniquely connected with the neutron absorption by the sample.

For a thin sample the change in the counting rate of the detecting system can be written in the form

$$\Delta N_x = N_0 - N_x = K F n \Sigma_c,$$

where N_0 is the number of counts in the detecting system without the sample; N_x is the number of counts after the introduction of the sample; K the efficiency of the detecting system; n the number of nuclei per cm^2 of sample; F is the neutron flux.

By comparing the magnitude of the effects for the sample studied, ΔN_x , and for a material with a known value of the capture cross section the required value of the resonance integral Σ_c can be obtained.

The samples investigated were made into disks 22 mm in diameter and 10 mm thick. A sample of the same size, made from a mixture of boric acid and graphite powder and containing 0.256 g of boron, was used as a standard. The total scattering cross section of this sample was the same as that for the zirconium sample. A series of measurements of ΔN_x were made: the absorber sample was repeatedly put into and taken out of the beam, which facilitated the elimination of errors connected with the instability of the apparatus and the obtaining of a sufficiently high statistical accuracy for the measurements.

The value of the resonance integral for boron was taken to be $\Sigma_{cB} = 375 \cdot 10^{-24} \text{ cm}^2$.

Because of the scattering of neutrons in the samples the block effect was small ($n\sigma_s \approx 0.25$); self-absorption was practically absent since the measured effects did not exceed 0.3%. The results of measurement of the resonance integrals are given in the Table.

The evaluation of the contribution of hafnium to the magnitude of the resonance integral was carried out on the basis of measurements made earlier in our laboratory [1]. By comparison with hafnium, the contribution of other impurities is negligible.

The value of the resonance integral for pure zirconium, calculated from the Table, is equal to $(2.3 \pm 0.5) \times 10^{-24}$ and is in satisfactory agreement with the value $3 \cdot 10^{-24}$ given in reference [3], where no errors of measurement are indicated.

LITERATURE CITED

[1] P. E. Spivak and B. G. Erozolimskii, "Physical research," Reports of the Soviet Delegation at the International Conference on the Peaceful Uses of Atomic Energy [in Russian] (Izd AN SSSR, 1955) p. 184.

[2] Yu. G. Nikolaev, "Reactor building and reactor theory," Reports of the Soviet Delegation at the International Conference on the Peaceful Uses of Atomic Energy [in Russian] (Izd AN SSSR, 1955) p. 91.

[3] R. L. Macklin and H. S. Pomerance, Progress in Nuclear Energy, Ser. I, 1 (Pergamon Press, London, 1956) p. 179.

Received May 20, 1957

DEUTERON SPLITTING IN SCATTERING BY NUCLEI

A. G. Sitenko

When a deuteron collides with a nucleus the following processes may occur: elastic deuteron scattering (d, d), inelastic deuteron scattering (d, d'), stripping reactions (d, p) and (d, n) and deuteron splitting (d, np).

The theory of deuteron stripping has been given by Butler [1] who found the angular distribution of the products of the stripping reaction from the condition that the wave functions are continuous on the nuclear surface. Later [2, 3] it was shown that the Born approximation leads to the same results as does Butler's theory. Although it is difficult to justify the use of the Born approximation for nuclear processes in the energy range from 10 to 15 Mev, its success in treating the stripping reaction indicates that it may be possible to apply it also to other similar reactions. Huby and Newns [4] have considered inelastic deuteron scattering by nuclei and obtained results which have since been verified by experiment. In the present note the Born approximation is used to consider the splitting of deuterons by nuclear scattering.

As in the theory of the stripping reaction [2] we shall assume that only the neutron of the deuteron interacts with the nucleus. The differential scattering cross section of the deuteron can then be written in the form

$$d\sigma_d = \frac{2\pi}{\hbar v_0} |V_{if}|^2 \delta(E_f - E_i) \frac{d\vec{x}}{(2\pi)^3} \frac{d\vec{f}}{(2\pi)^3}, \quad (1)$$

$$V_{if} = \int \psi_f^{(s)*}(\vec{r}) e^{-i\vec{k}_d \cdot \vec{r}_d} \chi_{s\mu_d}^* \chi_f^*(\xi) V(r_n, \sigma_n, \xi) \times \\ \times \psi_0(r) e^{i\vec{k}_d \cdot \vec{r}_d} \chi_{1\mu_d} \chi_i(\xi) d\xi d\vec{r} d\vec{r}_d, \quad (2)$$

where $\chi_i(\xi)$ and $\chi_f(\xi)$ are the wave functions of the nucleus in the initial and final states, $\chi_{1\mu_d}$ and $\chi_{s\mu_s}$ are the spin functions of the deuteron and the $n + p$ system in the final state (where $s = 1$ and 0), $\psi_0(r) = (\alpha/2\pi)^{1/2} \cdot [\exp(-\alpha r)]/r$ is the wave function of the deuteron ground state;

$$\psi_f^{(s)}(\vec{r}) = \exp(i\vec{f} \cdot \vec{r}) - \exp(-i/r)/(z_s - i) r -$$

is the wave function of the $n + p$ system in the final state (with $z_1 = \alpha = (M_d/\hbar^2)^{1/2}$, where ϵ is the deuteron binding energy, and $\alpha_0 = (M_{n'}/\hbar^2)^{1/2}$, where ϵ' is the energy of the virtual deuteron level), \vec{f} is the wave vector of the neutron-proton relative motion, \vec{k}_d is the wave vector of the incident deuteron, and \vec{k} is the wave vector of the center of mass of the $n + p$ system in the final state.

The neutron interacts with the nucleus only at the nuclear surface, so that

$$\int \chi_{s\mu_d}^* \chi_f^*(\xi) V(r_n, \sigma_n, \xi) \chi_{1\mu_d} \chi_i(\xi) d\xi = \\ = \frac{\delta(r_n - R)}{r_n^2} \sum_{l, m} \langle \mu_f \mu_s | V | \mu_i \mu_d l m \rangle Y_{lm}^*(\Omega_n),$$

where R is the nuclear radius and \mathbf{l} is the angular momentum transferred by the neutron to the nucleus. Going over from the variables \mathbf{r} and \mathbf{r}_d to \mathbf{r} and \mathbf{r}_n and integrating (2) over $d\mathbf{r}_n$, we obtain the matrix element for the transition probability in the form

$$V_{if} = \int \varphi_f^{(s)*}(\mathbf{r}) \varphi_0(\mathbf{r}) e^{\frac{i}{2} \mathbf{q} \cdot \mathbf{r}} d\mathbf{r} \sum_{l, m} 4\pi (-i)^l \times \\ \times \langle \mu_f \mu_s | V | \mu_i \mu_d | l m \rangle Y_{lm}(\Omega_q) j_l(qR),$$

where $\mathbf{q} = \mathbf{k} - \mathbf{k}_0$.

Averaging the square modulus of this matrix element over the spin projections in the initial state and summing over spin projections in the final state, we obtain

$$\frac{1}{3(2j_i+1)} \sum_{\mu_i \mu_d \mu_f \mu_s} |V_{if}|^2 = \\ = \left| \int \varphi_f^{(s)*}(\mathbf{r}) \varphi_0(\mathbf{r}) e^{\frac{i}{2} \mathbf{q} \cdot \mathbf{r}} d\mathbf{r} \right|^2 \times \\ \times \sum_l \frac{\pi^3 \hbar^4}{M^3} |B_l^{(s)}|^2 j_l^2(qR),$$

where

$$|B_l^{(s)}|^2 = \frac{4M^3}{3\pi(2j_i+1)\hbar^4} \sum_{\mu_f \mu_s \mu_i \mu_d} |\langle \mu_f \mu_s | V | \mu_i \mu_d | l m \rangle|^2$$

Thus the differential scattering cross section for the deuteron is

$$d\sigma_d^{(s)} = \sum_l |B_l^{(s)}|^2 \frac{\hbar^2}{2M\omega_0} \times \\ \times \left| \int \varphi_f^{(s)*}(\mathbf{r}) \varphi_0(\mathbf{r}) e^{\frac{i}{2} \mathbf{q} \cdot \mathbf{r}} d\mathbf{r} \right|^2 j_l^2(qR) \times \\ \times \delta \left\{ \epsilon_{fi} + \frac{\hbar^2 f^2}{M} + \frac{\hbar^2 \omega^2}{4M} + \epsilon - \frac{\hbar^2 \omega_0^2}{4M} \right\} d\mathbf{q} \frac{d\mathbf{f}}{(2\pi)^3}, \quad (3)$$

where ϵ_{fi} is the difference in energy between the initial and final nuclear states. The quantity $B_l^{(s)}$ can be treated as an undetermined coefficient entering into the theory. The summation is taken over those values of l which are given by the selection rules

$$\vec{j}_f = \vec{j}_i + \vec{l} + \vec{1}, \quad s=0, \\ \vec{i}_f = \vec{i}_i + \vec{l}, \quad s=1.$$

Noting that

$$\int \varphi_f^{(s)*}(\mathbf{r}) \varphi_0(\mathbf{r}) e^{\frac{i}{2} \mathbf{q} \cdot \mathbf{r}} d\mathbf{r} = \sqrt{8\pi\alpha} \times \\ \times \left\{ \frac{1}{\alpha^2 + \left(\frac{\mathbf{f} - \frac{\mathbf{q}}{2}}{2} \right)^2} + \frac{1}{q(i\alpha_s - f)} \ln \frac{\mathbf{f} + \frac{\mathbf{q}}{2} + i\alpha}{\mathbf{f} - \frac{\mathbf{q}}{2} + i\alpha} \right\}, \quad (4)$$

and integrating (3) over $d\mathbf{f}$, we obtain the momentum distribution for the center of mass for the $n + p$ system in the form

$$\begin{aligned}
d\sigma_d^{(s)} = & \sum_l |B_l^{(s)}|^2 \frac{f}{\pi x_0} \frac{\alpha}{2\pi} \times \\
& \times \left\{ \frac{1}{f^2} \left[\frac{1}{\alpha^2 + \left(f - \frac{q}{2} \right)^2} - \frac{1}{\alpha^2 + \left(f + \frac{q}{2} \right)^2} \right] + \right. \\
& + \frac{2}{f^2} \ln \frac{\alpha^2 + \left(f + \frac{q}{2} \right)^2}{\alpha^2 + \left(f - \frac{q}{2} \right)^2} R_l \frac{1}{i\alpha_s - f} \times \\
& \times \ln \frac{f + \frac{q}{2} + i\alpha}{f - \frac{q}{2} + i\alpha} + \frac{2}{q^2 (\alpha^2 + f^2)} \times \\
& \times \left. \left| \ln \frac{f + \frac{q}{2} + i\alpha}{f - \frac{q}{2} + i\alpha} \right|^2 \right\} j_l^2(qR) d\vec{\alpha}, \tag{5}
\end{aligned}$$

where

$$f^2 = \frac{1}{4} x_0^2 - \frac{1}{4} x^2 - \frac{M}{\hbar^2} (\varepsilon + \varepsilon_{fi}).$$

If we assume that $q r_{\text{eff}} \ll 1$ ($r_{\text{eff}} \sim 1/\alpha$), Equation (5) simplifies to

$$d\sigma_d^{(1)} = \sum_l |B_l^{(1)}|^2 \frac{\alpha}{3\pi x_0} \frac{f^2 q^2}{(\alpha^2 + f^2)^4} j_l^2(qR) d\vec{\alpha}, \quad s=1; \tag{6}$$

$$\begin{aligned}
d\sigma_d^{(0)} = & \sum_l |B_l^{(0)}|^2 \frac{\alpha}{\pi x_0} \frac{f (\alpha - \alpha_0)^2}{(\alpha^2 + f^2)^2 (\alpha_0^2 + f^2)} j_l^2(qR) d\vec{\alpha}, \\
s = 0. \tag{7}
\end{aligned}$$

If the wave function of the final state of the $n + p$ system is taken as $\varphi_0(r)$, we obtain a formula for the deuteron inelastic scattering cross section [4], namely

$$d\sigma_s = \sum_l |B_l^{(1)}|^2 \frac{\alpha}{\pi x_0} \left[\frac{4\alpha}{q} \operatorname{arctg} \frac{q}{4\alpha} j_l(qR) \right]^2 d\alpha. \tag{8}$$

Noting that $\vec{f} = \frac{1}{2} (\vec{k}_n - \vec{k}_p)$ and $\vec{\kappa} = \vec{k}_n + \vec{k}_p$ (\vec{k}_n and \vec{k}_p are the wave vectors of the neutron and proton liberated), Equation (3) can be written in the form

$$\begin{aligned}
d\sigma_d^{(s)} = & \sum_l |B_l^{(s)}|^2 \frac{\alpha k_n}{2\pi^2 x_0} \left| \frac{1}{\alpha^2 + \left(\frac{1}{2} x_0 - k_p \right)^2} + \right. \\
& + \frac{1}{|\vec{k}_n + \vec{k}_p - \vec{x}_0|} \cdot \frac{1}{i\alpha_s - \frac{1}{2} |\vec{k}_n - \vec{k}_p|} \times \\
& \times \ln \frac{|\vec{k}_n - \vec{k}_p| + |\vec{k}_n + \vec{k}_p - \vec{x}_0| + 2i\alpha}{|\vec{k}_n - \vec{k}_p| - |\vec{k}_n + \vec{k}_p - \vec{x}_0| + 2i\alpha} \times \\
& \times j_l^2(|\vec{k}_n + \vec{k}_p - \vec{x}_0| R) d\vec{k}_p d\alpha_n, \\
k_n^2 = & \frac{1}{2} x_0^2 - \frac{2M}{\hbar^2} (\varepsilon + \varepsilon_{fi}) - k_p^2. \tag{9}
\end{aligned}$$

This expression gives the differential angular and energy distributions of the neutrons and protons liberated in deuteron splitting. It is not in general possible to integrate Equation (9). If $f_{\text{eff}} \ll \kappa$, the momentum distributions of the neutrons and protons is given approximately by (5) or by (6) and (7).

The author expresses his sincere gratitude to N. A. Vlasov for helpful discussions.

LITERATURE CITED

- [1] S. Butler, Proc. Roy. Soc. 208A, 559 (1951).
- [2] A. Bhatia et al., Phil. Mag. 43, 485 (1952).
- [3] P. Daitch and J. French, Phys. Rev. 87, 900 (1952).
- [4] R. Huby and H. Newns, Phil. Mag. 42, 1442 (1951).
- [5] J. Haffner, Phys. Rev. 103, 1398 (1956).

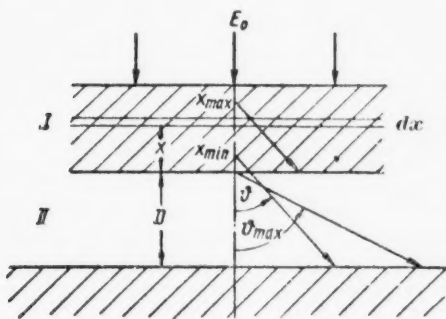
Received June 26, 1957

IONIZATION LOSSES BELOW THE THRESHOLD IN A PULSE IONIZATION DOSIMETER OF FAST NEUTRONS

Yu. I. Petrov

In the absolute measurements of neutron doses, a considerable difficulty is caused by the γ -background which usually accompanies a beam of neutrons. Therefore, the proportional counter working on the principle of a small tissue-equivalent chamber, proposed by Hurst [1-4] and which has received widespread use abroad, deserves attention.

The elimination of the γ -background is based on the sharp difference between the specific ionizations of recoil protons and electrons. The small potential pulses produced by the electrons are "cut off" by the threshold discriminator of the amplifier. The total ionization produced by the recoil proton is measured by a special pulse-amplitude integrator [5]. A considerable disadvantage of this method is the uncontrolled ionization losses below the threshold. The tentative calculations of Hurst [1], leading to the conclusion that these losses are negligible, are not applicable to a real counter.



The escape of recoil protons from a thick radiator into the gas-filled slit.

angle θ , end either on the lower, or on the upper, boundary layers of the gas-filled slit (in the figure, x_{\min} and x_{\max}), and also enables the calculation of the limiting emission angle θ_{\max} of the recoil protons, at which angle the protons emitted can still reach the lower boundary of the gas-filled slit.

Let us introduce the following symbols: E_0 is the energy of the registered neutrons; B is the threshold of the registration system; ν is the neutron flux in neutrons per $\text{cm}^2 \text{ sec}$; N is the number of hydrogen atoms in 1 cm^3 of the radiator; $\sigma(E_0)$ is the cross section for the scattering of neutrons of energy E_0 on hydrogen; A is the area of the radiator, which is assumed to be sufficiently large to exclude edge effects; D is the slit thickness in centimeters; k and n are the constants in the range-energy relation $R = kE^n$; $f(R)$ and $F(R)$ is the proton

The results of an accurate calculation of the sub-threshold ionization losses are given below for the case when the recoil protons from a thick infinite flat radiator enter a gas-filled slit, with the neutrons being normally incident on the surface of the radiator (see Figure).

Let us assume that the n-p scattering is spherically symmetrical in the center-of-mass system, that the radiator thickness is greater than the range of the most energetic recoil proton and that the thickness of the gas-filled slit is less than the range of a proton of energy 0.4 Mev. This limitation of the slit thickness is useful because in the energy interval of 0.4 to 10 Mev the proton range-energy relation for a large number of light substances (H_2 , C_2H_2 , C_2H_6 , $(\text{CH})_n$ and others) can be correctly represented by the relation $R = kE^{1.73}$. This relation enables the determination of those limiting positions of infinitely-thin layers inside the radiator for which the recoil-proton ranges, for a given emission

energy corresponding to a range R in the gas and the radiator, respectively; R_I^B is the range of a proton of energy B in the radiator; $R_{II}^{\min} = \frac{D}{\cos \theta}$; $R^B = kE_0^n \cos^{2n} \theta$; θ_{\max} and θ_1 are given by the relations:

$$\cos \theta_{\max} = \left(\frac{D}{k_{II} E_0^{\frac{1}{n}}} \right)^{\frac{1}{2n+1}}; \quad E_0 \cos^2 \theta_1 = B.$$

The subscripts I and II refer to the radiator and the gas, respectively.

The total measured energy losses of the recoil protons in the gas-filled slit, when $E_0 < \left(\frac{k_{II} n B}{D} \right)^{\frac{1}{1-n}}$, are given by the relation

$$\epsilon' = 2\gamma N \sigma (E_0) A [\epsilon'_1 + \epsilon'_2 + \epsilon'_3], \quad (1)$$

where

$$\begin{aligned} \epsilon'_1 = \frac{k_I}{k_{II}} \left\{ \int_0^{\theta_{\max}} \sin \theta \cos^2 \theta d\theta \left[\int_{R_{II}^{\min}}^{R_I^B} f(R) dR - \right. \right. \\ \left. \left. - \int_0^{(R_I^B - R_{II}^{\min})} f(R) dR \right] - \frac{k_{II} E_0^n B}{2n+3} \left[1 - \left(\frac{D}{k_{II} E_0^n} \right)^{\frac{2n+3}{2n+1}} \right] + \right. \\ \left. + \frac{BD}{2} \left[1 - \left(\frac{D}{k_{II} E_0^{\frac{1}{n}}} \right)^{\frac{2}{2n+1}} \right] \right\}; \end{aligned} \quad (2)$$

$$\begin{aligned} \epsilon'_2 = \int_0^{\theta_{\max}} \sin \theta \cos^2 \theta d\theta \left[\int_{R_I^B}^{\frac{DK_I}{k_{II} \cos \theta}} F(R) dR - \right. \\ \left. - \frac{BD k_I}{2k_{II}} \left[1 - \left(\frac{D}{k_{II} E_0^n} \right)^{\frac{2}{2n+1}} \right] + \right. \\ \left. + \frac{BR_I^B}{3} \left[1 - \left(\frac{D}{k_{II} E_0^n} \right)^{\frac{3}{2n+1}} \right]; \right. \end{aligned} \quad (3)$$

$$\begin{aligned} \epsilon'_3 = \int_{\theta_{\max}}^{\theta_1} \sin \theta \cos^2 \theta d\theta \left[\int_{R_I^B}^{R_I^B} F(R) dR - \right. \\ \left. - \frac{B k_I E_0^n}{2n+3} \left[\left(\frac{D}{k_{II} E_0^{\frac{1}{n}}} \right)^{\frac{2n+3}{2n+1}} - \left(\frac{B}{E_0} \right)^{\frac{2n+3}{2}} \right] + \right. \\ \left. + \frac{BR_I^B}{3} \left[\left(\frac{D}{k_{II} E_0^n} \right)^{\frac{3}{2n+1}} - \left(\frac{B}{E_0} \right)^{\frac{3}{2}} \right]. \right. \end{aligned} \quad (4)$$

In order to calculate the actual energy losses of the recoil protons in the gas filled slit (ϵ), it is necessary to put $B = 0$ in Equations (2)-(4) and replace the limits of integration in Equation (4) and (3): $\theta_1 \rightarrow \frac{\pi}{2}$, $R_I^B \rightarrow 0$.

The calculations were carried out by means of numerical integration for the system polystyrene-acetylene, taking into account the actual range-energy curve obtained from the data of reference [6].

TABLE 1

 $D=1$ cm

E_0 , Mev	1	2	3	
$\frac{\epsilon'}{\epsilon}$	$B=0.05$ Mev	0.884	0.875	0.845
$\frac{\epsilon'}{\epsilon}$	$B=0.1$ Mev	0.767	0.748	0.691

TABLE 2

 $D=4$ cm

E_0 , Mev	2	5	
$\frac{\epsilon'}{\epsilon}$	$B=0.1$ Mev	0.800	0.885
$\frac{\epsilon'}{\epsilon}$	$B=0.2$ Mev	0.780	0.770

TABLE 3

The Contribution of Recoil Protons from the Radiator to the Total Ionization in 1 cm^3 of the Gas

E_0 , Mev	$D=1$ cm			$D=4$ cm	
	1	2	3	2	5
$\frac{\Delta}{I}$	0.500	0.773	0.852	0.443	0.830

For polystyrene $R = 2 \cdot 10^{-3} E^{1.73}$ (R in cm, E in Mev). The range of a proton of a given energy is 955 times longer in acetylene (15°C , 760 mm) than it is for polystyrene.

The ratio of ϵ' , the registered energy losses of the recoil protons, to ϵ , the actual energy losses, is given in Tables 1 and 2 for a number of values of E_0 , B and D.

According to Equation (1), the recoil protons, leaving the radiator, in 1 cm^3 of the gas lose an amount of energy

$$\Delta = 2(\epsilon_1 + \epsilon_2 + \epsilon_3) \frac{\sqrt{N\sigma(E_0)}}{D}. \quad (5)$$

Since polystyrene and acetylene have the same composition (CH group), the total energy losses of the recoil protons from the radiator and the gas, per cm^3 of gas, are determined by the equation

$$I = \frac{\sqrt{N\sigma(E_0)} E_0}{2\rho}, \quad (6)$$

where $\rho = 955$ is the ratio of the numbers of CH groups in a unit volume of polystyrene and acetylene.

The value of the ratio Δ/I for several values of the neutron energy are given in Table 3.

From the Table it follows that if the width of the slit is comparable with the proton range ($D = 1$ cm corresponds to the range of a proton of 0.65 Mev, while $D = 4$ cm to the range of a proton of 1.55 Mev), then the "gas effect" and the "radiator effect" are approximately the same. As the energy of the incident neutrons is increased the "radiator effect" becomes bigger.

The data of Tables 1 and 2 show that for real measurements, when the threshold reaches a value $B = 0.1$ to 0.2 Mev [1], the uncontrolled ionization losses can be of the order of several tenths of one %. For example, with $D = 1$ cm; $E_0 = 3$ Mev and $B = 0.1$ Mev the losses amount to 31%, whereas according to Hurst's evaluation they should be $\sim 0.1\%$.

The author considers it his duty to express his gratitude to V. V. Miller for valuable advice and to V. N. Popov for help with the calculations.

LITERATURE CITED

- [1] G. S. Hurst, Brit. J. Rad. 27, No. 318, 353 (1954).
- [2] G. S. Hurst and Ritchie, Radiology 60, No. 6, 846 (1953).

- [3] T. A. Barr, and G. S. Hurst, Nucleonics 12, No. 8, 33 (1954).
- [4] G. W. Cure, and G. S. Hurst, Nucleonics 12, No. 8, 36 (1954).
- [5] F. M. Glass and G. S. Hurst, Rev. Sci. Instr. 23, 67 (1952).
- [6] J. O. Hirschfelder and J. L. Magee, Phys. Rev. 73, 207 (1948).

Received May 24, 1957

A COMPARISON OF THE STANDARD NEUTRON SOURCES OF THE USSR AND SWEDEN

G. A. Dorofeev, I. E. Kutikov and A. M. Kucher

The standardization of the neutron sources was carried out in a number of laboratories in the USSR by various methods [1-5]. The results of these measurements agree to within 10%.

Similar measurements of the absolute intensity of neutron sources were carried out in other countries and the results of the calibrations have been compared [6].

The determination of the absolute neutron fluxes is important for the measurement of the atomic constants. Therefore, the comparison of the results of the measurements in the USSR with the data from other countries is of considerable interest.

A relative comparison of the neutron source H-26 of the USSR and that of Sweden was carried out in the beginning of April 1957, during a special trip to Stockholm by A. M. Kucher.

The USSR source H-26 was calibrated in 1952 by Davidenko and Kucher [4]. Its intensity, according to the data of these authors, was

$$Q_{H-26} = (4.70 \pm 0.30) \cdot 10^6 \text{ neutrons/sec}$$

The intensity of the Swedish source, denoted in the following by Q_1 and calibrated in 1952-1954 by Larsson, was

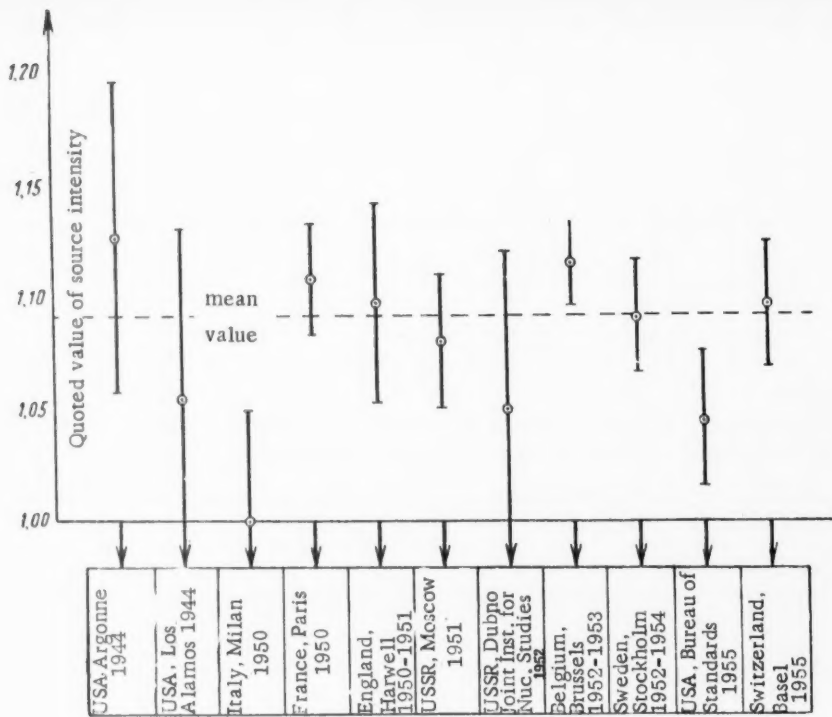
$$Q_1 = (2.65 \pm 0.05) \cdot 10^6 \text{ neutrons/sec}$$

The comparison of the intensities of the USSR source H-26 and that of Sweden was carried out in a large tank, filled with a solution of boric acid, by the determination of the distribution of neutron density in the tank by two long proportional BF_3 counters.

In this method, the ratio of the intensities of the sources being compared is expressed as the ratio of the areas enclosed by the curves giving the distribution of neutron density:

$$\frac{Q_1}{Q_2} = \frac{\int_0^{\infty} J_1 r dr}{\int_0^{\infty} J_2 r dr}.$$

A correction was introduced into this ratio to take into account the self-absorption in the sources, the correction being taken equal to 1.01 for the Stockholm source and 1.005 for the USSR source H-26, which was somewhat smaller in size.



Results of absolute measurements of neutron source intensities.

As a result of these measurements it was found that

$$\frac{Q_{H-26}}{Q_1} = 0.1856 \pm 0.7\%.$$

From this, taking $Q_1 = (2.65 \pm 0.05) \cdot 10^6$ neutrons/sec, we obtain

$$Q_{H-26} = (4.92 \pm 0.11) \cdot 10^6 \text{ neutrons/sec [8].}$$

At the end of April 1957, during a visit to Moscow by Dr. Larsson, a comparison of the neutron source H-22 was carried out by Dr. Spivak and Erozolimskii [3] and according to the data of these authors its intensity was

$$Q_{H-22} = (5.96 \pm 0.17) \cdot 10^6 \text{ neutrons/sec.}$$

The comparison of the sources was made in a large graphite prism. The source was placed at the center of the prism. Neutrons were detected by a group of BF_3 counters placed in the prism at a distance of 150 cm from the source.

Where the measurements were made	Year of calibration	Absolute value of $Q \cdot 10^4$ neutrons per second	Experimental error, %	Method used for the absolute calibration	The sources compared	Quoted value for the intensity
USA (Argonne)	1944	5.5	7	The determination of the quantity of He^4 produced as the result of the reaction $\text{Be}^8(n, \alpha)\text{Li}^7$	Argonne — Los Alamos — Brussels	1.127
USA (Los Alamos)	1944	5.80	7.5	Water tank method. Determination of the absolute number of interactions $\text{Be}^8(n, \alpha)\text{Li}^7$	Los Alamos — Harwell — Bureau of Standards	1.056
Italy (Milan)	1950	3.12	5	Water-tank method. Determination of the absolute number of interactions $\text{Li}^6(n, \alpha)\text{He}^4$	Milan — Paris — Brussels	1.000
France (Paris)	1950	5.3	2.5	Activation of a solution of Mn salt. Absolute β counting with a 4π counter	Paris — Harwell — Brussels	1.108
England (Harwell)	1950-1954	9.66	4.5	Reactor oscillator method. Absolute determination of the Na^{24} and p^{21} activities ($\beta - \gamma$ coincidence and β counting in a definite solid angle)	Harwell — Paris — Stockholm — Los Alamos	1.097
USSR (Moscow)	1951	5.96	3	Comparison of the source intensity with the "flow" of thermal neutrons in a graphite prism. Absolute determination of the Au^{198} activity	Moscow — Stockholm	1.080
USSR Joint Institute for Nuclear Research (Brussels)	1952	0.47	7	Activation of an aqueous solution of KMnO_4 and the absolute determination of Mn^{55}	Joint Institute for Nuclear Research — Stockholm — Brussels — Argonne — Basel	1.040
Belgium (Brussels)	1952-1953	7.87	2	Water-tank method. Absolute determination of the Au^{198} activity by the method of $\beta - \gamma$ coincidences	Milan — Stockholm — Basel — Brussels	1.115
Sweden (Stockholm)	1952-1954	2.65	2.5	Water-tank method. Correlated-particle method. Counting of recoil protons. Determination of the absolute number of interactions $\text{Be}^8(n, \alpha)\text{Li}^7$, of Au^{198} activity, of α -particles from the reaction $\text{H}^3(d, n)\text{He}^4$. Absolute determination of the current.	Stockholm — Harwell — Basel — Brussels	1.090
USA (Bureau of Standards)	1955	1.265	3	Water-tank method. Determination of the absolute number of interactions $\text{Be}^8(n, \alpha)\text{Li}^7$. Absolute determination of Mn activity	Bureau of Standards — Los Alamos — Argonne	1.045
Switzerland (Basel)	1955	1.51	2.8	Water-tank method. Absolute determination of Au^{198} activity	Basel — Stockholm — Milan — Harwell — Brussels	1.096

With this method of comparing neutron sources, differences in shape and in the material of the sheath are not important. The ratio of the source intensities was obtained from the ratio of the counting rates. The total error of the relative measurements did not exceed 0.5%.

In addition, during these measurements a comparison was made of the standard sources indicated with the source H-26.

As a result of the measurements a comparison was made of the standard sources indicated with the source H-26.

As a result of the measurements it was found that

$$\frac{Q_1}{Q_{H-22}} = 0.439 \pm 0.5\%$$

and

$$\frac{Q_{H-26}}{Q_{H-22}} = 0.082 \pm 0.5\%.$$

Taking $Q_{H-22} = (5.96 \pm 0.17) \cdot 10^6$ neutrons/sec, according to the data of Spivak and Erozolimskii, then for the Stockholm source

$$Q_1 = (2.62 \pm 0.08) \cdot 10^6 \text{ neutrons/sec}$$

and for H-26

$$Q_{H-26} = (4.89 \pm 0.13) \cdot 10^5 \text{ neutrons/sec}$$

which is in good agreement with the data of Dr. Larsson:

$$Q_1 = (2.65 \pm 0.05) \cdot 10^6 \text{ neutrons/sec}$$

and with the data of Davidenko and Kucher

$$Q_{H-26} = (4.70 \pm 0.30) \cdot 10^5 \text{ neutrons/sec}$$

The Stockholm source was compared with the standard sources of England, Switzerland and Belgium.

The latest data on the absolute and relative measurements of the standard sources of various countries are given in the Table and the Figure.*

The intensity of the Italian source has been arbitrarily taken as unity.

It must be pointed out that the table of standard neutron sources does not altogether represent the absolute values of the intensities as of April 1957 because the intensity of Ra- α -Be sources increases with time on account of the accumulation of the isotope Po²¹⁰ in the radium decay products [9-10].

* These data were kindly communicated to us by Dr. Larsson.

Therefore, the value of the intensity of each neutron source in 1957 must be corrected by taking into account the date at which the radium of the given standard was prepared and the interval of time between the date of calibration and April 1957. The equation giving the correction is

$$Q = Q_0 \frac{1 + 0.17 [1 - e^{-\frac{0.7}{T} (t_1 + t_2)}]}{1 + 0.17 (1 - e^{-\frac{0.7}{T} t_1})},$$

where Q is the intensity of the neutron source at the present time; Q_0 is its intensity at calibration; t_1 the time interval between the preparation of the radium and the calibration of the source; t_2 the time interval which has elapsed after calibration; T is the half-life of isotope RaD (22 years) which determines the rate at which Po^{210} accumulates.

For the USSR sources H-22 and H-26 the corrections amount to 1.8 and 2.5%; their intensities at the present time are $6.07 \cdot 10^6$ and $4.82 \cdot 10^6$ neutrons/sec, respectively.

The intensity of the Stockholm source at the same time, according to Larsson's data is $(2.68 \pm 0.06) \times 10^6$ neutrons/sec.

We consider it a pleasant duty to express our gratitude to Dr. S. Edlund and Dr. K. Larsson for their kind cooperation during the comparison of USSR and Swedish sources.

LITERATURE CITED

- [1] V. M. Bezotosnyi and Yu. C. Zamyatnin, *J. Atomic Energy (USSR)* 2, 4, 313 (1957).
- [2] K. A. Petrzhak, M. A. Bak and B. A. Fersman, *J. Atomic Energy (USSR)* 2, 4, 319 (1957).
- [3] B. G. Erozolimskii and P. E. Spivak, *J. Atomic Energy (USSR)* 2, 4, 327 (1957).
- [4] V. A. Davidenko and A. M. Kucher, *J. Atomic Energy (USSR)* 2, 4, 334 (1957).
- [5] N. N. Flerov and V. M. Talyzin, *J. Atomic Energy (USSR)* 3, 10, 291 (1957).
- [6] D. J. Hughes, *Nucleonics* 12, No. 12, 26 (1957).
- [7] K. E. Larsson, *Ark. f. Fys.* Bd 7, No. 25, 1954; *Ark. f. Fys.* Bd 9 No. 18 (1955).
- [8] K. E. Larsson, *Record of Measurements in Stockholm*, [in Russian] (1957).
- [9] E. Bretscher, G. B. Cook, G. R. Martin and D. H. Wilkinson, *Proc. Roy. Soc.* 196 A, 436 (1949).
- [10] A. De Troyer, and G. C. Tavernier, *Bulletin de la classe des sciences*, 5 ser. 50, 150 (1954).

Received May 20, 1957

V
3
/
I
C
-
3

SCINTILLATIONS PRODUCED BY α PARTICLES IN HELIUM AT HIGH PRESSURES

S. A. Baldin, V. V. Gavrilovskii and F. E. Chukreev

The investigation of scintillations, occurring in helium when a charged particle passes through it, was undertaken in an attempt to develop a sufficiently effective method for the measurement of the degree of polarization of neutron beams of energy from 2 to 20 Mev, based on the registration of coincidences between the scattered neutron and the recoil nucleus in a gas scintillation chamber filled with helium at a pressure of a few tens of atmospheres.

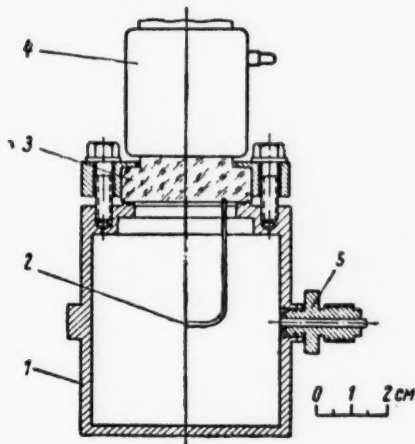


Fig. 1. Schematic diagram of the gas chamber.
1) Chamber case; 2) Po²¹⁰ specimen; 3) plexiglas window; 4) FEU-19M; 5) connection for evacuation and introduction of gas.

A specimen of Po²¹⁰ served as the source of α -particles with an intensity of about 1000 particles per sec. The registration of scintillations in the gas was made by a photomultiplier FEU-19M.

The counting rate, for a given discrimination level of the registering apparatus and a fixed multiplier amplification, served as the measure of the magnitude of the scintillation intensity. To improve the signal-to-noise ratio the optimum distribution of potentials on the dynodes was chosen.

The first experiments, carried out with technical helium from cylinders (pressure 150 atm, containing nominally about 0.03% of impurities), showed that the light yield depends on the degree of purity of the gas and changes considerably from cylinder to cylinder. Therefore, in further work, the cleaning of the gases used

Up to the present time only a comparatively small number of papers, dealing with scintillation phenomena in gases, have been published. The data existing in the literature mainly refer to argon, krypton, and xenon at comparatively low pressures (5-10 atm). These investigations, in a number of cases are not sufficiently detailed or systematic and their results are not always completely definite [1-5].

We have carried out a systematic investigation of the intensity of the light flashes occurring in helium and its mixtures with various gases under the action of polonium α -particles. The dependence of the light yield on the pressure in the interval 1-80 atm and on the concentration of the various admixtures to the helium (xenon, neon, nitrogen, oxygen and argon) was determined.

For the investigation of the scintillation properties of gaseous mixtures a steel chamber was used which was intended for operation at a pressure of 150 atm (Fig. 1). The internal walls of the chamber were covered with magnesium oxide. The window was tightened by pressing a steel flange onto the plexiglas.

from the impurities contained in them was carried out by means of activated coal, cooled to liquid nitrogen temperature. Particular attention was paid to the cleanliness of the connecting attachments.

In considering the question of the criterion for the purity of the helium used in our experiments, it is necessary to point out that the problem is one of finding extremely small amounts of impurities, for example, the addition of nitrogen or oxygen to the purified helium appreciably changes the light yield even at concentrations of $\sim 10^{-3}\%$. The role played by the impurities is most clearly seen in the investigation of the dependence of the light yield on the pressure. Thus, in the case of technical helium the counting rate decreases substantially with rising pressure from 5 to 80 atm (Fig. 2, Curve II). Depending on the time taken for purification, the characteristic curve "counting rate-pressure" gradually changes. For helium which had been subject to purification for an hour or more a rise of the counting rate with pressure was observed (Curve I). A further increase of the purifying time did not lead to a change in the curve "counting rate-pressure." The linear increase of the counting rate with increasing pressure was then adopted as a practical criterion for the purity of the helium. A qualitative spectral analysis of the purified helium showed that the spectrum of helium, purified in this way, was markedly different from the spectrum of helium which had not been sufficiently thoroughly purified. In the former spectrum the lines of gases other than helium are practically absent, with the exception of weak lines of hydrogen which is apparently given off by the discharge-tube walls.

The method used by us for working with gases enabled us to obtain results which were reproducible and stable in time.

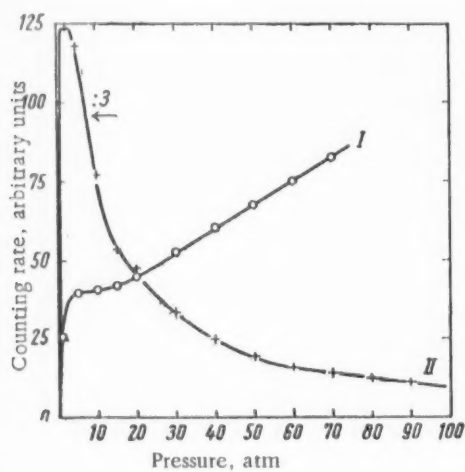


Fig. 2. The counting rate as a function of the pressure for pure (Curve I) and technical (Curve II) helium.

The results of the investigation of the dependence on the pressure of the scintillation properties of pure helium are given in Figure 2 (Curve I). After a sharp rise of the counting rate with increasing pressure from 0 to 2 atm and a small plateau extending to 10 atm, a practically linear increase of the scintillation intensity with pressure is observed. The amplitude of the pulses at any given pressure does not exceed the amplitude of the amplifier noise.

It is very difficult to separate the mixtures investigated into any definite groups according to the nature of the dependence of the light yield on the pressure and on the concentration of impurities in the helium even if some mixtures have many features in common. This refers, for example, to such mixtures as He + Xe and He + Ne. Figure 3 gives the dependence of the quantity

$$\eta_{\text{Xe}} = \frac{N_{\text{He}}^{\text{Xe}} - N_{\text{He}}}{N_{\text{He}}}$$

(where $N_{\text{He}}^{\text{Xe}}$ and N_{He} are the counting rates for a mixture of helium with xenon and for pure helium) on the xenon concentration. The total pressure is 5 atm. In the region of concentrations from 0.03 to 0.3% a small, but quite distinct, decrease of the counting rate is observed as compared with pure helium. In the case of neon this decrease is very marked; at a neon concentration of about 0.3% and a total pressure of 5 atm the value of $\eta_{\text{Ne}} = 0.3$.

With a further increase of the xenon or neon concentration in the helium (above 1%) the light yield rises monotonically; in the case of xenon this increase is considerably smaller than that for neon. Thus, at a neon concentration equal to 3% and a total pressure of 5 atm $\eta_{\text{Ne}} = 0.7$, while under the same conditions η_{Xe} is equal to 16.

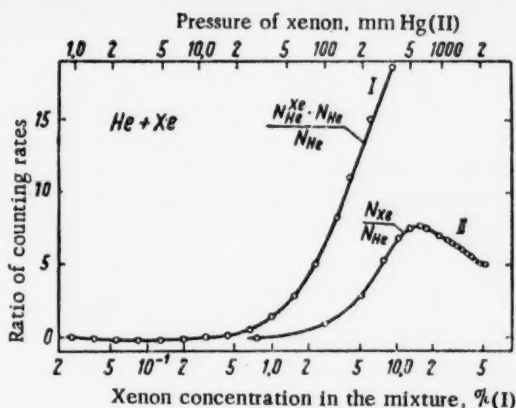


Fig. 3. The ratios of the counting rates for pure xenon and for the mixture He + Xe to the counting rate for pure helium as a function of the xenon pressure. The total pressure of the mixture is 5 atm. N_{He} — the counting rate for pure helium at a pressure of 5 atm; N_{He}^{Xe} and N_{He}^{Xe} are the counting rates for pure xenon and for the mixture He + Xe, respectively.

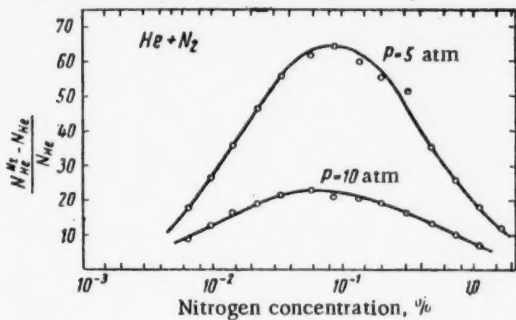


Fig. 4. The relative increase of the counting rate for the mixture He + N₂ as a function of the N₂ concentration. N_{He} and N_{He}^{N2} are the counting rates for pure helium and for the mixture He + N₂, respectively; P is the pressure of the mixture.

of the scintillation intensity as a function of the nitrogen and oxygen concentrations. While the maximum value of η_{N_2} at 10 atm is about three times smaller than the value at 5 atm, the maximum values of η_{O_2} are practically the same at these pressures, but the maxima are observed at different concentrations of the impurity. In addition, the scintillation intensities for these mixtures differ markedly one from the other. Thus, at the optimum concentration of oxygen in the helium the counting rate is only 3.5 times higher than the counting rate in pure helium, while the pulse amplitude does not exceed the amplifier noise level. In the case of a mixture of helium and nitrogen, however, the counting rate is 60-70 times higher than for pure helium, while the pulse amplitude is 8-10 times bigger than the amplitude of the amplifier noise. It must be pointed out that the

The curves "counting rate — pressure" for the mixtures He + Xe and He + Ne are similar. This curve for the mixture He + 3% Ne is given in Figure 7 by Curve II, which after a sharp rise with an increase in pressure to 5 atm monotonically increases with increasing pressure up to 80 atm.

It must be pointed out that spectrally-pure neon and xenon, under the action of α -particles, emits visible light which is registered by the photomultiplier without the help of a converter. This radiation is observed starting from a pressure of the order of 5 mm Hg and its intensity in the case of neon increases monotonically with increasing pressure. The dependence of the intensity of the flashes on the pressure in the case of neon is given by Curve II of Figure 3.

In the case of mixtures of helium with nitrogen and oxygen, phenomena which were qualitatively different to those for neon and xenon mixtures were observed. Figures 4 and 5 give the dependence of η_{N_2} and η_{O_2} on the concentration of nitrogen and oxygen for mixtures at a pressure of 5 and 10 atm.

With the addition of xenon to helium a practically monotonic increase of the light yield is observed, while the addition of oxygen can lead to an increase, as well as to a considerable decrease of the light yield depending on the oxygen concentration. A qualitative difference in the effect of N₂ or O₂ on the light yield, as compared to the case of neon, can also be seen from the curves "counting rate-pressure" for the mixtures He + 0.1% N₂ and He + 0.01% O₂ (Curves IV and V Fig. 7). The position of the maxima of these curves is apparently determined by the relation of the α particle range to the size of the chamber. Together with some similarity between the scintillation properties of He + N₂ and He + O₂ mixtures, there are also considerable differences between them. The chief of these, apparently, must be considered the difference between the curves of the relative increase

of the scintillation intensity as a function of the nitrogen and oxygen concentrations. While the maximum value of η_{N_2} at 10 atm is about three times smaller than the value at 5 atm, the maximum values of η_{O_2} are practically the same at these pressures, but the maxima are observed at different concentrations of the impurity. In addition, the scintillation intensities for these mixtures differ markedly one from the other. Thus, at the optimum concentration of oxygen in the helium the counting rate is only 3.5 times higher than the counting rate in pure helium, while the pulse amplitude does not exceed the amplifier noise level. In the case of a mixture of helium and nitrogen, however, the counting rate is 60-70 times higher than for pure helium, while the pulse amplitude is 8-10 times bigger than the amplitude of the amplifier noise. It must be pointed out that the

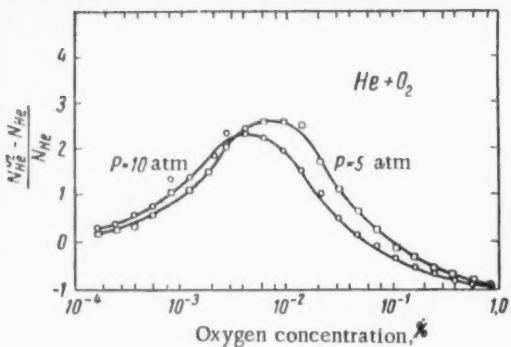


Fig. 5. The relative increase of the counting rate for the mixture $\text{He} + \text{O}_2$ as a function of the O_2 concentration. N_{He} and $N_{\text{He} + \text{O}_2}$) the counting rate for pure helium and for the mixture $\text{He} + \text{O}_2$, respectively; P) pressure of the mixture.

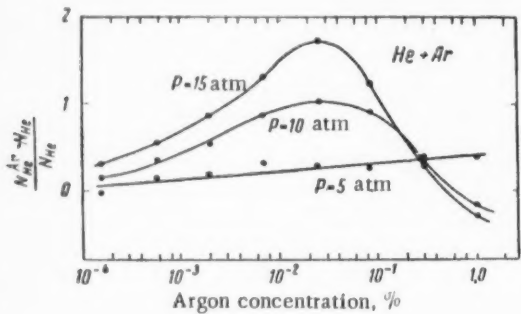


Fig. 6. The relative increase of the counting rate for the mixture $\text{He} + \text{A}$ as a function of the A concentration. N_{He} and $N_{\text{He} + \text{A}}$) the counting rate for pure helium and for the mixture $\text{He} + \text{A}$, respectively; P) pressure of the mixture.

Figure 7 gives the counting rate as a function of the gas pressure obtained for one and the same amplifier setting and registration threshold. For a threshold equal to 0.07 about 20 noise pulses were registered per second, while the counting efficiency for α particles, with the chamber filled by a mixture of $\text{He} + 0.1\% \text{N}_2$, was equal to 10% in the pressure range 2-5 atm (the ordinate of the corresponding curve in Figure 7 has been reduced 15 times). For the other mixtures the maximum efficiency under these conditions was 3, 6, 6 and 3% for the mixtures $\text{He} + 0.01\% \text{O}_2$, $\text{He} + 3\% \text{Ne}$, $\text{He} + 0.03\% \text{A}$ and pure He, respectively.

In addition to the mixtures already considered, for which the light yield is greater than that for pure helium, mixtures of helium with O_2 and vapors of organic liquids (ether, alcohol) were investigated which quench considerably the scintillations in the helium.

The results obtained by us are qualitative in nature. This is due to the limited region of spectral sensitivity of the photocathode, (3500-6000 AU), as well as to the measure of the light yield - the counting rate -

curve "counting rate - pressure" for this mixture is the more easily reproducible when the measurements are repeated, and also depends little on the degree of purity of the helium.

An intermediate position between nitrogen and oxygen on the one hand, and neon and xenon on the other, is taken by argon (Fig. 6). The relative increase of the counting rate for a mixture of helium with argon η_A at pressures of 10 and 15 atm depends on the concentration of argon in the same way as η_{O_2} and η_{N_2} , while at a pressure of 5 atm it rises monotonically as η_{Ne} and η_{Xe} . The counting rate as a function of the pressure for the mixture $\text{He} + 0.03\% \text{A}$, given in Figure 7 (Curve III), has a maximum at about 50 atm. The reason for its appearance is unexplained and, possibly, it is due to some impurities in the argon which we have used.

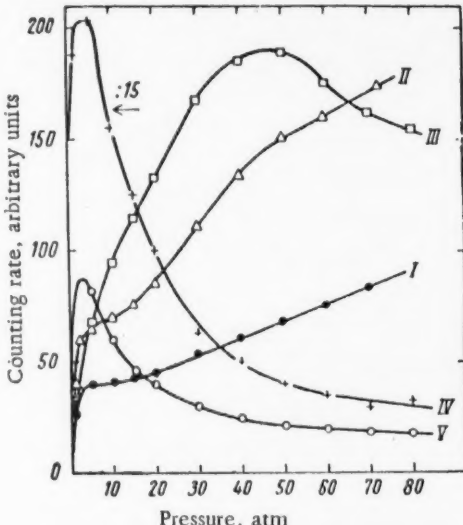


Fig. 7. The counting rate as a function of the pressure for various mixtures. I) He ; II) $\text{He} + 3\% \text{Ne}$; III) $\text{He} + 0.03\% \text{A}$; IV) $\text{He} + 0.1\% \text{N}_2$; V) $\text{He} + 0.01\% \text{O}_2$.

which we have taken. The disadvantage of this measurement method is the nonlinear relation between the counting rate and the light yield. However, in the case of a low counting efficiency, the counting rate is a quite sensitive measure of the variation of the scintillation intensity as a function of various factors.

The interpretation of the curves obtained by us for the variation of the α -particle counting efficiency as a function of the pressure of the mixtures and their composition is difficult in view of the complexity of the phenomena. When an α -particle passes through a mixture of helium with a small quantity of another gas, mainly helium atoms are excited and the transfer of the excitation from them to the impurity atoms leads to the emission of visible light. The production of a large number of metastable helium atoms [6] "sub-excited electrons", [7], emission in the far ultraviolet which is strongly absorbed by the impurities [8-10], — all of these can play an important role in the transfer of energy to the atoms and molecules of the impurities. Our results are not adequate for establishing the relative importance of the various processes which affect the transformation of the excitation energy into visible radiation. The satisfactory agreement between the experimental and theoretical dependence of the scintillation amplitude on the concentration of nitrogen, obtained in reference [4] for the mixture $A + N_2$, must be pointed out. The calculation was based on the assumption that the light yield is only determined by two competing factors. Our results for mixtures do not agree with these premises. Apparently, for mixtures of helium with various gases it is not possible to limit the calculation to only two factors.

The authors thank E. K. Zavoiskii for his attention to and interest in the present work and Yu. P. Dontsov for help in carrying out the spectral analysis.

LITERATURE CITED

- [1] A. Ward, Proc. Phys. Soc. 67 A, 841 (1954).
- [2] C. Muelhouse, Phys. Rev. 91, 495 (1953).
- [3] M. Forte, Nuovo Cim. 3, 6, 1443 (1956).
- [4] C. Eggler, and C. M. Huddleston, Nucleonics 14, 4, 34 (1956).
- [5] J. A. Northrop and R. Nobles, Nucleonics 14, 4, 36 (1956).
- [6] W. P. Jesse and J. Sadauskis, Phys. Rev. 100, 1755 (1956).
- [7] R. L. Platzman, Radiation Research 2, 1 (1956).
- [8] G. L. Weissler, Po Lee and E. I. Mohr, J. Opt. Soc. Am. 42, 84 (1952).
- [9] G. L. Weissler and Po Lee, J. Opt. Soc. Am. 42, 200 (1952).
- [10] Po Lee, and G. L. Weissler, J. Opt. Soc. Am. 42, 214 (1952).

Received February 5, 1957



GROSS γ -ACTIVITY OF FISSION PRODUCTS OF U^{235}

V. N. Sakharov and A. I. Malofeev

Measurements were made of the γ -activity $Q(t)$, representing the average for the products of a single fission of U^{235} , in the time interval $1 < t < 1000$ hours after fission.

The value Q was determined by comparing the γ -activity J of specimens of U^{235} and Na^{23} after simultaneous irradiation in a homogeneous stream of slow neutrons emitted from the heavy-water reactor of AN SSSR.

Comparison of the γ -activities was carried out using a Geiger counter, the construction of which was described in work [1]. This counter possessed a constant sensitivity to γ -rays over a wide range of energies. Therefore, in standard conditions of measurement the ratio of the γ -activities of the specimens J_U/J_{Na} was equal to the ratio of the counting rates C_U/C_{Na} independent of variation in the emission spectrum of the U^{235} fission products with time.

The ratio of γ -activities of the specimens in the conditions of the experiment was equal to

$$\frac{J_U}{J_{Na}} = \frac{P_U}{P_{Na}} \frac{A_{Na}}{A_U} \frac{\sigma_{fiss}}{\sigma_{act}} \frac{1}{q\lambda} e^{\lambda t} Q(t),$$

where P_U/P_{Na} is the ratio of weights of irradiated specimens; $A_{Na}/A_U = 23/235$ is the ratio of atomic weights of Na^{23} and U^{235} ; $\lambda = 1.27 \cdot 10^6 \text{ sec}^{-1}$ is the decay constant of Na^{24} ; $q = 4.2 \text{ Mev}$ — energy of γ -radiation emitted in a single decay of Na^{24} ; $\sigma_{fiss}/\sigma_{act} = 945$ — ratio of fission cross section of U^{235} to the activation cross section of Na^{23} .

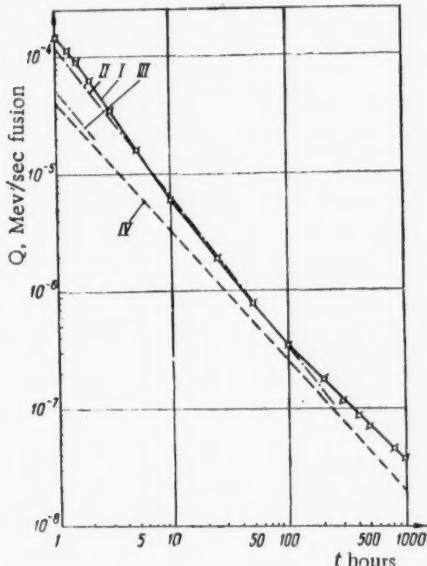
For determining this ratio we used data on the spectral distribution of slow neutrons emitted from the reactor [2] and data on the deviation of the fission cross section of U^{235} from the $1/v$ law [3]. The activation cross section of Na^{23} was taken equal to 0.565 barns. This value was found by comparison with the activation cross section of Au^{197} . The ratio of the activation cross sections of gold and sodium was obtained in the same way as in [4] but the activation cross section for gold was taken equal to 96 barns, i. e., somewhat greater than in [4].

The values of Q for the interval $1 < t < 1000$ hours are given on the figure. The accuracy of

Gamma-activity, representing the average for the products of a single fission of U^{235} . I) Experimental data of authors; II) experimental data of [5]; III) experimental data of [6]; IV) calculated values of [7], [8].

determining Q throughout the whole time interval examined is estimated at $\pm 20\%$.

$Q(t)$ can be represented in the form



$$Q = 23t^{-1.45} \frac{\text{Mev}}{\text{sec} \cdot \text{fission}} \text{ for } 1 < t < 10 \text{ hrs.}$$

$$Q = 0.76 t^{-1.12} \frac{\text{Mev}}{\text{sec} \cdot \text{fission}} \text{ for } 10 < t < 1000 \text{ hrs.}$$

The values of $Q(t)$ determined from these formulas do not differ by more than $\pm 7\%$ from the results given on the figure.

Values of the function $Q(t)$ obtained by other authors are also plotted on the figure. The results of our measurements are in good agreement with those of Borst [5] whose work gave experimental values of Q for the time interval $20 \text{ min} < t < 240 \text{ hrs}$. The results of Sugarman and others [6] may be compared with ours in the interval $1 < t < 2 \text{ hrs}$. The values which we obtained for Q are 2-3 times greater than those of Sugarman.

The figure also gives values of the function $Q(t)$ obtained by summing the γ -activities of separate fission products of U^{235} according to the tabular data of [7], [8]. The results of these calculations with $t < 10-20 \text{ hrs}$ give values of $Q(t)$ 2-3.5 times smaller than the experimental ones. This discrepancy can be accounted for by our incomplete knowledge of the γ -emission of the separate fission products. With increase of t the experimental and calculated values approach one another.

The authors thank O. I. Leipunskii for suggesting the theme and for guidance in this work.

LITERATURE CITED

- [1] V. N. Sakharov, J. Atomic Energy (USSR) 3, 61 (1957).
- [2] Iu. G. Abov, Session of AN SSSR on the Peaceful Uses of Atomic Energy, July 1-5, 1955 (Session of the Section of Phys.-Math. Sciences) [in Russian] (Izd. An SSSR, 1955), p. 294.
- [3] D. Popovic, and N. Rajsic, J. Nucl. Energy 1, 2, 170 (1954).
- [4] R. M. Bartolomew, R. C. Hawkings, W. F. Merritt and L. Yaffe, Can. J. Chem. 31, 204 (1953).
- [5] L. B. Borst, Nat. Nucl. Energy Ser., div. IV, 9, book I, McGraw-Hill, N. Y., 1951, p. 344.
- [6] N. Sugarman, S. Katcoff, B. Finkle, N. Elliott and J. D. Knight, Ibid. p. 371.
- [7] J. Moteff, Nucleonics 13, 5, 28 (1955).
- [8] M. Ia. Gen, M. S. Ziskin and E. I. Intezarova, Private Communication.

Received May 16, 1957

DETERMINATION OF THE ABSOLUTE INTENSITY OF THE 2.5 Mev LINE OF γ -EMISSION OF La^{140}

V. A. Arkhipov

The value of the absolute intensity of the line of γ -emission of La^{140} with energy 2.5 Mev is of great practical interest. This value has been determined earlier in other works. The following results were obtained: using the reaction $D(\gamma, p) = 0.04$ quanta/disintegration [1]; using the reaction $D(\gamma, n) = 0.01-0.1$ quanta per disintegration [2]; using ritron ≈ 0.055 quanta/disintegration [3]. We decided to determine this value more exactly, using the reaction $D(\gamma, n)$.

As is known, the nuclear photo-effect in heavy water is produced by γ -rays with energy more than 2.23 Mev, and in beryllium by γ -rays with energy more than 1.67 Mev [4]. Therefore γ -quanta with energy 2.5 Mev produce the photo-effect both in heavy water and in beryllium. Besides this, the photo-effect in beryllium is produced by the principal line of γ -emission of La^{140} with intensity 0.94 quanta per disintegration, if its energy exceeds 1.67 Mev.

In our experiment neutrons, formed as a result of the photo-effect in heavy water or in beryllium, after slowing in paraffin, fell on a rhodium (or silver) target, and the β -activity induced in the target was registered by a β -counter. The number of γ -quanta with energy 2.5 Mev emitted per second by La^{140} was determined by comparing the photo-effects in heavy water produced by preparations of La^{140} and RdTh . In addition we introduced a correction for the dependence of the cross section of the photo-effect in heavy water on the energy of γ -quanta.

For the 2.5 Mev line of γ -emission of La^{140} the value of the cross section of the photo-effect was taken equal to $11 \cdot 10^{-28} \text{ cm}^2$, and for the 2.6 Mev line of γ -emission of $\text{RdTh} = 13.9 \cdot 10^{-28} \text{ cm}^2$ [5]. The absolute number of γ -quanta K_{La} with energy 2.5 Mev emitted per second by the La^{140} preparation was determined from the formula

$$K_{\text{La}} = K_{\text{RdTh}} \frac{N_{\text{La}} \sigma_{2.5}}{N_{\text{RdTh}} \sigma_{2.6}},$$

where $K_{\text{RdTh}} = 1.03 \cdot 10^9$ is the number of γ -quanta with energy 2.6 Mev emitted per second by the RdTh preparation; N_{La} , N_{RdTh} are the values proportional to the activities of the rhodium (or silver) target after its activation by photo-neutrons from the preparations of La^{140} and RdTh respectively (these values were determined experimentally); $\sigma_{2.5}$ and $\sigma_{2.6}$ are the cross sections of photo-effect for lines of γ -emission of La^{140} and RdTh with energies 2.5 and 2.6 Mev respectively.

The La^{140} preparation used was an equilibrium preparation of $\text{Ba}^{140} + \text{La}^{140}$ in solution. Comparative measurements of the La^{140} and RdTh preparations were carried out several times over a period of 12 days. The value of the ratio $N_{\text{La}}/N_{\text{RdTh}}$ was equal to 0.051. The obtained effect was due to the La^{140} , and not to any radioactive contamination, since the value N_{La} varied in approximate correspondence with the half-life period of Ba^{140} (12.8 days). The value of K_{La} was found equal to $6.6 \cdot 10^7$ quanta/sec.

* Transliteration of Russian — Publisher's note.

The absolute activity of the La^{140} preparation was determined on a $4\pi - \beta$ -counter and found equal to 35 mC.

In addition, the activity of the preparation used was estimated by an ionization method. For this purpose comparison measurements were made with an electrometer SG-1M on the preparation and a radium standard. The radiation was filtered through 5 mm of lead. The activity of the preparation was found equal to 47.1 mg-equiv of radium. For evaluating the absolute activity of the equilibrium preparation of $\text{Ba}^{140} + \text{La}^{140}$ we calculated the relative gram-equivalent of radium in filtration through 5 mm of lead. It was found to be 1.3. The yields of γ -emission for Ba^{140} and La^{140} were taken from data of [3, 6]. The value of the activity of the La^{140} preparation, measured by the ionization method, coincided with the activity value determined by the $4\pi - \beta$ -counter.

The value of the absolute intensity of the line of γ -emission from La^{140} with energy 2.5 Mev was found equal to

$$\frac{6.6 \cdot 10^7 \text{ quanta/sec}}{35 \cdot 3.7 \cdot 10^7 \text{ disintegrations/sec}} = 0.05 \text{ quanta/disintegration}$$

The mean square error in determining this value was estimated at 15%.

We detected a slight photo-effect in beryllium from the γ -emission of the La^{140} preparation which was due solely to γ -rays with energy 2.5 Mev. This indicates that the energy of the principal line of γ -emission from La^{140} is actually less than the threshold energy for the photo-effect in beryllium. From the literary data the energy of this line is equal to 1.597 Mev [3].

In conclusion the author expresses thanks to Professor G. V. Gorshkov for valuable observations during the course of this work.

LITERATURE CITED

- [1] G. R. Bishop, R. Wilson and H. Halban, *Phys. Rev.* 77, 416 (1950).
- [2] E. Hylleraas and A. Ore, *Phys. Rev.* 71, 497 (1947).
- [3] L. V. Arkhangelskii, B. S. Dzhelepov, N. N. Zhukovskii, V. P. Prikhodtseva, and Iu. V. Khol'nov, *Izv. AN SSSR (Ser. Phys.)* 19, 251 (1955).
- [4] R. Star, J. Halpern and A. K. Mann, *Phys. Rev.* 84, 387 (1951).
- [5] E. Segré, Ed., *Experimental Nuclear Physics* (Russian Translation), (IL, 1955).
- [6] B. S. Dzhelepov and L. K. Peker, *Decay Schemes of Radioactive Isotopes* [in Russian] (Izd AN SSSR, 1957).

Received May 20, 1957

POLARIZATION OF γ -EMISSION PRODUCED IN THE REACTION $\text{Si}^{30}(\text{p}, \gamma)\text{P}^{31}$

P. M. Tutakin, S. P. Tsytko, A. N. L'vov, A. K. Val'ter
and Iu. V. Gonchar

In recent times measurements of polarization of γ -rays have been used successfully in the study of proton captures by light nuclei. Polarization of γ -rays has been studied in works [1], [2], where electric dipole transitions were observed and the parities of nuclei for ground and excited levels were determined. Marked polarization of γ -emission may be expected in every case where asymmetry in angular distribution is detected in the study of γ -rays of proton γ -resonance.

In order to determine the parity of the resonance level of the P^{31} nucleus with excitation energy 8.2 Mev we measured the polarization of γ -rays from the reaction $\text{Si}^{30}(\text{p}, \gamma)\text{P}^{31}$ with proton energy 940 kev. This reaction has been studied earlier [3]. It was found that the P^{31} nucleus with excitation energy 8.2 Mev undergoes a transition to the ground state with $J = \frac{1}{2}^+$ both by direct γ -transition and by intermediate levels with energies 1.26 and 2.35 Mev. The angular distribution of γ -quanta with energy $E_\gamma = 8.2$ Mev has the form $\omega(\theta) \sim 1 - a_2 \cos^2 \theta$, where $a_2 = -0.60 \pm 0.15$, which leads to a unique fixed spin of the excited state of P^{31} , equal to $J = 3/2$.

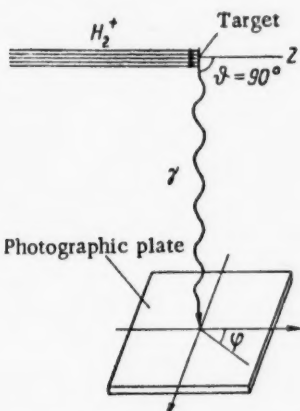


Fig. 1. Scheme of experiment.

The scheme of the experiment is shown in Figure 1. A beam of monoenergetic molecular H_2^+ ions accelerated by an electrostatic generator falls on a thin target of the isotope Si^{31} obtained by magnetic separation. Gamma-rays, flying from the target at an angle $\theta = 90^\circ$, fall normally on a photographic plate impregnated with heavy water. By microscope we determined the direction and lengths of tracks produced in the emulsion as a result of photo-disintegration of the deuterons. Proton tracks in the plane of the emulsion were measured at all angles φ reckoned from the direction of the beam of charged particles. For measurement we chose proton tracks which did not go outside the limits of the emulsion and with angles of penetration not exceeding 45° . The thickness of emulsion on the plates was equal to 230μ . Energy losses in the target by protons with energy 940 kev reached about 5 kev which excluded the possibility of excitation of neighboring γ -resonances. The plates were exposed for 30 hours with a mean current of $25 \mu\text{amp}$ on the target.

The method of measuring the polarization of γ -rays using photo-emulsions impregnated with heavy water is as follows. If J_{\parallel} is the intensity of γ -rays polarized in the plane P defined by the directions of the incident proton and emitted γ -quantum, and J_{\perp} the intensity of γ -rays polarized perpendicular to the plane P , then the degree of polarization is determined by the ratio $R = J_{\parallel}/J_{\perp}$. If the angular distribution of γ -rays has the form $\omega(\theta) \sim 1 + a_2 \cos^2 \theta + \dots$, then R may be expressed by the coefficients a_n [2], [4]. In particular, with $\theta = 90^\circ$ for the electrical dipole transition E1

$$R_{\text{E1}} = \frac{1 - a_2}{1 + a_2}, \quad (1)$$

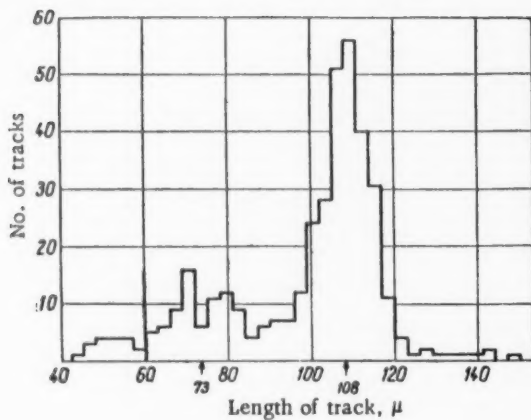


Fig. 2. Length distribution of photo-proton tracks. The wavy line denotes the cut-off.

and for the magnetic dipole transition M1

$$RM1 = \frac{1 + a_2}{1 - a_2} . \quad (2)$$

As is known, the angular distribution of photo-disintegration products of the deuteron follows a $\cos^2 \varphi$ law where φ is the angle between the direction of flight of the disintegration product and the direction of the vector of polarization of the γ -quantum. Hence in the general case of elliptical polarization of emission the angular distribution of photo-protons will have the form $w(\varphi) = 1 + (R - 1) \cos^2 \varphi$. The experimentally observable angular distribution of photo-protons makes it possible to determine the value R. Comparing it with the values for R obtained from Formulas (1) and (2), it is possible to discover the nature of the dipole transition (E1 or M1) and after this to determine uniquely the parity of the excited level if the parity of the ground level is known.

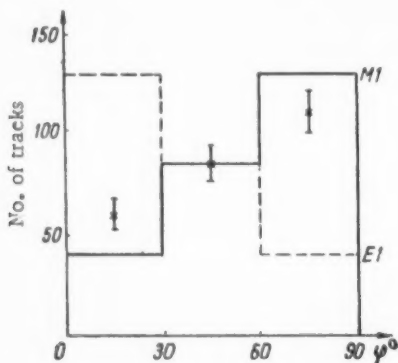


Fig. 3. Angular distribution of photo-protons corresponding to γ -rays with energy 8.2 Mev. Continuous line) calculated angular distribution for M1 transition; broken line) for E1 transition, experimentally obtained values designated by points.

The experimentally obtained distribution of the lengths of photo-proton tracks in the emulsion is shown in Figure 2. Mean values of paths equal to 108 and 73 μ correspond to two observable groups. For finding the energies of photo-protons corresponding to these groups we used the relation between path and energy for a damp emulsion which was obtained by calculation. The obtained energies of photo-protons corresponded to energies of γ -rays equal to 8.2 and 7.0 Mev, i. e., to known transitions of the excited P^{31} nucleus to the ground state and to the level with energy 1.26 Mev.

An examination of control plates with emulsion impregnated with ordinary water, irradiated simultaneously with the plates impregnated with heavy water, showed that a background of tracks longer than 60 μ was absent. The fact that a high-voltage generator was never used for accelerating the deuterons contributed to this absence of background.

The angular distribution of photo-protons with track lengths from 96 to 120 μ with respect to the angle

ϕ is shown in Figure 3. These photo-protons arose from γ -rays with energy 8.2 Mev. The angular distribution of photo-protons corresponding to the γ -transition to a level with energy 1.26 Mev is not shown in Figure 3, since the number of tracks was small. The angular distributions calculated using the values of R taken from Formulas (1) and (2) with $a_2 = -0.6$ are also given in Figure 3.

From the results of measuring the polarization of the γ -emission we may draw the following conclusions:

1. The observed emission produced in the reaction $\text{Si}^{30}(\text{p}, \gamma)\text{P}^{31}$ in the transition from a nuclear level of P^{31} with energy 8.2 Mev ($J = \frac{1}{2}^+$) to the ground state ($J = \frac{1}{2}^+$) is strongly polarized. In the experimentally observable angular distribution of photo-protons the coefficient $(R - 1) = -0.51$, and the degree of polarization $R = 0.49$.

2. The experimentally measured angular distribution of photo-protons excludes the possibility of an E1 transition and shows that the given transition is of the M1 type. Hence it follows that the P^{31} nucleus with excitation energy 8.2 Mev and spin $J = \frac{1}{2}$ has positive parity.

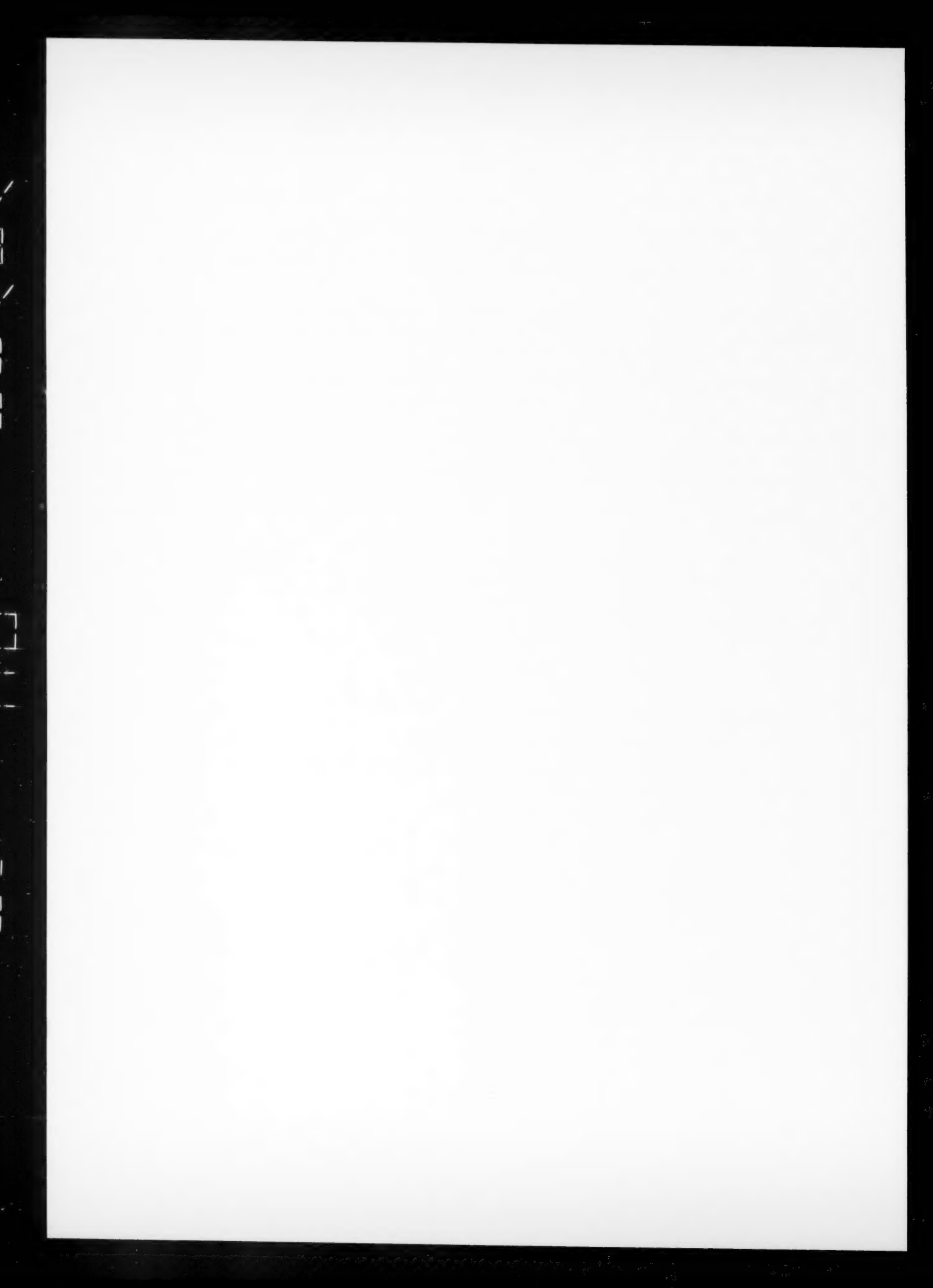
3. From the obtained value of the degree of polarization R the value of coefficient a_2 calculated from Formula (2) is $a_2 = -0.34 \pm 0.12$. The divergence from the value $a_2 = -0.6$ calculated theoretically on the assumption of a purely dipole transition $\frac{1}{2} \rightarrow \frac{1}{2}$ is apparently due to a small "admixture" of the electrical quadrupole transition E2. We do not exclude the possibility also of some contribution of γ -quanta from the transition between energy-levels 8.2 and 0.43 Mev, which was difficult to resolve. For γ -rays, emitted in this transition, the mean path of the photo-protons is equal to 96μ . As may be seen from the distribution of track lengths of photo-protons (Fig. 2) the value of this contribution could not, it seems, lead to a marked reduction of asymmetry of the angular distribution of photo-protons. Additional experiments will be devoted to clearing up these questions.

The authors express their thanks to the collective of workers headed by A. A. Tsygikalo who serviced the electrostatic generator during the course of the experiments, to Iu. P. Antuf'yev and E. G. Kopanets who took part in measurements on the generator, to E. V. Inopin for discussion of the results obtained and valuable advice. The authors are particularly grateful to M. I. Guseva who was responsible for developing methods of magnetic separation of the isotopes and the preparation of targets from them.

LITERATURE CITED

- [1] J. S. Hughes and P. J. Grant, Proc. Phys. Soc. 67A, 481 (1954).
- [2] J. S. Hughes and D. Sinclair, Proc. Phys. Soc. 69A, 125 (1956).
- [3] Thesis of reports of the VIIth annual conference on nuclear spectroscopy in Leningrad, 1947. Izv. AN SSSR, Ser. Phys. (in press).
- [4] D. R. Hamilton, Phys. Rev. 74, 782 (1948).

Received June 20, 1957



CALCULATION AND MEASUREMENT OF γ -FIELD FROM A PLANE SOURCE

U. Ia. Margulis and A. V. Khrustalev

Within recent years a great deal of attention has been given to the question of using artificial radioactive isotopes in powerful γ -ray irradiators. Such appliances could be used for investigation of the laws governing the action of radiation on biological material and living organisms, for cold sterilization of medical preparations and food products, for accelerating the chemical processes of polymerization and halogenation [1-3], and also for many other purposes.

For uniform irradiation of large objects the geometry of a point source is inadequate because the radiation field rapidly diminishes in inverse ratio to the square of the distance. A more uniform field of radiation is produced by a plane source.

In the present work we present a calculation and the results of experimentally measuring the γ -field from such a source.

Calculation of Dose from Plane Source

We will examine a plane source of emission in which the specific activity q of unit surface is constant. We will consider the thickness of the plane source as insignificant and thus we may neglect the self-absorption factor.

The dose D_A at point A (x_0, y_0, h_0) in time t (Fig. 1) can be calculated from the formula

$$D_A = kqt \int_{-L/2}^{+L/2} \frac{1}{\sqrt{(x-x_0)^2 + h_0^2}} \times \times \left(\arctan \frac{y_0 - \frac{d}{2}}{\sqrt{(x-x_0)^2 + h_0^2}} + \arctan \frac{y_0 + \frac{d}{2}}{\sqrt{(x-x_0)^2 + h_0^2}} \right) dx, \quad (1)$$

where L is the length; d is the width of source; k is the ionization constant of the source.

For the partial case of a plane source where the ratio d/L is close to 1, we suggest a formula for calculating the dose at a point lying over the center of the source, the deduction of which is as follows. The plane is divided by diagonals into two pairs of equal triangular sources (Fig. 2). The dose at the common vertex of these triangles is calculated as the mean dosage value from the inscribed and circumscribed sectors of each of the triangular sources, taking the specific activity of the sectors as equal. Using this method we may replace the source of triangular form by an equivalent sector, the dose at the vertex of which is calculated by the known formula, obtained in the following way. We will consider a sector defined by the angle φ_0 and radius R . The dosage power at point A (Fig. 2) is determined from the formula

$$P_{AR_i} = kq \int_0^{\varphi_0} \int_0^R \frac{r d\varphi dr}{r^2 + h_0^2} = \frac{1}{2} kq\varphi_0 \ln \left(1 + \frac{R^2}{h_0^2} \right). \quad (2)$$

Using the symbols of Figure 2, we may write

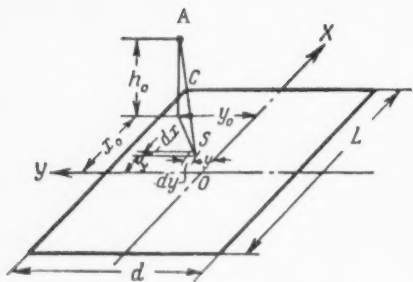


Fig. 1. Diagram for calculation of dose from a plane source in the general form.

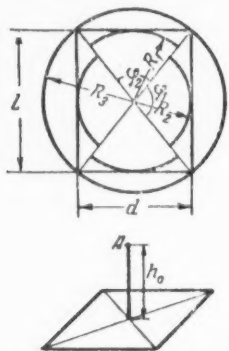


Fig. 2. Diagram for calculation of dose in case where point A is situated over center of source.

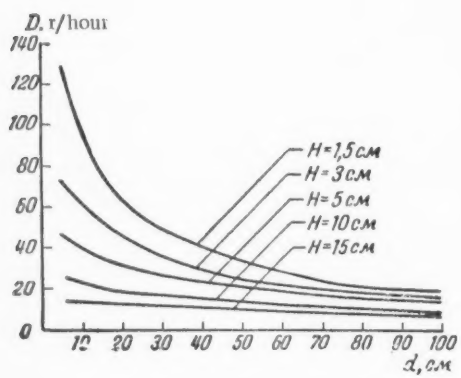


Fig. 3. Curves for calculation of dose for different distances of point from center of plane source and with varying width of source (source length 100 cm).

* As in original — Publisher's note.

$$\begin{aligned}
 p_A &= 2 \left(\frac{p_{AR_3} + R_{AR_1}}{2} \right)_{\varphi_2} + 2 \left(\frac{p_{AR_3} + p_{AR_2}}{2} \right)_{\varphi_1} = \\
 &= \frac{1}{2} \frac{kQ}{Ld} \cdot \left[(\varphi_2 + \varphi_1) \ln \left(1 + \frac{R_3^2}{h_0^2} \right) + \varphi_2 \ln \left(1 + \frac{R_2^2}{h_0^2} \right) + \right. \\
 &\quad \left. + \varphi_1 \ln \left(1 + \frac{R_1^2}{h_0^2} \right) \right] \text{r/hour}
 \end{aligned} \tag{3}$$

where Q is the total activity of source in mg-equiv of radium; φ_1 and φ_2 are sector angles in radians, and R_1, R_2, R_3 are radii of sectors in centimeters.

The results of calculation from Formula (3) agree to within 10% with results of calculation from Formula (1) for cases where $1 \geq d/L > 0.6$.

On the basis of dosage calculations for different plane sources by numerical integration of Formula (1) we plotted curves which would give the dose at a point situated at a fixed distance h from the center of a plane of different widths d , with length $L = 100$ cm and $Q = 1000$ mg-equiv of radium (Fig. 3).

Measurement of Dose From Plane Source

A plane source was imitated by 11* aluminum rods filled with radioactive Co^{60} , with the length of the active zone 1 m, diameter 6 mm and wall thickness 0.5 mm. The total activity of the source was 675 mg-equiv of radium (418 mC).

Measurement of the dose at various points above the solid source was carried out using tablets of scintillation phosphors (method of individual luminescent control — ILC). After exposure for 5 minutes the tablets were simultaneously removed from the radiation field. Since the accuracy of the ILC method is $\pm 15\%$, each point was measured by different tablets 3-5 times.

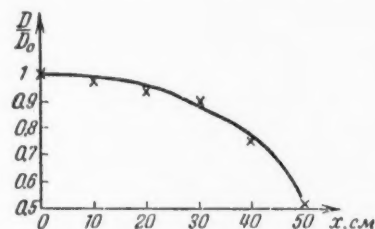


Fig. 4. Relative variation of dose between two parallel planes along length of source (x-axis). $D/D_0 = f(x)$. $H = 20$ cm.

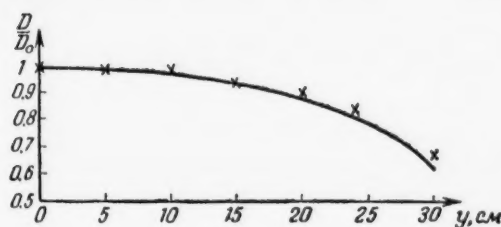


Fig. 5. Relative variation of dose between two parallel planes along the width of source (y-axis). $D/D_0 = f(y)$, $H = 20$ cm.

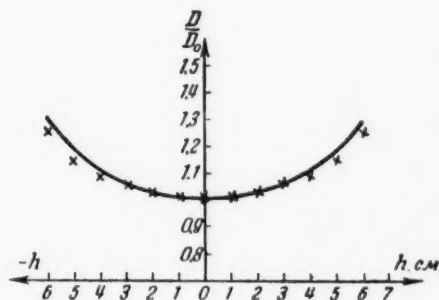


Fig. 6. Relative variation of dose between two parallel planes along the (h-axis). $D/D_0 = f(h)$, $H = 15$ cm.

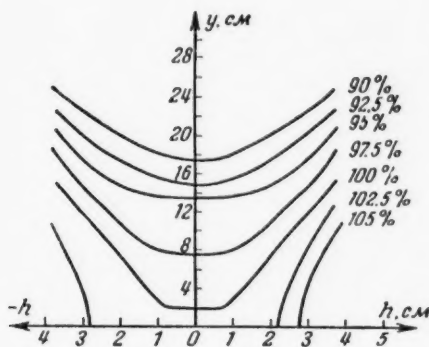


Fig. 7. Isodose curve of source formed of two parallel planes.

essential parameters is the uniformity of the γ -field. The greater the region of uniformity, the greater the capacity of the appliance for a given exposure time.

From the results obtained we constructed curves which enabled us to examine the dose distribution between two parallel plane sources, to compare the volumes of zones of uniform dose distribution in plane and cylindrical sources, and hence to decide on the suitability of applying one or the other source form.

As an illustration we show on Figures 4, 5 and 6 the relative variation D/D_0 in air between two parallel planes for planes of width $d = 60$ cm and length $L = 100$ cm. Here D is the dose at a given point between planes; D_0 is the dose at the center of the source cavity; H is the distance between the planes; d is the width of the plane, L is the length.

From the results obtained on the distribution of the γ -field between parallel planes, we constructed isodose curves for planes with $L = 100$ cm, $d = 20, 40$ and 60 cm and $H = 10$ and 15 cm. One of such isodose curves for two planes with $L = 100$ cm, $d = 60$ cm and $H = 10$ cm is given on Figure 7.

Isodose curves enable us to determine the true dose which can be produced at any point between two active planes, and also to decide the dimensions of the object which can be uniformly irradiated.

An analysis of the given curves characterizing the γ -field distribution between two active planes shows that the dose variation along the h -axis is the same as in the case of a hollow cylindrical source. Thus the region of uniformity in which the dose deviation does not exceed 10% both for the cylinder and for two parallel planes along the h -axis is the same and equal to $0.5 H$ or $0.5 D_1$, and $0.7 L$, where D_1 is the cylinder diameter; H is the distance between planes, and L is the length of plane or cylinder.

As regards the distribution along the y -axis, the γ -field region uniform to within 10% is considerably larger than in the cylinder where it is also equal to $0.5 D_1$, whereas for two planes it amounts to $0.7 d$.

Comparison of Cylindrical Source with a Source Formed by Two Parallel Planes

In the design of powerful irradiators one of the

For animals with approximately cylindrical body form (rabbits, dogs), the cylindrical irradiator is the most suitable. For the irradiation of plane objects, however, two planes are better because of the greater uniformity of the dosage field along the y-axis.

This can be illustrated by the following calculation from which we may compare the efficiency of appliances using these forms of sources.

Consider a cylinder with diameter $D_1 = 25.44$ cm and length $L = 100$ cm. Let the time of passage of the product through the irradiator be 1 minute. We will consider also that the degree of nonuniformity of irradiation of different parts of the product does not exceed 10 %. In this case the transverse dimension of the object must be equal to $0.5 D_1$, i. e., 12.72 cm.

If the object is a parallelopiped of square cross section, the capacity of the cylindrical irradiator will be

$$C = 0.5 D_1 \cdot 0.5 D_1 \cdot L \cdot \rho = 12.72 \cdot 12.72 \cdot 100 \cdot 1 = 16.18 \text{ kg}$$

(for simplicity we take the density of the object as $\rho = 1 \text{ gm/cm}^3$). If the activity of the source $Q = 1000 \text{ mg-equiv of radium}$ the dosage power at the center is equal to 0.291 rpm.

The form equivalent to the given cylindrical source will be two planes, the total surface of which is equal to the curved surface of the cylinder, total activity $Q = 1000 \text{ mg-equiv radium}$, and distance between planes $H = 25.44 \text{ cm}$.

Each plane has length $L = 100 \text{ cm}$ and width $d = \frac{\pi D_1}{2} = 40 \text{ cm}$. As we showed earlier, the region of 10% uniformity is equal to $0.5 H$ and $0.7 d$. Hence, the capacity of the machine will be

$$C = 0.5 H \cdot 0.7 d \cdot L \cdot \rho = 35.616 \text{ kg},$$

and the dosage at the center between the two plates is equal to 0.21 rpm. Hence, the capacity of the source formed of two planes is 1.6 times greater than the capacity of an equivalent cylindrical source.

This comparison clearly reveals the advantages of a source consisting of two planes.

LITERATURE CITED

- [1] Industrial uses of radioactive fission product, A Report to the United States Atomic Energy Commission, Stanford, California, 1951.
- [2] D. Duffey, Nucleonics 11, 10, 8 (1954).
- [3] G. J. Lewis, J. V. Nehemias, D. E. Harmer and J. J. Martin, Nucleonics 12, 1, 40 (1954).

Received October 26, 1956

ON THE MOTION OF CHARGED PARTICLES IN THE CENTRAL REGION OF A CYCLOTRON

V. S. Panasiuk

New methods of physical experimentation have sharply increased the stability requirements of cyclotrons. Lack of precision in the ion optics in the central region of a cyclotron has remained for many years one of the causes of operational instability of accelerators and has delayed improvements due indirectly to poor operation of the first cycle lens or ion focusing system in the first acceleration cycle.

A. A. Naumov has directed his attention to the fact that the high-frequency power expended on accelerating the ions is several times greater than the beam power at the outermost radius. Measurements made on a cyclotron with 15 Mev deuterons showed that the beam current at the outermost radius is lower by a factor of 150 than the ion current passing through the ion source. *

Calculation of the ion losses in this cyclotron, based on theoretical works with which we are familiar [1-3], has shown that they should be no greater than fifteen-fold. The difference between the calculated and experimental results gives reason to suppose that the actual motion of an overwhelming majority of the ions in the cyclotron does not correspond to that used in the theoretical calculations. Investigation showed that the difference can be explained by processes not previously accounted for, taking place in the central region of the cyclotron.

Ion motion in the horizontal plane. Figure 1 shows the equipotential lines of the electric field between the dees in the horizontal plane, taking into account the perturbing action of the open column of the ion source plasma. In studying the field in an electrolytic tank, the open plasma column was replaced by a metal rod and the dee by a metal plate parallel to the rod at a distance equal to the field-penetration depth in the first acceleration cycle.

The calculation of the phases and orbits of the ions showed that in the first cycle particles emitted at a nonzero angle φ have semicircular orbits whose centers are displaced from the plane midway between the dees (Fig. 1). Therefore the second cycle of these ions starts with phases which differ sharply from those calculated for ions with a zero emission angle (this is a case of an unperturbed electric field [3]). Many ions starting from the ion source with an emission angle $\varphi > 0$ do not leave the electric field region during the first cycle. Lens effects for these ions start at large negative phases, which leads to strong electric defocusing of the beam. Thus in the first cycle of acceleration there appears a harmful angular divergence of the ion beam in the horizontal plane.

To decrease this effect, the open plasma column was enclosed in a groove milled out of a special fitting in the housing for the cathode and anticathode of the ion source (Fig. 2). The dimension of this fitting was chosen so that ions which do not leave the electric field region in the first cycle collide with its walls. It is extremely difficult to calculate theoretically the groove depth which will give maximum focusing. An experimental method was therefore used.

Experiments with a grooved ion-source holder which were performed in 1953 showed that with a slight decrease of the ion current on a target outside the cyclotron chamber, the high-frequency power expended on the acceleration of unused ions decreased from 50 to 20 kw.

* The ion current of the source was evaluated by measuring the ion current in the source discharge tube when the high-frequency voltage was turned on.

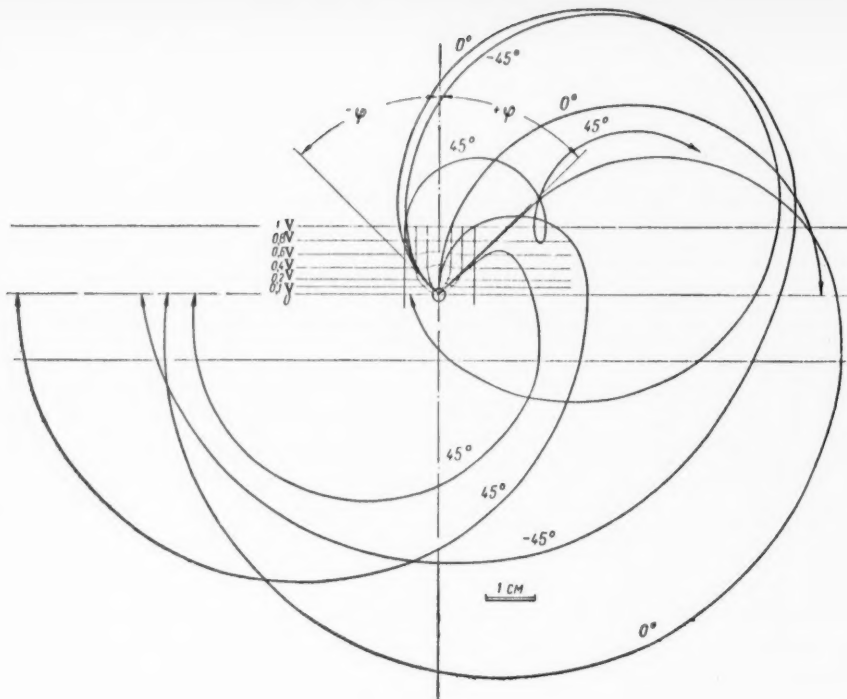


Fig. 1. Electric field of an ordinary first cycle lens in the horizontal plane, and the ion trajectories for various initial phases and angles of emission from the source. (The dee potential is taken as 1 v.)

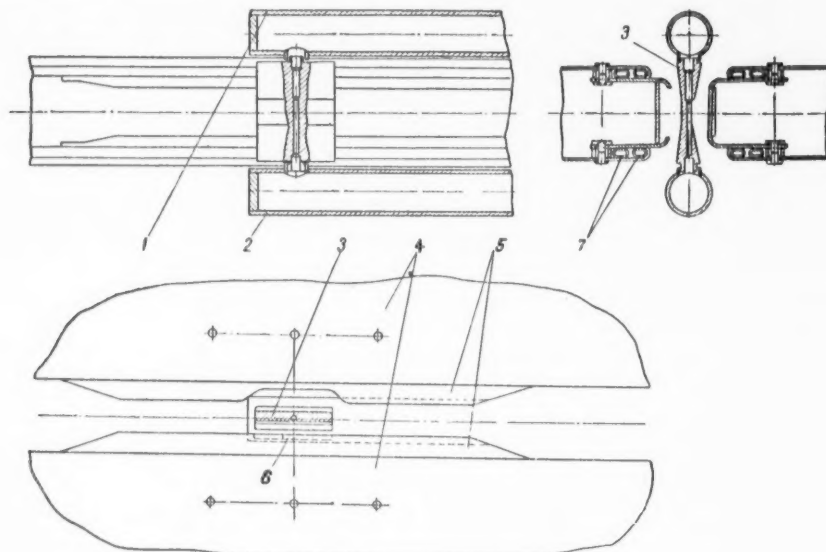


Fig. 2. The design of the new first cycle lens. 1) Anticathode casing; 2) cathode casing; 3) source holder; 4) dees; 5) projections on the dees; 6) drawing electrode slit; 7) water cooling for the dees.

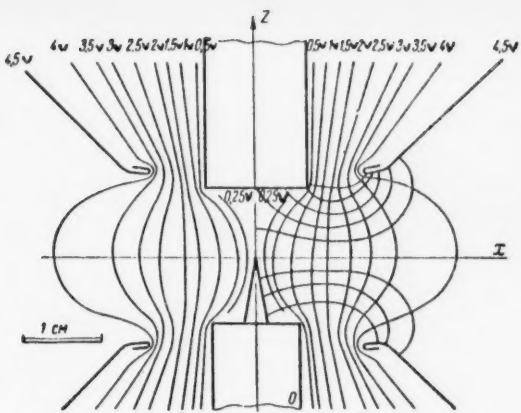


Fig. 3. Electric field of an ordinary first cycle lens in the vertical plane. (The potentials of the source casing and of the dees are taken as 0 and 4.5 v, respectively.)

We also obtained a much better ratio between the beam current at the final radius and that of the deflected beam. Whereas in the case of an ordinary first cycle lens the current in the deflected beam was 30% of that at the final radius, for the new lens this fraction was 55%. This is explained by the decrease in the region occupied by the orbit centers in the first cycle of acceleration, and therefore also in the spread of angles at which the ions approach the deflecting apparatus.

Ion motion in the vertical plane. As is well known, the surface of a plasma in contact with an electric field decreases if the number of ions removed by the field from the discharge is greater than the number of ions formed in the discharge per unit time. The electric field strength in the central regions of large cyclotrons usually attains values of several times 10 kv/cm. This field strength is sufficient to deform the ordinarily cylindrical open plasma column of the ion source into a somewhat conical shape. This column shape was observed visually and recorded photographically. The ion (deuteron) current emitted by the plasma was then 200-300 ma.

An electrolytic tank was used to investigate the field of the set of electrodes shown in Figure 3 (the plasma column was replaced by a metal cone). It was found that with this deformation of the open column most of the ions have an initial vertical velocity so great that they are lost to the covers of the dees. This situation was verified experimentally.

There are two ways to decrease the deformation of the plasma column: either by increasing the ion density in the discharge or by decreasing the number of ions emitted by the plasma. The current of ions emitted from the open plasma column is so large that with the existing ion optics all the ions cannot be accelerated to the outermost radius due to the electrostatic repulsion of the particles. It is therefore desirable to decrease the number of ions emitted. It is obvious that from this point of view the grooved holder improves the vertical ion motion by screening the electric field of the dees.

An effective measure to combat defocusing properties of the first cycle lens in the vertical plane involves providing the dees having a special drawing electrode with a slit (Fig. 2). The dimensions of this electrode should lead to minimum fringing of the electric field into the dees but should not interfere with the motion of those ions which can be accelerated to the final energy (the evaluation of the dimensions of the drawing electrode in each specific case necessitates constructing the particle trajectories in the central region). It is clear that the use of such an electrode leads to a decreased penetration of the electric field and therefore to an increase in the useful distribution of initial phases [1, 3]. In connection with the strong electrostatic repulsion of the ions in the first acceleration, the electrodes of the lens (the ion-source fitting and the drawing electrode on the dees) may remind one of Pierse's electrodes [4]. The particular conditions of the cyclotron, however, require further refinement of their shape.

Tests of the new first cycle lens, consisting of the grooved holder and the electrode with the slit, on a one-and-a-half meter cyclotron showed that the part of the high-frequency power expended on the acceleration of unused ions was decreased to 15 kw. The current in the deflected beam was 37% of the current at the final radius. The decrease of the current in the deflected beam compared to that obtained without the drawing electrode is explained by the increase in the region occupied by the orbit centers as a result of the defocusing action of the electric field at the electrode slit.

It should be noted that the application of a negative potential equal to the potential of the saturated ion current to the anticathode of the new source ("electron reflection") leads to a 30% increase of the ion current at the final radius over that obtained with an ungrounded anticathode. For an ordinary source (with an open plasma column) the accelerated ion current is practically independent of the anticathode potential. Such a source always operates with "electron reflection" due to the fact that on the boundary of the plasma the electric field has components directed along the lines of force of the magnetic field (Fig. 3).

The use of the new type of the first cycle lens has led to a sharp increase in the operational stability of the cyclotron and to a significant increase in the electric stability in the central region of the accelerating chamber. The "liberated" high-frequency power was used in achieving stability of the high-frequency potential on the dee to which the electrode with the slit is attached.

One year after the author developed this new type of first acceleration lens, R. S. Livingston [5] described the design of a lens which seemed to be based on concepts similar to ours.

The author expresses his gratitude to L. M. Nemenov and A. A. Chubakov who suggested performing the investigation, and to A. A. Naumov for valuable advice and constant interest in the work. The author also thanks L. I. Iudin for participating in the development of the method and adjusting the apparatus.

LITERATURE CITED

- [1] B. L. Cohen, *Rev. Sci. Instr.* 24, 589 (1953).
- [2] M. E. Rose, *Phys. Rev.* 53, 392 (1938).
- [3] N. D. Fedorov, *J. Atomic Energy (USSR)* 2, 4, 385 (1957).
- [4] J. R. Pierse, *J. Appl. Phys.* 11, 548 (1940).
- [5] R. S. Livingston, *Nature* 9, 173, 54 (1954).

Received October 9, 1956

THE IODIDE METHOD OF REFINING ZIRCONIUM

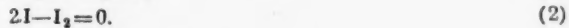
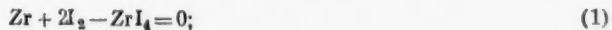
G. I. Stepanova and F. I. Busol

A considerable amount of experimental work has been devoted to investigations of the iodide method of refining zirconium (see for example [1, 2]). Certain features of the method, particularly the existence of a maximum rate of zirconium transport, have not yet, in our opinion, been correctly explained.

In [1-3], it is shown that maximum rate of transport is determined by the pressure of tetraiodide in the working range. The increase which takes place in the flow of zirconium to the filament on increasing the pressure is explained in [2] and [3] by the increase in the number of independent carriers. This is true for the pressure range in which the length of the free path is greater than, or is of the order of, the dimensions of the vessel. It is known, however, that increase in the zirconium flow also occurs at pressures in which the above-mentioned condition does not apply. The descending portion of the curve of zirconium flow as a function of tetraiodide pressure is explained in [2] as due to a decrease in the diffusion coefficient with increase in pressure. The authors of reference [2] do not take into account the increase in density of the particles, compensating for the decrease in the diffusion coefficient.

The authors of the present paper advance a different explanation for the dependence of zirconium flow upon pressure.

It will be assumed that in steady conditions of the iodide process of refining zirconium, there is chemical equilibrium in the vicinity of both filament and crude metal. Ignoring the formation of lower iodides, the following reactions occur



The molecular and atomic iodine and tetraiodide are in the gaseous state and the zirconium is in the solid state (the vapor pressure of zirconium at the working temperatures is negligibly small).

For a given pressure, the equilibrium concentrations of the reacting substances are determined by the temperature and are different for the filament and the crude metal. In the vicinity of the filament, iodine predominates, in the vicinity of the crude metal tetraiodide predominates. The resulting concentration gradient produces a diffusion flow. The equilibrium upset by the flow is restored by the chemical reactions. There is thus a constant transport of zirconium from the crude metal to the filament.

We shall characterize the rate of zirconium transport by the magnitude of the tetraiodide flow, disregarding the reverse flow of iodine. The flow of tetraiodide molecules j established in the apparatus is proportional to the diffusion coefficient, density and difference in the boundary concentrations. Since the diffusion coefficient is inversely proportional to the pressure and the density is directly proportional to the pressure, the dependence of the flow j upon the pressure is determined by the dependence of the difference in concentrations upon the pressure. Consequently:

$$j = A(c_1 - c_2), \quad (3)$$

where A is a quantity independent of the pressure; c_1 is the tetraiodide concentration in the vicinity of the crude metal and c_2 that in the vicinity of the filament. We note that Expression (3) is true for tetraiodide flow only at pressures such that the length of the free path is much less than the dimensions of the vessel.

The concentrations c_1 and c_2 are determined from the law of mass action:

$$\frac{p_{I_2}^2}{p_{ZrI_4}} = k_1 \quad (4)$$

$$\frac{p_{I_2}^2}{p_{I_2}} = k'_1 \quad (5)$$

where k_1 and k'_1 are temperature-dependent equilibrium constants of the Reactions (1) and (2); p_{I_2} , p_I and p_{ZrI_4} are the partial pressures of molecular and atomic iodine and tetraiodide, respectively. In the apparatus, with a total pressure which is the same at all points, a gradient of partial pressures is established, in particular a gradient of tetraiodide pressure. In experiments on zirconium refining, the pressure of the tetraiodide in the vicinity of the crude metal is determined by the temperature of the latter. For simplification in writing, we shall denote it by p . The problem is to determine j as a function of p .

In the vicinity of the crude metal, which usually has a low temperature, the dissociation of molecular iodine may be neglected. Then, according to (4)

$$c_1 = \frac{1}{1 + k_1^{1/2} p^{-1/2}}, \quad (6)$$

where k_1 is the value of the equilibrium constant of reaction (1) at the temperature of the crude metal. In accordance with (4), the total pressure in the apparatus is

$$p_{\text{total}} = p (1 + k_1^{1/2} p^{-1/2}). \quad (7)$$

In the vicinity of the filament, the tetraiodide concentration c_2 is determined, as follows from (4), (5) and (7), by the equation

$$c_2 + c_2^{1/2} \frac{k_2^{1/2} p^{-1/2}}{(1 + k_1^{1/2} p^{-1/2})^{1/2}} + c_2^{1/4} \frac{k_2^{1/4} k'_2^{1/2} p^{-3/4}}{(1 + k_1^{1/2} p^{-1/2})^{3/4}} = 1, \quad (8)$$

where k_2 and k'_2 are the equilibrium constants of reactions (1) and (2) at the filament temperature. Substituting in (3) the value for c_1 from (6) and for c_2 from (8), we obtain an explicit expression for the flow as a function of pressure. In limit cases, the solution of Equation (8) may be found in an explicit form. It is therefore possible to obtain a sufficiently complete conception of the way in which the flow depends upon pressure. In what follows, it will be considered that the filament temperature is much higher than the temperature of the crude metal, i. e., $k_2 \gg k_1$.

At low pressures ($k_1 \gg p$), the first item on the left in Equation (8) may be ignored. We then have

$$c_2 = \frac{k_2^{1/2} p^{-1/2}}{24 k_1^{1/2} k_2} \left[\left(1 + 4 \frac{k_1^{1/2} p^{1/2}}{k'_2} \right)^{1/2} - 1 \right]^4. \quad (9)$$

If

$$k'_2 \gg k_1 \quad c_2 = \frac{k_1^3}{k_2 k'_2^2} \frac{p^{3/2}}{k_1^{3/2}}.$$

In the opposite limit case of low values of k'_2 , for which $\frac{4k_1^{1/2} p^{1/2}}{k'_2} \gg 1$, the quantity c_2 has the value

$$c_2 = \frac{k_1}{k_2} \frac{p^{1/2}}{k_1^{1/2}}.$$

Since $c_1 \approx \frac{p^{1/2}}{k_1^{1/2}}$ is much greater than c_2 , determined by Expression (9),

$$j = A \frac{p^{1/2}}{k_1^{1/2}}. \quad (10)$$

Thus, for low pressures, the flow j increases as $p^{1/2}$.

For high pressures ($k_2 \ll p$), Equation (8) gives

$$c_2 = 1 - \frac{k_2^{1/2}}{p^{1/2}} - \frac{k_2^{1/4} k_2^{1/2}}{p^{3/4}}. \quad (11)$$

Taking into consideration that in this case $c_1 = c_2 = 1 - \frac{k_1^{1/2}}{p^{1/2}}$, we have approximately

$$j = A \left(\frac{k_2^{1/2}}{p^{1/2}} + \frac{k_2^{1/4} k_2^{1/2}}{p^{3/4}} \right), \quad (12)$$

i. e., at high pressures, the flow diminishes with increase in pressure.

Taking into account the condition $k_2 \gg k_1$, it is possible to find an expression for the flow also for intermediate values of the pressure $k_2 \gg p \gg k_1$. In this case

$$c_2 = \frac{k_2'^2}{2^4 k_2 p} \left[\left(1 + \frac{4p}{k_2'} \right)^{1/2} - 1 \right]^4. \quad (13)$$

The magnitude of the flow is determined by the relationship

$$j = A \left\{ 1 - \left(\frac{k_1}{p} \right)^{1/2} - \frac{k_2'^2}{2^4 k_2 p} \left[\left(1 + \frac{4p}{k_2'} \right)^{1/2} - 1 \right]^4 \right\}. \quad (14)$$

If $k_2' \gtrsim k_2$, Equation (13) gives

$$c_2 = \frac{p^3}{k_2 k_2'^2}. \quad (15)$$

The flow

$$j = A \left(1 - \frac{k_1^{1/2}}{p^{1/2}} - \frac{p^3}{k_2 k_2'^2} \right) \quad (16)$$

at the pressure

$$p_m = \frac{1}{6^{2/7}} (k_1 k_2^2 k_2'^4)^{1/7} \quad (17)$$

has a maximum value, equal to

$$j_m = A \left[1 - \frac{7}{6^{6/7}} \left(\frac{k_1^3}{k_2 k_2'} \right)^{1/7} \right]. \quad (18)$$

For low values of k_2' (such that $\frac{4p}{k_2'} \gg 1$), Equation (13) gives

$$c_2 = \frac{p}{k_2}; \quad (19)$$

$$j = A \left(1 - \frac{k_1^{1/2}}{p^{1/2}} - \frac{p}{k_2} \right); \quad (20)$$

$$p_m = \left(\frac{k_1 k_2^2}{4} \right)^{1/3}; \quad (21)$$

$$j_m = A \left[1 - \frac{3}{2^{2/3}} \left(\frac{k_1}{k_2} \right)^{1/3} \right]. \quad (22)$$

The foregoing considerations explain the variation in the magnitude of the flow as a function of pressure. The quantity j , proportional to the difference $(c_1 - c_2)$ is a nonmonotonic function of the pressure (it has a maximum) despite the fact that c_1 and c_2 vary monotonically, since with increase in the pressure, c_1 and c_2 increase from zero to unity at different rates.

The above examination provides an explanation for a number of other features of the process. It has been found experimentally [4] that on increasing the filament temperature the flow (and in particular its maximum value) increases, and the pressure corresponding to maximum flow is shifted in the direction of higher values. Both these facts follow from the relationships (17) and (18) or (21) and (22) if it is borne in mind that the constants k_2 and k_2' increase with increase in the filament temperature. It is also known that with increase in the filament temperature, the flow increases at first rapidly and then gradually approaches a constant limit [3]. As follows from Equation (8), the value of c_2 approaches zero with increase in the filament temperature, i. e., with increase in k_2 and k_2' . At the same time, while c_2 is comparable to c_1 , the variation of c_2 has a substantial influence on the magnitude of the flow. As c_2 approaches zero ($c_2 \ll c_1$), further variation of c_2 does not affect the magnitude of the flow, which in this case is determined solely by the value of c_1 .

It should be noted that the values of the flow as determined by Expressions (10), (12), (14) and (20) are somewhat high, since actually equilibrium is incomplete at the boundaries of the region. In addition, in the steady process, for each molecule of tetraiodide arriving at the filament, there should be four atoms or two molecules of iodine arriving at the crude metal. Generally speaking, this is not observed in diffusion flow. In the reaction vessel, therefore, the total pressure shows a slight gradient which, by creating a macroscopic flow of gas, additional to the diffusion flow from the filament to the crude metal, will increase the total flow of iodine and diminish the flow of tetraiodide.

Verification of the theory proposed will require its comparison with experimental data and this will form the subject of a subsequent communication.

The authors wish to express their indebtedness to K. D. Sineinikov and I. M. Lifshits for discussions of the results obtained.

LITERATURE CITED

- [1] F. I. Busol, G. T. Nikolaev and L. N. Ryabchikov, *Otchet FTI Academy of Sciences, Ukrainian SSSR*.
- [2] V. S. Emelyanov, P. D. Bystrov and A. I. Evstyukhin, *Atomic Energy*, No. 1, 43 (1956); No. 3, 122 (1956).

[3] Z. M. Shapiro, *The Metallurgy of Zirconium*, Edited by Lustman and Kerze (McGraw-Hill Book Company Inc., USA) 1955, p. 135.

[4] J. H. Döring and K. Möller, *Z. f. Elektrochem.* 56, 403 (1952).

Received August 1, 1956

V

3

/

-

3

3

MEASUREMENT OF SMALL CONCENTRATIONS OF α -ACTIVE SUBSTANCES IN WATER BY THE FREEZING-OUT METHOD

N. G. Gusev, D. P. Osanov and V. P. Mashkovich

One of the most important problems of radiometry is the measurement of α -contamination of water. Yet this is very difficult to accomplish since, firstly, the α -particle path in water is extremely short ($40-50 \mu$) and secondly, the maximum permissible levels for α -contamination of water are of the order of $5 \cdot 10^{-11}$ curie per liter, which is equivalent to one disintegration per 1 cm^3 in 10 minutes.

It was found [1] that α -contamination of water could be measured if a fixed volume was evaporated on a substrate, the substrate with the active deposit then being placed in the sensitive volume of a diffusion cloud chamber and a count made of the number of α -particle tracks emitted from the deposit in unit time.

For certain α -emitters however, the evaporation method of treating the sample involves large losses which are difficult to determine (for instance, due to the volatility of the substance on heating). In addition, it requires additional equipment and a considerable expenditure of time. The introduction of a correction for self-absorption is also laborious. Hence we made an attempt to measure the α -activity of water by introducing a liquid sample into the sensitive volume of a diffusion cloud chamber.

Since the temperature of the base of the chamber was about -60°C , the introduced liquid rapidly froze. This resulted in the freezing-out of the active material in the same direction as the positive temperature gradient and hence produced a considerable increase in the activity of the upper layers.

As a value quantitatively characterizing the enrichment process we may choose the ratio of the α -activity, recorded on the upper surface of the sample after freezing, to that which is registered on the upper surface of the liquid sample. We will name this value the enrichment coefficient K .

Let the number of α -particles emitted in 1 minute from the upper surface of the frozen sample be equal to N and from the upper surface of the liquid sample $- N_0$.

Then the enrichment coefficient

$$K = \frac{N}{N_0} . \quad (1)$$

It is clear that the upper surface will only emit those α -particles which are formed in a layer h_0 cm thick, equal to the length of the α -particle path in water (critical layer). We will suppose that in the water there occurs A_0 disintegrations/min/ml (without enrichment).

Only a quarter of the α -particles formed in the critical layer of the liquid sample will be emitted from the upper surface [2] i. e.,

$$N_0 = \frac{A_0}{4} h_0 S,$$

where S is the area of the surface in cm^2 .

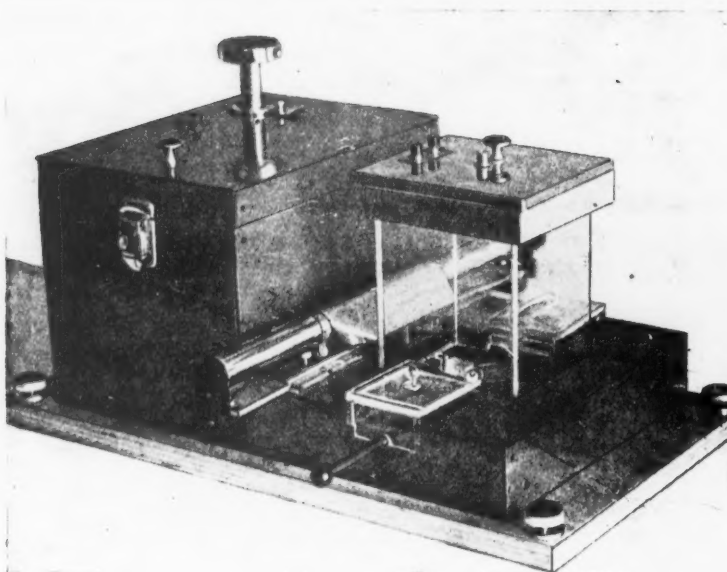


Fig. 1. General view of diffusion cloud chamber.

The concentration of α -activity in the water, expressed in curie per liter will be equal to

$$C_0 = \frac{A_0 \cdot 1000}{2.22 \cdot 10^{12}} = \frac{4N_0 \cdot 1000}{2.22 \cdot 10^{12} h_0 S}.$$

On freezing the sample by the method mentioned above and with enrichment coefficient equal to K,

$$C_0 = \frac{4N \cdot 1000}{2.22 \cdot 10^{12} h_0 K S}.$$

For α -particles with energy about 5 Mev, $h = 4.2 \cdot 10^{-3}$ cm [3]. Hence

$$C_0 = 4.3 \cdot 10^{-7} \cdot \frac{N}{K \cdot S}. \quad (2)$$

It is to be expected that the value K will not be constant but will depend on the conditions in which the freezing-out takes place and will be largely determined by the freezing temperature and the height of the sample.

Below we describe experiments to investigate these dependences.

For making up the samples we used solutions of various concentrations of uranyl nitrate hexahydrate $UO_2(NO_3)_2 \cdot 6H_2O$ in distilled water and cylinders with thin ebonite side walls and bases of metallic foil.

The latter were placed on a cooled surface which had a temperature $T < 0^\circ C$.

The counting of the number of α -particle tracks was carried out visually over a period of three minutes using a manual mechanical counter. It was found that during this period the alcohol precipitated in the diffusion chamber covered the surface of the specimen with such a fine layer that it could not affect the measurements.

A general view and a diagram of the diffusion cloud chamber used for the measurements are shown in Figures 1 and 2.

In Figure 3 there is a photograph of the track of an α -particle emitted from the surface of a frozen sample.

Dependence of K on The Concentration of the α -Active Liquid

The nature of this dependence determines the suitability of the suggested method of treating the sample.

In fact, if the enrichment coefficient varied in any way with change of C_0 , then in Equation (2) there would be two related unknowns C_0 and K and the determination of C_0 would be impossible.

The data given in the table show that the enrichment coefficient is practically independent of the concentration of α -activity in the water.

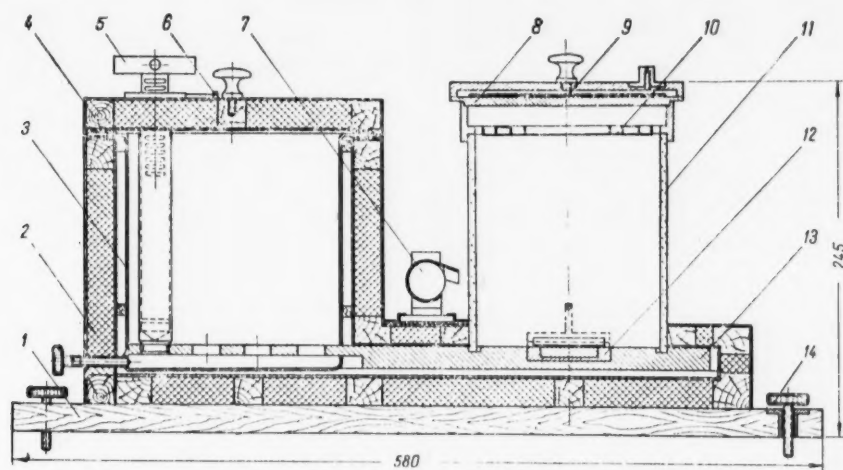


Fig. 2. Diagram of diffusion cloud chamber. 1) Base of chamber; 2) wall of ice container; 3) wall of brass tank; 4) roof of container 5) movable stage for freezing of sample; 6) stop; 7) daylight lamp; 8) roof of chamber; 9) electric heater; 10) evaporator grooves; 11) walls of diffusion chamber; 12) sample carrier; 13) coolable bottom of diffusion chamber; 14) leveling screws.

Dependence of K on Freezing Temperature T

For freezing the liquid samples we used a cooler with which we could obtain cooling surface temperatures from 0 to 79° .

The temperature of the aluminum cooling plate, on which the sample was placed for freezing, was measured by an alcohol thermometer, with the bulb inserted in a spherical depression in the plate.

The results of measuring the activity of samples of height 0.22 cm and cross sectional area 4.0 cm^2 , produced by freezing α -active water with concentration $C_0 = 1.19 \cdot 10^{-7}$ curie/liter are given in the form of a curve 1 in Figure 4. It is easy to see that the experimental points conform well to a straight line.

Curve 2 is plotted from the results of measuring samples of a different height.

C_0 curie/liter	K	\bar{K}	$\frac{\delta K}{\bar{K}} \cdot \%$
$6.17 \cdot 10^{-9}$	5.3		+6.0
$3.17 \cdot 10^{-8}$	4.4		-12.0
$1.19 \cdot 10^{-7}$	5.7	5.0	+14.0
$2.38 \cdot 10^{-7}$	4.5		-10.0
$3.17 \cdot 10^{-7}$	5.1		+2.0



Fig. 3. Photograph of track of α -particle emitted from frozen sample.

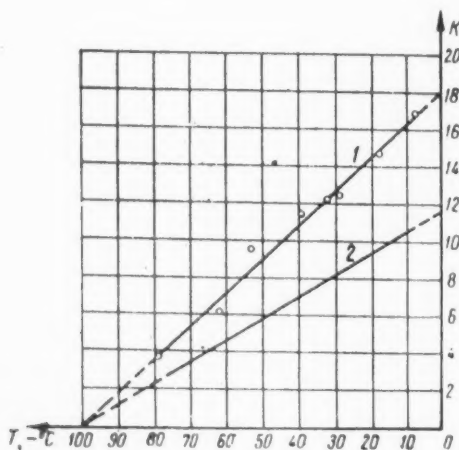


Fig. 4. Dependence of enrichment coefficient on the freezing temperature of sample.

K on h . In principle the height h can be further increased but, with the exception of the case of volatile substances, this is inadvisable since the freezing of such a sample demands almost as much time as is required for the evaporation of a corresponding volume of water.

The dependence of the enrichment coefficient on the temperature for curve 1 is described by the intercept form of the equation of a straight line

$$\frac{K}{18} + \frac{T}{100} = 1. \quad (3)$$

The behavior of the curves shows that temperatures close to 0°C are more favorable for freezing-out of the activity.

It is clear that there must be some temperature at which the freezing-out practically disappears, and this is apparently determined by the height of the sample. For the samples used this temperature was about 100°C .

The physical aspect of this effect is clear: at very low temperatures the cooling process of a liquid sample approximates to a bulk effect and the sample freezes before the concentration of α -activity manages to redistribute itself along its height.

Dependence of K on Height h of Sample

We should expect that K will in some measure depend on the height of the sample. The results of measuring, illustrated by the curves of Figure 5, confirmed this assumption. Curve 1 is plotted for specimens frozen in molds with aluminum side walls. In this case increase of the sample height up to $h = 0.22$ cm favored the freezing-out of activity. With further increase of height ($h > 0.22$ cm) the aluminium sides, which cool much more quickly than the liquid column, begin to show an effect (the coefficient of heat conduction of aluminum is 350 times greater than that of water).

Thus the freezing-out begins to take place in a horizontal as well as a vertical direction. The horizontal freezing-out reduces the enrichment of the upper surface of the sample by displacing the activity towards the center of the liquid volume. As the height increases ($h > 0.22$ cm) the horizontal effect becomes stronger and leads to a decrease in the enrichment coefficient. In order to eliminate horizontal freezing-out we used molds with ebonite sides, since the coefficients of heat conduction of water and ebonite are of the same order.

Curve 2 in Figure 5 is plotted from the results of measuring samples frozen in cylinders with ebonite sides. In this case we found a linear dependence of

Curve 2 shows that the enrichment coefficients for different heights are connected by the relation

$$\frac{K_2}{K_1} = \frac{h_2 + 0.5}{h_1 + 0.5}, \quad (4)$$

where h_1 and h_2 are given in centimeters.

In these experiments we also established that the enrichment coefficient was independent of the area of the sample.

Effect of Chemical Composition of the Water on the Freezing-Out Process

We found that an increase in the quantity of foreign matter added to the solution led to a reduction of the enrichment coefficient while the same amounts by weight of substances of different chemical nature reduced it in various degrees.

Fig. 5. Dependence of enrichment coefficient on height of sample.

Hence, it might be suggested that the freezing-out itself is "impeded" by chemical impurities which to some extent dissipate the directed process. This theory was confirmed by experimental results; the greatest enrichment coefficient was found in the case where the solvent was distilled water.

For our measurements we used solutions of uranyl nitrate hexahydrate in water with eight different chemical admixtures. From the results of our measurements, the maximum error due to difference in chemical composition was 70% relative to distilled water.

From the experiments we have conducted we can find the dependence of the value of the enrichment coefficient on the conditions of preparing the sample. Since Equation (3) is valid only for samples of height $h = 0.22$ cm, the dependence of K on T for any height of sample h is written in the form

$$\frac{K}{18 \frac{h_1 + 0.5}{h_2 + 0.5}} + \frac{T}{100} = 1. \quad (5)$$

Hence

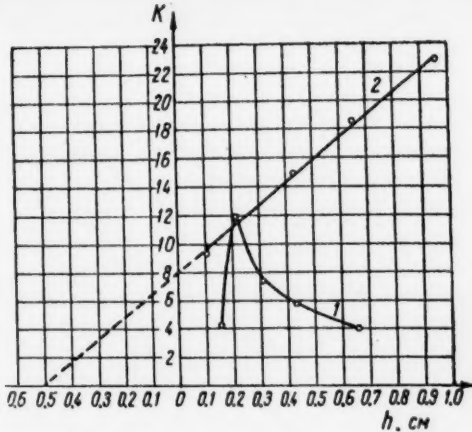
$$K = 25 (h + 0.5) (1 - 0.01T). \quad (6)$$

We substitute the value of K from Formula (6) in Expression (2):

$$\begin{aligned} C_0 &= 4.3 \cdot 10^{-7} \frac{N}{K \cdot S} = 4.3 \cdot 10^{-7} \frac{N}{25(h + 0.5)(1 - 0.01T)S} = \\ &= 1.7 \cdot 10^{-8} \frac{N}{(h + 0.5)(1 - 0.01T)S}. \end{aligned} \quad (7)$$

In the case where the counting of the number of α -particle tracks is carried out in a period of t minutes, the activity C_0 in curie/liter is determined by the formula

$$C_0 = 1.7 \cdot 10^{-8} \frac{N}{(h + 0.5)(1 - 0.01T)S \cdot t}. \quad (8)$$



Formula (8) was confirmed for solutions of uranyl nitrate hexahydrate in distilled water in a range of concentrations $3 \cdot 10^{-7}$ to $5 \cdot 10^{-10}$ curie/liter. The deviation of the experimental results from those calculated from Formula (8) did not exceed 15%. The application of Formula (8) for determining the concentration of other α -active salts in water requires further verification.

Thus, we may consider it established that the freezing-out of α -activity dissolved in water permits the determination of α -contamination of water without evaporation up to concentrations of $5 \cdot 10^{-10}$ curie/liter. We may expect that a similar method could also be used to produce enrichment of β -active solutions.

It is hoped that these investigations might lead to the application of the freezing-out method for the purification of highly radioactive effluent waters.

The authors take this opportunity to express their thanks to V. I. Popov for help in this work.

LITERATURE CITED

- [1] N. G. Gusev, V. I. Popov and D. P. Osanov, "Measurements of α -contamination of water using a diffusion cloud chamber," Collection of Works of the Faculty of Dosimetry and Defence [in Russian] in print MIFI.*
- [2] M. Curie, Radioactivity [Russian Translation], (Goztekhizdat, 1947).
- [3] H. Carvalho, Phys. Rev. 78, 330 (1950).

Received April 24, 1956

*As in original — Publisher's note.

FIXATION OF NITROGEN UNDER THE ACTION OF IONIZING RADIATIONS

S. Ia. Pshezhetskii and M. T. Dmitriev

The modern development of nuclear energy has raised the problem of developing various methods for utilizing the energy of nuclear transformations. The reaction of direct oxidation of nitrogen under the action of radiations and high-energy particles may be one way of utilizing atomic energy.

We have studied the main characteristics of the reaction of nitrogen oxidation under the action of electron impact and γ -radiation. The radiation sources were a 2 kv electron radiation tube, a 200 kv linear accelerator, and Co^{60} isotope of 1400 curie activity.

From the results of the measurements of the formation rates of nitrogen oxides in relation to the irradiation time, the composition of the gaseous mixture, the pressure, and the temperature, the following equation for the reaction rate was derived:

$$V = K P_{N_2} \cdot P_{O_2}, \quad (1)$$

where V is the reaction rate; K is a constant; P_{N_2} and P_{O_2} are the partial pressures of nitrogen and oxygen.

Equation (1) is valid for pressures of ~ 0.1 and ~ 760 mm Hg.

The activation energy of the reaction is 7.5 ± 1 kcal/mole at low pressures and about 2 kcal/mole at atmospheric pressure.

As has been shown [1], [2], the reaction begins at electron energy of 16.2 ev, which corresponds to the potential at which molecular nitrogen ions N_2^+ appear. A substantial acceleration of the reaction occurs at electron energy of 24 ev. This may be associated with the formation of atomic ions and atoms of nitrogen in the primary process. The reaction rate constant is proportional to the ionization function of nitrogen. The determining role of nitrogen ionization processes is also confirmed by experiments in which positive ions were removed from the reaction zone on a probe. The rate of the oxidation reaction then fell.

These results, and data on the reaction kinetics, indicate the following mechanism for the oxide formation reaction:

Basic processes for the formation of chemically active particles:

1. $N_2 \longrightarrow N_2^+ + e$ ($N_2^{+*} + e$, $N_2^{+*} + 2e$).
2. $N_2 \longrightarrow N^* + N + e$ ($N^* + N^* + e$, $N^{+*} + N^* + e$).
3. $N_2 \longrightarrow N_2^* \longrightarrow N^* + N$ ($N^* + N^*$).
4. $N_2^+ + e \longrightarrow N^* + N$ ($N_2^+ + [e] \longrightarrow N^* + N$).

The principal reactions of the active particles:

5. $N_2^+ + O_2 \rightarrow NO^* + NO$.
6. $N_2^{+*} + O_2 \rightarrow NO_2^* + N$.
7. $N_2^+ + O_2 \rightarrow N_2O^+ + O$.

8. $N + O_2 \rightarrow NO + O$.
9. $N + O_2 + M \rightarrow NO_2 + M$.
10. $N_2 + O + M \rightarrow N_2O + M$.

Processes leading to loss of active particles:

11. $N_2^+ + O_2^- \rightarrow \overset{\leftrightarrow}{N_2} + \overset{\leftrightarrow}{O_2}$.
12. $N_2^+ + O_2 \rightarrow N_2 + O_2^+$.
13. $N_2^+ + NO \rightarrow N_2 + NO^+$.
14. $N + N + M \rightarrow N_2 + M$.
15. $N + NO_2 \rightarrow N_2 + O_2$.
16. $N_2^+ + [e] \rightarrow \overset{\leftrightarrow}{N_2}$.

Our data show that under electron impact (up to 100 ev) the probability of Process 1 is about 10 times the probability of Process 2. The main reactions of the active particles are Processes 5, 6, 8 and 9. The interaction and decomposition reactions of nitrogen oxides are not considered here. The rate constant in Equation (1) is expressed as:

$$K = \frac{K_0 \cdot I}{E_{cr}} \sqrt{\frac{K_1 \cdot R \cdot T}{\alpha \cdot M \cdot P}} e^{-\frac{7500}{RT}} \int_0^{E_{max}} F(E) q(E) dE, \quad (2)$$

where K_0 is a proportionality factor; I is the radiation intensity; E_{cr} is the ionization potential of a nitrogen molecule; K_1 is the effective constant for the processes of chemically-active particle formation; R is the gas constant; T is the temperature; α is the coefficient of ion recombination; M is the molecular weight of nitrogen; P is the pressure; $q(E)$ is the ionization function of nitrogen; $F(E)$ is radiation energy distribution function; E_{max} is the maximum energy of the ionizing particles.

Equations (1) and (2) make it possible to analyze the oxidation process in relation to the conditions and the radiation characteristics.

Equation (2) was verified for pressures of 0.1 and 760 mm Hg, electron energies of 20-400 and $2 \cdot 10^5$ ev, and temperatures of 0-200°.

The reaction rate constant is independent of the pressure if $\alpha \sim T/P$ (which is the case at moderately low temperatures and pressures up to ~ 15 atm).

The table gives some of the values obtained in our laboratory for the yield of nitrogen dioxide as a function of the absorbed radiation energy under various conditions.

Data for electric discharges are also given for comparison.

It follows from the table that the highest yields are obtained at elevated temperatures and low pressures. This is due to competition between the elementary reactions leading to formation of nitrogen oxides, processes leading to loss of active particles, and reactions of oxide decomposition. The stationary NO_2 concentration when air is irradiated by high-speed electrons (at 20-30°) is 5.5-6%. This concentration is considerably higher than the equilibrium concentration in the thermal reaction.

Transition to the liquid phase at low temperatures does not have a significant influence on the reaction yield.

If nitrogen dissolved in water, or over water, is irradiated the oxide yields are relatively low. Similar results were obtained by Proskurnin et al [3] and Haissinsky et al [4] in the oxidation of nitrogen by the radiolysis products of water in alkaline aqueous solutions.

Radiation		Composition oxygen: ni- trogen mix- ture	Pressure, mm Hg	Tempera- ture °C	Reaction yield, mole- cules per 100 ev
form of radiation	energy, kev				
γ -radiation	≤ 1330	1:4	760	15-25	1.2
γ -radiation and high-speed electrons	200-1330	2:1*)	760	15-25	0.1-0.3
Slow electrons	0.02-0.40	1:4	≤ 0.1	~ 5	5-6
High-speed electrons	240	1:1	liquid phase	-183	1-2
High-speed electrons	200	1:1**)	760	40-50	2
High-speed electrons	200	1:4**)	760	40-50	1.3
High-speed electrons	200	0:1**)	40-50	0.2
High-speed electrons	200	1:4	760	15-25	1.5
High-speed electrons	200	1:4	760	~ 200	3-3.5
Silent discharge	≤ 6	2:1	1	< 50	2.5
High-frequency discharge	≤ 4	2:1	1	< 100	4.0
High-frequency discharge	≤ 15	1:1	760	< 200	1.7

*) In saturated aqueous solution.

**) Over water surface

As the Table shows, the reaction yields in experiments under atmospheric pressure are approximately the same with high-speed electrons and γ -radiation. Similar yields were obtained in a nuclear reactor.

Wright et al [5] obtained a yield of about one atom of fixed nitrogen per 100 ev by irradiation of air over water at atmospheric pressure. Primak and Fuchs [6] obtained a yield of 3 atoms per 100 ev by irradiation of moist air at 1 atm and 40°. Harteck and Dondes [7] obtained 2.5 NO_2 molecules per 100 ev at 140° and 1 atm and 5 molecules of NO_2 per 100 ev at 175° and 25 atm. An increase of the energy yield of the reaction can evidently be obtained by neutralization of negative ions [8] or by sensitization of processes of nitrogen atom and ion formation. However, there are no experimental data at present relating to yields of over 6 molecules of NO_2 per 100 ev. This yield corresponds to a consumption of 7000 kw/hr/1 ton of anhydrous nitric acid, which is the approximate consumption in the ammonia process.

Radiochemical oxidation of nitrogen can only become technically important if it can be effected with the utilization of most of the energy of nuclear fission, i. e., in a nuclear reactor.

A complicating factor in this case is the capture of neutrons by nitrogen as the result of the reaction ${}^7\text{N}^{14} + n \rightarrow {}^6\text{C}^{14} + p$, which should have an unfavorable effect on the reactor performance (neutron capture cross section by nitrogen $\sigma_N \approx 1.5 \cdot 10^{-24} \text{ cm}^2$, and by oxygen $\sigma_O \approx 2.8 \cdot 10^{-28} \text{ cm}^2$). In principle, nitrogen can be used for controlling a nuclear reactor by absorbing excess neutrons. Its adverse effect can be compensated to some extent by partial replacement of other neutron absorbers by it. At the same time, the proton liberated in each elementary act of the above nuclear reaction has an energy of ~ 600 kev, which can give rise to $\sim 10^4$ ionization acts and hence $\sim 10^4$ molecules of nitrogen dioxide per one thermal energy neutron absorbed by nitrogen.

The capture of neutrons by nitrogen can evidently be decreased by enrichment of the gaseous mixtures with oxygen.

LITERATURE CITED

[1] S. Ia. Pshezhetskii, Session of AN SSSR on the Peaceful Uses of Atomic Energy (Div. Chem. Sci.) [in Russian] (Izd. AN SSSR, Moscow, 1955) p. 64.

[2] S. Ia. Pshezhetskii and M. T. Dmitriev, Doklady Akad. Nauk SSSR, 103, 4, 647 (1955).

[3] M. A. Proskurnin, V. D. Orekhov and E. V. Bareiko, Session of AN SSSR on the Peaceful Uses of Atomic Energy (Div. Chem. Sci.) [in Russian] (Izd. AN SSSR, Moscow, 1955) p. 41.

[4] C. Vermeil, M. Cottin and M. Haissinsky, *J. Chim. Phys.* 49, 437 (1952).

[5] J. Wright, J. K. Linacre, W. R. Marsh and T. H. Bates, Conference on the Peaceful Uses of Atomic Energy, Paper 445, 7 (New York, 1956) 560.

[6] W. Primak and L. H. Fuchs, *Nucleonics* 13, No. 3, 38 (1955).

[7] P. Jarteck and S. Dondes, *Nucleonics* 14, No. 7, 22 (1956).

[8] M. T. Dmitriev and S. Ia. Pshezhetskii, Abstracts of papers at the All-Union Conference on Radiation Chemistry [in Russian] (Izd. AN SSSR, Moscow, 1957) p. 5.

Received May 20, 1957

THE USE OF RADIOACTIVE ISOTOPES IN STUDYING THE KINETICS OF SCRAP MELTING AND SLAG FORMATION IN THE SCRAP-ORE PROCESS

A. I. Osipov, L. A. Shvartsman, V. I. Alekseev, V. F. Surov, M. L. Sazonov,
M. T. Bulskii, S. A. Telesov, A. M. Skrebtsov, A. M. Ofengenden,
L. G. Goldshtein and F. F. Sviridenko

The problem of improving the technology of steel production necessitates an investigation of the kinetics of scrap melting and the kinetics of slag formation.

The use of radioactive isotopes in a variant of the well known "isotope attenuation" method provides a fundamentally new means of studying melting rate and slag formation and — what is particularly important — it enables the absolute weight of slag to be determined during the course of melting.

A Study of the Kinetics of Scrap Melting

The rate of scrap melting in experimental melts in 130- and 350-ton open-hearth furnaces was determined from the diminution in specific activity of metal samples containing Co^{60} . Under the conditions existing in the molten steel bath this indicator does not oxydize, does not pass into the slag and does not volatilize, thus enabling the quantity of Co^{60} atoms to be taken as constant and a balance of the number of impulses to be attained. To effect a rapid equilibrium distribution, a preparation of Co^{60} was introduced into the ladle car during the pouring of the last pig iron from the mixer. A sample was taken from the Co^{60} containing pig iron in the ladle. Further samples of metal were taken from the furnace throughout the melting period.

The values of the specific rates of count of all the samples were reduced to the specific rate of count of an arbitrarily chosen standard sample weighing 400 g. The activity of the metal samples was measured by means of 12 type-MS-4 counters built up into a block as described earlier [1].

Knowing the specific rate of count of the pig-iron samples and the weight of pig iron in the ladle and also the specific rate of count of the metal samples taken from the furnace during melting, it is possible to arrive at an equilibrium equation of the form

$$A_t = \frac{A_0 i_0}{i_t}, \quad (1)$$

where A_t is the weight of liquid metal (in tons) in the furnace at the time t when a certain quantity of scrap is melted; A_0 is the weight (in tons) of liquid pig iron containing Co^{60} in the ladle; i_0 is the specific rate of count of pig-iron samples in impulses per min · g; and i_t is the specific rate of count (in impulses per min · g) of metal samples taken from the furnace at time t .

Taking into account the quantity of impurities that have been oxidized, the actual weight of scrap melted x , at time t will be

$$x = \frac{A_0 i_0}{i_t} \left(1 - \frac{\sum C_t}{100} \right) - A_0 \left(1 - \frac{\sum C_0}{100} \right), \quad (2)$$

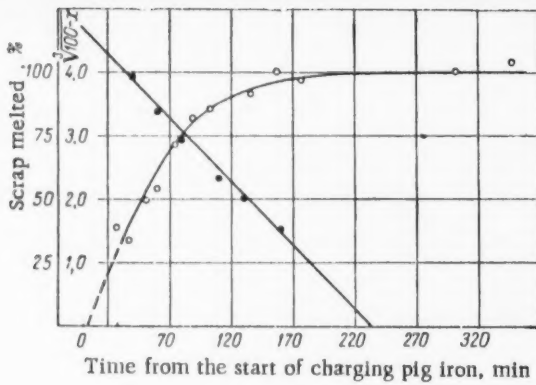


Fig. 1. Relationship between the quantity of scrap melted and time. ○) percentate of total weight: ●) $\sqrt{100-x}$.

where $\sum C_t$ is the sum of the percentage contents of impurities in the metal at time t , and $\sum C_0$ is the sum of the percentage contents of impurities in the pig iron at the time when it was poured into the furnace.

Thus conclusions concerning the kinetics of scrap melting can be drawn from calculations of the value of x based on measurements of the activity of the metal samples and on the results of chemical analysis. From

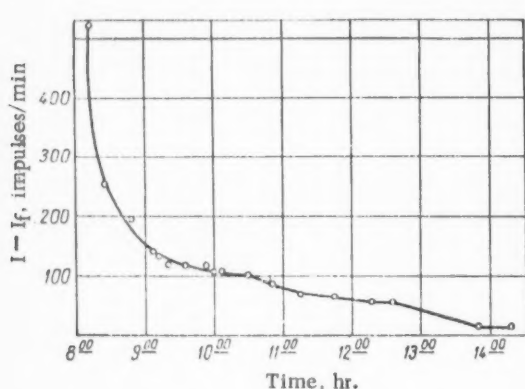


Fig. 2. Attenuation curve for Ca^{45} in slag.

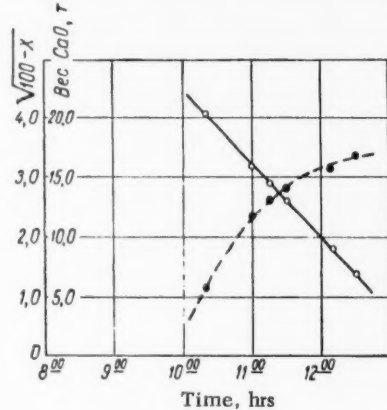


Fig. 3. Kinetics of solution of calcium oxide in slag. ●) weight of CaO ; ○) $\sqrt{100-x}$.

the relationship of the quantity of melted scrap (as a percentage of the total weight) and time, it is clear that the melting process can be represented by a smooth kinetic curve and that it apparently conforms to a definite law (Fig. 1). The completion of the melting process is indicated by the flattening out of the curve. The plateau can be used to determine the total weight of metal.

Similar data were obtained from 20 experimental melts.

Under the actual conditions of open-hearth furnace operation, the scrap melting process is complicated to a greater or lesser extent by a whole series of associated factors.

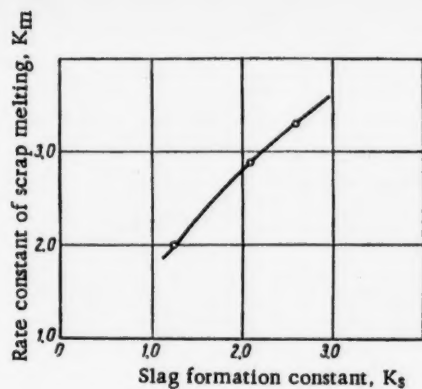


Fig. 4. Relation between the rate constant of scrap melting and the slag formation constant.

In the present work the authors have confined themselves to an attempt at determining the kinetic equation which describes the melting of scrap in the scrap-ore process. If it is assumed that the rate of melting dG/dt (G is the weight of scrap melted) is proportional to the surface of separation between the scrap and the molten pig iron or approximately equal to the surface of the scrap, S , then

$$\frac{dG}{dt} = KS, \quad (3)$$

where K is the proportionality constant.

The following relationship applies in the case of a body having a definite correlation between its weight and surface

$$S = \alpha G^{2/3}, \quad (4)$$

where α is a geometrical coefficient depending on the shape of the body. For scrap consisting of separate pieces more or less varied in shape, the coefficient α can be represented by some mean value. Hence

$$\frac{dG}{dt} = K \alpha G^{2/3}. \quad (5)$$

We will express the rate of melting scrap as a percentage of its total weight, i. e., we replace dG/dt by dx/dt . It is obvious that the weight per cent of scrap remaining solid at a given time is $100 - x$. In accordance with the assumption stated, the rate of melting is proportional to the extent of the surface of the solid scrap and consequently

$$\frac{dx}{dt} = K_M (100 - x)^{2/3}, \quad (6)$$

where $K_M = K\alpha$.

Integration of this equation gives

$$3 \sqrt[3]{100 - x} = K_M t + C, \quad (7)$$

where C is the integration constant.

From Equation (7) it follows that the quantity $\sqrt[3]{100 - x}$ is a linear function of time. The dependence of $\sqrt[3]{100 - x}$ on time (a straight line) is given in Figure 1. Points taken from the smoothed kinetic curve fall quite satisfactorily on the straight line.

By introducing the rate constant K_M it is possible to evaluate objectively the rate of melting in each given melt, to compare the melting conditions in different furnaces and to determine the dependence of K_M on the technological parameters. In addition, knowing the value of K_M for a given melt, it is easy to calculate the quantity of scrap melted up to a certain moment and thus to work out the true rate of oxidation of impurities during melting.

The investigation carried out has enabled us to establish the dependence of the rate of scrap melting on the size of the thermal loads during charging, heating up and melting, on the length of time of charging the

pig iron and also on the concentration of carbon in the molten bath and the rate of oxidation of carbon dissolved in the metal.

A Study of the Kinetics of Slag Formation

To study the formation of liquid slag during melting, use was again made of the isotope attenuation method, using CaO containing Ca⁴⁵. The choice of this isotope was indicated by the fact that under melting conditions in the open-hearth furnace CaO is not reduced, does not dissolve in the metal and occurs only in the slag phase.

A preparation of calcium oxide tagged with Ca⁴⁵ was placed in a sealed metal tube and introduced into the furnace at the start of pouring the pig iron.

Sampling was begun 30-35 min after the introduction of the isotope into the furnace, a time which was sufficient for the isotope to become uniformly distributed throughout the whole volume of slag.

The quantity of slag in the furnace was determined from the formula

$$G_i = \frac{I_0 Q_i G_0}{I_i Q_0}, \quad (8)$$

where G_i is the quantity of liquid slag (in tons) in the furnace at a given time; I_0 is the activity of the "standard" slag in impulses/min; Q_i is the activity of Ca⁴⁵ introduced into the slag of the melt being studied in mC; G_0 is the weight of "standard" slag in tons; I_i is the rate of count of slag samples from the melts being studied at a given time; and Q_0 is the activity of Ca⁴⁵ introduced into the "standard" slag, in mC.

If at a certain time a known quantity of slag is removed from the furnace, which gives a mean rate of count I_r^m , then Equation (8) becomes

$$G_i = \frac{I_0 Q_i G_0}{I_i Q_0} - \frac{G_r I_r^m}{I_i}. \quad (9)$$

where G_r is the weight of slag removed.

The attenuation curve for Ca⁴⁵ for one of the melts investigated is presented in Figure 2.

To a first approximation it may be assumed that after oxidation of the silicon and manganese in the pig iron and melting of the ore further slag formation is determined by the rate of solution of pieces of disintegrated limestone in the molten system FeO-Fe₂O₃-SiO₂-MnO.

This process can apparently proceed within the mass in separate regions of material charged onto the hearth, into which the initial slag flows. Solution goes on for a fairly long time and hence may be the limiting factor in slag formation. The "lime boiling" observed is evidence of this and so is the fact that pieces of limestone come to the surface at the end of the melting stage.

In the absence of special theoretical considerations for estimating the rate of solution of calcium oxide, it is convenient to use the same consideration as that employed in investigating the kinetics of scrap melting and to use Equation (6) in the form

$$\frac{dx}{dt} = K_s (100 - x)^{2/3}, \quad (10)$$

where x is the weight of calcium oxide dissolved in the slag (as a percentage of total weight in the nonmetallic charge) fed into the furnace up to the end of the melting stage.

Experimental data from the melts studied confirm the validity of this equation.

The curve characterizing the solution of calcium oxide in the slag is presented in Figure 3. It is typical of saturation processes. The flattening out of the curve indicates the end of the solution of limestone. The ordinate of the plateau corresponds to 100% dissolved calcium oxide. From Figure 3 it can also be seen that the experimental points plotted on the graph in coordinates of $\sqrt[4]{100 - x}$ against time obey the straight-line relationship perfectly satisfactorily.

The validity of Equation (10) is confirmed by data from several of the melts investigated.

The use of the quantity K_s as a criterion of the rate of slag formation provides an explanation of the effect of the order of charging powdery materials and their physical properties on the rate of this process. As can be seen from Figure 4, a definite connection is observed between K_M and K_s .

Such a connection reflects the similarity between the physicochemical conditions which determine the course of the processes of scrap melting and solution of lime.

LITERATURE CITED

- [1] A. I. Osipov, L. A. Shvartsman, V. E. Iulin and M. L. Sazonov, Conference of the Academy of Sciences USSR on the Peaceful Uses of Atomic Energy (Session of the Division of Technical Sciences), p. 29 (AN USSR Press, 1955).
- [2] A. I. Osipov, L. A. Shvartsman, V. E. Iulin and M. L. Sazonov, "A study of the mixing processes in the steel bath during the reduction of high-phosphorus pig irons" (Report of the Central Scientific Research Institute for Ferrous Metallurgy, 1955).

Received January 15, 1957

SCIENTIFIC AND TECHNICAL NEWS

ON THE PHYSICS OF IONIZED GASES

The Third International Conference on the study of Physical Phenomena in Ionized Gases took place in Venice, June 11-15, 1957.

The reports read at the conference were devoted to elementary processes occurring in plasmas, various types of discharges, the technology of gas-discharge tubes, and problems of the radiation of plasmas at high temperatures.

There was great interest in the reports devoted to researches on powerful gas discharges and plasmas in a magnetic field, i. e., to questions connected in a certain degree with the problem of the production of a controlled thermonuclear reaction.

Physicists of a number of countries have been occupied with the solution of this problem during the last several years. Work is being carried on in two main directions, as regards basic principles: the study of pulsed processes, and the study of stationary systems in which a plasma at high temperature is kept in an isolated state by means of a magnetic field.

As is well known, the Soviet Union has been the initiator of publication of work in thermonuclear research. In April 1956, during a visit of a Soviet government delegation to England, Academician I. V. Kurchatov presented at Harwell a report "On the Possibility of Producing Thermonuclear Reactions in Gas Discharges," devoted to a survey of several researches on pulsed processes which were being carried on in the Soviet Union. This report together with a number of researches by Soviet physicists, carried out under the direction of Academician L. A. Artsimovich and M. A. Leontovich, is published in the journal "Atomic Energy" [1-8].

Soon after the report by I. V. Kurchatov, E. Teller [9] presented a lecture in the USA on general problems of controlled thermonuclear reactions. There was also published a paper by R. Post [10] on the use of the physics of high-temperature plasmas in the realization of controlled thermonuclear reactions. At the beginning of the present year a number of papers by English physicists were published [11-16]. Most of the papers in question were mainly devoted to the discussion of general problems of principle in the production of a thermonuclear reactor.

At the conference in Venice a number of papers were presented devoted to the search for practical ways of realizing controlled reactions of synthesis.

A brief survey of a number of studies in this field is given below.

Some of the experimental researches reported at the conference were devoted to the study of the instabilities of a filament of plasma carrying a current ("pinch" effect), to the determination of the parameters characterizing discharges of large currents, and also to the observation and study of the hard radiation appearing in discharges in deuterium.

T. K. Allen (England) had studied the instability of discharges in toroidal and race-track chambers at currents of several thousand amperes and pressures from 0.5 to 20 mm Hg.

J. E. Allen and Reynolds (England) had carried out experiments with a ring discharge. The maximum current strength was 20 thousand amperes, the pressure 0.1 to 1.5 mm Hg. The temperatures of the electrons and ions were determined spectroscopically. The results are in agreement with a theory developed earlier by J. E. Allen [14], in which the compression of the discharge is related to the formation of a shock wave.

Hemmings, Miles, and Ware (England) had studied the instability of a toroidal discharge in argon at pressures 10^{-2} - 10^{-3} mm Hg. The large and small diameters of the chamber were 30 and 10 cm respectively.

The current in the chamber was of the order of 2000 amperes. Photographs of the discharge show that the application of a toroidal magnetic field, and also application of a field of short magnetic lenses, leads to the appearance in the discharge of a number of luminous channels.

Bickerton (England) had studied the characteristics of a discharge at great current strength in a longitudinal magnetic field.

Breton, Charon, Hubert, Vendryes, and Yvon (France) had studied discharges in deuterium in linear and toroidal chambers, and had also studied the effect of a longitudinal magnetic field.

A most interesting research was that of Colgate, Anderson, Becker, Ise and Pyle (USA) on the emission of neutrons in a linear pulsed discharge in deuterium. As is well known, this effect was discovered and studied in the USSR by Artsimovich and his co-workers. The American physicists observed the emission of neutrons in a powerful pulsed discharge to the number of about 10^8 per discharge. The experiments were carried out with quartz tubes of length 45 or 90 cm and diameter of from 5 to 8 cm. The source of energy was a battery of 25 condensers, each of capacity $0.5 \mu\text{f}$, charged to a potential of 50 kv. The maximum current was about 200,000 amp. The oscillograms of the current and voltage are of the same character as in the researches of the Soviet physicists. The neutrons appeared at the second and third breaks of the current curve.

By means of scintillation counters Colgate and others measured the spatial distribution of the neutrons and found that they arise from a region near the axis of the discharge, of diameter not greater than 2 cm, and appear simultaneously along the whole length of the tube. The recoil protons in an emulsion were used to determine the energy of the neutrons as a function of the angle between the axis of the tube and direction of emission of the neutrons. These authors also found that the yield of neutrons is decreased when a longitudinal magnetic field is applied. These facts, together with a study of the effects of the applied voltage and of impurities in the discharge chamber, made it possible to conclude that these neutrons did not arise from a thermonuclear process. Studies of the dependence of the energies of the neutrons on their angle of emission led the authors to the conclusion that the neutrons are produced by a small group of deuterons accelerated along the axis of the tube in the direction of the applied electric field. The measured neutron energies correspond to the deuteron energy of 50 kev with an average spread of ± 50 kev. For this, the energies of individual neutrons must reach 200 kev. The occurrence in the discharge of the large electric fields in which deuterons acquire such an energy is ascribed by these authors to the constrictions of the discharge caused by instability of the "sausage" type.

Short communications not on the original conference program were also given by English and Swedish physicists about the observation of neutrons in discharges in deuterium.

Some of the theoretical reports at the conference were devoted to studies of the conditions of magnetohydrodynamic stability of the discharge.

Rosenbluth (USA) had found that a filament of plasma carrying surface current and surrounded by an ideally conducting case can be stable, when a longitudinal magnetic field is present, over a rather wide range of variation of the parameters that fix its initial equilibrium state (ratio of longitudinal and azimuthal magnetic field, ratio of the radii of the filament of plasma and the coaxial case). The studies were carried out both on the basis of the magneto-electrodynamic equations and by means of an improved system of equations based on the existence of an adiabatic invariant of the motion of a charged particle in a magnetic field. For an initially isotropic distribution of velocities the results obtained for both cases are the same.

Hain, Lust and Schlüter (West Germany) showed that when dissipation is neglected in the study of the stability of magnetohydrodynamic equilibrium systems one obtains a differential equation of second order with respect to time. This equation is self-adjoint, so that a number of general theorems can be established for all equilibrium configurations. Sufficient conditions for stability have been obtained for a certain class of configurations.

Bernstein, Frieman, Kruskal and Kulsrud (USA) have developed the energetic principle for studying stability (introduced by Lundquist) in applications to ideally conducting and completely ionized plasmas. This principle can be applied to obtain criteria of stability of equilibrium systems of plasma in a magnetic field in cases in which the magnetic field does not penetrate into the plasma, when the magnetic fields exist inside the plasma but the system is axially symmetric, and also for a number of other special cases.

Taylor (England) had studied the stability of a filament of plasma with distributed current in the presence of a longitudinal field. In this case no absolutely stable state exists. The rate of growth of disturbances can, however, be decidedly reduced. With a sufficiently strong longitudinal magnetic field the only disturbances that remain unstable are those with wave length exceeding the dimensions of the system.

Some individual theoretical papers were devoted to the study of rarefied plasma in a magnetic field and to the study of discharges in a magnetic field.

Kruskal (USA) proved the existence of an adiabatic invariant of the motion of a charged particle in a magnetic field in arbitrary order of the expansion in a power series with respect to a small parameter of the drift theory.

Schlüter (West Germany) had studies the possibility of heating plasmas in a slowly varying magnetic field.

Thompson (England) considered the effect of a magnetic field on a discharge, and in particular the effect of the magnetic field of the discharge itself on the breaking away of the discharge from the walls.

Post (USA) presented to the conference a report containing the same information as his previously published article.

The researches presented at the conference and also the remarks of foreign scientists in private conversations give evidence of the large-scale achievements up to the present time in researches on pulsed processes in a number of countries (USA, England, France, West Germany, Sweden, and others), and also of the high scientific level of these researches.

The Soviet delegation participating in the work of the conference was composed of: S. E. Frish, (head of the delegation), A. I. Akhiezer, R. A. Emikhranov, V. M. Kukel'skii, S. L. Mandel'shtam, V. G. Tel'kovskii, N. V. Fedorenko and V. D. Shafranov.

The conference was well organized. The participants in the conference had an opportunity to become acquainted with the sights of Venice and of the other cities of Italy. The relations between the delegates were of the most friendly sort. Personal conversations with the foreign scientists were very interesting. The fact is to be regretted that the delegation of the USSR arrived at the conference very belatedly and could be present only at the sessions of the last two days.

V. D. Shafranov

LITERATURE CITED

- [1] I. V. Kurchatov, J. Atomic Energy (USSR) No. 3, 65 (1956).
- [2] L. A. Artsimovich, A. M. Andrianov, O. A. Bazilevskaya, Iu. G. Prokhorov and N. V. Filippov, J. Atomic Energy (USSR) No. 3, 76 (1956).
- [3] M. A. Leontovich and S. M. Osovets, J. Atomic Energy (USSR) No. 3, 81 (1956).
- [4] L. A. Artsimovich, A. M. Andrianov, E. I. Dobrokhотов, S. Iu. Luk'ianov, I. M. Podgornyi, V. I. Sinitsyn and N. V. Filippov, J. Atomic Energy (USSR) No. 3, 84 (1956).
- [5] S. Iu. Luk'ianov and V. I. Sinitsyn, J. Atomic Energy (USSR) No. 3, 88 (1956).
- [6] S. Iu. Luk'ianov and I. M. Podgornyi, J. Atomic Energy (USSR) No. 3, 97 (1956).
- [7] A. L. Bezbachchenko, I. N. Golovin, D. P. Ivanov, V. D. Kirillov and N. A. Iavlinskii, J. Atomic Energy (USSR) No. 5, 26 (1956).
- [8] V. D. Shafranov, J. Atomic Energy (USSR) No. 5, 38 (1956).
- [9] E. Teller, Uspekhi Fiz. Nauk 61, 331 (1957).
- [10] R. Post, Uspekhi Fiz. Nauk 61, 491 (1957).
- [11] W. B. Thompson, Proc. Phys. Soc. 70B, 1 (1957).

- [12] J. D. Lawson, Proc Phys. Soc. 70B, 6 (1957).
- [13] R. S. Pease, Proc. Phys. Soc. 70B, 11 (1957).
- [14] J. E. Allen, Proc. Phys. Soc. 70B, 24 (1957).
- [15] P. J. Tayler, Proc. Phys. Soc. 70B, 31 (1957).
- [16] P. Carruthers, and P. W. Teale, Proc. Phys. Soc. 70B, 31 (1957).

AT THE ALL-UNION INDUSTRIAL EXHIBITION

Section. "The atomic nucleus and methods for its study." The section entitled "The atomic nucleus and methods for its study" gives us an insight into the structure of atoms and nuclei, the phenomenon of radioactivity, methods of obtaining nuclear energy, the chain reaction, problems of controlled thermonuclear reactions and so on.

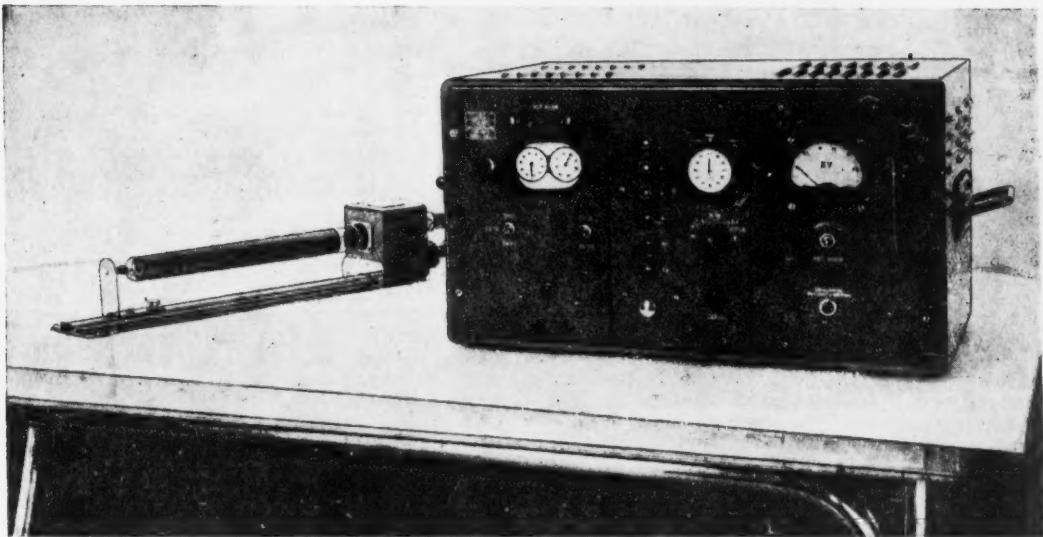


Fig. 1. B-2 type scaler.

There is a display of diverse measuring equipment designed for research on the properties of nuclear emission. There are various types of gas-discharge and scintillation counters which, in conjunction with pulse analyzers, are widely used for the spectral analysis of radiation. Two types of analyzers are also on display — a 24-channel analyzer on an electronic switch and a scintillation γ -ray spectrometer. The analyzer is intended for the amplitude analysis of pulses and is designed for positive and negative input pulses of 0.03-0.5 v. The scintillation γ -ray spectrometer is used for measuring the energy of x-rays and γ -rays in the 10 kev to 5 Mev region. From the amplitude distribution of the pulses the γ -ray energies can be determined. The counting rate is 100 pulses/sec.

Scalers of type B-2 (Fig. 1), BK-3 (Fig. 2), PS- 10^4 and PS- 10^6 , on display in the section, are used for the registration of pulses. Of great interest is a model of a standard scaling decade on a ring trochotron (Fig. 3), designed for counting electrical pulses statistically distributed in time. The decade forms a component part of a high-speed scaling device. The scaling factor of the latter depends on the number of decades composing the device. The scaling device on trochotrons, developed by the Institute of Radio-engineering and Electronics AN SSSR, has a resolving time of 0.2 microseconds.

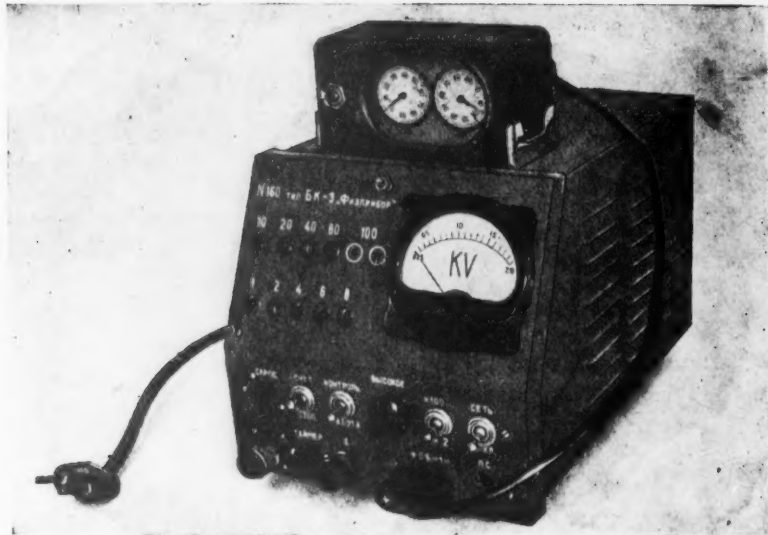


Fig. 2. BK-3 type scaler.

For the detection and recording of slow neutrons there is a SCh-3 unit (Fig. 4) which can be used for determining the intensity and half-life of radioactive substances. The sensitive element of the unit is a SNM-5 counter. With an apparatus of the "Bambuk" type, also on display, it is possible to measure the intensity of x-radiation; the measured radiation intensity is registered on an indicator, the resolving time of the apparatus (without counting tube) is 50 microsecond. Its sensitive element is an end-window counter.



Fig. 3. Model of standard scaling decade on a ring trochotron.

An apparatus of the "Iablonia" type, which is used for separating and counting coincidences and anticoincidences, is on view. The resolving time for coincidence can be varied within the limits $2 \cdot 10^{-6}$ and 10^{-7} sec. The apparatus operates with input pulses of amplitude 0.2 v and more.

Also displayed in this section are a broad-band amplifier of the "Kashtan" type, a double-beam electronic oscilloscope, an electronic microsecond timer and an amplitude comparator. The amplifier has a frequency band from 500 c/sec to 2 Mc/sec, maximal amplification factor 300,000 and gives positive output pulses with a maximal amplitude of 100 v.

The double-beam pulsed electronic oscilloscope DIO-56 is designed for the study of electrical pulse processes by visual display on the oscilloscope screen. The sweep range is from 5 microseconds to 2 milliseconds and the nonlinearity of sweep does not exceed 10%.

The electronic microsecond timer of type MS makes it possible to measure time intervals bounded by two pulses of positive or negative sign passing through one or two channels, as well as pulse durations of any sign.

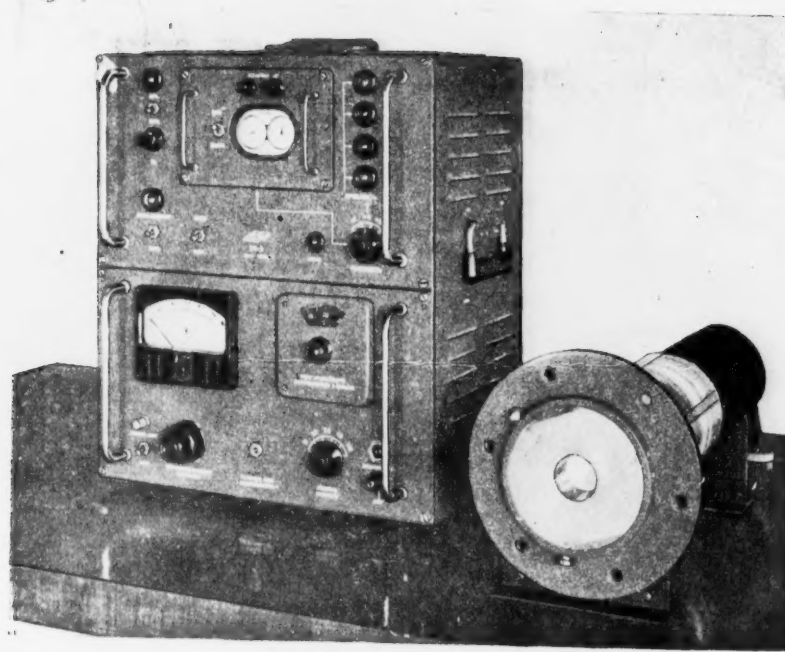


Fig. 4. SCh-3 unit.

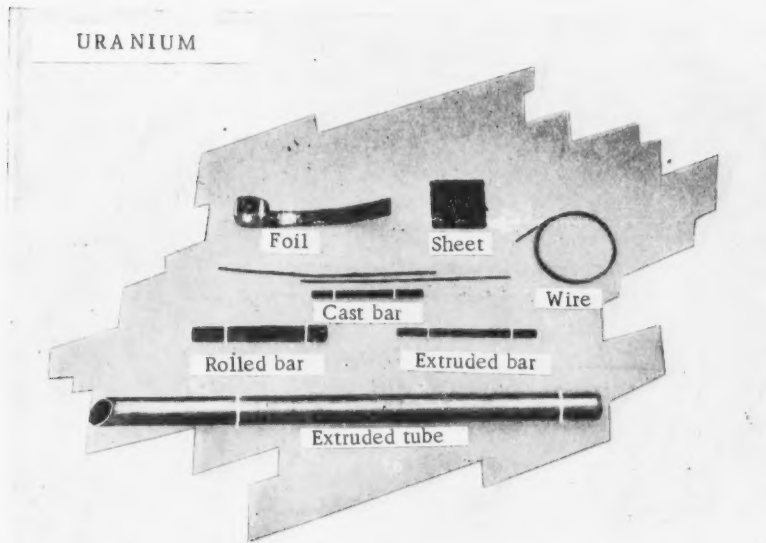


Fig. 5. Articles made from uranium.

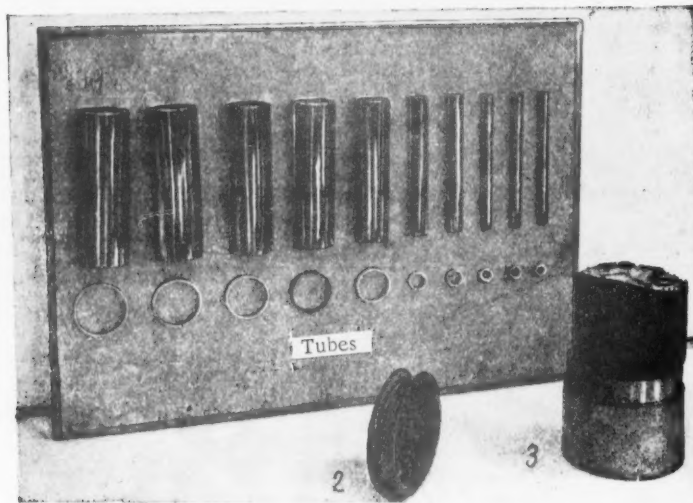


Fig. 6. Articles made from zirconium.
 1) Tubes of various diameter; 2) wire; 3) blank.

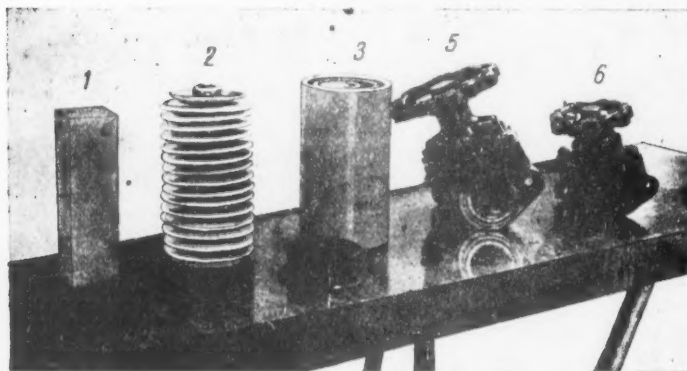


Fig. 7. Samples of nonmetallic materials. 1) Polyethylene block; 2) bellows of "ftoroplast"; 3) polyvinyl chloride tubes of various diameters; 4) resin packing ring; 5) polyethylene-lined valve; 6) resin-lined valve.

The duration of pulse fronts marking the beginning and end of measurement must not be greater than 1 microsecond, and the amplitude from 25 to 100 v.

The amplitude comparator is designed for measurement of the instantaneous value of a slowly-varying voltage. The range of measurable input voltages is 0-300 v, the accuracy of voltage measurement $200 \mu\text{v} \pm \pm 0.02\%$. The design of the comparator also allows it to be used for measuring constant voltage and also as a linear or narrow-band dc amplifier.

In addition, there is also on show a Wilson diffusion cloud chamber with transparent bottom, designed for the observation of α -particle tracks on a screen and also models and diagrams of different types of accelerators.

Section. "Materials for nuclear reactors." The stands in this section display "nuclear fuel" — uranium, "moderator" — beryllium, and construction material — zirconium.

Uranium is one of the heaviest metals. Its specific weight is 18.9-19.1, its fusion temperature 1130°. Dependent on the composition and treatment, the strength of uranium varies between 35 and 140 kg/mm². The surface of uranium polishes well. By pressure treatment (moulding, rolling, forging, drawing) in conjunction with heat treatment it is possible to obtain uranium articles in the form of rods, tubes, ribbon, foil and wire (Fig. 5).

Beryllium is one of the lightest metals, with a specific weight 1.85 and fusion temperature 1285°. Its hardness varies from 60 to 130 kg/mm². It is sufficiently strong within a large temperature range for technical purposes. A valuable property of beryllium is its resistance to oxidation at increased temperature. Besides being a good moderator for neutrons, beryllium can also be used as a construction material.

Zirconium is a metal possessing a high resistance to corrosion. It is practically unaffected by hydrochloric and nitric acid, dilute sulfuric acid, and aqueous alkaline solutions. In corrosion resistance zirconium is superior to titanium and comes close to tantalum and niobium. At high temperatures zirconium actively absorbs gases. Its specific weight is 6.4 and fusion temperature 1860°. Besides this, zirconium is very plastic, which makes it possible to manufacture all kinds of articles from it (Fig. 6).

On a stand are displayed some samples of nonmetallic materials which possess a number of properties of value to the radio-engineering industry. In particular, they are resistant to the action of radiation and are easily cleansed of radioactive contamination. Such are polyethylene, mixtures of POV* vinyl plastics, polyvinyl chloride plastic, polymethyl metacrylate, polystyrene, "ftoroplast-4" (fluoro-plastic), "grafitoplast" (graphite-plastic) and special resins. Besides the samples listed, there are also on view some industrial products lined with non-metallic materials (Fig. 7).

F. Musaev.

* Transliteration of Russian — Publisher's note.

✓
3
/
-
C
-
0
1
1

THE EXPERIMENTAL SODIUM GRAPHITE REACTOR, SRE, GOES CRITICAL

According to an announcement of the Atomic Energy Commission of the USA [1] dated April 25, 1957, the experimental sodium graphite reactor, SRE, located at Santa Susana near Los Angeles (California) was brought to criticality for the first time. This reactor is the prototype for the American power reactor, SGR.

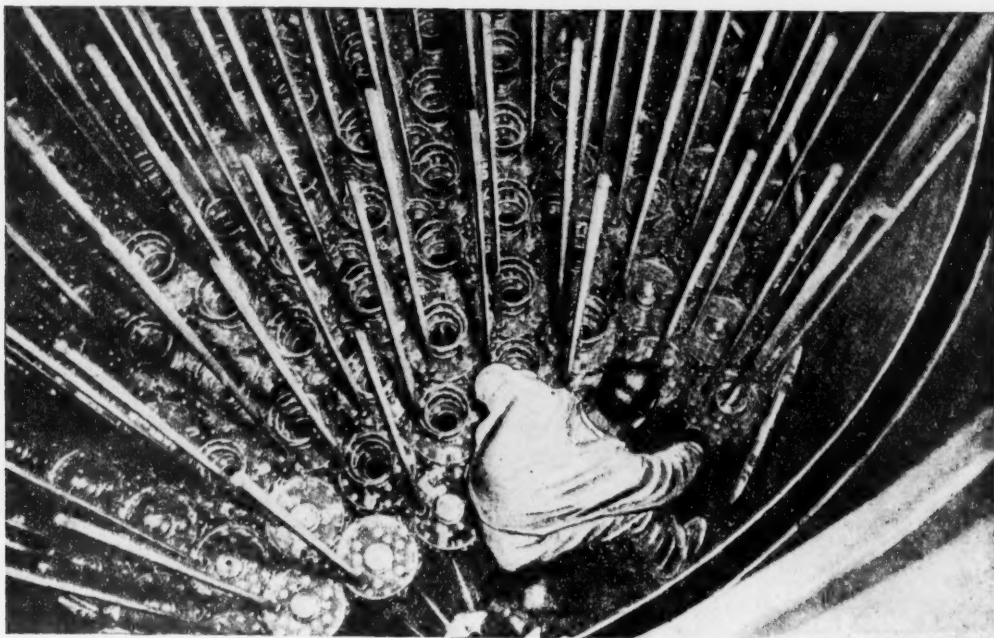


Fig. 1. Graphite columns mounted in tank of SRE reactor (view from above).

Thermal power of the SRE is 20 Mw. The initial intention had been to dissipate the heat generated through heat exchangers to air. However, during construction of this reactor it was decided to utilize this heat for generation of $7\frac{1}{2}$ Mw of electrical energy [2].

The SRE reactor was described in considerable detail in a report given by B. Perkins at the International Conference on Peaceful Uses of Atomic Energy at Geneva [3].

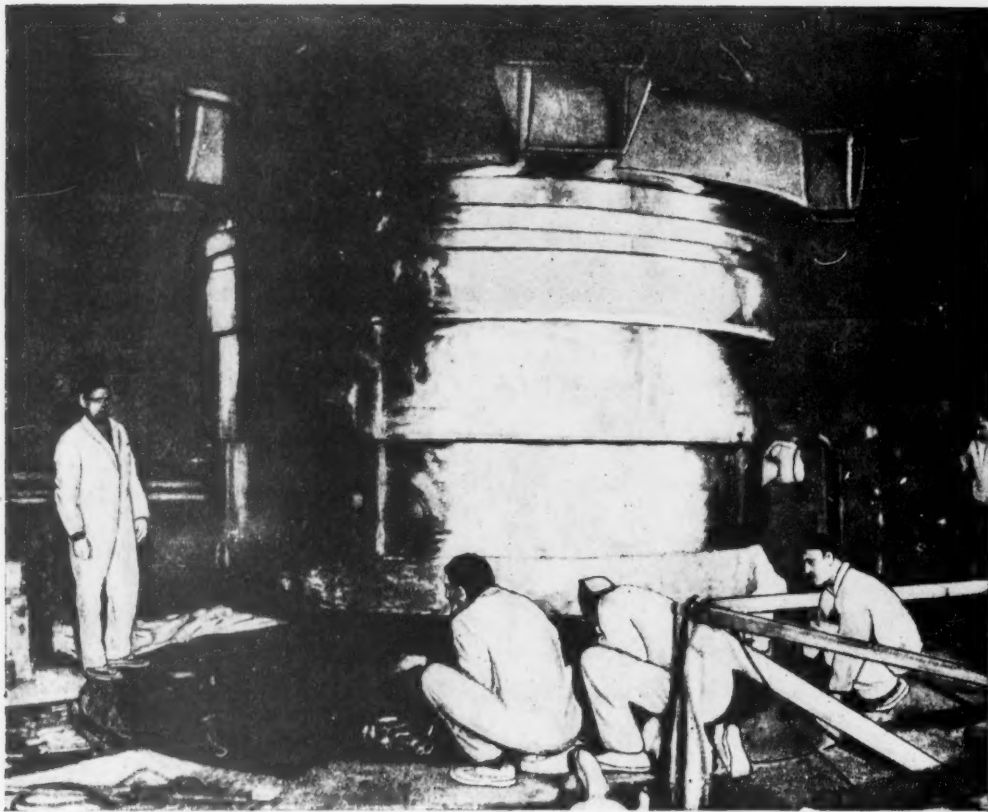


Fig. 2. Installation of the upper reactor shield, weighing 75 tons.

The coolant in the SRE reactor is sodium, which allows attainment of relatively high steam parameters. Sodium temperature at entrance to the reactor is 260°C and at outlet is 516°C.

The use of sodium for coolant, and of graphite for moderator requires special safety measures to preclude any contact between the graphite and the sodium. Such contact does not produce any significant chemical or volumetric changes in the graphite, but is undesirable since the graphite is saturated with sodium and this seriously impairs the neutron balance in the core through parasitic capture of neutrons by the sodium, which has a higher capture cross section for neutrons than the graphite. For this reason each of the 119 graphite columns are covered with a sheath of zirconium (side thickness 0.84 mm, face thickness 2.4 mm). Through a central opening in the graphite column passes a zirconium tube of 57.2 mm diameter and wall thickness 0.84 mm; this tube is welded at the top and bottom of the column with the face covering of the column. Within this tube is placed the fuel element assembly consisting of seven fuel elements of the rod type [4]. The control rods are located along the graphite block walls.

The sodium flows from bottom to top through the central tube, absorbing heat from the fuel elements and also through gaps between the sides of the hexagonal graphite column, thus cooling the sides. The gap between fuel elements is so chosen that rises in temperature of the sodium flowing through the tubes and through the gaps are equal [3]. The fuel elements are distributed in a grid of triangular pattern with fuel

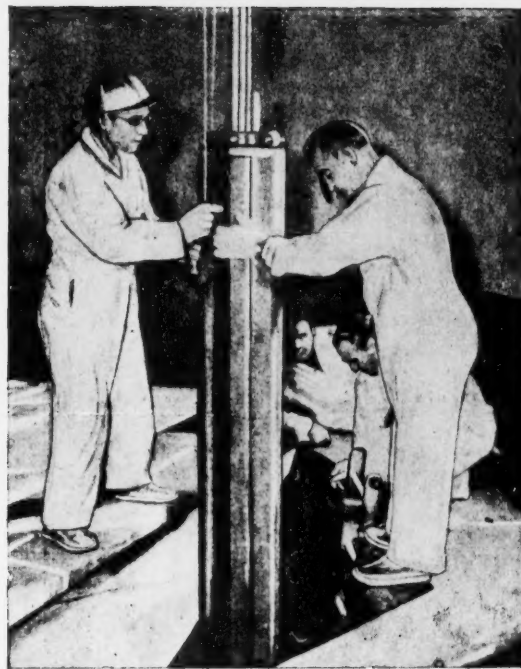


Fig. 3. Installation of a fully assembled graphite column in the reactor.

element spacing of 26.4 cm. The core and moderator are located within a sealed tank of approximately 330 cm diameter and 570 cm high.

The cost of the SRE reactor proper is placed within the limits of 3.5 to 6.8 million dollars, the fuel element assemblies including the fuel, are valued at 220 to 230 thousand dollars, the building and its equipment are valued at 0.5 to 0.9 million dollars [5].

Iu. K.

LITERATURE CITED

- [1] Engineering 183, 4758, 636 (1957).
- [2] Mechanical Engineering 79, 3, 245 (1957).
- [3] Atomic Energy (Gosenergoizdat, Moscow) 1956, p. 208.
- [4] Nuclear Engineering 2, 11, 78 (1957).
- [5] Engineering 183, 4763, 796 (1957).

THE USE OF ORGANIC COMPOUNDS IN REACTOR CONSTRUCTION

Recently organic liquids have been widely studied with a view to their use as moderators and coolants in nuclear reactors. Particular interest has been shown in organic compounds by firms and research organizations, working on the problem of using nuclear energy in transport systems.

The firm Atomics International is designing a reactor for a cargo ship using an organic compound as the moderator and coolant [1].

In Harwell, a reactor is projected for a submarine with an organic moderator and a liquid metal coolant. In a second form it is proposed to use a gas turbine. Besides this, a reactor with an organic moderator and coolant is being developed for a tanker with a displacement of 65 thousand tons [2], [3].

Organic compounds used as coolants have a series of advantages over other coolants:

- 1) low saturation vapor pressure, which makes it possible to have high temperatures at low pressures;
- 2) good moderating properties and low activity developed by neutron irradiation;
- 3) weak chemical reactivity, which produces little erosion and corrosion of construction materials because of the absence of reaction with these materials as occurs with sodium and potassium.

However, until recently, the problem of the stability of organic compounds under the combined effect of heat and radiation remained obscure.

The firm Atomics International investigated the behavior of ortho-, meta- and para-terphenyl at temperatures of 400 and 450°C and various radiation doses up to 90 watt-hours/g. The source of radiation was a Van de Graaf generator, giving electrons at an energy of 1 Mev with a beam current of 10-20 microamp. The experimental apparatus was arranged so that it was possible to perform experiments with and without radiation at the same time. As a result, curves were obtained of the rate of pyrolysis (decomposition by heat) and radiolysis (decomposition by radiation).

From the spectra of the products of fractional distillation of the irradiated compounds it was possible to establish the degree of polymerization of the terphenyl, which gave a measure of the stability of the sample.

Besides this, changes in the temperatures at which the samples began to melt and completely melted were studied. The curves obtained are given in Figures 1-6. On these diagrams are shown the temperature of complete melting (Curve 1), the temperature at which melting begins (Curve 2), the amount of polymer molecules formed per 100 ev of absorbed energy G_p (Curve 3), the percentage of polymerization on radiolysis and pyrolysis (Curve 4) and the percentage of polymerization on pyrolysis (Curve 5). As the diagrams show, the pyrolysis effect is not more than 3% of the total effect.

The most stable of all the substances studied is para-terphenyl. Comparison of the curves in Figures 1 and 6 shows that the stability of meta-terphenyl is increased by adding a small amount of para-terphenyl to it.

Tests showed the possibility of applying polyphenyls under conditions of high temperature and radiation [4].

The firm Monsanto Chemicals, together with the construction department of the US Navy ship building board, performed tests with a loop in the Brookhaven National Laboratory reactor on several types of organic compounds: biphenyl, a eutectic mixture of biphenyl, ortho-terphenyl and meta-terphenyl (36% biphenyl, 45% orthoterphenyl and 19% meta-terphenyl), a hydrogenated mixture of terphenyl isomers (HB-40) and monoiso-propylbiphenyl (MIPB) [5], [6]. The physical properties of these compounds are given in Table 1.

TABLE 1

Physical characteristics	Units of measurement	Biphenyl	Eutectic	HB-40	MIPB
Melting point	°C	70	20	-25	-47
Boiling point	the same	255		362	290
Vapor pressure at:					
100° C	mm Hg	4			
150° C	the same	43		2	10
200° C	»	185		15	63
250° C	»	670		69	290
300° C	atm.	2.4		0.33	1.25
350° C	the same	5.55		0.82	3.5
Density at:					
100° C	g/cm³	0.980	1.000	0.930	0.925
200° C	the same	0.880	0.918	0.858	0.857
300° C	»	0.790	0.837	0.786	0.776
Viscosity at:					
100° C	centistokes	0.980	2.3	3.800	1.400
200° C	the same	0.430	0.65	1.200	0.560
300° C	»	0.240	0.36	0.520	0.310
Heat capacity at:					
100° C	cal/g·°C	0.428	0.413		0.470
200° C	the same	0.508	0.495		0.555
300° C	»	0.590	0.575		0.637
Thermal conductivity (100—220° C)	cal/°C·cm·sec	$31.5 \cdot 10^{-8}$			$28.8 \cdot 10^{-8}$
Hydrogen content	%	6.53			8.28

TABLE 2

Physical characteristics	Units of measurement	Biphenyl	Eutectic	HB-40	MIPB
Integral dose of fast neutrons	nvt	$1.393 \cdot 10^{18}$	$1.66 \cdot 10^{18}$	$3.94 \cdot 10^{17}$	$1.36 \cdot 10^{18}$
Amount of decomposition products at end of experiment	%	7.4	7.0		10
Decomposition rate in percentages for irradiation of 10^{18} nvt		29	17	~120 (estimated)	40—20
Amount of gaseous decomposition products per g of decomposition products	cm³/g	12		56	15
Composition of gases	%	H₂(37)		H₂(95)	H₂(85) CH₃CH₂CH₃ (14)
Coefficient of heat transfer at 227° C and a liquid rate of 3 m/sec	kcal/m² hr °C	5 500	4 000	3 000	4 250
Induced radioactivity	mC/g	0.45	0.38	0.15 ÷ 4	0.111
Induced radioactivity of the filtered sample	mC/g	0.23	0.21	0.15	0.109
Composition of the induced radioactivity (unfiltered sample)	%	Fe ⁵⁹ (6.6) Na ²⁴ (20.6) Mn ⁵⁶ (72.8)	Fe ⁵⁹ (13.3) Na ²⁴ (10) Mn ⁵⁶ (60.2) Ce ¹⁴⁸ (16.5)		Fe ⁵⁹ (5.4) Na ²⁴ (8.1) Mn ⁵⁶ (37.8) Ce ¹⁴⁸ (48.7)
Maximum permissible temperature in an atmosphere of nitrogen	°C	>425	>425	<400	>400
Maximum permissible temperature in air	°C	>400	>400		375 ÷ 400

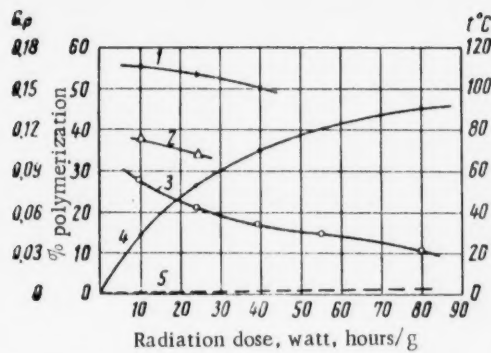


Fig. 1. The effect of radiation on meta-terphenyl at a temperature of 400°C .

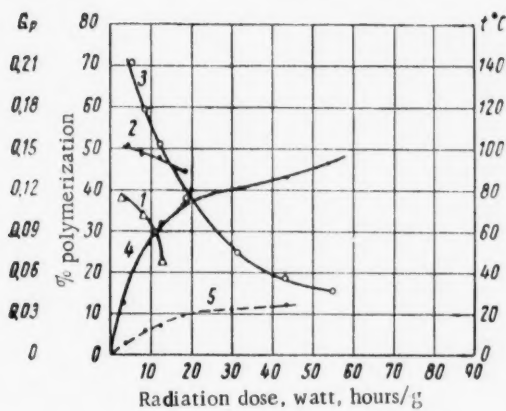


Fig. 2. The effect of radiation on meta-terphenyl at a temperature of 450°C .

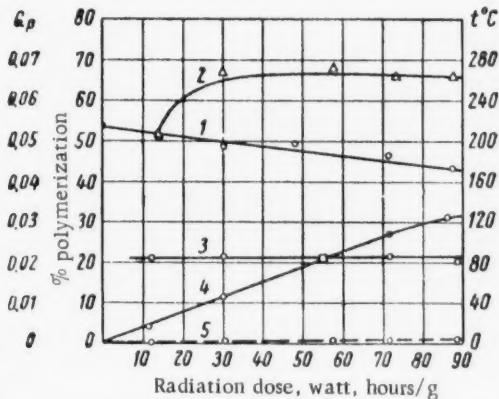


Fig. 3. The effect of radiation on para-terphenyl at a temperature of 400°C .

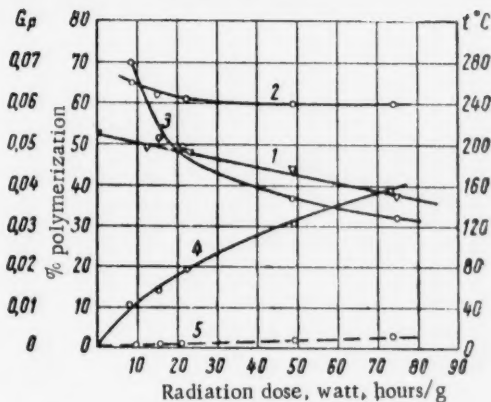


Fig. 4. The effect of radiation on para-terphenyl at a temperature of 450°C .

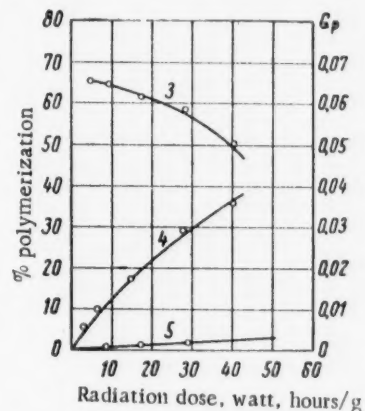


Fig. 5. The polymerization of ortho-terphenyl when irradiated and at a temperature of 400°C .

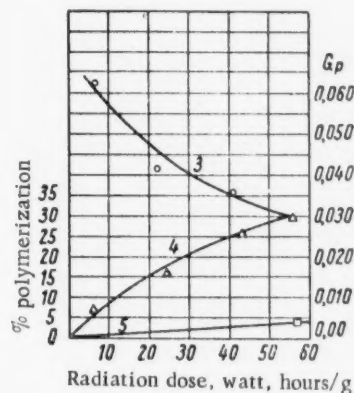


Fig. 6. The polymerization of a mixture of meta-terphenyl (95.65%) and para-terphenyl (4.35%) when irradiated at a temperature of 400°C .

The tests showed that the organic compounds were quite suitable for use as moderators and coolants. The main drawback of organic compounds is their tendency towards radiolysis. The decomposition rate, which equals the percentage of the substance decomposing relative to the integral flux (nvt), of the substances investigated was quite high (of the order 30). However, in a reactor of a large electrical generating station, for example of 100,000 kilowatts capacity, this leads to a calculated loss of coolant of only about 50 kg/hr.

The high solubility of the decomposition products in the compound used does not lead to contamination of the coolant and the comparatively small effect of the decomposition products on the heat transfer properties makes 10% decomposition of the liquid tolerable. In the coolants examined, the percentage of coolant decomposed did not exceed this figure. The decomposition products have much higher boiling points so that they may be removed by distillation.

The main results of the investigation are given in Table 2.

A thorough analysis of the properties of the organic compounds confirms that the most promising one is monoisopropylbiphenyl, which was recommended for use in an experimental reactor.

I. S.

LITERATURE CITED

- [1] Atomic Energy, Guideletter No. 108, 4 (1957).
- [2] Engineering 183, No. 4272, 123 (1957).
- [3] Financial Times 1, 2, 8 (1957).
- [4] Nucleonics 15, No. 2, 72 (1957).
- [5] Nucl. Eng. 2, No. 12, 126 (1957).
- [6] Nucl. Eng. 2, No. 13, 156 (1957).

DOSIMETRIC EQUIPMENT

In recent years (1954-1956) dosimetric equipment, in which new recording principles (luminescence, etc.) have been used, has been developed, whereby dosimetric measurements can be extended and accuracy improved.

The following are some such equipments.

x-Ray dosimeter type DIB, for measuring x-ray dose-rates and doses from 10 to 10^4 r. Automatic signalling and source cut-off devices are built in.

Type IDK-3 equipment, consisting of a set of individual dose-meters and a charging and measurement unit, for recording external γ -ray doses.

A new chamber-operation principle makes it possible to measure doses from 0.01 to 50 r with a single chamber, automatic scale-switching being used in the measurement unit.

The EF-2 portable electroprecipitation filter for concentration determinations on α - and β -active aerosols; deposition efficiency 85-90% for aerosols of varying dispersions at airflow rates up to 1600 liters/min.

The ILK-3 equipment for measuring individual γ -ray and thermal neutron doses with finely-divided phosphor buttons. Range $0.02-10^3$ r.

A clinical radiometer for measuring blood-flow rates (with Na^{24}) and iodine localization in the thyroid. A γ -ray scintillation head is used.

A universal scintillation dosimeter for measuring external γ -radiation, thermal neutron fluxes and α and β surface contamination in the presence of γ -radiation.

A pocket radiometer, being a portable counter for recording external γ -radiation in the range 0.1 to 100 $\mu\text{r/sec}$ and β -particle fluxes from 5 to 500 β -particles/cm².sec. The equipment is built of transistors and fed from a single cell giving a running time of 200 hours. Weight 580 g.

The DIB unit and the clinical radiometer have been demonstrated at international exhibitions in Geneva, Prague, Delhi, Warsaw and at the All-Union Industrial Exhibition in Moscow.

Iu. Sh.

3
1
2
4
5
6
7
8
9

THE DEVELOPMENT AND INTRODUCTION OF SOME RADIATION SCREENING AND HANDLING DEVICES

In recent years Soviet designers have devoted much attention to radiation screening and handling devices for safe operation, and have also developed methods.

Busygin's simple and original "self-locking" handling tongs have been mass-produced and have proved a valuable item of equipment in laboratories preparing and using artificial radioactive preparations.

The author and colleagues have developed a selection of manual clamps for radiochemical operations of a preparational or therapeutic character. The range provides medium-remote handling devices for all normal laboratory chemical vessels etc., has long been of value, and is now being mass-produced.

The laboratory dish (evaporating basin) is a basic and very common piece of equipment and yet one of the most difficult to adapt to remote handling in radiochemistry. Its shape and size are very variable, as are its weight and center of gravity as between the filled and empty states. In working with large objects containing hazardous materials it is very difficult to devise mechanical hands for remote control.

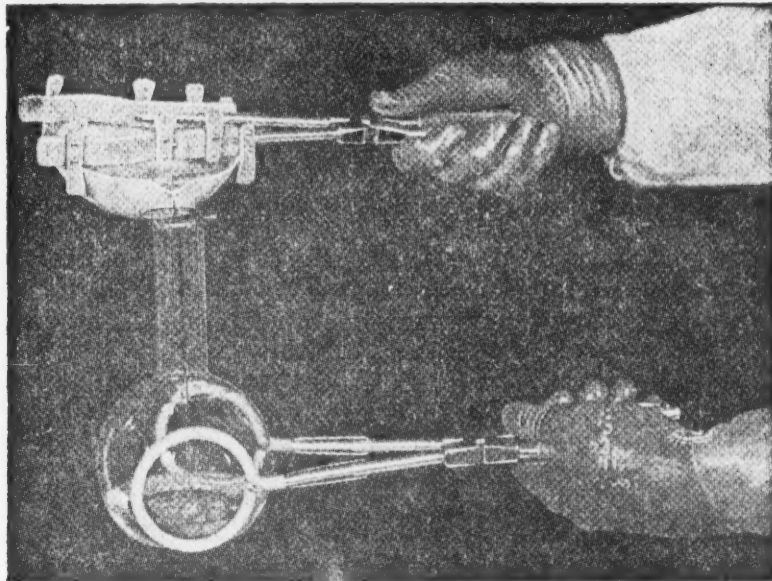


Fig. 1. An operation using two different kinds of tongs — pouring a liquid from an evaporating dish into a spherical flask.

Some typical points about the clamps are the two or four strong sprung working rods terminating in rubber-covered gripping jaws of various shapes appropriate to the dishes and fitted where necessary with additional side-arms to give sensitive and reliable "feel" in use (Fig. 1).

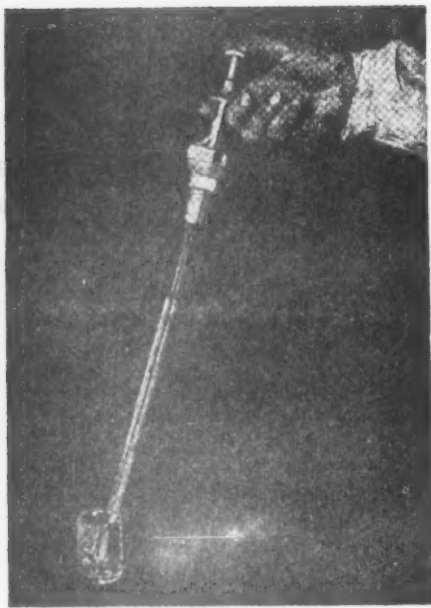


Fig. 2. A radiochemical autopipette.

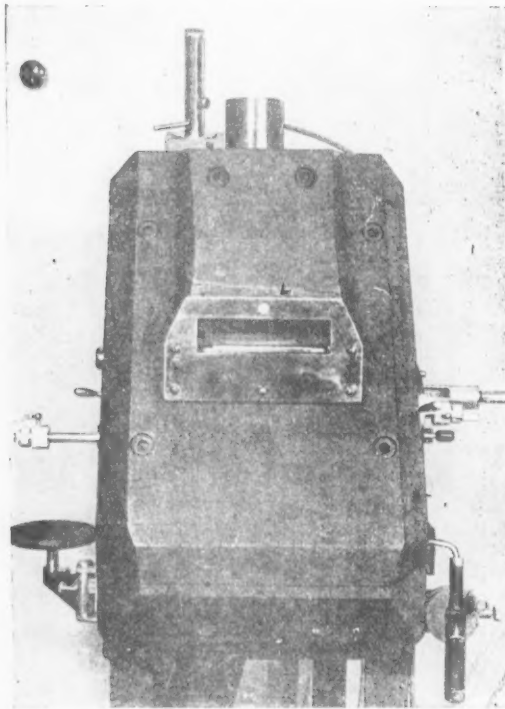


Fig. 3. A shielded box for loading radiotherapy needles and applicators.

All the clamps, as a rule, are suitable for objects of any shape and can grip them in any position so the center of gravity can be kept approximately in the principal plane of the tongs. This feature is an aid to safety, particularly with heavy objects, as they can be held steady and manipulations are easy and convenient.

The fixed pneumatic handling devices and manual pneumatic tongs developed by the author are intended for remote control of vessels containing radioactive preparations in shielded glove-boxes or in open conditions. They are very simple in design and suitable for use with comparatively light objects of various shapes and sizes even in very inaccessible locations.

Operations involving radioactive liquids required special safe methods and equipment to be designed and put into production.

A micropump* for use with micropipettes, a sampling autopipette (Fig. 2) and several modifications to liquid-handling devices for volume measurement and transfer operations with radioactive and other toxic liquids involving pneumatic or hydraulic remote controls were developed. The manipulations could be carried out at differing activity levels with the appropriate accuracy. The liquid-handling devices eliminated the need to move vessels containing liquids and to manipulate them off the bench, and also enabled one to perform transfer operations.

The micropumps and autopipettes have now been produced commercially for several years, the liquid-handling devices being presently introduced.

A shielded box containing new handling and transfer facilities designed by Busygin under the direct guidance of the author is intended for use with needles, applicators and molds for radiotherapeutic use.

A number of new features were introduced into the box including a sectional storage container made of cast-iron rings and a sterilizer-container with additional water shielding; a viewing-window unit with a combination of organic and lead-glass shielding, or thick glass plus water, or transparent liquids of high density; a movable hand-shield with tong manipulators in a ball joint, etc.

Honeycomb containers for storing and transporting needles and applicators, developed by Busygin et al, have been produced and applied in radiotherapy. The ingenious positioning of the preparations utilizes the partial self-absorption in the materials to increase the shielding.

The equipment developed by Busygin for the preliminary handling of radioactive needles and applicators

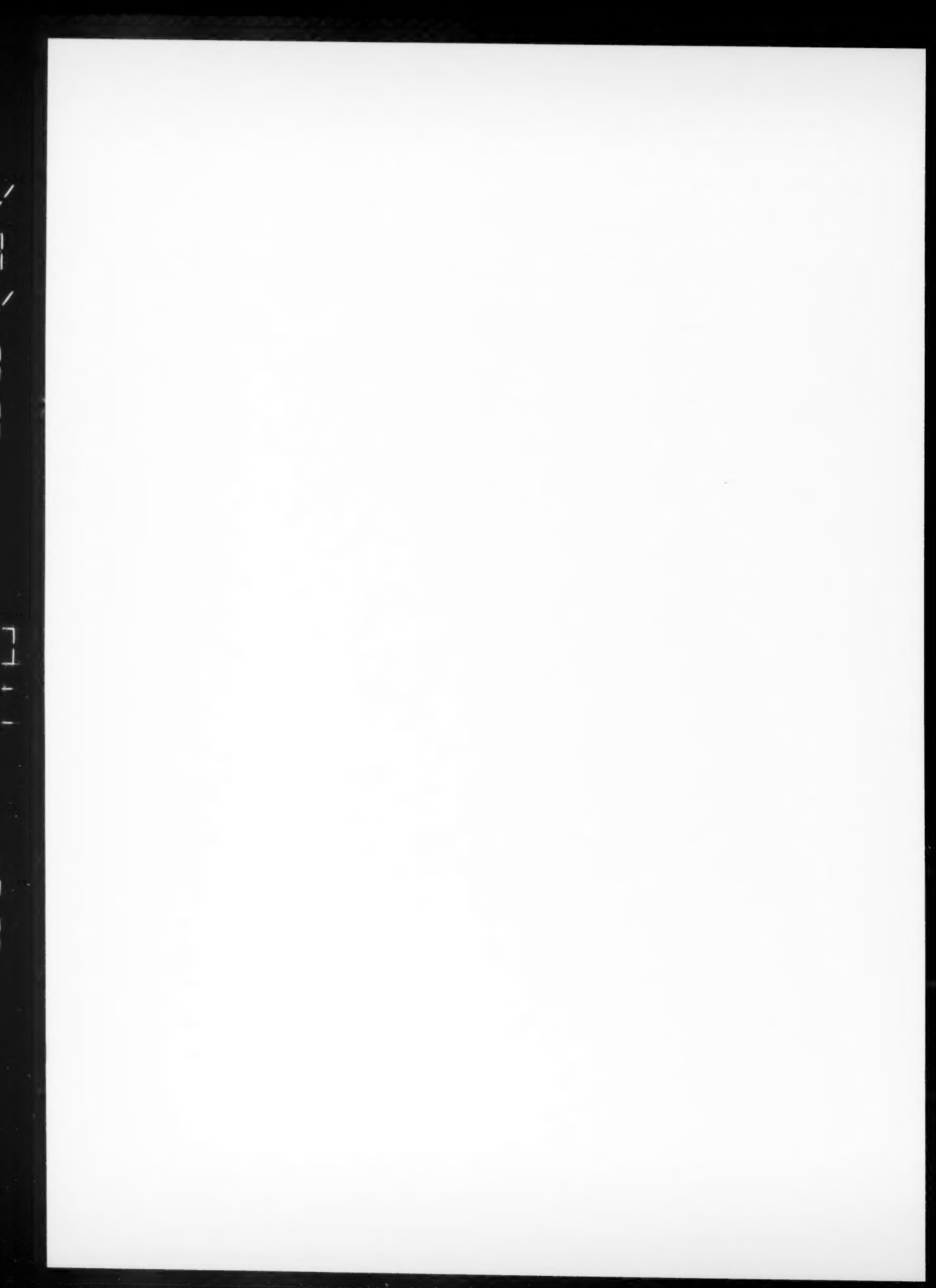
*Certificate in the name of N. V. Samokhvalov.

includes a box with a special combination of remote-controlled instruments and measuring units for operation in water and a shielded box (not employing water shielding) for loading radioactive cobalt into needles and applicators (Figure 3). This equipment enables one to carry out many delicate operations on a large scale by remote control while providing high productivity.

A variety of containers developed under the direction of the author and Busygin are now used, together with a fork-lift trolley for carrying heavy containers recently developed.

A simple manual washdown device for remote-controlled hydromechanical cleaning of a variety of activity-contaminated surfaces is at present being introduced.

N. V. Samokhvalov.



THE DEVELOPMENT OF IRRADIATION FACILITIES AND OF APPARATUS FOR RADIobiological WORK

The variety of conditions required in current radiobiological work demand many special irradiation set-ups and methods and apparatus for studying the vital functions of irradiated organisms.

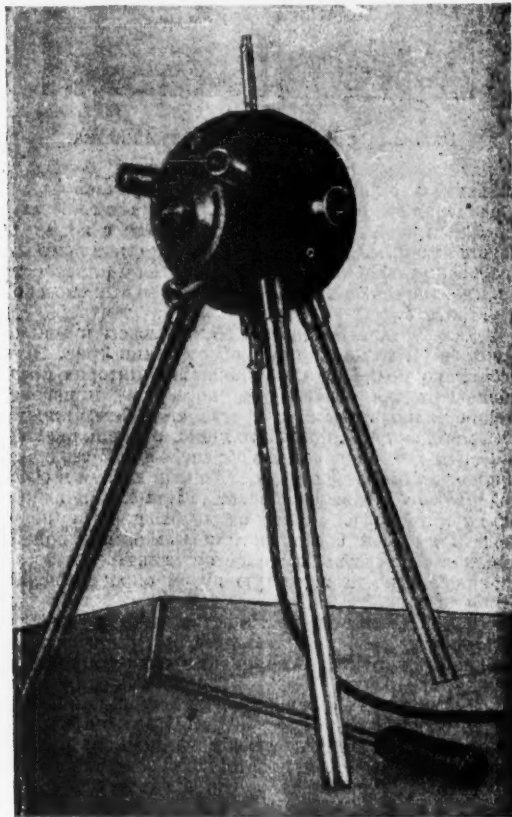


Fig. 1. TRK-2 transport and working container.

A team of scientists and designers (Busygin, Frank, etc) developed the GOP-1 γ -irradiator for treating malignant neoplasms. The GUT-Co-400-1 irradiator (400 g-equivalent Ra) was developed from this.

A design team of scientists and engineers (Bibergol, Busygin, etc.) developed the EGO-1 experimental cobalt irradiator.

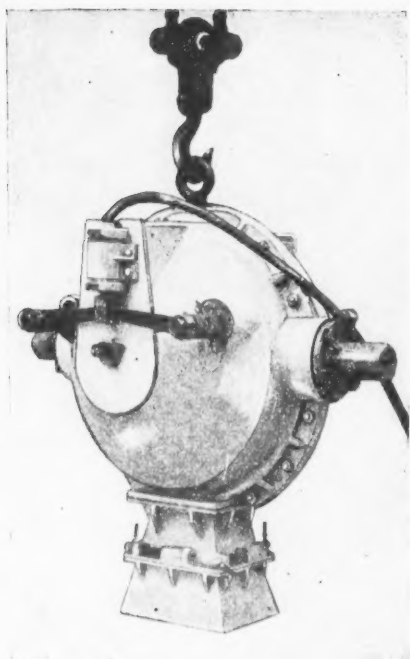


Fig. 2. Experimental GOD-1 setup for industrial γ -defectoscopy.

Subsequently the sources (in tubes) were arranged in a cylindrical array around the working volume, as in the EGO-2 and EGO-20, this giving comparatively uniform irradiation over a large volume; by combining this with a horseshoe-shaped working channel ("ray trap") and remote control of a powered trolley for the irradiated object, its use could be extended to quite powerful sources. Using the same principle, but with water shielding, V. G. Khrushchev (with others) produced the EGO-2 * designed for whole-body irradiation of experimental animals.

The EGO-20 unit (32,000 g-equivalent Ra) has been developed by V. G. Khrushchev and N. V. Samokhvalov, but not yet put into production.

The experimental short-focus OKFO-1 irradiator (designed by B. I. Kochstov, Z. I. Lisitsina, V. G. Khrushchev and V. E. Busygina) is designed for dose-rate studies in local irradiation and for irradiating small biological objects. Two radio-cobalt sources of 0.4 and 400 g-equivalent Ra of identical geometries are used for this. The object is placed 1-2 mm away from the sources. This gives very high dose-rates and relatively local irradiation. Using the 400 g-equivalent source the dose-rate is 500 r/sec, and with the 0.4 g-equivalent source 0.5 r/sec. The setup is remote-controlled and includes several devices ensuring accurate doses.

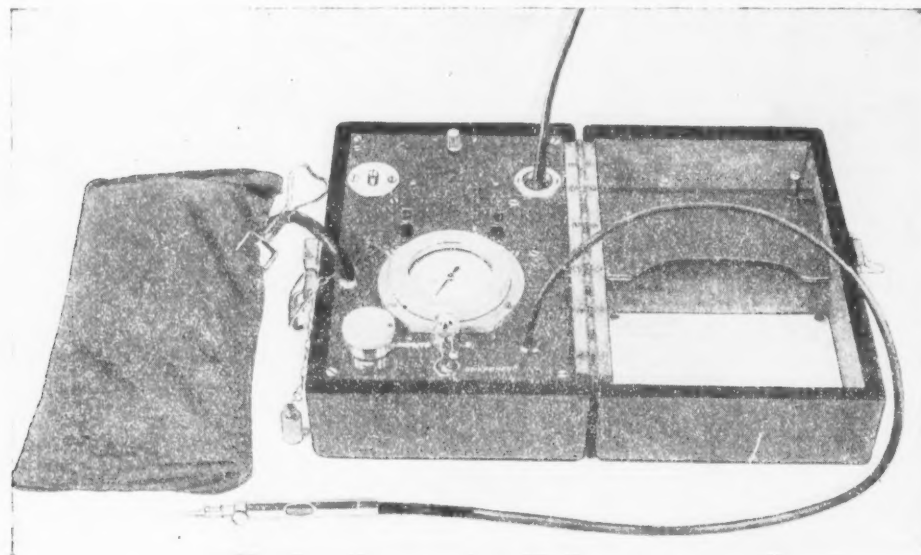


Fig. 3. AVK-1 unit for oxygen therapy in eye disorders.

* Described in detail in J. Atomic Energy 2, 197 (1957).

A 12-tube x-ray apparatus (V. G. Khrushchev et al) is intended for whole-body x-irradiations (up to 200 kev) with experimental animals. Twelve T-200 x-ray tubes are used. The tubes (in threes) are arranged on four sides of the working cavity. The cavity walls are of 0.5 mm Cu plus 1 mm Al and also filter the radiation. The dose-rate in the center of the cavity is 140 r/min.

The apparatus can be worked with 4 x-ray tubes (much overloaded). Small animals (rats, mice) can be irradiated under pulsed conditions (dose rates up to 150 r/sec). The 12-tube unit is at present being redesigned to give dose-rates up to 600 r/sec.

The design team which produced the GOP-1 also produced the TRK-2 γ -irradiator (transport and working container — Figure 1), intended for use with radio-cobalt up to 0.6 g-equivalent Ra, mainly for flaw-detection in metals. In 1950 the TRK-2 was adopted by Gostekhnika* as the type model used in developing the production model irradiator GUT-Co-0.5-1. The UG-1 γ -irradiator proposed by Samokhvalov and developed by him together with Busygin, was intended for flaw detection in inaccessible sites and was used as the basis for the GUP-Co-5-1 and GUP-Co-50-1 irradiators. The main distinguishing features of these are the separate storage and comparatively small irradiation containers, which are joined by a flexible metal tube for transferring the source from storage to irradiation containers and back again.

Previously Samokhvalov and Frank had directed the design, production, and testing of the first experimental units for radiotherapy and industrial γ -radiography: RP-4, GOT-1 and GOD-1 (Fig. 2) with 50-100 g-equivalent Ra and mercury or folding shutters in the working channel, which furthered the design and production principles of radiation units.

Of the physiological apparatus designed by the Academy of Medical Sciences we must mention Ananyev and Livanov's electroencephaloscope, which uses electronic switching to record the spatial distribution of the bioelectric potentials from 50 points on the cortex on a cathode-ray tube (using man and animals) as a mosaic of bright points of intensity proportional to the potential. This apparatus was used to demonstrate a number of regularities in radiation-induced cortical activity changes.

Polivoda and Gudin produced a device for determining the erythrocyte, leucocyte, neutrophil and eosinophil counts of blood automatically. The pulses produced in the scan by the differentially stained cells are amplified and recorded on counting equipment. This greatly accelerates the laborious analyses widely employed in medical radiobiology.

Two models (of very simple and original design and construction) of an apparatus for oxygen therapy of radiation cataract (Figure 3), methods and transducers for recording muscle respiration, devices for measuring gas and liquid pressures, including blood pressures in acute experiments, were developed by Busygin; he, together with Nefedov, developed methods of recording arterial pressures continuously in extended experiments and of recording pulse wave propagation velocities, methods and apparatus for recording arterial pressures in man and animals objectively; with Iu. G. Grigor'ev methods and apparatus for taking blood from animals by remote control during irradiation; with E. N. Kondrat'ev apparatus for digital plethysmography; with R. M. Liubimova methods and apparatus for recording intracranial and intravenous pressures photographically, together with certain other devices required in radiobiological work.

L. L. Vannikov and N. V. Samokhvalov

* Transliteration of Russian — Publisher's note.

V
3
/
-
0
[
-
0
1

RADIOACTIVE DYNAMITE*

It often happens that some charges remain undetonated when multiple charges are detonated simultaneously in mining, building, etc., operations. When dynamite or other such explosives are used the unexploded charges are very dangerous.

In Canada the Mines Department has investigated the manufacture and testing of radioactive dynamite, as this could be used to detect unexploded charges.

The dynamite was made by adding radioisotopes to normal dynamite. Those of half-life between 30 and 70 days, e. g., Sb¹²⁴, were found most suitable.

The experiments showed that unexploded charges were easily detected with the radioactive dynamite using Geiger counters or other such units to record the radiation.

In the opinion of the Department the use of radioactive dynamite would not displace existing methods of checking but would be useful where other methods do not give reliable results.

M. K.

* South Africa Mining and Engineering Journal, May 17, 1957, p. 927.

✓
3
-
3
[]
-
3

PROVISIONAL AGENDA OF THE 2nd INTERNATIONAL CONFERENCE ON
THE PEACEFUL USES OF ATOMIC ENERGY, GENEVA, 1958

(Brief Summary)

Plenary sessions.

Session A. Opening of the Conference.
Session B. The future of nuclear energy.
Session C. Nuclear power station experience.
Session D. Nuclear power station building projects.
Session E. 1. Uses of nuclear energy other than for generating electricity.
Session E. 2. Progress in the use of radioisotopes.
Session F. 1. Health-experience and operational safety.
Session F. 2. The latest developments in theoretical physics.
Session G. Controlled thermonuclear reactor possibilities.

Closing sessions.

Session Y. a) Development of international cooperation in nuclear energy in subsequent years.
b) Procurement and training of technical staff.
Session Z. Final plenary session.

Parallel sectional meetings.

Section 1.

Sessions 1.1 and 1.2 Reactor technology and chemistry
Sessions 1.3 and 1.4 The main applications of chemistry in nuclear energetics.
Sessions 1.5, 1.6 and 1.7 Properties of reactor materials.
Sessions 1.8 and 1.9 Processing irradiated fuel elements.
Sessions 1.10 and 1.11 Treatment of radioactive wastes.
Sessions 1.12 Experience with the radioactivity produced when using reactors and operating chemical plants.

Section 2.

Sessions 2.1, 2.2 and 2.3 Problems of nuclear synthesis:
a) energy balances in synthesis systems.
b) experimental systems.
c) stability and other properties of a plasma.
Sessions 2.4 Physics of elementary particles.
Sessions 2.5 Physics of fission.
Sessions 2.6 and 2.7 Nuclear data.
Sessions 2.8 and 2.9 Reactor theory and design.
Sessions 2.10 and 2.11 Fuel cycles and nuclear energy economies.
Sessions 2.12 Prototype power reactors.
Sessions 2.13 and 2.14 Use of experimental reactors.
Sessions 2.15 and 2.16 Reactor experiments.

Section 3.

Sessions 3.1 Dosimetry and standards.
Sessions 3.2 and 3.3 Technological aspects of high-intensity ionizing radiations.
Sessions 3.4 and 3.5 New medical uses of isotopes.
Session 3.6 Use of isotopes in biochemistry and physiology.
Session 3.7 Use of isotopes in research for control purposes and in industrial technology.
Session 3.8 Use of isotopes in agriculture.
Session 3.9 Production and distribution of radioactive and stable isotopes.
Sessions 3.10 and 3.11 The biological effects of radiation.
Sessions 3.12 and 3.13 Radiation protection and experience.
Session 3.14 Reactor operational hazards and reactor siting.
Session 3.15 Meteorological and oceanographic aspects of the large-scale use of nuclear energy.

Section 4.

Sessions 4.1, 4.2 and 4.3 Raw material supplies.
Sessions 4.4 and 4.5 Ore enrichment, preparation
and purification of uranium and thorium.
Sessions 4.6, 4.7 and 4.8 Isotope separation methods
(with particular attention to uranium
and the technology of UF_6).

Sessions 4.9 and 4.10 Fuel element production
(including the metallurgy of uranium,
thorium, plutonium and their alloys).
Sessions 4.11 and 4.12 Treatment of other nuclear
materials (graphite, zirconium, beryl-
lium, etc.).

BRIEF COMMUNICATIONS

USSR. An International Seminar on the Peaceful Uses of Atomic Energy was held at Moscow State University during the VIth Festival of Youth and Students. The director of the United Institute of Nuclear Studies, D. I. Blokhintsev, lectured on the physical foundations of nuclear energy and on Soviet work on high-energy particles; A. M. Samarin (corresponding member, Academy of Sciences of the USSR) lectured on the use of radioisotopes in science and technology, and G. M. Frank (corresponding member, Academy of Medical Sciences of the USSR) lectured on the work of Soviet geneticists on producing new plant forms with radiation-induced mutations.

Young people from England, Czechoslovakia, etc., participated in the discussion following the lectures.

The participants, in conclusion, adopted a combined resolution that nuclear energy should only be used for peaceful ends. (Iu. K.)

FGR. The Bundestag committee on atomic matters has recommended that a Calder-Hall type power station be erected on Hardwald Island (in the river Rhine, near Karlsruhe). (Nuclear Engineering 2, 17, 341, 1957).

FGR. A centrifugal method of separating uranium isotopes has been developed in the Federal Republic. Gaseous UF_6 is fed continuously to two centrifuges operating at 40,000 rpm. Some centrifuge parameters are given: height of steel rotor 150 mm, internal diameter 50 mm, wall thickness 20 mm.

Nine large centrifuges are to be set up in Bonn University in fall 1957; 50 will be installed at the new Nuclear Research Institute at Durenhagen (N. Rhine-Westphalia). Output 5 tons of uranium (2 % enrichment) per annum; power consumption 8-10 times less than in the diffusion method. (Nucleonics, 15, 6, 23, 1957).

UK. The third annual report of the UKAEA has been published. The report consists mainly of information on Calder Hall, commissioned during the period covered by the report and on the development of nuclear power in UK (Engineer, 204, 5297, 145, 1957).

Switzerland. The nuclear power development plan for Switzerland envisages the construction of a boiling-water reactor using slightly enriched uranium to produce 5 Mw of electrical energy. The reactor will be located in a cave near Lausanne. The station will be on view during the Swiss National Exhibition in Lausanne in 1964. The reactor will be commissioned earlier. It is proposed to use the reactor for instructing students from Lausanne University and Polytechnical Institute. (Nuclear Power, 2, 16, 309, 1957).

India. The Indian Atomic Energy Commission states that a new uranium deposit has been found in Rajasthan, 480 km southwest of New Delhi in the Bhilvar region. The ore is suitable for industrial use. The deposit is said to be the largest uranium deposit in Asia. (South Afr. Min. and Eng. Journ., 68, 3355, 1053, 1957).

South Korea. The South Korean Government states that the uranium deposit found in the Kosung region (25 km north of the 38th parallel on the eastern coast) will be developed in collaboration with the USA. The US Government has already assigned 310,000 dollars for this development. The bilateral agreement provides that all ore mined will be exported to USA. (Appl. Atomics, 90, 14, 1957).

Japan. The Japanese Atomic Energy Research Institute is preparing plans for a center to handle the production, distribution and import of radioisotopes. Specialists will also be trained in radioisotope work at the center. The center will cost 4.7 million dollars.

The center will possess a Van de Graff generator, a cyclotron and isotope and radiation laboratories.

The Japanese Government has prepared a program on peaceful uses of atomic energy to cover the next 4 years. This program provides for setting up a research center to deal with methods of using isotopes in agriculture and in the food and textile industries. This program will cost 400,000 dollars in the coming financial year. (Nucleonics, 15, 3, 10, 1957).

Venezuela. One-Hundred and sixty-seven million bolivars have been assigned by the government for setting up an isotope production reactor. The project includes building research laboratories. It is proposed to open the nuclear center in 1958. (Chem. Age, 77, 1980, 1051, 1957).

USA. The number of dismantled, operative and projected reactors at the Argonne National Laboratory given the symbol CP (Chicago Pile) is now seventeen:

CP-1, the first reactor (commissioned at the end of 1942).
CP-2, a modification of CP-1 (Palace Park, Chicago).
CP-3, the first heavy-water reactor,
CP-4, the experimental fast neutron reactor EBR-1,
CP-5, Argonne heavy-water research reactor,
CP-6, design reactor for Savanna River,
CP-7, (EBWR) experimental boiling water reactor,
CP-8, (EBWR-2) experimental fast neutron reactor,
CP-9, Army Low-Power Reactor, boiling water (ALPR),
CP-10, radioisotope production design reactor,
CP-11, instructional zero-power graphite reactor ("Argonaut"),
CP-12, (ARBOR), boiling-water reactor,
CP-13, ("Mighty mouse") 250 Mw research reactor,
CP-14, ("Hot box") sodium-graphite materials testing reactor,
CP-15, combined thermal and fast neutron reactor,
CP-16, reactor with gas-turbine setup,
CP-17, research reactor for research under power swing conditions. (Nucleonics, 15, 4, 24, 1957).

USA. The Dresden (Illinois) nuclear power station has been begun. This is being built by General Electric and the Nuclear Power Group and will be run by Commonwealth Edison. Its power will be 180 Mw. Completion set for 1960. (Nuclear Engineering, 2, 17, 346, 1957).

USA. Union Carbide Nuclear has dismantled its experimental aircraft reactor at Oak Ridge after continuous testing for four days at 2500 kw peak power. The reactor was run red-hot at fuel temperatures of 650 to 815° C. (Atomic Energy Guideletter, 117, 8, 1957).

USA. The Texas Oil Company will build a large nuclear radiation laboratory at its research center in Beacon, New York State. Three radiation sources will be available: a 6 Mev linear accelerator, a 3 Mev Van de Graaf generator and a 35,000 curie cobalt source. (Chem. Trade J. 140, 3655, 1491, 1957).

USA. The Atomic Energy Commission has published new guaranteed purchase prices for plutonium deriving from power and research reactors operated under license. The new price is effective from July 1, 1963. Up to July 1, 1962 the price will vary from 30 to 45 dollars per gram, depending on the Pu^{240} content. From July 1, 1962 to July 1, 1963 the price will be 30 dollars per gram. The earlier price (12 dollars per gram) is deleted. (Appl. Atomics, 86, 12, 1957).

USA. Scientists at the Batelle Institute have developed a method of producing super-purity chromium. Irradiated crystals of this have been used (by Ohio University) as an interstitial γ -ray therapy source. The Cr^{61} in the crystals provides the γ -rays. As Cr^{61} has a half-life of 28 days it may be better than Au^{198} , Rn^{222} and other short-lived isotopes used in radiotherapy. (Financial Times, July 26, 1957.)

USA. A silver-activated phosphate glass has been developed at the Naval Research Laboratory. This glass is becoming widely used in dosimeters for use in medicine and the food industries. About 3 million buttons for individual radiation checks have already been produced. (Science News Letter 72, 1, 9, 1957).

USA. Westinghouse Electric has developed at the Pittsburgh radiation and nuclear physics laboratory a radiation shield consisting of two steel plates enclosing small spheres in the gap. Total weight of spheres 35 tons. The shield is easily shifted as the spheres are easily run off through special ports at the bottom of the walls. (New York Times of August 6, 1957).

BIBLIOGRAPHY

BOOK REVIEW

A. N. Tokarev and A. V. Shcherbakov, Radiohydrogeology, State Geological Technical Press, 1956, pp. 262. 13 roubles, 40 kopecks.

The appearance of Radiohydrogeology, which is the first major Soviet review on the radioactivity of natural waters, will be very welcome to uranium geologists.

The book is divided into two parts. The first "Fundamentals of Radiohydrogeology" contains three chapters.

The first chapter deals with the conditions under which natural waters become enriched in radioelements. Their general physicochemical and geochemical properties and their contents and forms in natural rocks are given and the conditions for the formation of radioactive waters are discussed (as dependent on climate, extent of fracturing in the structure, the physical properties of the rocks and underground waters as well as the chemical composition and gas contents of the latter).

The second deals with typical natural radioactive waters (surface waters from sedimentary rocks, acid magmatic rocks and uranium deposits) and gives their radioelement contents; a scheme for the formation and classification of radioactive waters is presented and the classification characteristics and formation conditions differentiated.

The third deals with the hydrogeological conditions for uranium deposit formation and destruction (pp. 96-118). This topic of practical and theoretical interest has thus far been inadequately examined and therefore is not dealt with exhaustively in this book. It is pointed out that the role of underground waters in uranium deposit dynamics has only been dealt with cursorily (p. 98). But nevertheless this chapter is of great interest as constituting the first generalization of the accumulated information.

The conditions for uranium deposit formation, persistence and destruction depend on the following factors: the geological formation, which is itself determined by the orogenic and epeirogenic movements, the mineral compositions of rock and uranium-rich ore, the temperature, which depends on the closeness of magmatic foci, the salt and gas contents of the water, the pressure, water conditions etc.

These factors are then considered in relation to the general scheme at two stages (formation and destruction) in the life of the deposit. The text relating to each stage is supplemented by tables relating to the main factors producing or destroying the deposits.

The second part of the book "Radiohydrogeological Methods" consists of 6 chapters. The first deals with general topics, "radiohydrogeological prospecting criteria" being defined, the main tasks involved in detection being enumerated: data are given on the contents and migrations of radioelements (uranium, radium and radon) in underground waters, together with how to use these data in the search for uranium ore-bodies. Four stages in radiohydrogeological prospecting are indicated (prospecting and detection, mapping, exploratory development and full-scale working) together with the map scale and basic methods required at each stage.

The organization of radiohydrogeological work is dealt with in three separate chapters. Chapter two deals with the field work, chapter four with methods of determination for radioactive gases and waters and chapter five with the computation of radioactive water resources, although these three topics would be better combined in one chapter; they should not, in any case, be separated by chapter three, which is independent. This latter deals with the interpretation of radiohydrogeological test data for various hydrogeological conditions, with the hydrogeological interpretation of aerial radiation surveys data, and with the main requirements for uranium deposit detection methods in such work.

The above brief summary shows that the general theoretical problems in the subject are dealt with and the prospecting methods developed by the authors for uranium are presented. This book is the product of many years' experience in this field, combined with the work of others.

While emphasizing that the book is of value, we would not wish to imply that it is without defects. They are inevitable in a book of such broad scope in a field as young as the search for uranium deposits. The text has not been carefully edited and corrected. Some topics are considered too briefly or in outline only, or as contributions to a discussion. But it must be borne in mind that the material is often inadequate. Moreover many of the topics considered are new and as yet inadequately checked by experiment.

It is to be hoped that in a subsequent edition many topics will be considered in greater detail, particularly as regards interpretation methods, and evaluating and checking radiohydrogeological anomalies, as these are of particularly great importance in detecting true anomalies and rejecting false ones.

The book is not only valuable as a handbook of methods for use in detailed surveys for uranium but is also the first in the USSR to serve as a text-book for the new scientific discipline of "Radiohydrogeology" which is taught in several institutions in this country.

V. N. Popov.

REVIEWS

Atomic technique abroad. A collection of reviews and of translations from the foreign literature (No. 1, September 1957, Atomic Press, 128 pp., 5 roubles). This volume starts a series of such collections of translations and reviews of the foreign periodical literature on the most important current topics in atomic technique.

The collections will consist of translations and reviews of the foreign scientific atomic journals on nuclear reactors, particle accelerators technology and metallurgy of nuclear materials, radioisotope production and application in industry, agriculture, biology and medicine, radiation dosimetry and shielding and atomic raw materials. In the "News" section short translations and abstracts will give the most interesting information of a scientific, technical, military and economic character on the achievements of foreign atomic industries.

The collections are directed to a broad circle of engineering and scientific workers, and also to instructors, postgraduates and students in higher educational institutions.

The first number contains the following translations:

Current state of work on atomic energy in the USA.

Reactor construction in U. K.

The experimental power station and EBWR boiling-water reactor.

Closed-cycle nuclear gas-turbine power units for ships.

Metallic uranium production in France.

Production of high-purity uranium powder.

Remote control of operations in hot cells.

An electromagnetic isotope separator.

Mesoatoms.

Geology of the uranium deposits at L. Ambrosia.

News:

Controlled thermonuclear reactions work.

Brief notes (reactor construction, constructional materials, particle accelerators, nuclear-powered ships, nuclear-propelled aircraft, atomic weapons, work with radioactive materials, atomic batteries, radiation protection agents, use of radioisotopes).

The collection is profusely illustrated and well got up.

L. I.

Progress in Nuclear Energy. An International Library of Atomic Energy in 9 series. First volumes of series 8, 1957, published by Pergamon Press (in English). Editors-in-chief: D. I. Blokhintsev (USSR), J. W. Dunworth (U. K.), D. J. Hughes (USA), I. I. Novikov (USSR), F. Perren (France) and A. M. Weinberg (USA).

The International Library of Atomic Energy consists of 9 series:

1. Physics and Mathematics.
2. Reactors.
3. Process Chemistry.
4. Technology and Engineering.
5. Metallurgy and Fuels.
6. Biological Sciences.
7. Medical Sciences.
8. The Economics of Nuclear Power.
9. Analytical Chemistry.

The first volumes of series 1-8 have been published (in English), these consisting partly of material presented at the Geneva (1955) Conference.*

The first volume of series 1 (pp. 398) contains 7 articles. The first three, dealing with neutron interactions with U^{233} , U^{235} and Pu^{239} , give data on absorption and fission cross sections and numbers of secondary neutrons emitted in fission at thermal energies, the data on resonance structure of the fissile isotopes being summarized and analyzed. The fourth article discusses the measurement of elastic and inelastic neutron cross sections and reviews the current state of experimental neutron and γ -ray spectroscopy: The fifth deals with the cross section of Xe^{135} as a function of neutron energy, the sixth with resonance capture integrals, while the seventh reviews the work on delayed neutrons. The last four articles present theoretical and experimental data on some types of reactors.

The first volume of series two (pp. 492) deals with reactors under design, building, or operative. Some articles, e. g., "PWR-pressurized water reactor," "Graphite moderated gas-cooled reactors and their place in power production" and "Sodium-cooled graphite reactors" are just copies of Geneva Conference reports. The others are of review type, composed partly of Geneva material and partly of that published subsequently. The Canadian research reactors (NRX, ZEEP, NRU), some U. S. research reactors (MTR, a swimming-pool type reactor at Oak Ridge, three CP type heavy-water reactors, various homogeneous and "water boiler" reactors), five research reactors in Western Europe (two in France, one in Norway, one in Sweden and one in Switzerland), the British research reactors (Gleep, Bepo, Zephyr, Dimple, Dido, Pluto and Lido) and the U.S. homogeneous power reactors are described. The last short review deals with fast neutron reactors. Nuclear reactors are cataloged (by countries) at the end of the book.

The articles in the first volume of series three (pp. 480) cover the principle stages in the chemical technology of nuclear fuels, including the preparation of uranium and thorium from their ores, processing of irradiated materials and the production of radioisotopes. The problems of radiochemical process choice, the action of intense radiations on reagents, etc., are considered. Much attention is devoted to pyrometallurgy and distillation processes for separating fission products. A valuable review deals with the chemical aspects of distilling UF_6 from irradiated fuels.

The first volume of series four (pp. 420) consists of chapters headed "Heavy water," "Graphite," "Beryllium oxide," "Liquid metals," "Technology," "Reactor chemistry and corrosion." The most interesting articles are "Chemistry of water for pressurized reactors" which gives much data on the chemical processes in a water-cooled nuclear reactor, and "Metallurgical studies of liquid bismuth and bismuth alloys as nuclear fuel carriers or coolants."

The first volume of series five (pp. 805) has the following sections, "Production of uranium metal," "Thorium," "Beryllium and zirconium," "Metallurgy of plutonium," "Preparation and properties of the rare-earth metals," "Ceramics," "Fuel elements," "Action of radiation" and "Solid-state physics." The most interesting articles are "Metallurgy of plutonium," ** "Production of uranium metal" and "Preparation and

* This conference material has been published in Russian.

** "Problems of current metallurgy" [in Russian], Vol. 2, No. 32 (Izd. IL, Moscow) 1957, p. 63.

properties of the rare-earth metals". There are interesting data on the melting and casting of large masses (up to 250 kg) of uranium, on uranium processing and hot-pressing of powders. Systematic data on the properties of almost all the rare-earth metals are given. The remaining articles contain some interesting data on making uranium carbide and uranium and thorium oxide ceramics for use as high-temperature fuel elements.

In the first volume of series six (pp. 205) some topics in the biological action of ionizing radiations are considered; together with radiation genetics and the use of radioisotopes for metabolism studies in plants and animals.

In the first volume of series seven (pp. 165) are given data on the use of radioisotopes in medicine and on safety measures in irradiation processes. The physical bases of isotope techniques and of measuring concentrations of radioactive materials in living organisms are considered. Methods of determining the circulating blood volume and blood flow rate are described, as are methods of localizing certain malignant tumors.

In the first volume of series eight (pp. 513) many subjects are dealt with. There are five chapters "Requirements and resources", "Economics of nuclear power", Reactor construction programs and data on nuclear reactor economics", "Law and administration". The energy requirements of various countries and their power resources are discussed, together with the part of nuclear power in satisfying the energy requirements of states.

Iu. K.

NEW LITERATURE

JOURNAL ARTICLES

Akhiezer, A. E. and Sitenko, A. G., The diffraction scattering of fast deuterons by nuclei. *J. Exptl.-Theor. Phys. (USSR)* 32, No. 4, 1957.

Alekseev, A. I., The covariant equation for two mutually annihilating particles. *J. Exptl.-Theor. Phys. (USSR)* 32, No. 4, 1957.

Alimarin, I. P. and Zolotov, Iu. A., The analytic chemistry of neptunium. *Uspheki khim.*, 26, No. 6, 1957.

Alimarin, I. P. and Zolotov, Iu. A., Extraction of uranyl α -nitroso- β -naphthol and the separation of uranium from vanadium and iron. *J. Anal. Chem. (USSR)* 12, No. 2, 1957.

Andreeva, O. S., The efficiencies of some existing methods of removing radium salt contamination from the hands. *Meditinskaya Radiologiya*, No. 3, 1957.

Azimov, S. A., The decaying particles produced by electron-nucleon showers in dense absorbers. *Izv. AN Uzb. SSSR, Seriya fiz-mat. nauk*, No. 1, 1957.

Baiukov, Iu. D. and Tiapkin, A. A., The energy spectrum of the γ -rays from the decay of π^0 -mesons formed by 660-Mev protons in p-p collisions. *J. Exptl.-Theor. Phys. (USSR)* 32, No. 5, 1957.

Baiukov, Iu. D. et al., The energy and angular distributions of π^0 -mesons formed by protons in p-p collisions at 470 and 660 Mev. *J. Exptl.-Theor. Phys. (USSR)* 32, No. 4, 1957.

Burtsev, A. K. and Kolomenskii, A. A., The theory of the ring phasotron. *Pribory i tekhnika eksperimenta*, No. 2, 1957.

Butomo, N. V. and Shcherbakov, N. I., The use of sodium pentoxy1 and sodium nucleinate in radiation-induced leucopenia. *Voen.-med. Zh.*, No. 5, 1957.

Vavilov, V. S. et al., Effect of fast neutron irradiation in electron-hole recombination in germanium crystals. *J. Exptl.-Theor. Phys. (USSR)* 32, No. 4, 1957.

Vavilov, P. V. The ionization losses of high-energy charged particles. *J. Exptl.-Theor. Phys. (USSR)* 32, No. 4, 1957.

Vavilov, P. V., High-energy π -meson cross sections for interaction with nucleons. (Letter to the Editors) *J. Exptl.-Theor. Phys. (USSR)* 32, No. 4, 1957.

Varfolomeev, A. A., International Conference on photographic emulsion methods, Dubna, 1957. *Pribory i tekhnika eksperimenta*, No. 2, 1957.

Vladimirskii, V. V., Fission mechanism of heavy nuclei. *J. Exptl.-Theor. Phys. (USSR)* 32, No. 4, 1957.

Gramenetskii, I. M. et al., Nuclear interactions at $8 \cdot 10^{13}$ ev in emulsions. (Letter to the Editors) *Pribory i tekhnika eksperimenta*, No. 2, 1957.

Gerchikov, D. S. et al., Radioisotope studies of the nonmetallic impurity inclusions in blown steel. *Transactions of the Donets Division, Scientific and Technical Society of Ferrous Metallurgy*, 5, 1957.

Gorbunov, A. M., et al., Use of Wilson chambers for studying photonuclear reactions. *Pribory i tekhnika eksperimenta*, No. 2, 1957.

Gorshkov, V. K., An integral mass-spectrometer method for determining element concentrations. *Pribory i tekhnika eksperimenta*, No. 2, 1957.

Gribov, V. N., Effect of nuclear edge-diffuseness on neutron scattering. *J. Exptl.-Theor. Phys. (USSR)* 32, No. 4, 1957.

Gribov, V. N., Excited rotational states in the interactions of neutrons with nuclei. *J. Exptl.-Theor. Phys. (USSR)* 32, No. 4, 1957.

Davydov, A. S., and Fillipov, G. F., The moment of inertia of a system of interacting particles. *J. Exptl.-Theor. Phys. (USSR)* 32, No. 4, 1957.

Dennis, Metallurgy in Nuclear Power (translated from the English). *Problemy sovremennoi metallurgii*, No. 3, 1957.

Dzhelepov, B. S., Resonant γ -ray scattering by nuclei. *Uspekhi Fiz. Nauk.*, 62, No. 1, 1957.

Dzhelepov, V. P. et al., Neutral π -meson formation in n-D collisions and compound nuclei. *J. Exptl.-Theor. Phys. (USSR)* 32, No. 4, 1957.

Dmitriev, A. B., Gas-discharge counters for ionizing particles. Review, *Pribory i tekhnika eksperimenta*, No. 2, 1957.

Domshlak, M. P. et al., Radiation counter-agents experiments in the experimental x-ray therapy of tumors. *Meditinskaya Radiologiya*, No. 3, 1957.

Diatlov, I. I. et al., An asymptotic theory of meson-meson scattering. *J. Exptl.-Theor. Phys. (USSR)* 32, No. 4, 1957.

Zhernovoi, A. I. et al., Internal conversion electron spectrum from the active deposit from radiothorium. II. *J. Exptl.-Theor. Phys. (USSR)* 32, No. 4, 1957.

Zavoiskii, E. K., A source of polarized nuclei for accelerations. *J. Exptl.-Theor. Phys. (USSR)* 32, No. 4, 1957.

Zedgenizde, G. A., The VIII International Congress of Radiology (Mexico, July, 1956). *Klin. Meditsina*, 35, No. 6, 1957.

Zelevich, Ia. B., and Sakharov, A. D., The μ -meson induced reactions in hydrogen. (Letter to the Editors). *J. Exptl.-Theor. Phys. (USSR)* 32, No. 4, 1957.

Zeuss, G. and Urey, H., The distribution of the elements (translated from the English). *Uspekhi Fiz. Nauk.*, 62, No. 1, 1957.

Ivanov, L. I. and Matveev, M. P., A new device for studying vapor pressures and diffusion constants for metals by isotope exchange. *Transactions of the Baikov Institute of Metallurgy*, No. 1, 1957.

Kaipov, O. K. and Takibaev, Zh. S., Slow π -meson generation by cosmic ray particles. *J. Exptl.-Theor. Phys. (USSR)* 32, No. 4, 1957.

Karpman, V. I., The theory of "odd" particles. (Letter to the Editors). *J. Exptl.-Theor. Phys. (USSR)* 32, No. 4, 1957.

Kiselev, V. S. and Fliagin, V. B., The energy distribution of the neutrons produced by 680 Mev proton bombardment of beryllium. *J. Exptl.-Theor. Phys. (USSR)* 32, No. 5, 1957.

Klechkovskii, V. M., Distribution of atomic electrons. *Reports of the Timiriazevskoi Agricultural Academy* No. 1, 1957.

Kobzarev, I. Iu. and Okun', L. B., The simultaneous production of Λ - and Θ -particles. (Letter to the Editors). *J. Exptl.-Theor. Phys. (USSR)* 32, No. 4, 1957.

Korshunov, I. A. et al., Activity determinations of C^{14} labeled organic compounds. *Zh. Obshch. Khim.*, 27, No. 4, 1957.

Krylova, N. M., Effect of γ -rays on vitamins in food products. *Voen.-med. Zh.*, No. 5, 1957.

Kuznetsov, B. M., Separation of helium isotopes by distillation and thermo-osmosis. *J. Exptl.-Theor. Phys. (USSR)* 32, No. 5, 1957.

Kustanovich, S. D., The use of thulium-170 γ -rays in medical practice. *Voen.-med. Zh.*, No. 5, 1957.

Likhter, A. I., and Kikoin, A. K., Effect of neutron irradiation on the compressibilities of metals. (Letters to the Editors), *J. Exptl.-Theor. Phys. (USSR)* 32, No. 4, 1957.

Liapidevskii, V. K., Use of diffusion chambers in determining low activities. *Pribory i tekhnika eksperimenta*, No. 2, 1957.

Maksimenko, V. M. and Rozental', I. L., Some problems in the statistical theory of multiple charge formation. *J. Exptl.-Theor. Phys. (USSR)* 32, No. 4, 1957.

Matalin, A. L. and Ivanov, A. A., A neutron flux monitor. *Pribory i tekhnika eksperimenta*, No. 2, 1957.

Matinian, S. G., The energy spectrum of the μ -mesons from K_{μ_3} decay. (Letter to the Editors), *J. Exptl.-Theor. Phys. (USSR)* 32, No. 4, 1957.

Migdal, A. B., Bremsstrahlung and pair formation at high energies in a condensed medium. *J. Exptl.-Theor. Phys. (USSR)* 32, No. 4, 1957.

Mints, A. L., The largest establishment for nuclear studies. *Vestnik Akad. Nauk SSSR*, No. 6, 1957.

Novikova, G. I. et al., The α -decay of Pu^{239} . *J. Exptl.-Theor. Phys. (USSR)* 32, No. 4, 1957.

Petrov, V. A., The BB-DKZ device for checking γ -ray shielding. *Meditinskaia radiol.*, No. 3, 1957.

Poluektov, N. S. et al., Compleximetric titration of zirconium and hafnium. *Zavodskaiia Lab.*, No. 6, 1957.

Prokoshkin, Iu. D. and Triapkin, A. A., π^0 meson formation in p-p and p-n collisions at 390-660 Mev. *J. Exptl.-Theor. Phys. (USSR)* 32, No. 4, 1957.

Rapp, A., Production of radioisotopes. *Khimiia i khimicheskaiia tekhnologija*, No. 5, 1957.

Sviderskaia, Z. A. et al., Study of the microinhomogeneities in magnesium alloys with radioisotopes. *Trudy Inst. metallurgii im Baikova*, No. 1, 1957.

Sermenov, L. F. and Prokudina, E. A., The use of combined adrenaline-acetylcholine in radiation sickness prophylaxis. *Meditinskaia radiologija*, No. 3, 1957.

Soroko, L. M., Resonant π -meson - nucleon interactions and π -meson formation by nucleons. *J. Exptl.-Theor. Phys. (USSR)* 32, No. 5, 1957.

Spitsyn, V. I. and Lavrukhina, A. K., Utilization of atomic energy in Czechoslovakia. *Vestnik Akad. Nauk* No. 6, 1957.

Spitsyn, V. I. and Mikheev, N. B., Use of radiometric analysis to study the compositions of phosphotungstates. *Zhurnal neorg. khimii* 2, No. 5, 1957.

Strashnin, A. I., Efficiency of cysteamine preparations in clinical radiation sickness prophylaxis. *Meditinskaia radiologija*, No. 3, 1957.

Takibaev, Zh. S. and Usik, P. A., Allowance for the primary α -particles in nucleon cascade development in the stratosphere. (Letter to the Editors), *J. Exptl.-Theor. Phys. (USSR)* 32, No. 4, 1957.

Wichers, E., Report on atomic weights in 1954-1955 (translated from the English). *Uspekhi Khimii*, 26, No. 6, 1957.

Fainberg, Ia. B. and Khizhniak, N. A., Energy loss by a charged particle passing through a layered dielectric, I. *J. Exptl.-Theor. Phys. (USSR)* 32, No. 4, 1957.

Shchepot'eva, E. S., Medical uses of α -emitting isotopes (α -therapy). Meditsinskaia radiologiya, No. 3, 1957.

Epel'baum, V. A. and Gurevich, M. A., The phase diagram of the zirconium-boron system I. Formation of solid solutions of boron and zirconium. Zh. Fiz. Khimii, 31, No. 3, 1957.

Estulin, I. V. et al., The soft γ -rays emitted by nuclei on thermal neutron capture. J. Exptl.-Theor. Phys. (USSR) 32, No. 5, 1957.

Ian'shin, V. S., A sighting single-slit x-ray kymograph. Voen.-med. Zhurnal, No. 5, 1957.

Ianushkovskii, V. A. and Banashek, V. E., A radioactive method of checking the filling of nontransparent vessels in flow production. Masloboina-zhirovaia promyshlennost', No. 5, 1957.

COMMISSION ON HIGH-LEVEL ISOTOPE DEVICES

To improve the coordination and guidance of research and design workers involved in using and designing high-level isotope devices, the Atomic Energy Directorate of the USSR Council of Ministers has organized a Commission on high-level isotope devices.

The commission will deal with the technical and design aspects of all high-level isotope devices to be used in various branches of the national economy and science, and will provide advice on design and assistance in procuring the radioisotopes.

The Directorate has organized the design of high-level devices and of laboratories for work with radioisotopes both in response to individual requests, for organizations and for general use in various branches of the national economy and science.

It is now dealing with typical designs for laboratories for work with radioisotopes in metallurgy and metalworking, in agriculture, biology, and chemistry, for wear studies on materials, parts and assemblies, for radiation chemistry and for flow detection work.

Atomic Energy Directorate of the USSR
Council of Ministers.

TABLE OF CONTENTS

	Page	Russ. Page
Formation of Na^{24} and P^{32} in the Interaction of High-Energy Protons with Compound Nuclei. <u>A. K. Lavrukhina, L. P. Moskaleva, L. D. Krasavina and I. M. Grechishcheva</u>	1087	285
The Measurement of the Absolute Intensity of Neutron Sources by a Comparison with the Reaction $\text{T}(\text{d}, \text{n})\text{He}^4$. <u>N. N. Flerov and V. M. Taluzin</u>	1095	291
Investigations of the Performance of Gas-Discharge Counters with a Controlled Pulsed Power Supply. <u>V. V. Vishnyakov and A. A. Tyapkin</u>	1103	298
Determination of the Composition and Instability Constants of Complex Pu^{+3} Oxalate Ions. <u>A. D. Gel'man, N. N. Matorina and A. I. Moskvin</u>	1115	308
Investigation of the Formation Conditions and Stability of Complex Pu^{+3} Compounds by a Spectrophotometric Method. <u>A. D. Gel'man and A. I. Moskvin</u>	1121	314
Letters to the Editor		
On the Question of Neutron Thermalization. <u>V. V. Smelov</u>	1125	317
The Chemical Behavior of Mo^{99} Formed on Irradiation of Uranium Compounds by Neutrons. <u>L. V. Shiriaeva and G. M. Tolmachev</u>	1129	318
On the Measurement of Neutron Absorbtion in Heterogeneous Uranium-Heavy Water Systems. <u>V. F. Belkin, P. A. Krupchitskii and Yu. V. Orlov</u>	1133	320
The Measurement of the Resonance Integrals of Absorption for Zirconium Samples. <u>Yu. P. Dobrynin, G. A. Dorofeev and I. E. Kutikov</u>	1139	323
Deuteron Splitting in Scattering by Nuclei. <u>A. G. Sitenko</u>	1141	324
Ionization Losses Below the Threshold in a Pulse Ionization Dosimeter of Fast Neutrons. <u>Yu. I. Petrov</u>	1145	326
A Comparison of the Standard Neutron Sources of the USSR and Sweden. <u>G. A. Dorofeev, I. E. Kutikov and A. M. Kucher</u>	1149	328
Scintillations Produced by α -Particles in Helium at High Pressures. <u>S. A. Baldin, V. V. Gavrilovskii and F. E. Chukreev</u>	1155	331
Gross γ -Activity of Fission Products of U^{235} . <u>V. N. Sakharov and A. I. Malofeev</u>	1161	334
Determination of the Absolute Intensity of the 2.5 Mev Line of γ -Emission of La^{140} . <u>V. A. Arkhipov</u>	1163	335
Polarization of γ -Emission Produced in the Reaction $\text{Si}^{30}(\text{p}, \gamma)\text{P}^{31}$. <u>P. M. Tutakin, S. P. Tsytko, A. N. L'vov, A. K. Val'ter and Iu. V. Gonchar</u>	1165	336
Calculation and Measurement of γ -Field From a Plane Source. <u>U. Ia. Margulis and A. V. Khrustalev</u>	1169	338

	Page	Russ. Page
On the Motion of Charged Particles in the Central Region of a Cyclotron. <u>V. S. Panasiuk</u>	1173	341
The Iodide Method of Refining Zirconium. <u>G. I. Stapanova and F. I. Busol</u>	1177	344
Measurement of Small Concentrations of α -Active Substances in Water by the Freezing-Out Method. <u>N. G. Gusev, D. P. Osanov and V. P. Mashkovich</u>	1183	346
Fixation of Nitrogen Under the Action of Ionizing Radiations. <u>S. Ia. Pshezhetskii, and M. T. Dmitriev</u>	1189	350
The Use of Radioactive Isotopes in Studying the Kinetics of Scrap Melting and Slag Formation in the Scrap-Ore Process. <u>A. I. Osipov, L. A. Shvartsman, V. I. Alekseev, V. F. Surov, M. L. Sazonov, M. T. Bulskii, S. A. Telesov, A. M. Skrebtsov, A. M. Ofengenden, L. G. Goldshtain and F. F. Sviridenko</u>	1193	352

Scientific and Technical News

On the Physics of Ionized Gases (1199). At the All-Union Industrial Exhibition (1203).

The Experimental Sodium Graphite Reactor, SRE, Goes Critical (1209). The Use of Organic Compounds in Reactor Construction (1213). Dosimetric Equipment (1217). The Development and Introduction of Some Radiation Screening and Handling Devices (1219). The Development of Irradiation Facilities and of Apparatus for Radiobiological Work (1223). Radioactive Dynamite (1227). Provisional Agenda of the 2nd International Conference on the Peaceful Uses of Atomic Energy, Geneva, 1958 (Brief Summary) (1229).

Brief Communications	1231
--------------------------------	------

Bibliography

Book Review	1233	376
Reviews	1234	376
New Literature	1237	379



Announcing A NEW expanded program for the translation and publication of six leading Russian physics journals. Published by the American Institute of Physics with the cooperation and support of the National Science Foundation.

Soviet Physics - Technical Physics. A translation of the "Journal of Technical Physics" of the Academy of Sciences of the U.S.S.R. 12 issues per year, Vol. 3 begins July 1958, approximately 3,000 Russian pages. Annually \$75.00 domestic.

Soviet Physics - Acoustics. A translation of the "Journal of Acoustics" of the Academy of Sciences of the U.S.S.R. Four issues per year, Vol. 4 begins July 1958, approximately 400 Russian pages. Annually \$12.00 domestic.

Soviet Physics - Doklady. A translation of all the "Physics Section" of the Proceedings of the Academy of Sciences of the U.S.S.R. Six issues per year, Vol. 3 begins July 1958, approximately 800 Russian pages. Annually \$35.00 domestic.

Soviet Physics - JETP. A translation of the "Journal of Experimental and Theoretical Physics" of the Academy of Sciences of the U.S.S.R. Twelve issues per year, Vol. 7 begins July 1958, approximately 3,700 Russian pages. Annually \$75.00 domestic.

Soviet Physics - Crystallography. A translation of the journal "Crystallography" of the Academy of Sciences of the U.S.S.R. Six issues per year, Vol. 2 begins July 1958, approximately 1,000 Russian pages. Annually \$25.00 domestic.

Soviet Astronomy - AJ. A translation of the "Astronomy Journal" of the Academy of Sciences of the U.S.S.R. Six issues per year, Vol. 1 begins July 1958, approximately 1,200 Russian pages. Annually \$25.00 domestic.

Back issues are available, either in complete sets or single copies.

All journals are to be complete translations of their Russian counterparts. The number of pages to be published represents the best estimate based on all available information now on hand.

Translated by competent, qualified scientists, the publications will provide all research laboratories and libraries with accurate and up-to-date information of the results of research in the U.S.S.R.

Subscriptions should be addressed to the

AMERICAN INSTITUTE OF PHYSICS

335 East 45 Street

New York 17, N.Y.

